Role of PKC during B cell development and transformation

Rinako Nakagawa

A thesis submitted for the degree of Doctor of Philosophy at the University of Glasgow

Faculty of Medicine

Submitted: July 2006

Summary

The objective of this thesis is to determine the role of specific PKC isotypes during B cell development and transformation. B cell generation systems were validated both *in vitro* and *in vivo*, by coculturing haematopoietic progenitor cells (HPCs) on the calvanial cell line, OP9, or by adoptively transferring HPCs into recombinase-activating gene 1-deficient (RAG-$1^{-/-}$) mice, respectively. In both cases, mature B cells were generated as determined by analysing surface B cell marker expression. Coupling of these *in vitro* and *in vivo* B cell generation systems with a retroviral gene transfer technique, plasmids-encoding PKC mutants in the retroviral vector MIEV were stably expressed in foetal liver (FL)-derived HPCs from wild type mice and cultured to assess the ability of individual PKC isoforms to modulate the development or transformation of B cells. Of note, expression of a plasmid-encoding dominant negative PKCα (PKCα-KR) in HPCs and placement in B cell generation system *in vitro* or *in vivo* resulted in the generation of a population of cells that displayed an enhanced proliferative capacity. Analysis of PKCα-KR-expressing cells *in vitro* revealed that these cells incorporated BrdU significantly more than the MIEV control, and unexpectedly upregulated cell cycle regulators, $p21^{waf-1}$ and $p27^{kip-1}$. Of surprise, PKCα-KR-expressing cells phenotypically resemble human B cell chronic lymphocytic leukaemia (CLL) cells. Expression of constitutively active PKCα, PKCα-CAT, or dominant negative PKCζ, PKCζ-KR in HPCs caused significant decrease in cell number.

CLL is characterised by the accumulation of long-lived phenotypically mature B cells with the distinctive phenotype: $CD19^{hi}$, $CD5^{+}$, $CD23^{+}$, IgM^{dim}, which are deficient in apoptosis and have undergone cell cycle arrest in the G_0/G_1 phase. Closer analysis of PKCα-KR-expressing cells uncovered that these cells undergo cell cycle arrest in the absence of growth factors and stroma and consistent with their ability to escape growth factor withdrawal-induced apoptosis, exhibited elevated levels of Bcl-2 and Mcl-1 expression. Upon stimulation with IL-7, PKCα-KR-expressing cells showed explosive proliferation,

suggesting that IL-7 is a proliferation factor for these cells. In accordance with this, IL-7R expression was upregulated in these cells, which may contribute to the increased sensitivity to IL-7. Mice injected with wildtype PKCα-KR-HPCs bore solid intraperitonial tumours at the injection site and the cells from both tumour and spleen showed CLL-like phenotype. Interestingly, splenocytes from these mice were cycling whereas the tumour cells were arrested at the G_0/G_1 stage, probably reflecting the two phases of this disease, a quiescent stage and an extensive proliferative stage, respectively. The expansion of the leukaemic cells was halted when they were cultured on OP9-DL1, OP9 cells with ectopic expression of Notch ligand, DL1, suggesting that Notch signalling mediates tumour suppression in CLL cells.

As PI3K and ERK-MAPK pathways have been implicated in mediating the survival of human CLL cells, cellular and molecular mechanisms that govern the initiation and maintenance of CLL were investigated. MIEV- and PKCα-KR-expressing cells were treated with pharmacological inhibitors, LY294002 and U0126, against PI3K- and ERK-MAPK- mediated pathways respectively, and the amount of apoptosis was analysed by Annexin V staining. MIEV-expressing cells increased apoptosis followingLY294002 treatment, in agreement with AKT phosphorylation in MIEV-expressing cells, whereas this inhibitor also induced apoptosis in PKCα-KR-expressing cells although AKT phosphorylation was not detected in these cells. Analysis of ERK phosphorylation in MIEV- and PKCα-KR-expressing cells revealed that while ERK1 and 2 remained just weakly phosphorylated in MIEV-expressing cells throughout the culture period, ERK1 was phosphorylated during the early stage of PKCα-KR-HPCs culture and both ERK1 and 2 were constitutively phosphorylated in longer cultured PKCα-KR-expressing cells. However, neither MIEV- nor PKCα-KR-expressing cells were affected upon treatment with U0126 compared with DMSO treated controls. In contrast, a cell line derived from PKCα-KR-expressing cells, M-1, underwent apoptosis in the presence of U0126, however, phosphorylation in ERK1 or 2 was not detected in this cell line. Collectively, these studies suggest that PI3K-

and ERK-MAPK signalling pathways are differentially-regulated to induce survival during the progression of CLL cells.

In an effort to identify the developmental stage at which B lineage cells are susceptible to transformation, RAG-1$^{-/-}$-derived HPCs were retrovirally infected with either vector control, MIEV, or PKCα-KR and then placed into B cell generation systems *in vitro* or *in vivo*. RAG-1$^{-/-}$ mice lack the ability to generate mature B lymphocytes because they are blocked at the late pro-B cell stage due to an inability to initiate recombination at the immunoglobulin heavy chain gene locus. Therefore, the onset of leukaemiagenesis in these HPCs suggests that CLL originates from an early B lineage cell or HPC population. Of interest, flow cytometric analysis of the cells from either the *in vitro* HPC-OP9 cocultures or the lymph node (LN) of the reconstituted RAG-1$^{-/-}$ mice *in vivo*, revealed that a similar population of CLL-like cells (CD23^{+}, CD5^{+}, CD19^{hi}) was generated from RAG-1$^{-/-}$ mouse-derived HPCs as observed from wildtype mouse-derived HPCs. Hence, these results suggest that PKCα-mediated development of CLL occurs at a very early stage of B cell development, and challenges current dogma indicating that CLL is commonly considered to arise from an outgrowth of a mature subset of B lymphocytes.

Overall, this thesis identifies a unique oncogenic trigger for the development of a CLL-like disease resulting from the subversion of PKCα signalling.

Declaration

This work represents original work carried out by the author and has not been submitted in any form to any other University.

Rinako Nakagawa

July 2006

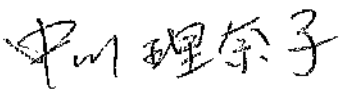

'Now here is my secret. It is very simple. It is only with one's heart that one can see clearly. What is important is invisible to the eye.'

Antoine de Saint-Exupéry

Acknowledgements

I would like to thank my supervisor, Dr. Alison M Michie. Her enthusiasm and precise advice for the project have been a great driving force for keeping me positive in undertaking research. In addition, her kindness and consideration in general life has supported me to survive in an "alien" country. I would also like to thank all the members of the Dr. Michie's, Professor Maggie Harnett's and Professor Tessa Holyoake's labs-past and present-for their friendship and practical expertise.

I would like to thank my parents, my sister and my friends both in Japan and Glasgow to encourage me for stepping forward and keep me in sanity.

Contents

List of Figures

List of Tables

Abbreviations

aa	amino acid
7-AAD	7-Amino-actinomycin D
AKAP	a kinase anchoring protein
ALL	acute lymphoblastic leukaemia
AML	acute myeloid leukaemia
AMV	avian myeloblastosis virus
APC	allophycocyanin
aPKC	atypical PKC
APRIL	a proliferation-inducing ligand
AP-1	activating protein-1
ATM	ataxia telangiectasia mutated
ATP	adenosine triphosphate
BAFF	B cell activating factor
BASH	B cell-restricted adaptor protein
BCMA	B cell maturation antigen
BCR	B cell receptor
BisI	bisindolylmaleimide I
BLNK	B cell linker protein
BM	bone marrow
β-ME	β-mercaptoethanol
BrdU	5-bromo-2'-deoxyuridine
BSA	bovine serum albumin
BSAP	B cell specific activator protein
Btk	Bruton's tyrosine kinase
CBF-1	c-promoter binding factor 1
CDK	cyclin dependent kinase
CD40L	CD40 ligand
CFSE	5-(and-6)-carboxyfluoresceindiacetate-succinimidyl ester
CLL	chronic lymphocytic leukaemia
CLP	common lymphoid progenitor

CML	chronic myeloid leukaemia
cμ	μH chain in the cytoplasm
CMP	common myeloid progenitor
CMV	cytomegalovirus promoter
cPKC	classical PKC
CSL	CBF-1 for humans, Su(H) for drosophila, Lag-for *Caenorhabditis elegans*
D	diversity
DAG	diacylglycerol
DC	dendritic cell
DN	double negative
DP	double positive
EBF	early B cell factor
ECL	enhanced chemiluminescence
EDTA	ethylenediaminetetraacetic acid
Eμ	heavy chain enhancer
ER	endoplasmic reticulum
ERK	extracellular signal-regulated kinase
ES	embryonic stem
FBS	foetal bovine serum
FCM	flow cytometry
FITC	fluorescein isothiocyanate
FISH	fluorescence in situ hybridization
FL	foetal liver
FSC	forward scatter
FT	foetal thymocytes
GC	germinal centre
GEF	guanine nucleotide exchange factor
GFP	green fluorescent protein
GDP	guanosine diphosphate
GTP	guanosine triphosphate
H	heavy

HA	hemagglutinin
HBSS	Hank's Balanced Salt Solution
Hes	Hairy enhancer of split
HPC	haematopoietic progenitor cell
HRP	horseradish peroxidase
HSC	haematopoietic stem cell
IAP	inhibitor of apoptosis protein
Ig	immunoglobulin
IKK	IκB kinase
IL-7R	IL-7 Receptor
i.p.	intra-peritoneally
IP_3	inositol-1,4,5-triphosphate
IRES	internal-ribosomal entry site
ITAM	immunoreceptor tyrosine-based activation motif
J	joining
JNK	c-Jun amino-terminal kinase
L	light
Lag-2	Lin-12 and Glp-1 phenotype 2
LDL	lithium dodecyl sulfate
LN	lymph nodes
LPS	lipopolysaccharide
MAPK	mitogen activated protein kinase
MAPKK	MAPK kinase
MAPKKK	MAPKK kinase
M-CSF	macrophase colony-stimulating factor
MFI	mean fluorescence intensity
MHC	major histocompatibility
MMLV	Moloney murine leukaemia virus
MOPS	3-(N-morpholino) propane sulfonic acid
NF-κB	nuclear factor kappa B
NK	natural killer
nPKC	novel PKC

NIC	cytoplasmic domain of Notch
NLC	nurse-like cell
OD	optical density
OP9-DL1	OP9 cells expressing the Notch Ligand Delta-like1PBS phosphate buffered saline
PDK1	phosphoinositide-dependent kinase-1
PE	Phycoerythrin
PH	pleckstrin homology
PI	Propidium iodide
PI3K	phophatidylinositol-3-kinase
PIP_2	phophatidylinositol-4,5-bisphosphate
PIP_3	phosphatidylinositol-3,4,5-triphosphate
PICKs	proteins that interact with C kinases
PKB	protein kinase B
PKC	protein kinase C
PLC	phospholipase C
PM	plasma membrane
PP2A	Protein phosphatase 2A
PS	phosphatidylserine
PTEN	phosphatase and tensin homolog
PVDF	polyvinyliden difluoride
RACKs	receptor for activated C kinases
RAG	recombination-activating gene
RBP-Jκ	recombining binding protein-J kappa
RT	room temperature
RT-PCR	reverse transcription-PCR
SA	streptavidin
s.c.	subcutaneous
sCD23	soluble CD23
SCF	stem cell factor
SCID	severe combined immuno deficiency
SDF-1	stromal cell-derived factor

SDS-PAGE	sodium dodecyl sulphate polyacylamide gel electrophoresis
SEM	standard error of the means
SH	Src homology
SHIP	SH2 domain-containing polyinositol phosphatase
SL	surrogate light
SP	single positive
Sos	son of sevenless
SSC	side scatter
Su(H)	suppressor of hairless
Syk	spleen tyrosine kinase
TACI	transmembrane activator and CAML Interactor
TAO	thousand-and-one amino acid
TBS	Tris buffered saline
TCRβ	T cell receptor β
TdT	terminal deoxynucleotidyl transferase
TEY	threonine-glutamate-tyrosine
Tg	transgenic
TPA	12-*o*-tetradecanoylphorbol-13-acetate
V	variable
XLA	X-linked agammaglobulinaemia
xid	X-linked immunodeficiency
ZAP-70	70 kDa zeta associated protein

Chapter 1:
Introduction

1.1 The humoral immune system

The innate and adaptive immune systems together provide a remarkably effective defence system. A specific immune response, such as the production of antibodies against a particular pathogen, is known as an adaptive immune response, which confers lifelong protective immunity to re-infection with the same pathogen in many cases. Innate immunity, on the other hand, provides a front line of host defence through effector mechanisms that engage the pathogen directly, act immediately, and are unaltered in their ability to resist a subsequent challenge with either the same or a different pathogen. Many infections are handled successfully by the innate immune system and cause no disease; others that cannot be resolved by innate immunity trigger an adaptive immune response and are then overcome successfully, followed by lasting immunological memory (Janeway et al, 2001).

Adaptive immunity is triggered when the numbers of a pathogen exceed the threshold dose of antigen required for an adaptive response and thereby an infection eludes the innate defence mechanisms. Several days are required for antigen-specific T cells and B cells to locate their specific foreign antigen, proliferate, and differentiate into armed effector cells. Adaptive immunity mainly consists of $CD8^+$ T cell-mediated immunity and B cell-mediated humoral immunity. The production of antibody usually requires the action of $CD4^+$ helper T cells that are specific for a peptide fragment of the antigen recognised by the B cell. The B cell then proliferates and differentiates, first at the T to B zone boundary in secondary lymphoid tissues and later in the germinal centre (GC), where somatic hypermutation diversifies the B-cell receptors expressed by a clone of B cells. $CD4^+$ helper T cells also direct both the production of antibody by B cells and the isotype that determines the effector function (Janeway et al, 2001).

The humoral immune response to infection involves the production of antibody by plasma cells derived from B lymphocytes, binding of this antibody to the pathogen, and subsequent elimination of the pathogen. Antibodies contribute

to immunity in three main ways, neutralisation, opsonisation and complement activation. Neutralisation is a process by which antibody binding to pathogen, such as viruses and intracellular bacteria, can prevent their binding to specific molecules on the cell surface, thus preventing entry into the host cells. Opsonisation is the process that results in antibodies coating the pathogen and being recognised as foreign by phagocytotic cells. The phagocytotic cells then bind to the antibody constant C region by Fc receptors, thus facilitating pathogen phagocytosis. Antibodies binding to the surface of a pathogen can also activate the complement system, which results in complement proteins being bound to the pathogen surface. This enhances opsonisation of the pathogen by phagocytes that bind to the pathogen-complement complex via complement receptors or even lyses certain microorganisms directly by forming pores in their membranes (Janeway et al, 2001).

1.2 B cell development

B cells consist of three different populations, B-1a, B-1b and B-2. The B-1a/B-1b/B-2 nomenclature is based predominantly on surface phenotypic criteria, expression of IgM and/or IgD and/or CD5: B-1a cells are IgM^{hi}, $IgD^{lo/-}$, $CD5^{+}$; B-1b cells are IgM^{hi}, $IgD^{lo/-}$, $CD5^{lo/-}$; B-2 cells are IgM^{lo}, IgD^{hi}, $CD5^{-}$ (Hayakawa and Hardy, 2000). In this thesis, B cell describes B-2 cells unless otherwise stated.

1.2.1 B-2 cell development

The development of B cells from committed progenitors into differentiated plasma cells is a multistep process, involving the ordered expression of various genes. Mouse B cell development can be divided into several stages based on the rearrangement status of the immunoglobulin (Ig) genes and the expression of specific cell markers. Currently, two nomenclatures are used to define the B cell developmental stages: the Hardy (Philadelphia) (Hardy et al, 1991, Hardy and Hayakawa, 2001) and the Rolink/Melchers (Basel) (Osmond et al, 1998) classification (Table 1.1). In this thesis, the Hardy nomenclature is used. The surface developmental markers are shown in Figure 1.1.

Fraction	A	B/C		C'	D	E	F	
Hardy (Philadelphia)	pre-pro-B	pro-B		Early pre-B	Late pre-B	immature-B	Mature-B	
Rolink (Basel)	pro-B	Pre-BI	Transitional pre-BI	Large-pre-BII	Small pre-BII	Immature-B	Transitional-B	Mature-B
BCR expression			cμ⁺	Pre-BCR⁺	Pre-BCR⁺	BCR⁺		
IgH locus	Germline	D-J rearranging	V-DJ rearranging	VDJ	VDJ			
IgL locus	Germline	Germline	Germline	Germline	V-J rearranging	VJ		

Table 1.1 Names for B cell stages and Ig rearrangement status

Modified from Annu. Rev. Immunol. (2001); 19: 595-621.

Figure 1.1 Diagram of B lineage development in mouse

B cell development from CLP to B cell committed stages is delineated. Concomitant expression of cell surface markers and B-lineage genes are shown. Relative expression levels are indicated by line thickness. Abbreviation definitions are included in the text. TdT, terminal deoxynucleotidyl transferase.

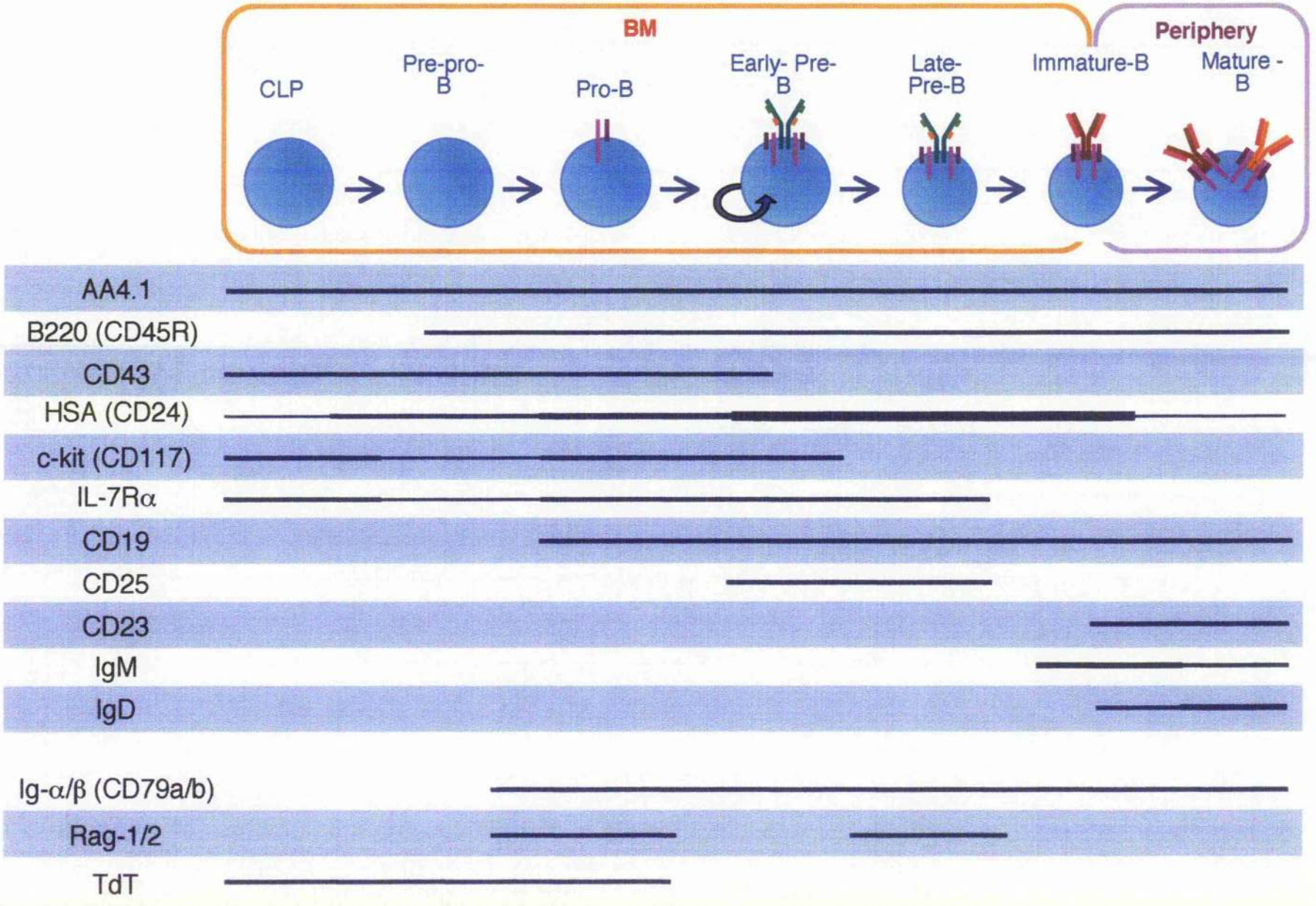
BM
Periphery
CLP
Pre-pro-B
Pro-B
Early- Pre-B
Late-Pre-B
Immature-B
Mature - B
AA4.1
B220 (CD45R)
CD43
HSA (CD24)
c-kit (CD117)
IL-7Rα
CD19
CD25
CD23
IgM
IgD
Ig-α/β (CD79a/b)
Rag-1/2
TdT

In the mouse, B cells are generated from pluripotent haematopoietic stem cells (HSCs) in the liver during foetal development and in the bone marrow (BM) after birth. A population of Lin^- IL-$7R^+$ Thy-1^- Sca-1^{lo} c-kit^{lo} cells was discovered as a common lymphoid progenitor (CLP) subset that is a lymphoid-restricted (T, B and NK) progenitor cell (Kondo et al, 1997). Following the CLP stage, the very early B lineage is recognised by expression of B220 (CD45R) and lack of CD19 (Li et al, 1996). At the next, pro-B cell stage, the cells start to rearrange D (diversity) to J (joining) gene segments on both alleles of the immunoglobulin (Ig) heavy (H) chain loci and express CD19 and the disulphide-linked Igα and Igβ (CD79a and CD79b) heterodimers on the surface as invariant signal-transducing subunits together with calnexin, a chaperone protein (Nagata et al, 1997). Subsequently, the cells begin rearranging V_H (variable) to D_HJ_H on individual alleles and express μH chain in the cytoplasm (cμ) (Benschop and Cambier, 1999). V(D)J recombination is initiated by recognising recombination signal sequences which flank V, D and J segments by recombination-activating gene (RAG) 1 and 2, expressing only in lymphocytes (Notarangelo et al, 1999). Progression to the early-pre-B cell stage is accompanied by surface expression of pre-B cell receptor (BCR), which is formed by μH chain and surrogate light (SL) chain; VpreB and λ5, associated with Igα and Igβ. The cells downregulate CD117 and CD43, and upregulate CD25 and CD24. Among cells expressing VDJ_H/DJ_H recombined alleles, when the VDJ_H-recombined allele is functional, the second IgH allele is no longer available for V_H to DJ_H rearrangements and thereby this μH chain from the first IgH allele is expressed on the cell surface as a pre-BCR, a process known as allelic exclusion (Melchers et al, 1999). In 2-4 % of cells carrying two productively V_HDJ_H-rearranged IgH chain loci, however, only one of these can pair with SL chain and therefore allelic exclusion is maintained at the level of pre-BCR expression (ten Boekel et al, 1998). Due to the induction of proliferation by surface expression of pre-BCR, the cells divide several times and differentiate into small late-pre-B cells (Rolink et al, 2000), which rearrange V_LJ_L (κ and λ) at the light (L) chain locus (Hardy and Hayakawa, 2001). When this is accomplished, the cells express the newly synthesised IgL chain together with μH chain as a BCR;

IgM, and progress to the immature-B cell stage. During progression from immature to mature B cells, there is a checkpoint to scrutinise their BCR. Encounter of immature B cells with antigen capable of cross-linking their BCR leads to one of three results; i) clonal deletion by high-affinity interactions; ii) anergy; iii) revision of their BCR to eliminate self-reactivity by editing. Unless the BCR is auto-reactive, the cells can leave the BM and migrate to peripheral lymphoid organs, where they differentiate into mature B cells expressing levels of IgD that exceed IgM (Havran et al, 1984), CD23 and CD21/35 (Hardy and Hayakawa, 2001).

In the peripheral organs, such as lymph nodes (LN) and spleen, mature but naïve B cells encounter an antigen, and most of them are activated in T cell dependent way. Antigen-activated B cells transform into larger B blasts, some differentiate short-living, IgM producing plasma cells for first-line defence and other B cells migrate to the primary B cell follicle and differentiate into GC B cells (MacLennan, 1994). GC B cells undergo somatic hypermutation, which is a process by which randomised mutations are introduced into the Ig gene region (Diaz and Casali, 2002). GC cells with unfavourable mutations do not bind to the antigen with high affinity, which results in apoptosis. The positively selected GC B cells activate T cells to express CD40 ligand (CD40L) and secrete IL-4 and IL-10, which in turn induces the expansion and class switching of GC B cells (Sagaert and De Wolf-Peeters, 2003). After accomplishing affinity maturation and isotype switching, GC B cells may differentiate into either post GC B cells, such as plasma cells producing antibodies or memory B cells. The interaction of CD27 and CD40L with T cells is an important interaction in directing GC B cells to become memory cells (Liu and Banchereau, 1997).

1.2.2 B-1 cell development

B-1 cells were originally described as a type of distinctive foetal B cell developed in the mouse, different from B-2 cells generated in adult BM. B-1 cells reside in the peritoneal cavity, pleural cavities and spleen. B-1 cells present in the peritoneal cavity express CD11b, however, this is not applicable

to B-1 cells present in spleen (Berland and Wortis, 2002). B-1 cells develop *de novo* and persist thereafter by self-renewal, while B-2 cells develop *de novo* and continue to enter the mature B-2 pool (Kantor and Herzenberg, 1993, Kantor et al, 1992). B-1 cells produce most of natural IgM, which is weakly autoreactive and reactive with many pathogen-associated carbohydrate antigens (Boes et al, 1998, Hayakawa et al, 1999, Hayakawa et al, 1984), and contribute significantly to IgA producing plasma cells in the lamina propria of the gut (de Waard et al, 1998, Kroese et al, 1993).

Regarding B-1 cell origin, there are two models available, the layered model and single-lineage model. The single-lineage model proposes that B-1 and B-2 cells derive from different, committed precursors and therefore represent two different lineages. The B-1 lineage is considered to be predominantly from foetal and the B-2 lineage from adult origin because only foetal liver (FL) could reconstitute mice with both the B-1 and B-2 cells, whereas adult BM could not generate B-1 cells (Kantor and Herzenberg, 1993). Alternatively the layered model is an induced-differentiation model, proposing that the B-1 lineage is a consequence of antigen-driven differentiation and selection (Berland and Wortis, 2002). The decision to differentiate into the B-1 cells rather than B-2 cells reflects different responses of mature B cells to stimulation with the different types of antigens, therefore, when the cells have encountered repetitive antigens during neonatal life, these cells with BCR that recognises these antigens differentiate into the B-1 lineage. On the contrary, cells that have encountered exogenous antigens during adult life become B-2 cells and their BCR recognises these antigens (Herzenberg and Tung, 2006). Based on this hypothesis, B-2 cells can be converted into B-1 cells when they are stimulated via BCR in certain conditions (Herzenberg, 2000). However, a recent study has shown that B-1 and B-2 progenitors can be physically separated from each other (Montecino-Rodriguez et al, 2006), as CD138 and major histocompatibility (MHC) class II molecule expression distinguishes the B-1a, B-1b and B-2 cell progenitors during early B cell development (Tung et al, 2006). Therefore,

functionally distinct B cells appear to be divided into separate developmental lineages rather than induced by differentiation.

1.3 Early B cell development and transcription factors

B cell development requires the coordinate expression of a series of transcription factors to regulate sets of genes in each differentiation stage (Fig. 1.2).

PU.1, a member of Ets transcription factor family, is crucial in the early stages of haematopoietic cell specification and essential for B cell development (Scott et al, 1997, Scott et al, 1994). Low concentrations of PU.1 induce B cell development, whereas high levels of PU.1 promote macrophage differentiation by suppressing the B cell fate (DeKoter and Singh, 2000). DeKoter *et al.*, showed that PU.1 directly activates *IL-7Rα* (DeKoter et al, 2002), thereby functioning as a regulator in early B cell development.

Differentiation of CLPs into pro-B cells critically depends on three transcription factors, E2A, early B cell factor (EBF) and Pax5 (Busslinger, 2004, Hagman and Lukin, 2005). *E2A* encodes the basic helix-loop-helix proteins E12 and E47 produced by alternative splicing (Busslinger, 2004). Both proteins are essential for pro-B cell development (Bain et al, 1997, Zhuang et al, 1998). E2A as well as EBF synergistically regulate the transcription of many B cell specific genes including *λ5* (Sigvardsson, 2000, Sigvardsson et al, 1997), *VpreB* (Gisler and Sigvardsson, 2002), *Igα* (mb-1) (Sigvardsson et al, 2002), *RAG-1* and *RAG-2* (Goebel et al, 2001, Hsu et al, 2003, Romanow et al, 2000). Both E2A- and EBF-null mice result in very early blockade in B cell development (Bain et al, 1994, Lin and Grosschedl, 1995).

Studies in $Pax5^{-/-}$ mice showed that B cell development is arrested at an early pro-B cell stage (Úrbanek et al, 1994) and pro-B cells from these mice can generate both myeloid and T lineage cells (Nutt et al, 1999, Rolink et al, 1999). These studies indicate that Pax5 (also known as B cell specific activator protein

Figure 1.2 Regulation of early B cell development

Multi-lineage precursor can adopt either myeloid or lymphoid cell fate depending on the level of PU.1 expression. CLPs develop into T cell lineage upon stimulation of Notch 1 signalling or else adopt a default B lineage. E2A and EBF facilitate B lineage commitment and Pax5 functions in pro-B cell to pre-B cell progression by suppressing alternative cell fates. Abbreviation definitions are included in the text. CMP, common myeloid progenitor.

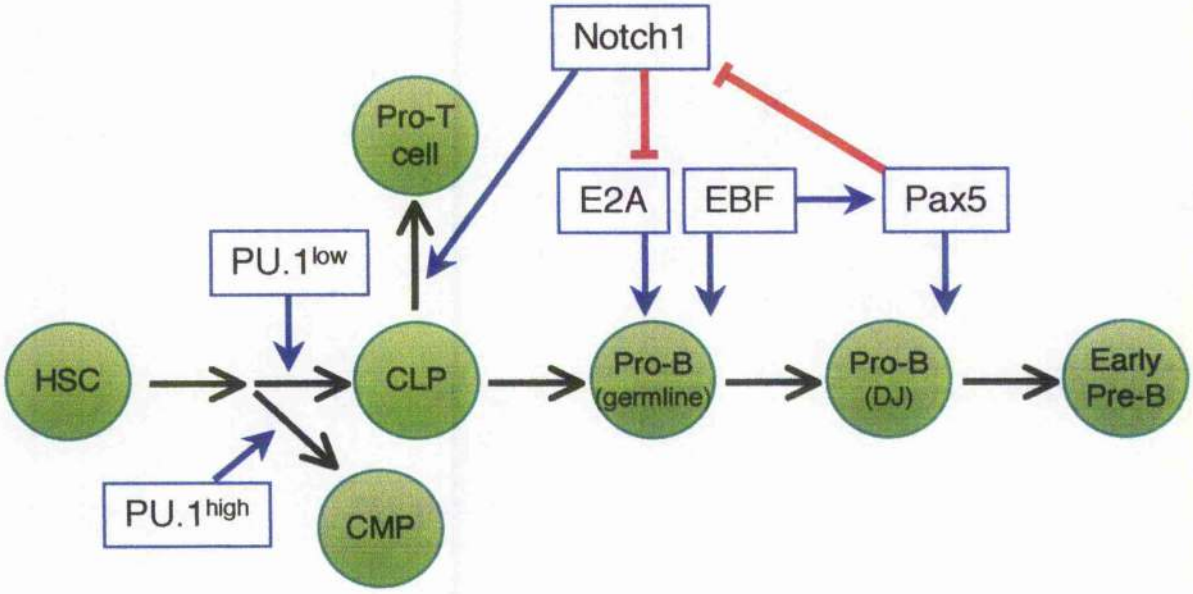
Notch1
Pro-T cell
E2A
EBF
Pax5
PU.1low
HSC
CLP
Pro-B (germline)
Pro-B (DJ)
Early Pre-B
PU.1high
CMP

(BSAP) (Adams et al, 1992)) is the key transcription factor in B cell commitment, as it suppresses alternative lineage cell fates early in development. Pax5 target genes encode essential components of the preBCR/BCR signalling pathway, including Igα (mb-1) (Nutt et al, 1999, Nutt et al, 1997), CD19 (Kozmik et al, 1992, Nutt et al, 1998) and the adaptor protein B cell linker protein (BLNK) (also called SLP-65 or B cell-restricted adaptor protein (BASH)) (Schebesta et al, 2002).

1.4 BCR signalling

Signals propagated through BCR are fundamental not only for the development, cellular selection, maturation and survival of B cells but are also imperative for antibody production (Gauld et al, 2002b). The BCR is a multiprotein structure containing membrane Ig, the disulfide-linked Igα and Igβ heterodimer, which is noncovalently associated with membrane Ig (Kurosaki, 1997). All BCR signal transduction is mediated through immunoreceptor tyrosine-based activation motifs (ITAMs) of this heterodimer (Papavasiliou et al, 1995, Teh and Neuberger, 1997). Both Igα and Igβ contain a single ITAM composed of two tyrosine residues (Kurosaki, 1997). BCR signalling is initiated upon ligand binding, which induces receptor aggregation and subsequent phosphorylation of the ITAM (Fig. 1.3). Phosphorylation of these tyrosine resides by the Src-family protein tyrosine kinases, such as Lyn, Fyn, Blk or Lck, residing in proximity of BCR, is essential for the recruitment (Dal Porto et al, 2004) and activation of spleen tyrosine kinase (Syk) that binds to phosphorylated ITAMs with its tandem Src homology (SH) 2 domains (Rowley et al, 1995). BLNK, a scaffold protein containing an SH2 domain and over five defined tyrosine phosphorylation sites (Chiu et al, 2002), is rapidly phosphorylated by Syk and serves as the primary docking site of the SH2 domain of Phospholipase C (PLC) γ2 (Fu et al, 1998, Ishiai et al, 1999). Phosphorylated BLNK brings PLCγ2 into the close proximity of the activated Syk in the membrane, thereby facilitating tyrosine phosphorylation of PLCγ2 by Syk (Ishiai et al, 1999). Membrane-localised Bruton's tyrosine kinase (Btk), a Tec family protein tyrosine kinase, which is recruited to plasma membrane (PM) by interaction between its

Figure 1.3 BCR signal transduction cascade

BCR signalling is initiated upon ligand-induced BCR aggregation. Signals are propagated by Src-family protein tyrosine kinase-mediated phosphorylation of ITAM on the Igα and Igβ, thereby recruiting and activating Syk, which leads to phosphorylate BLNK and in turn recruits PLCγ2. PLCγ2 is then phosphorylated by proximal Syk. PLCγ2 is further phosphorylated by Btk, fully activated and generate second messenger IP_3 and DAG, resulting in PKC activation. Grb/Sos also associates with phosphorylated BLNK and can activate Ras-MAPK family pathway. Abbreviation definitions are included in the text.

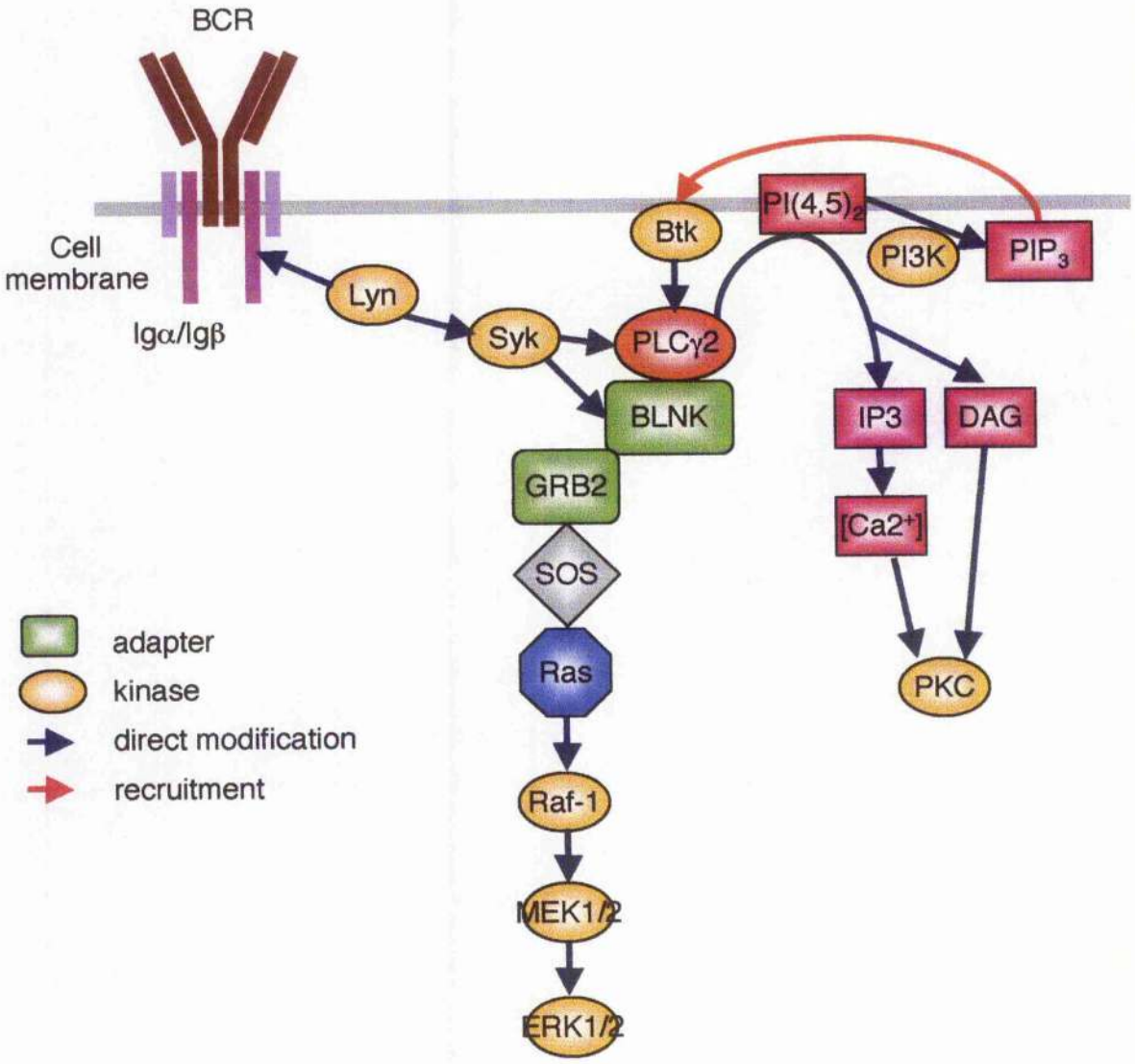
BCR
Cell membrane
Igα/Igβ
Lyn
Syk
Btk
PLCγ2
PI(4,5)2
PI3K
PIP3
BLNK
GRB2
SOS
Ras
Raf-1
MEK1/2
ERK1/2
IP3
DAG
[Ca2+]
PKC
adapter
kinase
direct modification
recruitment

pleckstrin homology (PH) domain and phosphatidylinositol-3,4,5-triphosphate; [PI(3,4,5)P_3], (PIP_3), further phosphorylates tyrosine residues on PLCγ2, resulting in full activation of PLCγ2 (Hashimoto et al, 1999, Takata and Kurosaki, 1996) (Fig. 1.3). PIP_3 is generated by phosphorylation of the ubiquitous PM lipid, phophatidylinositol-4,5-bisphosphate; [PI(4,5)P_2], (PIP_2) by phophatidylinositol-3-kinase (PI3K) (Marshall et al, 2000). Activated PLCγ2 hydolyses PIP_2 to produce soluble inositol-1,4,5-triphosphate (IP_3) and membrane-anchored diacylglycerol (DAG) (Marshall et al, 2000). IP_3 leads to elevation of cytosolic [Ca^{2+}] levels by activating release from the endoplasmic reticulum (ER) through IP_3-gated-Ca^{2+} channels, which results in activation of transcription factors, such as NFκ-B by protein kinase C (PKC) β [Saijo, 2002 #344], while DAG activates many PKC isoforms (See Section 1.5.2.1) (Guo et al, 2004). Phosphorylated BLNK also associates with Vav, a guanine nucleotide exchange factor of Rho-family, Grb2/Son of sevenless (SOS), while leads to the activation of p38 and c-Jun amino-terminal kinases (JNKs)-mitogen activated protein kinase (MAPK), and Ras, which results in the activation of extracellular signal-regulated kinase (ERK)-MAPK (Dal Porto et al, 2004) (Fig. 1.3).

1.5 Signalling molecules in B cell development

A number of molecules interact at or near the BCR and play essential roles in B cell function, however, signals from these molecules also influence stages of B cell development.

1.5.1 The roles of Btk and BLNK in development

Btk is involved in B cell development, and its dysfunction leads to severe immunodeficiencies. Naturally occurring mutations in the PH domain of Btk are responsible for X-linked agammaglobulinaemia (XLA) in humans, an inherited X chromosome-linked humoral immunodeficiency disease (Tsukada et al, 1993, Vetrie et al, 1993), which is characterised by an almost complete arrest of B cell differentiation at the pre-B cell stage (Conley et al, 2000) (Fig. 1.4). Afflicted males have an extremely low level of mature circulating B cells

Figure 1.4 The arrest of differentiation by gene disruption in mouse

The stages at which developmental arrest occurs in various knockout models are shown.

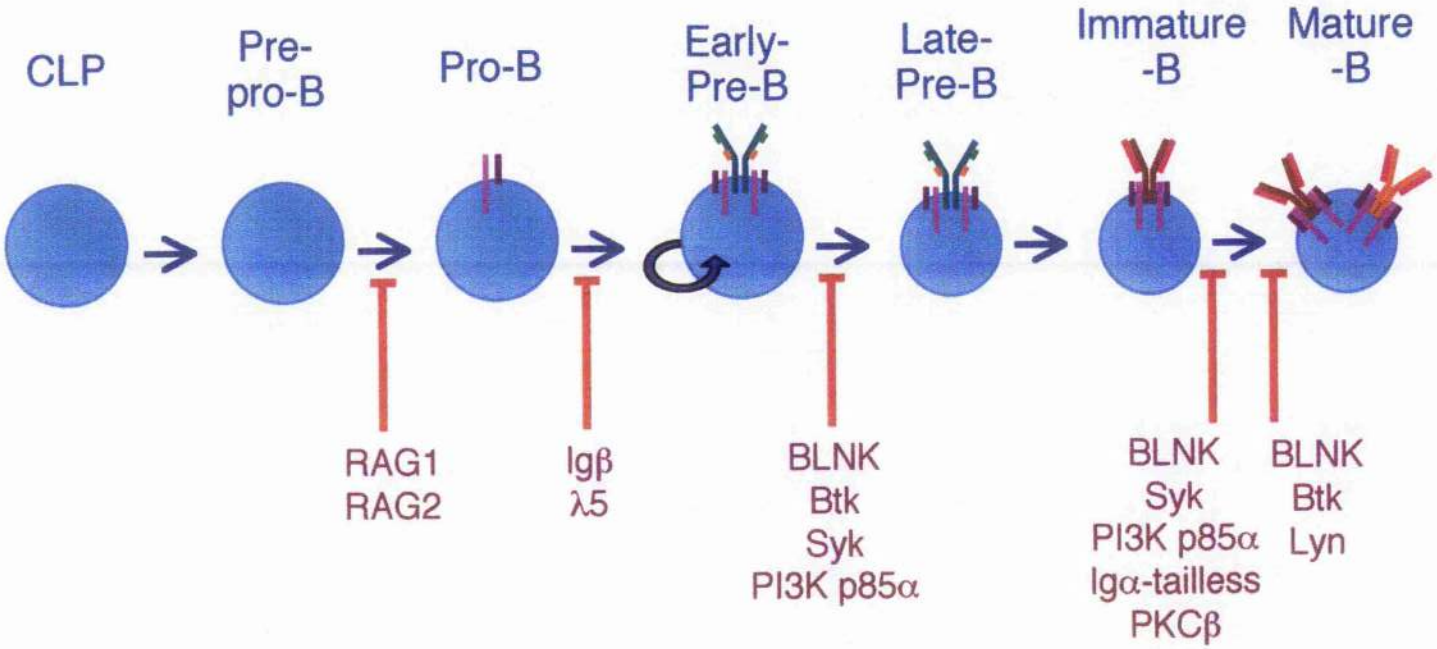
CLP
Pre-
pro-B
Pro-B
Early-
Pre-B
Late-
Pre-B
Immature
-B
Mature
-B
RAG1
RAG2
Igβ
λ5
BLNK
Btk
Syk
PI3K p85α
BLNK
Syk
PI3K p85α
Igα-tailless
PKCβ
BLNK
Btk
Lyn

and severe hypogammaglobulinaemia of all types of circulating Igs due to severe deficiency of peripheral mature B cells (Conley et al, 2000). A related deficiency in mice is called X-linked immunodeficiency (*xid*) and shares many features with human XLA although *xid* mice have a less dramatic decrease in the number of peripheral B cells (Rawlings et al, 1993, Thomas et al, 1993). The phenotype of $Btk^{-/-}$ mice is similar to *xid*, including reduced numbers of mature B cells, severe B-1 cell deficiency, serum IgM and IgG_3 deficiency (Kerner et al, 1995, Khan et al, 1995).

BLNK null mice have a striking block at pro-B cell to pre-B cell transition, but the block is leaky (Hayashi et al, 2000, Jumaa et al, 1999, Pappu et al, 1999, Xu et al, 2000), and thereby the deficiency is not as severe as that observed in humans which resembles XLA (Minegishi et al, 1999). BLNK is rapidly phosphorylated by Syk after BCR cross-linking, indicating that BLNK belongs to the same signal transduction pathway in B cell development, such as Syk and Btk. Indeed, the B cells present in $BLNK^{-/-}$ mice are phenotypically immature and a decrease in serum level of IgM and IgG_3 is observed, suggesting a blockade in development before pre-B cell stage, which is similar as observed in $Syk^{-/-}$ mice (Cheng et al, 1995, Turner et al, 1995), $PLC\gamma2^{-/-}$ mice (Wang et al, 2000) and $Btk^{-/-}$ mice (Kerner et al, 1995, Khan et al, 1995) (Fig. 1.4), although the phenotype of $BLNK^{-/-}$ mice is not as severe as that of $Btk^{-/-}$ mice. Of interest, an enlarged pre-B cell compartment is noted due to an enhanced proliferative capacity in a pre-BCR and IL-7 dependent way, indicating that BLNK limits pre-B cell expansion to promote differentiation, and acts as a tumour suppressor (Flemming et al, 2003).

1.5.2 PLCγ pathway

PLCγ2, the predominant isoform in B cells (Carpenter and Ji, 1999), contains a PH domain, two SH2 domain and an SH3 domain (Kurosaki et al, 2000). PLCγ2 is activated by Syk and Btk and cleaves PIP_2 to generate DAG and IP_3 as described in Section 1.4. IP_3 binds IP_3 receptors located in the ER, leading to Ca^{2+} release from internal stores (Takata et al, 1995). Cytosolic Ca^{2+}

elevation leads to the activation of downstream signalling molecules including calcineurin, calmodulin-activated serine/threonine phosphatase and classical protein kinase C (PKC) (α, β, γ) (Harnett et al, 2005, Kurosaki et al, 2000). A lipid second messenger, DAG, activates all phorbol ester-sensitive isoforms of PKC (α, β, γ, δ, ε, η, θ) (Guo et al, 2004).

1.5.2.1 PKCs

PKC is a family of serine/threonine protein kinases that are differentially regulated by Ca^{2+}, phospholipids, and DAG. This family of proteins are ubiquitously expressed and have differential cellular localization (Tan and Parker, 2003). The PKC family isotypes consist of up to ten members and are divided into three subfamilies depending on differences in their structures and cofactor requirement (Fig. 1.5). Classical PKC (cPKC) isoforms (α, βI/βII, γ) are regulated by both Ca^{2+} and DAG; novel PKC (nPKC) isoforms (δ, ε, η, θ) are regulated by DAG but not by Ca^{2+}, and; atypical PKC (aPKC) isoforms (ζ, ι/λ) do not require either Ca^{2+} or DAG (Tan and Parker, 2003). cPKCs are composed of a regulatory domains: C1 and C2 domains; and a catalytic domains; C3 and C4, while nPKCs and aPKCs lack C2 domain within their regulatory domain (Tan and Parker, 2003).

1.5.2.1.1 The roles of PKCβ in development and B cell survival

PKCβ-deficient mice exhibit a loss of peritoneal B-1 cells, slightly reduced numbers of splenic B-2 cells and decreased serum levels of IgM and IgG_3, indicating that PKCβ is important for B cell development (Leitges et al, 1996). However, the frequency and absolute number of pre-B and mature B cells in the BM of $PKC\beta^{-/-}$ mice is essentially identical to those of wildtype mice (Leitges et al, 1996), suggesting that PKCβ is not absolutely required for B cell maturation. Although it is less severe, the phenotype of these mice is similar to that seen in *xid* in $Btk^{-/-}$ mice (Kerner et al, 1995, Khan et al, 1995), which is consistent with that there is a functional link between Btk and PKCβ (Harnett et al, 2005). In supporting this view, Btk (Bajpai et al, 2000, Petro et al, 2000) and PKCβ (Saijo et al, 2002, Su et al, 2002) are both shown to be essential for nuclear factor

Figure 1.5 Structure of the PKC family

PKC are grouped into three subclasses based on regulatory domain composition, which dictates the cofactor-dependence. A regulatory domain comprises two basic modules, C1 and C2 domain. The C1 domain is a tandem repeat for cPKCs and nPKCs, but not for aPKCs. This domain mediates DAG/phorbol-ester-binding and contains autoinhibitory pseudosubstrate sequence in its N-terminus. C2 domain mediates Ca^{2+}-regulated phospholipid binding in cPKCs. All kinases have a conserved kinase domain in the C-terminus: C3 domain for ATP-binding and C4 domain for substrate-binding kinase core. Catalytic domain activity is highly regulated by phosphorylation and cofactor binding.

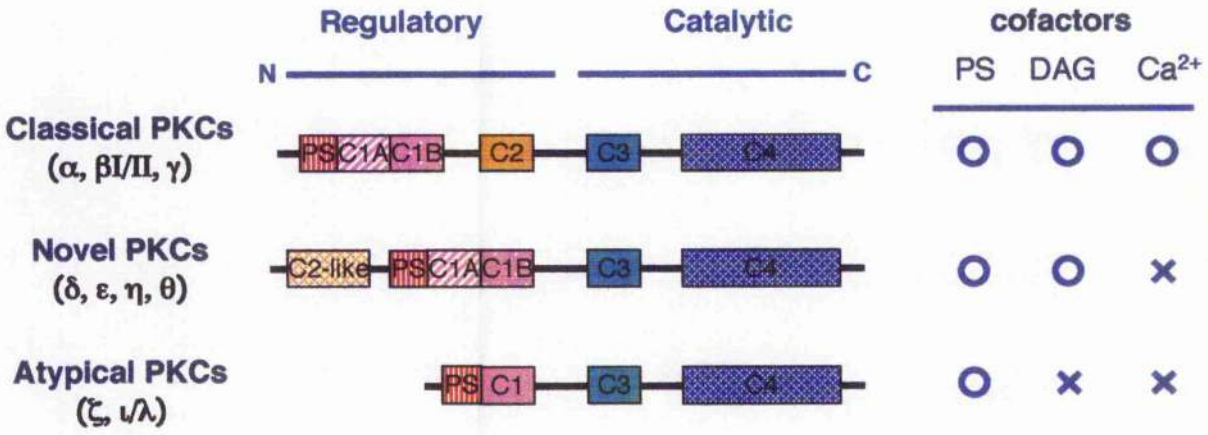

C1: DAG/phorbol ester binding
C2: Ca^{2+} binding
C3: ATP binding
C4: Kinase domain

kappa B (NF-κB) in response to BCR engagement. Successful activation of NF-κB and hence transcription of the NF-κB dependent genes requires activation of IκB kinase (IKK) and subsequent phosphorylation and degradation of inhibitory protein, IκB (Karin and Ben-Neriah, 2000). It is known that NF-κB controls the expression of Bcl-xL and Bcl-2 (Karin and Lin, 2002), and thus, mature B cells derived from PKCβ$^{-/-}$ mice fail to upregulate Bcl-xL in response to BCR stimulation (Saijo et al, 2002), similar as observed in Btk$^{-/-}$ B cells (Anderson et al, 1996). Taken together, these findings suggest that PKCβ regulates NF-κB pathway in response to BCR engagement and thereby acts to promote mature B cell survival.

1.5.2.1.2 The roles of PKCδ in B cell tolerance and survival

PKCδ$^{-/-}$ mouse studies showed that PKCδ functions as a negative regulator in activated B cells. PKCδ$^{-/-}$ mice exhibit expansion of the B cell population, infiltration of B cells in many organs, elevated antibody production, and are prone to autoimmunity (Mecklenbräuker et al, 2002, Miyamoto et al, 2002). Of note, PKCδ$^{-/-}$ mice develop autoreactive antibodies against DNA and nuclear proteins, thereby displaying an autoimmune phenotype (Mecklenbräuker et al, 2002, Miyamoto et al, 2002), which is associated with a specific loss of self antigen-induced B cell tolerance. In contrast with PKCβ$^{-/-}$ mice, PKCδ$^{-/-}$ mice do not develop an immunodeficiency resulting of decreased proliferation of B cells, suggesting that PKCδ plays a role in negatively regulating the proliferation and survival of B cells. Indeed, recent studies demonstrated that PKCδ regulates peripheral B cell survival by nuclear translocation following by phosphorylation of histone H2B at serine 14 (Mecklenbräuker et al, 2004), which has been shown to be associated with cell death (Ajiro, 2000, Cheung et al, 2003). Interestingly, this nuclear accumulation of PKCδ is prevented by B cell activating factor (BAFF), a member of TNF family, indicating that the existence of BAFF-dependent PKCδ-mediated nuclear signalling on B cell survival (Mecklenbräuker et al, 2004).

1.5.2.1.3 The roles of PKCζ in B cell survival and proliferation

PKCζ has been postulated to play roles in the survival and proliferation of B cells. The relative number and phenotype of splenic B cells in PKCζ$^{-/-}$ mice is similar to wildtype mice, however the loss of PKCζ leads to a temporal delay of B cell development in secondary lymphoid organs, increased spontaneous apoptosis and impaired BCR-dependent proliferation (Leitges et al, 2001, Martin et al, 2002). The impairment of BCR signalling correlates with decrease in ERK-MAPK activation, but not related to NF-κB or activating protein-1 (AP-1) complex (Martin et al, 2002). However, NF-κB-dependent genes, such as IκB and IL-6, seem to be regulated by PKCζ (Leitges et al, 2001), suggesting that PKCζ is important for promoting B cell survival.

1.5.2.1.4 The role of PKCε in B cell survival

PKCε have been postulated to play roles in survival and proliferation of B cells. PKCε is highly expressed in B lineage cells (Ting et al, 2002), promotes the activation of NF-κB via NF-κB-activating kinase, a kinase that phosphorylates and activates IKK (Tojima et al, 2000), also suggesting PKCε plays a role of B cell survival.

1.5.3 PI3K pathway

PI3Ks phosphorylate membrane phosphatidylinositol lipids on the 3-position of the inositol ring to generate the lipids, phosphatidylinositol-3-phosphate; [PI(3)P], phosphatidylinositol-3,4-bisphosphate; [$PI(3,4)P_2$], or PIP_3; described in Section 1.4 (Marshall et al, 2000) (Fig. 1.6).

The PI3Ks are divided into four classes; I_A, I_B, II and III on the basis of other structural characteristics and substrate specificity (Koyasu, 2003).
Each type of PI3K contains a C2 domain, which acts to bind phospholipids, and a catalytic domain (Koyasu, 2003). Class I and II PI3K, but not class III PI3K, contain a Ras binding domain at the N terminal. Class I_A family members are heterodimers comprising of a regulatory subunit and a catalytic subunit. Class I_A enzymes have the regulatory subunits: p85α, p55α, and p50α, products of

Figure 1.6 Phosphoinositide signalling pathways

The structure of the membrane phospholipid, phosphatidylinositol and the sites of phosphorylation/dephosphorylation are illustrated (top).

The metabolism of phosphoinositides is shown (bottom). Solid lines: Phosphorylation reactions, dotted lines: dephosphorylation reactions. SHIP, SH2 domain-containing polyinositol phosphatase; PTEN, phosphatase and tensin homolog.

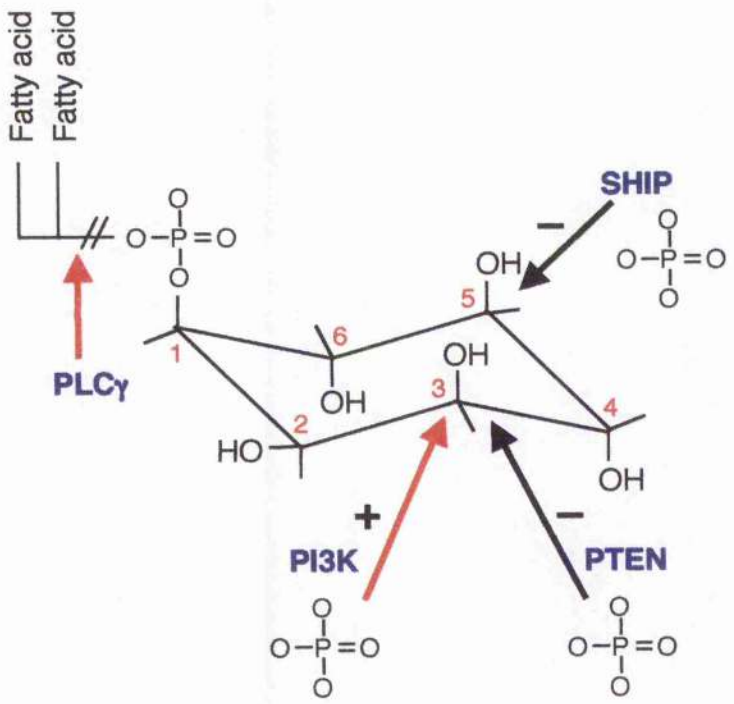
Fatty acid
Fatty acid
PLCγ
SHIP
PI3K
PTEN
OH
HO
1
2
3
4
5
6

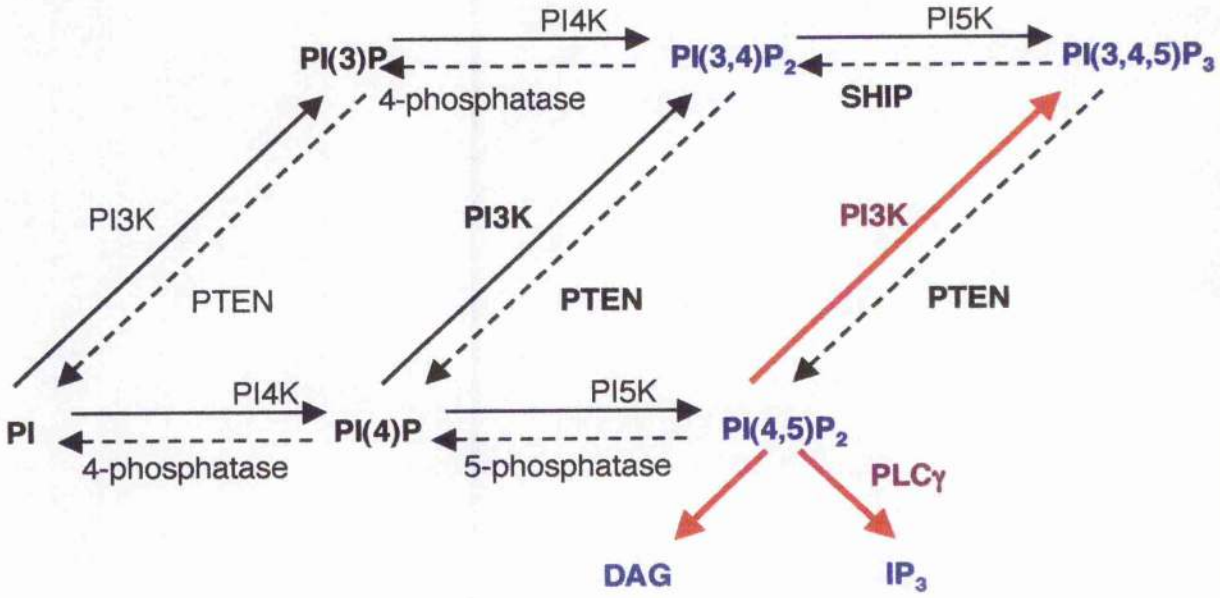
PI4K
PI5K
PI(3)P
PI(3,4)P2
PI(3,4,5)P3
4-phosphatase
SHIP
PI3K
PTEN
PI3K
PTEN
PI3K
PTEN
PI4K
PI5K
PI
PI(4)P
PI(4,5)P2
4-phosphatase
5-phosphatase
PLCγ
DAG
IP3

alternative splicing, p85β and p55γ, and catalytic subunits: p110α, p110β, p110δ (Koyasu, 2003). Class I_B has only one catalytic member p110γ that interacts with a p101 regulatory subunit. Class II has three members, PI3K-C2α, PI3K-C2β and PI3K-C2γ (Koyasu, 2003). Class III is a mammalian ortholog of a *Saccharomyces cerevisae* Vsp34p, and has not been well characterised (Koyasu, 2003).

1.5.3.1 The roles of PI3K in development and B cell survival

The phenotypes of two kinds of PI3K knockout mice: mice lacking p85α regulatory domain of class I_A and mice lacking p110δ catalytic domain of class I_A show a reduction in the number of mature B cells, decreased serum Ig level, reduced B cell proliferative responses, developmental block at pro-B cell stage and reduced numbers of B-1 cells (Clayton et al, 2002, Fruman et al, 1999, Jou et al, 2002, Okkenhaug et al, 2002, Suzuki et al, 1999), which is nearly identical to the phenotype of $Btk^{-/-}$ mice (Kerner et al, 1995, Khan et al, 1995) (Fig. 1.4). As suggested in other knockout model for BLNK, PKCβ, PLCγ2, PI3K also has a critical role during B cell development and proliferation.

1.5.3.2 The roles of AKT in development and B cell survival

AKT, also known as protein kinase B (PKB), is a serine/threonine kinase with a PH domain that allows the recruitment of AKT to the PM by binding to $PI(3,4)P_2$ and PIP_3 (Marshall et al, 2000) and consists of three isoforms, AKT1, AKT2 and AKT3 (Kandel and Hay, 1999). Activation of AKT requires phosphorylation on Thr 308 and Ser 473 (Gold et al, 1999). Thr 308 is phosphorylated by phosphoinositide-dependent kinase-1 (PDK1), a serine/threonine kinase, while the kinase that phosphorylates Ser 473 is unidentified. AKT is a major downstream target of the PI3K pathway and promotes various cell responses, such as cell division, survival, suppression of apoptosis and proliferation (Fruman, 2004). The pro-survival functions of AKT are exerted by phosphorylating bcl-2 family member, Bad (del Peso et al, 1997) and caspase-9 (Cardone et al, 1998), whose pro-apoptotic activities are inhibited by phosphorylation. AKT also helps to retain Bax in the cytoplasm, preventing it

from translocating to the mitochondria and thereby promoting survival (Tsuruta et al, 2002). NF-κB is known to have a pro-survival function in B cells (Ghosh et al, 1998) and it has been shown that AKT regulates NF-κB through phosphorylation and degradation of IκB (Ozes et al, 1999, Romashkova and Makarov, 1999), supporting the notion that AKT is an important mediator of B cell survival.

1.5.4 MAPK pathway

MAPKs, a group of serine/threonine kinases, are activated by a wide range of extracellular stimuli and are able to mediate a wide range of cellular functions. In general, ERK modules are activated in response to growth factors and phorbol esters, while p38 and JNK modules are more responsive to stress stimuli (Roux and Blenis, 2004). To date, five groups of MAPKs, have been identified in mammals: ERK1 and ERK2, JNK1, JNK 2, and JNK 3, p38 isoforms α, β, γ, and δ, ERK3 and ERK4, and ERK5 (Roux and Blenis, 2004). Although each MAPK has unique characteristics, each family is composed of a set of three evolutionarily conserved kinases: a MAPK, a MAPK kinase (MAPKK) and a MAPKK kinase (MAPKKK). MAPKKK activation leads to the phosphorylation and activation of a MAPKK, which in turn stimulates MAPK activity through dual phosphorylation on threonine and tyrosine residues (Roux and Blenis, 2004). The MAPK family is subdivided into three modules: ERK1/2 module, known as the classical mitogen cascade, consisting A-Raf, B-Raf and Raf-1 as MAPKKKs, MEK1 and MEK2 as MAPKKs, and ERK1 and ERK2 as MAPKs; p38 MAPK module, MEKK 1-4 and several other molecules as MAPKKKs, MEK3 and MEK6 as MAPKKs, four isoforms of p38 as MAPKs, and; JNK module, MEKK 1-4 and several other molecules as MAPKKKs, MEK4 and MEK7 as MAPKKs, three isoforms of JNK as MAPK (Roux and Blenis, 2004) (Fig. 1.7).

Figure 1.7 MAPK cascades

MAPK cascades are illustrated. Each family is composed of three levels of kinases: a MAPK; a MAPKK and; a MAPKKK. The MAPK family is subdivided into three modules: ERK1/2 module; p38 MAPK module and; JNK module. Abbreviation definitions are included in the text. TAO, thousand-and-one amino acid; ASK1, MAP3K5.

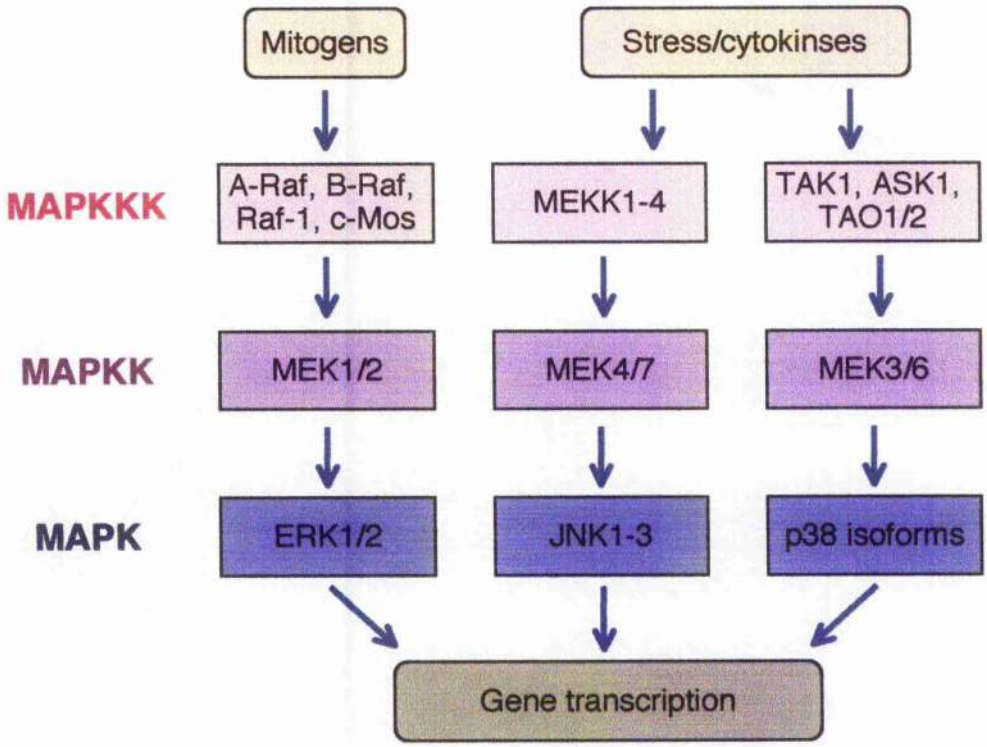
Mitogens
Stress/cytokinses
MAPKKK
A-Raf, B-Raf, Raf-1, c-Mos
MEKK1-4
TAK1, ASK1, TAO1/2
MAPKK
MEK1/2
MEK4/7
MEK3/6
MAPK
ERK1/2
JNK1-3
p38 isoforms
Gene transcription

1.5.5 The roles of $p21^{Ras}$ in B cell development and survival

RAS encodes a 21 kDa guanosine triphosphate (GTP)-binding protein, consisting of H-ras, K-ras and N-ras (Campbell et al, 1998). $p21^{Ras}$ is normally equilibrated between a GTP-bound active state and guanosine diphosphate (GDP)-bound inactive state. BCR ligation recruits adapter proteins, such as Grb-2, and subsequently Grb-2 binds Sos, a guanine nucleotide exchange factor, which stimulates $p21^{Ras}$ by exchanging GDP for GTP. GTP bound $p21^{Ras}$ activates the serine/threonine protein kinase, Raf-1, which in turn stimulates MEK1 and 2. Subsequently, the activated MEK phosphorylate ERK on the threonine-glutamate-tyrosine (TEY) motif of the activation loop (Campbell et al, 1998). Studies using a transgenic (Tg) mouse model expressing dominant negative form of $p21^{Ras}$, $p21^{H\text{-}RasN17}$, which is expressed under the regulation of the *Ig* intronic heavy chain enhancer (Eμ) and *lck* proximal promoter, revealed that $p21^{Ras}$-mediated Raf signals are essential for B cell differentiation since Tg mice expressing high levels of $p21^{H\text{-}RasN17}$ displayed a developmental block of pro-B and pre-B cells in the BM (Iritani et al, 1997). Moreover, expression of constitutively active $p21^{Ras}$, $p21^{Ha\text{-}RasV12}$, which is expressed under the regulation of Eμ and H chain V region promoter in $RAG^{-/-}$ mice, whose B cells are blocked at the pro-B cell stage due to an inability to initiate Ig gene rearrangement (Mombaerts et al, 1992, Shinkai et al, 1992), resulted in promotion of λ5 and germline κ locus transcripts and upregulation of surface markers associated with more mature stages of B cell development, such as CD23 and CD21(Shaw et al, 1999a, Shaw et al, 1999b). This suggests that $p21^{Ras}$ is involved in early B cell development and B cell survival.

1.5.6 ERK-MAPK

ERK1 and ERK2 are 43 and 41 kDa protein and are 83 % identical at the amino acid level (Chen et al, 2001). There are two activity levels in both ERKs, the phosphorylated form with high activity and unphosphorylated form with low activity (Chen et al, 2001). Activated ERK can phosphorylate membrane proteins, such as Syk and calnexin, and nuclear proteins, such as NF-AT, Elk-1, c-Fos and c-Jun, and cytoskeletal proteins, such as paxillin (Chen et al, 2001).

ERK-mediated biological responses seem to depend on the kinetics of ERK activation, subcellular compartmentalization of activated ERK; localised either cytosol or nucleus, its substrate targeting and interplays between cell types (Harding et al, 2005, Harnett et al, 2005, Kolch, 2005, Murphy et al, 2002). For example, the terminal differentiation of PC12 neuronal cells correlates with sustained activation of ERK and its translocation into the nucleus, while ERK mainly remain in the cytosol upon proliferative signals of the cells (Marshall, 1995). Moreover, ERK in mature B cells can stimulate proliferation, however, BCR-dependent activation of ERK is associated with apoptosis in immature B cells (Gauld et al, 2002a, Lee and Koretzky, 1998).

1.6 PKCα

1.6.1 Biological functions of PKCα

The cPKC, PKCα is expressed in wide range of tissues and predominantly in T cells among lymphocytes (Iwamoto et al, 1992, Nakashima, 2002). It has been reported that this enzyme promotes a wide variety of biological functions such as proliferation (Iwamoto et al, 1992, Mandil et al, 2001, Ways et al, 1995), cell cycle control (Besson and Yong, 2000, Detjen et al, 2000, Frey et al, 2000), apoptosis/cell survival (Jiffar et al, 2004, Leirdal and Sioud, 1999), and cell adhesion (Ng et al, 1999) (Fig. 1.8). However, PKCα$^{-/-}$ mice had no overt abnormalities in external characteristics, viability and fertility other than showing enhanced signalling capacity upon insulin stimulation (Leitges et al, 2002). In addition, PKCα has been shown to be involved in cellular differentiation. For instance, it provides signals for macrophage formation from macrophage colony-forming cells (Pierce et al, 1998), pro-platelet formation in megakaryocytes (Rojnuckarin and Kaushansky, 2001) and functions as a mediator of both differentiation and allelic exclusion in developing thymocytes (Michie et al, 2001).

Figure 1.8 Signal transduction pathways in biological functions of PKCα

Biological functions involving PKCα encompass cell survival/proliferation, cell cycle and cell motility. PP2A is a negative regulator of PKCα.

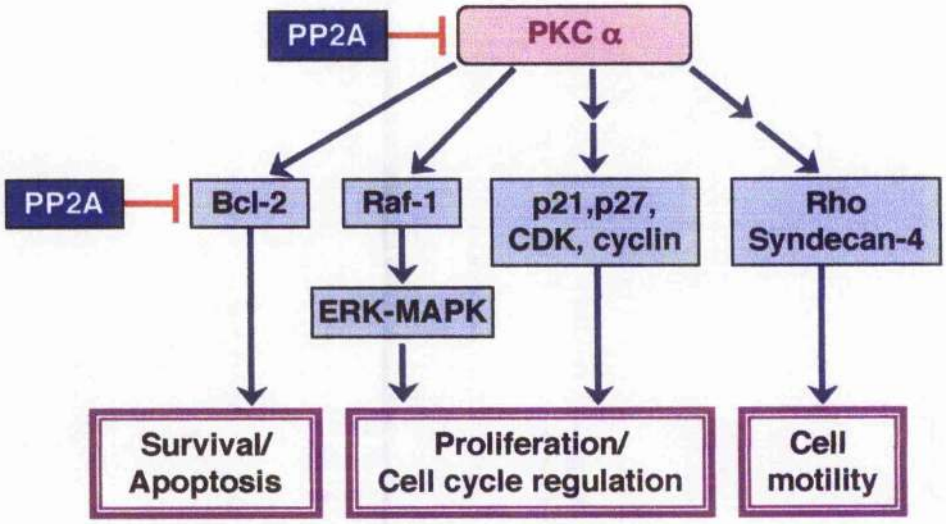
PP2A
PKC α
PP2A
Bcl-2
Raf-1
p21,p27,
CDK, cyclin
Rho
Syndecan-4
ERK-MAPK
Survival/
Apoptosis
Proliferation/
Cell cycle regulation
Cell
motility

1.6.2 The activation of PKCα

The generation of a mature, functional PKCα is regulated by three mechanisms: cofactor binding; phosphorylation, and; intracellular localisation. PKC cofactors comprise DAG, Ca^{2+} and phosphatidylserine (PS). DAG serves as an anchor to recruit PKC to the membrane and increases the affinity of c/nPKC for PS, anionic membrane phospholipid, upon its binding to C1 domain. Ca^{2+}

binding to C2 domain also increases the affinity of cPKC for acidic lipids. PS binding to C2 domain is accompanied by a conformational change, releasing its pseudo-substrate region from the substrate-binding site in the catalytic domain (Newton, 1995). PKC activity is also regulated by the phosphorylation of three conserved residues in its kinase domain, with the unphosphorylated precursor being inactive (Dutil and Newton, 2000). Previous work using mutagenesis analysis has identified three phosphorylation sites in PKCα catalytic domain noted as the activation-loop site (Thr-497), the autophosphorylation site (Thr-638), and the hydrophobic C-terminal site (Ser-657) (Parekh et al, 2000) (Fig. 1.9). Phosphorylation at both the Thr 638 in turn motif and the Thr 497 in the activation motif is essential for full activation of PKCα (Bornancin and Parker, 1996, Cazaubon et al, 1994). PDK1 initiates the maturation of cPKC by phosphorylating the residue at the activation loop, which promotes autophosphorylation at the turn motif and the hydrophobic motif (Dutil et al, 1998). Then, a conformational change occurs, which enables the pseudosubstrate to block the active site, and the enzyme is only activated and maintained at the membrane in response to second messengers (Dutil and Newton, 2000). Mutational analyses showed that phosphorylation at the turn motif and the hydrophobic motif contribute to phosphatase-resistance and thermal stability although the phosphorylation of hydrophobic motif is not necessary for full activation of PKCα (Bornancin and Parker, 1996, Bornancin and Parker, 1997). Of note, dephosphorylation of these residues is critical to control PKC signalling, which is mediated by protein phosphatase 2A (PP2A) (Hansra et al, 1996).

Figure 1.9 PKCα structure

PKCα (bovine illustrated here) protein comprises amino acid (aa) at the position of 2 to 672. The aa numbers shown indicate phosphorylation sites in PKCα, T497 in activation loop, T638 in turn motif and S657 in hydrophobic motif.

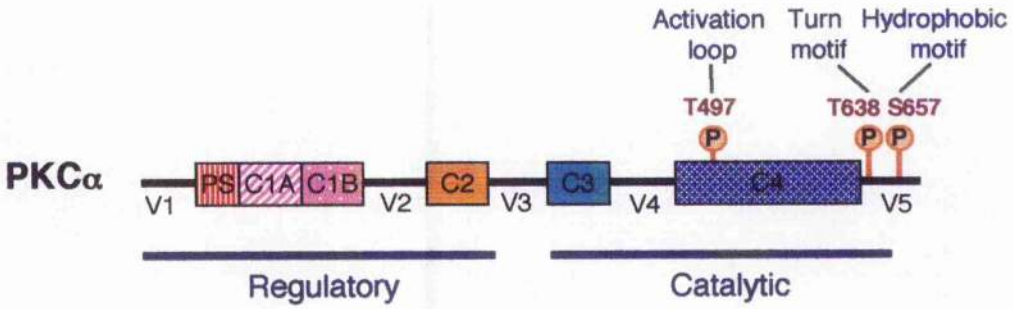
Activation loop
Turn motif
Hydrophobic motif
T497
T638
S657
P
P
P
PKCα
PS
C1A
C1B
C2
C3
C4
V1
V2
V3
V4
V5
Regulatory
Catalytic

A number of proteins regulate the intracellular localisation of PKC isoforms at different maturation stages. Scaffolding proteins, such as A Kinase Anchoring Protein (AKAP) family members (Klauck et al, 1996), Receptor for Activated C Kinases (RACKs) (Schechtman and Mochly-Rosen, 2001) and Proteins that Interact with C Kinases (PICKs) (Staudinger et al, 1995, Wang et al, 2003), contribute PKC to be in proximity of substrates, which is important for the precise targeting of PKCα.

1.6.3 PKCα and proliferation

PKCα has been related to proliferation. Indeed, overexpression of PKCα in human U87 glioma cells (Mandil et al, 2001) and PKCα-transfected human MCF-7 breast cancer cells (Ways et al, 1995) results in enhanced proliferation *in vitro*. Raf-1 is phosphorylated in a PKCα dependent manner (Kolch et al, 1993), which leads to activation of ERK-MAPK cascade, thereby causing cell proliferation (Buitrago et al, 2003, Schönwasser et al, 1998). Additionally, PKCα has been implicated in the activation of NF-κB in Jurkat cells upon TCR/CD28 stimulation (Trushin et al, 2003), suggesting that PKCα in involved in T cell proliferation. *In vivo*, thymocytes from 3 month old Tg mice overexpressing wildtype PKCα under the CD2 promoter displayed a higher proliferation rate and increased IL-2 production in response to anti-CD3 antibody stimulation in the absence of co-stimulation (Iwamoto et al, 1992). However, at 16 months, PKCα-overexpressing Tg mice showed increased PKCα expression but decreased proliferation during aging, thereby, the duration and timing of PKCα activation may have a profound effect on proliferation (Ohkusu et al, 1997).

1.6.4 The impact of PKCα on cell cycle regulation

Increasing evidence implicates PKCα is in the control of cell cycle progression and survival. Stable expression of constitutively active PKCα in NIH3T3 cells upregulates cyclin D1 and E and cycled faster compared to control cells (Soh and Weinstein, 2003). PKCα activation in glioma cells also promotes cell cycle progression concomitant with upregulated $p21^{waf-1}$ (Besson and Yong, 2000),

which implies that PKCα-mediated cell cycle progression is counter-intuitive, as it involves the upregulation of $p21^{waf-1}$, a cyclin dependent kinase (CDK) inhibitor.

However, several reports indicate that PKCα can function as an inhibitory factor in cell cycle regulation. In intestinal epithelial cells, PKCα activation leads to cell cycle withdrawal into G_0, which accompanies downregulation of cyclin D and upregulation of $p21^{waf-1}$ and $p27^{kip-1}$, CDK inhibitors (Frey et al, 2000). Similarly, PKCα activation results in growth arrest in the G_1 phase, by inducing $p21^{waf-1}$ expression (Detjen et al, 2000). Hence, PKCα may act as growth stimulator/inhibitor depending on the cell system.

1.6.5 The impact of PKCα on survival and apoptosis

The loss of PKCα activity generally correlates with the induction of apoptosis. In COS cells, dominant negative PKCα expression induced apoptosis (Whelan and Parker, 1998) and the inhibition of PKCα expression by ribozyme which can cleave specific mRNAs, triggered apoptosis with a reduction in Bcl-xL (Leirdal and Sioud, 1999). However, depending on cell types, PKCα appears to function as a pro-apoptotic factor (Okuda et al, 1999). Indeed, PKCα phosphorylates the anti-apoptotic protein, Bcl-2 (Ruvolo et al, 1998), the anti-apoptotic action of PKCα appears to be mediated via increasing phosphorylation/expression level of Bcl-2 (Blackburn et al, 1998, Jiffar et al, 2004) and/or Bcl-xL (Leirdal and Sioud, 1999). Cumulative evidence suggests that the activation and phosphorylation of PKCα (Boudreau et al, 2002, Hansra et al, 1996) and Bcl-2 (Ruvolo et al, 1998) are regulated by okadaic acid-sensitive PP2A. Moreover, overexpression of PKCα suppresses mitochondrial PP2A activity, thus maintaining constitutively phosphorylated Bcl-2 (Jiffar et al, 2004). In support of this finding, PKCα and Bcl-2 can colocalise at the mitochondrial membrane in myeloid leukaemia derived HL60 cells (Ruvolo et al, 1998). This colocalisation may involve PICK1, which targets PKCα for anchoring at mitochondria (Wang et al, 2003).

1.6.6 PKCα and cell adhesion

PKCα is involved in the regulation of cell morphology and cell motility. Cells overexpressing PKCα exhibited anchorage-independent growth and morphologic alterations (Ways et al, 1995, Zeng et al, 2002). Moreover, PKCα plays a pivotal role in focal adhesion formation and have been shown to be associated with adhesion molecules including β integrins (Ng et al, 1999), syndecan-4, transmembrane heparan sulphate proteoglycans (Lim et al, 2003), and fascin, an actin-bundling component (Anilkumar et al, 2003). PKCα is shown to interact with syndecan-4 directly (Lim et al, 2003) and PKCα activation is necessary for α5β1 integrin-mediated focal adhesion formation via syndecan-4 (Mostafavi-Pour et al, 2003). Recent studies showed that PKCα phosphorylates and activates p115 Rho guanine nucleotide exchange factors (GEFs) (Holinstat et al, 2003), and the integrin and syndecan-4-mediated focal adhesion is Rho-dependent (Saoncella et al, 1999), therefore, PKCα appears to contribute toward focal adhesion formation via two pathways, by the phosphorylation of syndecan-4 and Rho.

A naturally occurring mutant of PKCα, PKCα^{D294G}, has been identified in a subpopulation of human tumours, and the mutation is located in the V3 hinge region separating the catalytic domain and the regulatory domain (Fig. 1.9). The mutant has lost the ability of selective targeting to cell-cell contact (Vallentin et al, 2001) and exhibits aberrant translocation (Alvaro et al, 1997).

1.6.7 PKCα and cancer

It is perhaps unsurprising that dysregulation of PKCα has been implicated in a tumourigenicity. Indeed, PKCα-transfected breast cancer cells exhibit anchorage-independent growth, morphologic alterations, increased metastatic capacity in nude mice, and formation of mammary carcinomas in isografts model (Ways et al, 1995, Zeng et al, 2002). Treatment with antisense oligonucleotides for PKCα inhibited human lung carcinoma cells to proliferate and form colonies in soft agar, and it also reduced tumour formation in these cell inoculated nude mice (Wang et al, 1999). However, as described in

Section 1.6.4, PKCα appears to have opposing effects on the cell cycle regulation depending on types of cells. Of interest, Zhu *et al.*, propose that PKCα functions as anti-tumourigenic factor in the progression of endocrine tumours because PKCα^{D294G} mutant has been found in more invasive tumours. As this mutant has lost the membrane translocating ability, it fails to mediate several anti-tumourigenic signals (Zhu et al, 2005). Considering this, inhibition of PKCα activity may result in promoting tumourigenicity within cancer cells.

1.7 Chronic lymphocytic leukaemia (CLL)

1.7.1 Overall clinical symptoms

CLL is the most common leukaemia in the Western world, with increasing frequency in industrialised countries (Rozman and Montserrat, 1995), and mainly affects the aging population (Chiorazzi and Ferrarini, 2003). CLL is represented by a proliferation of B lymphocytes that express B cell markers, CD19 or CD20, CD5, CD23, and low levels of CD79b, CD22 and surface Igs that are monoclonal with regard to expression of either κ or λ. (Batata and Shen, 1992, Dighiero, 2005, Matutes et al, 1994, Moreau et al, 1997). These characteristics are generally adequate for a precise diagnosis of CLL (Dighiero, 2005). Whereas some patients with CLL have an indolent course and die after many years from unrelated causes, other patients progress very rapidly and succumb within a few years from this currently incurable leukaemia (Chiorazzi and Ferrarini, 2003).

While a central cytogenetic abnormality has not been identified (Chiorazzi and Ferrarini, 2003), recent progress in the identification of molecular and cellular markers, particularly, the mutational profile of Ig genes (Damle et al, 1999, Hamblin et al, 1999) and some cytogenetic abnormalities (Döhner et al, 2000), may allow a prediction of disease progression in patients with CLL.

1.7.2 Clinical staging and prognostic markers

One third of CLL patients never require treatment and have a long survival; in another third, an initial indolent phase is followed by disease progression; the remaining third exhibit an aggressive disease at the onset and need immediate treatment (Dighiero, 2005). The Rai (Rai et al, 1975) and Binet (Binet et al, 1981) staging systems have allowed CLL patients to be categorised into three prognostic groups. Both staging systems are based on the extent of lymphoadenopathy, splenomegaly, and hepatomegaly on physical exam and on the degree of anaemia and thrombocytopenia in peripheral cell counts (Hallek, 2005). However, neither the Rai nor the Binet staging system are sufficient to predict which individuals will develop progressive disease among patients diagnosed with good prognosis (Dighiero, 2005, Hallek, 2005). In order to develop risk-adapted therapeutic strategies, additional parameters have been identified allowing a more accurate prediction of clinical course of CLL at initial diagnosis. As shown in Table1.2 (Hallek, 2005), cytogenetic abnormalities, the IgV_H mutational profile and cytoplasmic ZAP-70 expression can help predict disease activity.

1.7.2.1 Chromosomal aberrations

Chromosomal abnormalities are detected in over 80 % of CLL cases. Although there is not a decisive cytogenetic alteration to characterise CLL, predominant cytogenetic abnormalities can be linked prognosis. Döhner *et al.*, analysed 325 cases by fluorescence in situ hybridization (FISH) and linked genomic aberrations to prognostic indicator (Döhner et al, 2000). The most frequent aberration was deletion 13q14 (55 %), followed by deletion 11q22-q23 (18 %), trisomy 12q13 (16 %), deletion 17p13 (7 %) and deletion 6q21 (7 %). They also demonstrated that the presence of 17p or 11q deletion is associated with reduced survival probability, whereas the 13q is associated with favourable prognosis (Döhner et al, 2000).

Throughout the molecular characterization of the critical region affected by deletions of 11q22-23, *ATM* (ataxia telangiectasia mutated), which is a kinase

Parameter
Aberrations in chromosomes 13 ($13q^-$),11($11q^-$) and 17 ($17p^-$)
Expression of cytoplasmic ZAP-70
Expression of surface CD38
Lymphocyte doubling time
Serum β2-microglobulin concentration
Serum levels of soluble CD23
Serum thymidine kinase activity
Mutational profiles of the IgV_H gene region

Table 1.2 Additional parameters for predicting the prognosis of CLL

Adapted from Hallec, M (2005); Hematology (Am Soc Hematol Educ Program): 285-291.

implicated in p53 activation (Pettitt, 2001), appears to be a tumour suppressor gene candidate (Stilgenbauer et al, 2002). However, *ATM* mutations were only found less than 25 % of CLL cases with 11q deletion (Schaffner et al, 1999) and its mutations occurred in normal cells in CLL patients as well as leukaemic cells from the same patients (Bullrich et al, 1999). Therefore, *ATM* may not be a causative gene for CLL. Yet, of interest, all *ATM* mutant CLL cells showed an absence of somatic V_H hypermutation indicating that loss of *ATM* function during B cell maturation may lead to tumourigenesis at pre-germinal stage by a defect in *p53* damage response and repair of chromosomal breaks (Stankovic et al, 2002). The discovery of the *p53* tumour suppressor gene located in 17p13 and assessment of its importance in the disease progression promoted investigations from a molecular genetic angle. Based on intensive reports, frequencies of *p53* mutation in CLL range from 7 % to 15 % (Stilgenbauer et al, 2002). As *p53* is important in the regulation of cell cycle arrest and cell death upon response to DNA damage (Levine et al, 1991), the presence of *p53* mutations correlates with poor prognosis and poor response to therapy (Cordone et al, 1998, Döhner et al, 1995, Lin et al, 2002).

1.7.2.2 IgV_H mutational profile

The widely confirmed method to determine to obtain patients' prognosis is based on the incidence of somatic mutations in the IgV_H gene. V_H gene sequences with differences of ≥2 % from the most similar germline gene were considered the 'mutated' subgroup, and <2 % differences were considered the 'unmutated' subgroup (Chiorazzi and Ferrarini, 2003). Damle *et al.*, and Hamblin *et al.*, associated IgV_H gene mutation status with clinical course and survival in CLL (Damle et al, 1999, Hamblin et al, 1999). The overall studies showed that patients bearing unmutated IgV_H genes result in more severe and poorer clinical outcome compared to those with mutated IgV_H genes (Hamblin et al, 2002, Kröber et al, 2002, Lin et al, 2002, Oscier et al, 2002).

The mutation status of the IgV_H region genes is correlated with the presence of genomic aberrations (Kröber et al, 2002, Oscier et al, 1997). Although overall

incidence of aberrations is not different between the mutated and unmutated subgroup, the unmutated subgroup are more likely to express the poor prognostic cytogenetic abnormalities, such as 17p deletion and 11q deletion, whereas those of the mutated subgroup were more likely to express the favourable aberrations, such as 13q deletion 13q14 deletion as a single abnormalities (Kröber et al, 2002).

1.7.2.3 CD38 expression

Damle *et al.*, subdivided CLL into two categories based on IgV_H gene mutation status and CD38 expression (Damle et al, 1999). In some cases, patients with unmutated IgV_H genes displayed higher percentage of $CD38^+$ CLL cells (≥ 30 %), whereas in other cases, patients with mutated IgV_H genes exhibited lower percentage of $CD38^+$ cells (Damle et al, 1999). This suggests that an inverse correlation exists between disease aggressiveness and higher percentages of $CD38^-$ CLL cells, however, other studies failed to find a strong correlation (Damle et al, 1999, Hamblin et al, 2002, Kröber et al, 2002, Thunberg et al, 2001), which makes CD38 inadequate for surrogate marker for the IgV_H gene mutational status.

1.7.2.4 Cytosolic ZAP-70 expression

ZAP-70, 70 kDa zeta associated protein, is a cytoplasmic tyrosine kinase essential for T cell receptor signal transduction. ZAP-70 was thought to be a key element in T and natural killer (NK) cells and be absent in normal B cells. However, recently it has shown that ZAP-70 is expressed in normal human splenic and tonsillar B cells (Nolz et al, 2005), and a subset of normal BM-derived B cells (Crespo et al, 2006). Murine studies show that ZAP-70 is expressed in most of the developmental stages, such as pro-B cell, pre-B cell and immature B cell stage (Meade et al, 2004, Schweighoffer et al, 2003) and the kinase is important for allelic exclusion at the IgH locus (Schweighoffer et al, 2003). This protein tyrosine kinase has emerged as a potential prognostic marker in CLL following gene expression profiling which compared unmutated CLL and mutated CLL cells (Rosenwald et al, 2001). In some studies, high

levels of ZAP-70 protein are detectable in the majority of cases of unmutated subgroup (Crespo et al, 2003, Wiestner et al, 2003), although there is more variation between clinical treatments in the group of mutated CLL patients with ZAP-70 expression (Crespo et al, 2003, Orchard et al, 2005, Rassenti et al, 2004, Wiestner et al, 2003). Other groups tested the correlation between ZAP-70 and mutational status, but there was discordance between ZAP-70 and IgV_H gene mutation status depending on the presence or absence of additional genetic high-risk features (Kröber et al, 2006, Orchard et al, 2004). ZAP-70 is not a complete surrogate for IgV_H gene, however, as it can be an independent prognostic marker in CLL to add supplemental information to that of mutational status.

In vitro studies demonstrated that the level of Syk phosphorylation (Chen et al, 2002) and $[Ca^{2+}]$ flux upon IgM cross-linking is greater in ZAP-70 positive CLL cells, suggesting that ZAP-70 is involved in the signal transduction initiated by BCR in CLL cells. This implies that ZAP-70 allows more effective IgM signalling in CLL cells and thereby contributes to the more aggressive course observed in ZAP-70 positive CLL cells, mostly consisting of unmutated subgroups.

1.7.3 Immunophenotype

Surface membrane phenotypic studies suggest that all CLL cells resemble memory cells which are antigen-experienced and activated (Damle et al, 2002, Klein et al, 2001, Rosenwald et al, 2001). Apart from low density of surface Ig, the markers on CLL cells are different from those on normal B cells and other B cell malignancies (Hamblin and Oscier, 1997), in that they overexpress CD23, CD5, CD25 and CD71, and underexpress CD22, FcγRIIb, CD79b (Chiorazzi and Ferrarini, 2003, Damle et al, 2002).

CD5 and CD23 are present on virtually all CLL cells, but absent from most B cell lymphomas, which make them CLL specific markers (Hamblin and Oscier, 1997). CD23, low affinity Fcε receptor, is cleaved into soluble fragments

(sCD23) displaying pleiotropic biological activities (Schwarzmeier et al, 2005). The CD23 protein and gene expression are abnormally regulated in CLL cells (Fournier et al, 1992). The serum level of sCD23 is elevated in some CLL patients and parallels to aggressiveness of the disease (Reinisch et al, 1994, Sarfati et al, 1996). A recent finding indicates that an anomalous overexpression of Notch2 in CLL cells leads to the upregulation of CD23 (Hubmann et al, 2002). Of interest, expression of a constitutively active form of Notch2 in developing B cells promotes development of B-1 cells while it results in a block of B-2 B cells at the pre-B cell stage (Witt et al, 2003). Although the regulatory mechanisms controlling Notch2 signalling in CLL cells are unknown, overexpression of CD23 may be a consequence of Notch2 signalling.

1.7.4 BCR molecule

Although 50-70 % of CLL cells have undergone somatic mutations of V_H genes (Dighiero, 2005), CLL cells use predominantly V_H1, V_H3 and V_H4 family genes in a distribution that is different from that reported for normal peripheral $CD5^+$ B cells (Fais et al, 1998). The most frequently used genes within these families are V_H1-69, V_H3-07, V_H 3-23, V_H 3-21 and V_H4-34 (Chiorazzi et al, 2005). Of interest, the V_H3-21 gene is associated with aggressive disease, even when it is expressed in a mutated form (Tobin et al, 2003, Tobin et al, 2002).

It is established that signals delivered through the BCR can have different consequences depending on the stage of maturation of the cells, and thus BCR ligation results in apoptosis for immature B cells, whereas BCR engagement leads to proliferation for mature B cells (Carey et al, 2000). Previously, Zupo *et al.*, reported that anti-IgM treatment of $CD38^-$ CLL cells causes apoptosis (Zupo et al, 1996), whereas surface IgD appeared not involved in apoptosis (Zupo et al, 2000). However, the results of IgM ligation varied from survival to apoptosis depending on the investigators (Bernal et al, 2001, Nédellec et al, 2005). Altogether, fine balance between the signals delivered through the BCR may dictate survival of CLL cells.

1.7.5 Possible mechanisms involved in evasion of apoptosis

Recent studies reported that *in vitro* apoptosis of CLL cells is prevented by exposure to IL-4 (Dancescu et al, 1992, Panayiotidis et al, 1993, Zupo et al, 2000) and/or stimulation via surface CD40 (Bernal et al, 2001, Fluckiger et al, 1992, Granziero et al, 2001). This inhibition of apoptosis may occur at particular site in lymphoid organs, such as the psuedofollicules, where CLL cells interact with T cells, resulting in substantial inhibition of the apoptosis and proliferation of the leukaemic cells (Ghia et al, 2002, Granziero et al, 2001). CD5 appears to contribute to survival of CLL cells because CD5 stimulation increased viability of CLL cells by upregulating Mcl-1, which is PKC-dependent manner (Perez-Chacon et al, 2006).

The microenvironment of CLL cells such as the presence of circulating nurse-like cells (NLCs) (Burger et al, 2000, Tsukada et al, 2002), BM stromal cells (Deaglio et al, 2005, Lagneaux et al, 1998) and follicular dendritic cells (DCs) (Pedersen et al, 2002) appear to be critical cellular components to confer prolonged viability to CLL cells. NLCs, derived CLL patient blood, and BM stromal cells can prevent apoptosis of CLL cells *in vitro*, mediated by the upregulation of anti-apoptotic factors, including Bcl-2, Mcl-1, and/or survivin (Granziero et al, 2001, Hanada et al, 1993, Kitada et al, 1998, Pedersen et al, 2002, Schena et al, 1992).

BAFF is a key regulator of B cell homeostasis (Moore et al, 1999) and was recently found aberrantly expressed in CLL cells (Novak et al, 2002). A proliferation-inducing ligand (APRIL), another TNF-related ligand, is a stimulator of tumour cell growth (Hahne et al, 1998), and is also expressed in CLL cells (Kern et al, 2004, Novak et al, 2002). An autocrine pathway via BAFF and APRIL seems to play a crucial role for apoptosis resistance and enhanced CLL cell survival. Indeed, NLCs secrete BAFF, APRIL (Nishio et al, 2005) and stromal cell-derived factor (SDF-1/CXCL12) (Burger et al, 2000), a TNF family CXC chemokine. Additionally, CLL cells express BAFF and APRIL receptors, such as BAFF-R (receptor only for BAFF), B cell maturation antigen (BCMA)

and transmembrane activator and CAML interactor (TACI) (receptors for both BAFF and APRIL), (He et al, 2004, Schneider, 2005) and CXCR4 (SDF-1 receptor) (Burger et al, 1999). Soluble forms of BAFF and APRIL prevented spontaneous/drug-induced apoptosis (Kern et al, 2004, Novak et al, 2002) and SDF-1 stimulated B cell growth (Nagasawa et al, 1994), suggesting that both autocrine and paracrine secretion of these factors rescue CLL cells from apoptosis.

Despite the rarity of Bcl-2 gene translocations in CLL, upregulation of Bcl-2 mRNA and protein expression are quite common. Indeed, 95 % of cases expressed Bcl-2 at higher levels than normal lymphocytes (Hanada et al, 1993). Relative expression of Bcl-2 and pro-apoptotic protein, Bax may also contribute to apoptosis resistance (Kitada et al, 1998, McConkey et al, 1996, Ringshausen et al, 2002). Some factors, such as cytokine effects, environmental stimuli or both, appear to contribute to the up-regulation of Bcl-2 protein.

Taken together, these studies underline the fact that CLL is a heterogeneous disease.

1.8 General aims and objectives

PKC regulates key biological functions including proliferation, differentiation and cell survival in various types of cells. Specific PKC isoforms, such as PKCβ, δ and ζ, have been shown to play important role in B cell development and signal transduction. The aim of this project is to elucidate the role of PKC isoforms, especially PKCα, in B cell development and transformation.

Chapter 2:
Materials and Methods

2.1 Animals and Plasmids

ICR mice were purchased from Harlan UK Ltd. and maintained at the University of Glasgow Central Research Facilities. ICR mice, which have an outbred Swiss background, aged between 6-10 weeks were used to isolate primary splenic cells and BM cells. RAG-1$^{-/-}$ mice (Mombaerts et al, 1992), which have a C57Bl/6 background and lack both T and B cells due to inability of V(D)J recombination, were bred and maintained in-house. Timed-pregnant mice were generated, and liver and thymus were extracted from foetuses at day 14 of gestation. All animals were maintained in accordance with local and home office regulations.

The dominant negative PKC isoforms (PKC-KR) were generated by introducing a point mutation at the lysine in the adenosine triphosphate (ATP) binding domain: PKCα, PKCα-KR ($K^{368}R$); PKCδ, PKCδ-KR ($K^{376}R$); and PKCζ, PKCζ-KR, ($K^{281}M$); and introduced into the backbone plasmid pHACE (Fig. 2.1 top) (Soh et al, 1999) derived from pcDNA3 (Invitrogen Life Technologies). The constitutively active PKC isoforms (PKC-CAT) were generated by deletion of the regulatory domain: PKCα-CAT, PKCδ-CAT and PKCζ-CAT, and introduced into the backbone plasmid pHANE (Fig. 2.1 bottom) derived from pcDNA3 (Soh et al, 1999). The original wildtype PKCα construct is expressed in the pHACE backbone and the original wildtype PKCα fused with GFP (PKCα-GFP) is expressed in the pGFP3 backbone (Fig. 2.2 top) (pEGFP-N1: Takara Bio Europe/Clontech). All the original PKC constructs were a kind gift from Dr. Jae-Won Soh (Soh et al, 1999). Retroviral constructs were generated by subcloning the gene of interest (mutated PKC isoforms (see below) and wildtype PKCα) into the retroviral backbone (MIEV) (Fig. 2.2 bottom) at the site of Bgl II and Not I, which is 5' of the internal-ribosomal entry site (IRES), allowing the bicistronic expression of the gene of interest and green fluorescent protein (GFP) (Fig. 2.3 and 2.4). The hemagglutinin (HA)-tag engineered onto the C-terminal (pHACE) or N-terminal of each PKC construct (pHANE) allowed confirmation of expression at the protein level utilizing an anti-HA antibody (Roche Diagnostics).

2.2 Antibodies and inhibitors

Fluorescein isothiocyanate (FITC)-, phycoerythrin (PE)-, allophycocyanin (APC)- and biotin-conjugated, and purified anti-mouse antibodies for flow cytometry (FCM) were purchased from BDBiosciences unless otherwise stated. Primary antibodies and horseradish peroxidase (HRP)- conjugated antibodies for Western blots were obtained from Cell Signalling Technologies unless otherwise stated. The list of antibodies used is supplied in the Table 2.1.

All the inhibitors were purchased from Calbiochem, Merck Biosciences. LY294002, [2-(4-Morpholinyl)-8-phenyl-4H-1-benzopyran-4-one], is a selective PI3K inhibitor (IC_{50}=1.4 μM) and acts on the ATP-binding site of the enzyme. Wortmannin, a fungal metabolite, is an irreversible, covalent inhibitor of PI3K (IC_{50}=5 nM). U0126, [1,4-Diamino-2,3-dicyano-1,4-*bis*(2-aminophenylthio)butadiene], is a specific inhibitor of MEK1 (IC_{50}=72 nM) and MEK2 (IC_{50}=58 nM). PD98059, [2'-amino-3'-methoxyflavone], inhibits MEK1 (IC_{50}=4 μM) more potently than MEK2 (IC_{50}=50 μM). SB 203580, [4-(4-Fluorophenyl)-2-(4-methylsulfinylphenyl)-5-(4-pyridyl)-1H-imidazole], is an inhibitor of p38 MAP kinase (IC_{50}=34 nM *in vitro*, 600 nM in cells). Rottlerin is a nPKC inhibitor that selectively inhibits PKCδ (IC_{50}=3-6 μM) and PKCθ. Rottlerin also inhibits PKCα, PKCβ and PKCγ, but significantly reduced potency (IC_{50}=80-100 μM). Chelerylthrine, naturally-occurring alkaloid, is an inhibitor of PKC (IC_{50}=660 nM) and acts on the catalytic domain of PKC.

2.3 Primers and PCR conditions

Primers were ordered from MWG Biotech AG at the scale of 0.2 μM or 0.05 μM for GC rich primers. Gene specific primers and conditions used for PCR are supplied in Table 2.2. Gene specific primer pairs were designed using the OLIGO program (Molecular Biology Insight Inc.), ensuring that no hairpin formation could occur within primers and no binding occurred between primer pairs. All the primers are designed for mouse genes.

2.4 Tissue culture

All cell culture reagents were purchased from Invitrogen Life Technologies unless otherwise stated. All procedures carried out in a under laminarspace flow hood to maintain sterile conditions.

2.4.1 Cell lines

2.4.1.1 GP+E.86 retroviral packaging lines

GP+E.86 (*gag-pol* and *env*) retroviral packaging line was used for retroviral gene transfer. These cells were generated by co-transfection of the plasmid containing the *gag* and *pol* genes derived from Moloney murine leukaemia virus (MMLV) and the plasmid containing the *env* gene derived from the helper virus into NIH-3T3 cells (Markowitz et al, 1988, Grady et al, 2004). These cells were cultured in complete media (High Glucose-DME media containing 10 % foetal bovine serum (FBS) (Cambrex), 100 U/ml penicillin, 100 μg/ml streptomycin, 2 mM glutamine, 1 mM sodium pyruvate, 10 mM HEPES, 50 μM β-mercaptoethanol (β-ME) and 10 μg/ml gentamicin) at 37°C in a humidified incubator containing 5 % (v/v) CO_2 in air.

2.4.1.2 PT-67 retroviral packaging lines

The PT-67 cell Line was obtained from Takara Bio Europe/Clontech. The cell line is an NIH-3T3-based packaging line expressing the 10A1 viral envelope. Virus packaged from PT-67 cells can enter cells via two different surface molecules, the amphotropic retrovirus receptor and the GALV receptor (Miller and Chen, 1996). These cells were maintained in complete media at 37°C in a humidified incubator containing 5% (v/v) CO_2 in air.

2.4.1.3 OP9 cells

Simple coculture of embryonic stem cells with the established stromal cell lines, such as ST2 (Nisitani et al, 1994), PA6 (Kodama et al, 1984) and RP0.10 (Gutierrez-Ramos and Palacios, 1992), without exogenous growth factors exclusively give rise to macrophages (Nakano et al, 1994). Therefore, Nakano *et al.* established a stromal cell line, OP9, from new born calvaria of B6C3F2-

op/op mice (Nakano et al, 1994) which lack functional M-CSF (macrophase colony-stimulating factor) due to a mutation generating stop codon in the coding sequence of the M-CSF gene (Yoshida et al, 1990). The coculture of embryonic stem (ES) cells with OP9 cells supports the development of erythroid, myeloid, and B cell lineages (Nakano et al, 1994), but ES cells could give rise to B cells more dominantly when IL-7 and β-ME were added to the culture (Nakano, 1995). Under this condition, OP9 cells were fully supportive of B cell development from ES cells and therefore, they were utilised to generate B cells *in vitro*. OP9 cells were cultured in complete media at 37°C in a humidified incubator containing 5 % (v/v) CO_2 in air.

2.4.1.4 OP9-DL1 cells

OP9 cells expressing the Notch ligand Delta-like1 (OP9-DL1) were established by retroviral transduction of the Notch ligand, DL1. This cell line loses its ability to support B lymphopoiesis, but gains the capacity to induce T cell differentiation (Schmitt and Zúñiga-Pflücker, 2002). The cells were cultured in OP9-DL1 media (α-MEM media containing 20 % FBS, 100 U/ml penicillin, 100 μg/ml streptomycin) at 37°C in a humidified incubator containing 5 % (v/v) CO_2 in air.

2.4.2 Primary cell preparation

2.4.2.1 Foetal Liver cells

Haematopoietic progenitor cell (HPC)-enriched-foetal liver (FL) cells were extracted from ICR or RAG-$1^{-/-}$ foetuses at day 14 of gestation and prepared by carrying out a CD24 (heat-stable Ag) antibody/complement-mediated cell lysis (Carlyle and Zúñiga-Pflücker, 1998). Briefly, FL single cell suspensions were prepared by crushing FL and filtered in 70μm nylon mesh (BioDesign) followed by a wash in complete medium (450 g, 6 min, 4°C). Then, the cells were incubated at 37°C for 30 min in medium with anti-CD24 antibody (final concentration; 100 $\mu g/10^7$ cells) and 1/10 dilution of 1 mL Low-Tox rabbit complement (Cedar Lane). After complement-mediated lysis, viable $CD24^{lo/-}$-HPCs were recovered by discontinuous density gradient centrifugation over

Lympholyte-Mammal (Cedar Lane) at 600 g for 15 min at room temperature (RT) (Fig. 2.5). Viable cells were removed from interphase of Lympholyte and medium, and washed in complete medium by centrifugation (450 g, 6 min, 4°C) once before the subsequent use. A representative FCM plots of a pre-antibody/complement mediated cell lysis and post-antibody/complement mediated cell lysis is shown in Figure 2.5.

2.4.2.2 Foetal thymocytes

Foetal thymocytes (FT) were extracted from ICR foetuses at day 14 of gestation. A single cell suspension was prepared by crushing the thymuses through a 70μm nylon mesh, in phosphate buffered saline (PBS). The cells were washed in complete medium by centrifugation (450 g, 6 min, 4°C) once before subsequent culture.

2.4.2.3 BM cells

Femurs were taken from 6-10 week old ICR mice and BM cells were flushed out of the femurs using a 18 gauge needle. Then, CD24 antibody/complement-mediated cell lysis was carried out and subsequently viable cells were recovered by discontinuous density gradient centrifugation as described in Section 2.4.2.1.

2.4.2.4 Splenocytes

Splenocytes were extracted from a spleen of 6-10 week old ICR mice. A single cell suspension was prepared by crushing a spleen in PBS and passing through a 70μm nylon mesh in PBS. The resultant suspension was centrifuged (300 g, 6 min, 4°C), and the pellet was resuspended in PBS. Red and dead cells were removed by discontinuous density gradient centrifugation and viable cells were collected described in Section 2.4.2.1.

2.4.3 Purification of $CD19^+$ Splenocytes

All procedures were performed at 4°C. A single cell suspension was resuspended in 5 ml ice-cold MACS buffer (PBS, 2 mM

Ethylenediaminetetraacetic acid (EDTA)) and counted by Trypan blue exclusion, and pelleted by centrifugation (300 g, 6 min). The cells were then resuspended in ice-cold MACS buffer (5×10^7 cells/ml) and incubated for 10 min with biotinylated anti-CD19 antibody ($1\mu g/10^7$ cells). These cells were washed in MACS buffer to remove primary antibody by centrifugation (300 g, 6 min) and resuspended in ice-cold MACS buffer ($90\mu l/1 \times 10^7$ cells) and incubated for 15 min with MACS Streptavidin (SA) micro beads ($10\ \mu l/1 \times 10^7$ cells) (Miltenyi Biotech). Labelled cells were washed in MACS buffer to remove unbound beads by centrifugation (300 g, 6 min), and resuspended in 3 ml ice-cold MACS buffer and applied to a LS-type positive selection magnetic column (Miltenyi Biotec) attached to the separator in a strong magnetic field. The column was washed with 3 ml ice-cold MACS buffer three times. The column was removed from the separator and flushed out in 5 ml ice-cold MACS buffer by applying the plunger, and purified cells ($CD19^+$) were collected in the eluent. The cells were centrifuged (450 g, 6 min), resuspended in complete media at 37°C in a humidified incubator. Typical FCM plots before $CD19^+$ purification and after are shown in Figure 2.6. The population of $CD19^+$ cells is nearly 1.8 times (from 55 % to 98 %) more concentrated in the post MACS sample.

2.4.4 Generation of retroviral packaging lines

A retrovirus vector is a powerful tool to introduce a nonviral gene into mitotic cells *in vitro* and *in vivo*. An integration of the retroviral insert into the genome requires active cell division (Miller et al, 1990). Of importance, retrovirus-mediated gene transfer leads to stable proviral integration in the target chromosomal DNA and its application is broad-ranging because many cells, including most primary cells, express viral receptors on the surface (Cepko and Pear, 2003). The retroviral vectors utilised in these studies have had all of the genes encoding virion structural proteins (*gag*, *pol*, *env*) removed to create space for inserted genes, and disable the retrovirus from replicating by itself. However, these vectors retain the efficiency of infection, therefore they are used in laboratory experiments (Cepko and Pear, 2003). To produce infectious viral

particles from a replication-incompetent retrovirus vector, retrovirus-packaging cells are utilised. These cells express gag, pol and env, thus supplying all of the viral proteins by *trans* that are necessary for encapsidation of vector RNA into virions and for subsequent infection, reverse transcription, and integration of the vector into the genomic DNA of infected cells (Cepko and Pear, 2003). In order to obtain packaging lines that produce higher viral titer, generally two packaging cell lines with different tropism, such as ecotropic and amphotropic, are employed. This is because the overexpression of *env* in a packaging cell line leads to binding and blocking of the cognate receptor, such that packaging cells can not be infected with a virus of the same tropism. One packaging cell line is transiently transfected with a vector DNA for transient production of virus and the produced virus is used to obtain stable virus producing lines. The virus from the stable packaging line is exploited for the further infection.

Retroviral constructs were engineered by subcloning the gene of interest into the retroviral vector (MIEV) as described in section 2.1 (Michie et al, 2001). The day before transfection, 5×10^4 PT-67 retroviral packaging cells were plated out into a 6 well-plate per well in complete medium. The retroviral vectors were transfected into the PT-67 cells using Effectene as per manufacturers instructions (Qiagen), utilising 0.4 μg DNA. The medium was replaced after 24 h and the transfected cells were cultured in complete medium until usage as a viral source. After 24 h, the supernatant from the transfected PT-67 was collected and filter-sterilised using a 0.45μm filter membrane (Millipore UK Ltd.) attached to a 10 mL syringe (BDBiosciences) to ensure that there was no carry over of PT-67 cells. 1×10^5 GP+E.86 retroviral packaging cells, which were plated 1 day before in complete medium, were spin-infected with supernatants from transfected PT-67 supplemented with 5 μg/ml polybrene (Sigma-Aldrich) by centrifugation at 600 g for 45 min at RT and then placed in culture for 48 h.

Retrovirally-transduced GP+E.86 packaging cells were trypsinised and then resuspended in sterile sorting buffer (Hank's Balanced Salt Solution (HBSS),

without phenol red, plus 1 % Bovine Serum Albumin (BSA)), and sorted on the basis of GFP expression using a FACSAria cell sorter (BDBiosciences) and FACSDiva software (BDBiosciences). After 2-3 weeks, the GP+E.86 packaging cells were resorted to a purity of >98 % GFP^+, thus establishing stable retroviral packaging cell lines. The established cell lines were maintained in complete media at 37°C in a humidified incubator containing 5 % (v/v) CO_2 in air.

2.4.5 Retroviral infection of HPCs

The retroviral GP+E.86 cell lines were seeded at 1×10^5 cells per 10 cm^2 dish and incubated with 10 μg/ml mitomycin C (Sigma-Aldrich) for 2-3 h at 37°C, 1 day before retroviral infection of primary cells, washing cells in complete medium 5 times post mitomycin C treatment. Single cell suspensions of viable HPCs isolated from either FL, FT or BM were cocultured with the mitomycin C-treated retroviral packaging line in FL-OP9 medium (complete medium supplemented with 3 % FBS), and 5 μg/ml polybrene, and IL-6, IL-7 and stem cell factor (SCF) (10 ng/ml of each) for 24-48 h prior to being placed either in an *in vitro* B cell generation system as described in Section 2.4.7 or adoptively transferred into RAG-$1^{-/-}$ mice as described in Section 2.4.8.

2.4.6 Retrovirus infection of $CD19^+$ splenocytes

The retroviral packaging lines were seeded and mitomycin C treated as described in Section 2.4.5. 1×10^6 $CD19^+$ splenocytes were prepared as described in Section 2.4.3 and placed on the packaging line with 50 μg/ml *E. Coli* derived lipopolysaccharide (LPS) (Sigma-Aldrich) for 48 h in complete media with IL-7 (10 ng/ml) in order to enhance retrovirus incorporation into the unproliferative mature $CD19^+$ B cells (McMahon et al, 1995). After the infection, the cells were washed in complete medium once and further cultured in an *in vitro* B cell generation system as described in Section 2.4.7.

2.4.7 B cell generation system *in vitro*

HPCs were cocultured on 60 % confluent layer of OP9 cells in the FL-OP9 medium together with 10 ng/ml IL-6, IL-7 and SCF until day 5 of coculture. Thereafter, FL-OP9 media was supplemented with IL-7 alone (10 ng/ml). OP9 layers were replenished every 4-5 days and HPCs were cocultured until FCM analysis at the indicated time points (Fig. 2.7).

2.4.8 *In vivo* adoptive transfer

Retrovirally infected/non-infected HPC's from ICR/RAG-1$^{-/-}$ mice (from Section 2.4.2.1) were centrifuged over Lympholyte-Mammal to ensure that dead cells and non-lymphoid cells were removed. The resultant cells were washed in PBS and resuspended in PBS at the concentration of 1×10^7 cells/ml. 1×10^5, 3×10^5, 1×10^6 cells were injected intra-peritoneally (i.p.) into neonatal RAG-1$^{-/-}$ mice as indicated in figure legends. The mice were sacrificed by cervical dislocation 2-6 wk post-injection and the BM, spleen, LN and tumours if present, were harvested. A single cell suspension was obtained by crushing organs in PBS and by passing through a 70μm nylon mesh in PBS (Fig. 2.8).

2.4.9 Purification of GFP$^+$ cells from ICR-PKCα-KR-FL injected mice

GFP$^+$ spleen/LN cells from PKCαKR-injected mice were obtained as described in Section 2.4.8, and purified by magnetic bead IgD negative-selection as described below.

All procedures were performed at 4°C. A single cell suspension was resuspended in 5 ml ice-cold MACS buffer counted by Trypan blue exclusion, and pelleted by centrifugation (300 g, 6 min). The cells were then resuspended in ice-cold MACS buffer (5×10^7 cells/ml) and incubated for 10 min with biotinylated anti-IgD antibody (1μl/10^7 cells). These cells were washed in MACS buffer to remove primary antibody by centrifugation (300 g, 6 min) and resuspended in ice-cold MACS buffer (90μl/1×10^7 cells) and incubated for 15 min with MACS SA micro beads (1 μg/1×10^7 cells). Labelled cells were washed in MACS buffer to remove unbound beads by

centrifugation (300 g, 6 min), resuspended in 10 ml ice-cold MACS buffer and applied to a CS-type negative selection magnetic column (Miltenyi Biotec) in a separator with strong magnetic field. Purified cells (IgD^-) were eluted from the column upon removing the column from the magnet by washing with 50 ml ice-cold MACS buffer. Next, IgD^- cells were positively selected as described in Section 2.4.3, except using anti-CD23 antibody. In brief, the cells were incubated for 10 min with biotinylated anti-CD23 antibody (1μg/10^7 cells), centrifuged in MACS buffer to remove primary antibody, resuspended in ice-cold MACS buffer (90μl/1 × 10^7 cells) and incubated for 15 min with MACS SA micro beads (1 μl/10^7 cells). The purified cells (IgD^-, $CD23^+$) were collected in the eluent using LS-type positive selection magnetic column. The cells were washed in medium and used for further experiments.

2.4.10 Generation of M-1 cells

Retrovirally PKCα-KR infected HPCs were cocultured with OP9 up to day 21 in the presence of IL-7 as described in Section 2.4.7. Next, the cultured PKCα-KR infected HPCs were transferred to a new tissue culture dish and cultured in the FL/OP9 medium in the presence of IL-7 and in the absence of OP9 for further 7 days. Every 2-3 days, medium was replenished. At day 30, cells were washed in medium by centrifugation (450 g, 6 min, 4°C), transferred to a new tissue culture and cultured for further 28 days without IL-7. Cells were prepared and stained with anti-CD5 antibody (diluted 1/200) in 500 μl sorting buffer for 20 min on ice and washed twice in sorting buffer prior to sorting. GFP^- $CD5^{lo}$ cells were sorted using a FACSAria and analysed with FACSDiva software; sorted cells were 99 % pure, as determined by post-sort analysis. The $CD5^{lo}$ cells that are able to survive without OP9 or IL-7 were selected and used for further experiments as the M-1 cell.

2.5 Flow Cytometry

2.5.1 Surface marker analysis

Cells were removed by gentle pipetting, washed in FACS buffer (HBSS supplemented with 1 % BSA and 0.05 % sodium azide) and then incubated with

anti-CD16/CD32 antibody (diluted 1/200) to block Fc receptors, and non-specific binding. After cells were washed in FACS buffer once by centrifugation (300 g, 1 min, RT), the appropriate antibodies (diluted 1/300) were added, as indicated in the text, and incubated for 30 min at 4°C. When biotin-conjugated antibodies were used, the cells were incubated with SA-APC (diluted 1/300) for 20 min at 4°C. The cells were then washed twice in FACS buffer, resuspended in FACS buffer, and filtered through a 70μm nylon mesh just before FCM analysis. Propidium iodide (PI) at final concentration of 25 μg/ml was added prior to analysis to discriminate dead cells. FCM was performed using a FACSCalibur flow cytometer (BDBiosiences). CellQuest software (BDBiosciences) was used to acquire the cells and FlowJo software (Tree Star) was employed to analyse the data. All data shown were live and size gated based on forward scatter (FSC) and side scatter (SSC) and lack of PI uptake.

2.5.2 Intracellular marker analysis

Cells were washed once in FACS buffer and fixed using the Cytofix/Cytoperm (BDBiosciences) solution by incubating for 20 min at 4°C, and were then washed in BDPerm/Washsolution (BDBiosciences) twice. Then, the cells were stained with fluorochrome-conjugated antibody (diluted 1/300), washed twice in the wash solution and analysed with a FACSCalibur flow cytometer. If a secondary antibody required, such as anti-rat IgG-PE antibody (diluted 1/200), cells were subsequently incubated with it for 20 min at 4°C, and then washed, and analysed with a FACSCalibur flow cytometer. CellQuest software was used to acquire the data and FlowJo software was employed to analyse the data. All data shown were size discriminated based on FSC and SSC.

2.5.3 FCM analysis of cell cycle and DNA content using PI

Cellular DNA content was detected by carrying out PI staining. Cells were lysed with 100 μl of 0.2 % Triton X-100-PBS solution and incubated for 10 min on ice. The lysed cells were treated with 0.5 % (w/v) RNase to remove RNA, followed by the addition of PI to a final concentration of 50 μg/ml (Vindelov et al,

1983). PI incorporation was analysed using a FACSCalibur flow cytometer with activated doublet discriminator module. The acquired data were analysed using the FlowJo software package. A figure showing basic cell cycle FCM analysis pattern is shown in Figure 2.9.

2.5.4 Measurement of DNA synthesis by BrdU incorporation

5-Bromo-2'-deoxyuridine (BrdU) is an analogue of the DNA precursor thymidine and is incorporated into newly synthesized DNA by cells entering and progressing through the S (DNA synthesis) phase of the cell cycle. Staining BrdU labelled cells with anti-BrdU antibody enables the FCM analysis, which allows enumeration of cells that are actively synthesizing DNA.

Cell samples were removed from the OP9 cell line two days prior to analysis and the dead cells were removed by discontinuous density centrifugation. The resultant cells were resuspended in complete media either in the absence or presence of IL-7 (10 ng/ml) at a concentration of 2×10^5 cells/ well. 50 μM BrdU was added 23 h prior to cell harvesting, at which time the cells were washed once in PBS and then fixed using the Cytofix/Cytoperm. To expose incorporated BrdU, cells were washed in BDPerm/Wash solution and treated with DNase at the final concentration of 300 μg/ml for 1 h at 37°C and then stained with anti-BrdU-APC antibody (diluted 1/300) for 20 min at 4°C. Cells were then resuspended in 7-amino-actinomycin D (7-AAD) to stain DNA, washed in the BDPerm/Wash solution and the samples were acquired on a FACSCalibur flow cytometer using the CELLQuest software package. All data shown were live and size gated by discrimination based on FSC and SSC. FlowJo software package was used to analyse the data.

2.5.5 Detection of apoptosis by Annexin V

Retrovirally infected HPCs were cocultured with OP9 for 16 days. Thereafter, 1×10^6 cells were plated on a OP9 cell layer in a 6 well-plate and incubated in the absence or presence of pharmacological inhibitors (1 μM, 3 μM, 10 μM LY294002, PI3K inhibitor; 0.2 μM, 2 μM, Chelerythrine, total PKC inhibitor; 2 μM,

20 μM, Rottlerin, PKCδ/θ inhibitor; 1μM, 10μM, U0126, MEK1/2 inhibitor; 0.5 μM, 5 μM, SB203580, p38 MAPK inhibitor) for 24 h at 37°C in a 5 % (v/v) CO_2 atmosphere. The cells were removed from OP9 layer by gentle pipetting, washed twice in ice-cold PBS, resuspended in 1 × Annexin V Binding Buffer (BDBiosciences) at the concentration of 1 × 10^6 cells/ml. 5 μl Annexin V-PE and 7-AAD were added to the cell suspension (100 μl, 1 × 10^5), and incubated for 15 min at RT in the dark. 400 μl of binding buffer was added to the sample and analysed by FCM. The samples were acquired on a FACSCalibur flow cytometer using the CELLQuest software package. FlowJo software package was used to analyse the data.

2.5.6 Cell number counting by flow cytometry

The retrovirally-infected HPCs were seeded in the following conditions: in the absence of OP9 and in the presence of IL-7, and in the absence of both OP9 cells and IL-7. The cells were cultured for up to three weeks. During this period, the cultures were sampled and analysed by FCM for the cell number, by collecting each for the same period of the time.

2.6 Western blotting

2.6.1 Cell stimulation and whole cell lysate preparation

Cell samples were removed from the OP9 cell line and either treated with phorbol ester (20 or 200 nM 12-O-tetradecanoylphorbol-13-acetate (TPA); Cell Signalling Technology) for 30 minutes or vehicle (DMSO). Then, cell samples were washed in ice-cold PBS twice and resuspended in ice-cold lysis buffer (50 mM Tris-HCl (pH=7.4), 150 mM NaCl, 1 mM EDTA, and 0.5 % (v/v) Triton X-100 supplemented with Complete Protease Inhibitor Cocktail (Roche Diagnostics)). After vortexing, the cells were solubilised for 30 min on ice before centrifugation of lysates at 10,000 g for 1 min. The resulting supernatant (whole cell lysate) was then collected and the protein concentration was determined by Bradford method (Bradford, 1976) using Coomassie Plus (Pierce). The samples were stored at -20°C before being used for Western blot analysis.

2.6.2 Sodium dodecyl sulphate-polyacylamide gel electrophoresis (SDS-PAGE) and transfer

Whole cell lysates (4 μg protein per lane) were resolved on the Xcell *SureLock* Mini-Cell kit with NuPAGE Novex high-performance pre-cast Bis-Tris gels and NuPAGE buffers and reagents (all supplied by Invitrogen). Lysates were diluted in lysis buffer to a constant final volume and the appropriate volume of 4 × NuPAGE LDS sample buffer (10 % (w/v) Glycerol, 1.7 % (w/v) Tris-Base, 1.7 % (w/v) Tris-HCl, 2.0 % (w/v) lithium dodecyl sulfate (LDL), 0.15 % (w/v) EDTA, 0.019 % Serva Blue G250 and 0.063 % Phenol Red (pH=8.5)) and 10 × NuPAGE reducing agent was added prior to heating samples to 70°C for 10 min. Samples were resolved using NuPAGE Bis-Tris gels (10 %) with NuPAGE MOPS running buffer (50 mM 3-(N-morpholino) propane sulfonic acid (MOPS), 50 mM Tris-Base, 3.5 mM SDS and 1.0 mM EDTA (pH=7.7); supplemented with NuPAGE antioxidant) at 150 V for 75 min following the manufacturers instructions. Polyvinyliden difluoride (PVDF) membrane (GH healthcare) was activated by immersing in methanol for 5 min and used. The gel was then transferred onto the PVDF membrane using NuPAGE transfer buffer (25 mM Bicine, 25 mM Bis-Tris, 1.0 mM EDTA, 50 μM Chlorobutanol (pH=7.2); supplemented with 20 % (v/v) methanol) at 30 V for 70 min.

2.6.3 Western Blot Analysis

Following transfer, PVDF membranes were washed once in Tris buffered saline (TBS; 0.5 M NaCl and 20 mM Tris pH=7.5) with 0.1 % (v/v) Tween-20 (TBS/Tween) and blocked for 1 h in TBS/Tween with 5 % non-fat milk. Membranes were then incubated with the appropriate primary detection antibody overnight at 4°C. All antibodies were diluted in TBS/Tween with either 5 % non-fat milk. Following incubation with primary antibody, PVDF membranes were washed (3 × 10 min) with TBS/Tween and incubated in the appropriate HRP-conjugated secondary antibody for 1 h at RT. PVDF membranes were then washed (6 × 10 min) with TBS/Tween and protein bands were visualised using SuperSignal West Pico Chemiluminescent Substrate (Pierce). PVDF membranes were incubated in a mixture of equal

volumes of Enhanced Chemiluminescence (ECL) solution A (2.5 mM luminol, 0.4 mM p-coumaric acid and 100 mM Tris pH=8.5) and ECL solution B (0.002 % hydrogen peroxide and 100 mM Tris pH=8.5) for 1 min before exposing membranes to Kodak X-Ray film.

2.6.4 Stripping Western blots

PVDF membranes were sometimes stripped and re-probed with a new primary antibody. Membranes were stripped at RT for 5 min in warm Restore Western Blot Stripping Buffer (Pierce). PVDF membranes were washed thoroughly in TBS/Tween and checked for residual signal before re-starting the Western blotting protocol.

2.7 *In vitro* protein kinase assay

2.7.1 ELISA-based assay

Retrovirally infected cells were washed in ice-cold PBS twice and resuspended in ice-cold sample preparation buffer (30 mM Tris-HCl (pH=7.0), 15 mM NaCl, 5 mM EGTA, 2.6 mM EDTA, 25 mM β-ME, and 0.05 % (v/v) Triton X-100 supplemented with Complete Protease Inhibitor Cocktail, Roche Diagnostics), and incubated on ice for 30 min. All the reagents were purchased from Sigma-Aldrich unless otherwise stated. Lysates were sonicated for 5 sec five times and then centrifuged at 15,000 × g for 60 min at 4°C. The supernatant was then collected and the protein concentration was determined using Bradford method. Protein (10 μg) per well was assayed per sample in triplicate. The PKC ELISA uses a synthetic PKC substrate and a monoclonal antibody that recognises the phosphorylated form of the peptide. In accordance with the protocol of the manufacturer (Merck Biosciences), 108 μl of component mixture was added to each well of a 96 well-plate and preincubated at 25°C for 5 min. The component mixture was prepared by combining the following components: 12 μl PKC reaction buffer (250 mM Tris-HCl (pH=7.0), 30 mM $MgCl_2$, 5 mM EDTA, 10 mM EGTA, and 50 mM β-ME), 12 μl 2 mM ATP, 12 μl 500 μg/ml PS, 12 μl 20 mM $CaCl_2$ and 72 μl distilled water. The negative control for the assay contained an equal volume of distilled water instead of PS and $CaCl_2$

solution. A 12 μl kinase sample was added to each well and mixed. Next 100 μl reaction mixture was transferred to each pseudosubstrate-coated well; the plate was incubated at 25°C for 20 min; and 100 μl 20 % H_2SO_4 was added to each well to stop the reaction. The wells were washed with PBS five times and the liquid was removed from each well by inverting and blotting on paper towel. Biotinylated antibody to phosphorylated PKC/PKA pseudosubstrate (2B9) (100 μl) was added to each well and incubated at 25°C for 60 min. After washing five times, 100 μl peroxidase-conjugated SA was added to each well and incubated at 25°C for 60 min. After additional washes, 100 μl substrate solution (1 tablet of *o*-Phenylenediamine in 12 ml hydrogen peroxide) was added to each well and allowed to develop until there was a medium bright yellow colour (3-5 min) at 25°C. The reaction was stopped by adding 100 μl 20 % H_2SO_4 to each well. The optical density (OD) value was measured at 490 nm wavelength. The PKC activity for each dominant negative PKC sample was analysed in triplicate and expressed as a ratio against the value of the control (MIEV).

2.7.2 ^{32}P-based assay

The kinase samples were prepared as described in Section 2.7.1. PKC activity was measured based upon the PKC catalysed transfer of the γ-phosphate group of adenosine-5'-triphosphate to a peptide which is specific for PKC according to the manufacturer's protocol (GE Healthcare). 25 μl kinase sample and 25 μl component mixture (3 mM Calcium acetate, 75 ng/ml Lα-phosphatidyl-L-serine, 6 μg/ml phorbol 12-myristate 13-cetate, 225 μM substrate peptide, 7.5 mM dithiothreitol, 50 mM Tris/HCl (pH=7.5) containing 0.05 %(w/v) sodium azide) were mixed, and the reaction was started by adding 0.2 μCi Mg^{2-} [^{32}P]ATP. The samples were incubated at 37°C for 15 min and stopped by adding 10 μl stop reagent (300 mM orthophosphoric acid containing carmosine red) to terminate the reaction. 35 μl terminated reaction mixture was transferred on to the centre of individual paper discs and allowed to air dry for 5 min. The discs were washed in 5 % (v/v) acetic acid for 5 min to remove leftover radioactivity, and then the discs were individually transferred to

scintillation vial using forceps. 10 ml scintillation cocktail (GE Healthcare) was added to each vial and the activity was counted for 60 sec in a scintillation counter appropriate for ^{32}P. Data expressed as percentage of MIEV counts.

2.8 PCR

2.8.1 Genomic DNA extraction

Cells were pelletted by centrifugation (450 g, 6 min, 4°C) and resuspended in 200 μl PBS. Genomic DNA was isolated using the Easy-DNA kit (Invitrogen Life Technologies) and then dissolved in DNase-free water.

2.8.2 Total RNA extraction

Cell pellets collected from HPC-OP9 cocultures at day 0, 3, 8 and 14 were homogenised using QIAshredder spin column (Qiagen). Total RNA was isolated from homogenised cells using the RNA-Easy RNA purification procedure (Qiagen) followed by DNase I (Qiagen) treatment to digest residual genomic DNA, and dissolved in RNase-free water.

2.8.3 RT-PCR/genomic PCR

cDNA was prepared from 1 μg RNA using oligo$(dT)_{15}$ primers and first strand cDNA synthesis kit (Roche Diagnostic). First, RNA and primer mixture was incubated at 70°C for 10 min and chilled on ice immediately. Then, the following component mixture; 10 mM Tris (pH=8.3), 50 mM KCl, 5 mM $MgCl_2$, 1 mM dNTP, 60 units RNase inhibitor, 20 units avian myeloblastosis virus (AMV) reverse transcriptase (all the reagents were from Roche Diagnostic) was added to the mixture, and incubated at 42°C for 1 h. Following the incubation, the reaction was heated at 90°C for 5 min to denature the AMV reverse transcriptase, followed by cooling the reaction to 4°C. Semi-quantitative PCR reactions were performed using the same serially diluted cDNA batches shown for β2m. Subsequent PCR analysis was performed using titrations of cDNA in a 1/3 dilution series in dH_2O. Reverse transcription-PCR (RT-PCR) reactions carried out in the absence of AMV were included as negative controls.

100 ng each cDNA/genomic DNA sample was amplified in Pfu reaction buffer (20 mM Tris-HCl (pH=8.8), 10 mM $(NH_4)SO_4$, 10 mM KCl, 0.1 % Triton X-100, 0.1 mg/ml BSA) with DNA polymerase mixture, Taq-Pfu polymerase (Taq polymerase to Pfu polymerase (6:1), (Fermentas Life Sciences)), using a Master cycler personal (Eppendorf). PCR was performed for 15-20 sec at 94°C, 30 sec at 57 to 62°C (depending on primer Tm's) (Table 2.2), and 20 sec-2 min 30 sec at 72°C for 32 cycles, with a hot start at 94°C for 2 min and a final extension at 72°C for 6 min. Products were separated by 1 % agarose gel electrophoresis in a TAE (0.48 % (w/v) Tris-Base buffer, 0.11 % (w/v) Acetic acid and 0.29 % (w/v) EDTA) filled tank and visualized using ethidium bromide staining. 1Kb ladder (Fermentas life Sciences) was run along side of the samples to detect the size. All PCR products correspond to the expected molecular sizes (Table 2.2).

2.9 Statistical analysis

Statistical comparisons of the values were carried out by two-tailed Student's t-test with an option of equal variances. The results are expressed as the mean standard error of the mean (SEM). Statistical significance was defined as $p<0.05$.

2.10 Supplier's addresses

Supplier's address was supplied in table 2.3.

Table 2.1 Antibodies

Description	reactive species	Clone	Format	Isotype	Use	Manufacturer
CD2	mouse	RM2-5	PE conjugated	Rat(SD)IgG2b, λ	FCM	BDBiosciences
CD4	mouse	RM4-5	PE conjugated	Rat(DA)IgG2a, κ	FCM	BDBiosciences
CD5	mouse	53-7.3	APC conjugated	Rat(LOU/Ws1/M) IgG2a, κ	FCM	BDBiosciences
CD8α	mouse	53-6.7	APC conjugated	Rat(LOU/Ws1/M) IgG2a, κ	FCM	BDBiosciences
CD11b	mouse	M1/70	PE conjugated	Rat(DA) IgG2b, κ	FCM	BDBiosciences
CD16/CD32	mouse	2.4G2	Purified	Rat(sprague-Dawley)IgG2b, κ	Blocking	BDBiosciences
CD19	mouse	1D3	PE-, APC-, Biotinylated	Rat(Lewis) IgG2a, κ	FCM / MACS	BDBiosciences
CD21/CD35	mouse	7G6	Purified	Rat(SD)IgG2b, κ	FCM	BDBiosciences
CD23	mouse	B3B4	PE conjugated, Biotinylated	Rat(LOU/M) IgG2a, κ	FCM / MACS	BDBiosciences
CD24	mouse	J11d	Purified	Rat(Lewis) IgM, κ	cell purification	BDBiosciences
CD24	mouse	M1/69	Biotinylated	Rat(DA) IgG2b, κ	FCM	BDBiosciences
CD25	mouse	PC61	PE conjugated	Rat(Outbred OFA)IgG1, λ	FCM	BDBiosciences
CD45	mouse	30-F11	PE-conjugated	Rat(LOU/Ws1/M) IgG2b, κ	FCM	BDBiosciences
CD45R/B220	mouse/Human	RA3-6B2	PE-conjugated	Rat(LOU) IgG2a, κ	FCM	BDBiosciences
CD90.2	mouse	53-2.1	PE conjugated	Rat(LOU/Ws1/M) IgG2a, κ	FCM	BDBiosciences
CD117	mouse	2B8	APC conjugated	Rat(Wistar) IgG2b, κ	FCM	BDBiosciences
Ly-51(6C3 / BP-1)	mouse	BP-1	PE conjugated	Mouse(Mus spretus) IgG2a, κ	FCM	BDBiosciences
Ly-6A/E (Sca-1)	mouse	D7	PE conjugated	Rat(Lewis) IgG2a, κ	FCM	BDBiosciences
Ly-6G and Ly6C (Gr-1)	mouse	RB6-8C5	Biotinylated	Rat IgG2b, κ	FCM	BDBiosciences
NK1.1	mouse	PK136	APC conjugated	Mouse[(C3H x BALB/c)F1]IgG2a, κ	FCM	BDBiosciences
TER-119 / Erythroid cells	mouse	TER-119	Biotinylated	Rat(Wistar) IgG2b, κ	FCM	BDBiosciences
H-2K^{d}	mouse	AF6-88.5	FITC conjugated	Mouse (BALB/c) IgG2a, κ	FCM	BDBiosciences

Description	reactive species	Clone	Format	Isotype	Use	Manufacturer
H-2K^a	mouse	KH114	FITC conjugated	Mouse (BALB/c) IgG2a, κ	FCM	BDBiosciences
IgD^a	mouse	AMS9.1	Biotinylated	Mouse (SLJ) IgG_{2b}, κ	FCM/cell purification	BDBiosciences
IgM	mouse	II/41	APC conjugated	Rat IgG2a, k	FCM	BDBiosciences
Ig, κ light chain	mouse	187.1	PE conjugated	Rat(sprague-Dawley)IgG1, κ	FCM	BDBiosciences
Rat IgG(H+L)	rat		PE conjugated	goat polyclonal	FCM	Caltag-Medsystems
HA		BMG-3F10	Peroxidase conjugated	Rat IgG1	FCM/Western blots	Roche Diagnostics
BrdU	human	3D4	APC conjugated	Mouse IgG1, κ	FCM	BDBiosciences
PKC/PKA phosphorylated psuedosubstrate	All	2B9	Biotinylated	N.D.	ELISA	Merck Biosciences (Calbiochem)
Streptavidin	-	-	APC conjugated	-	FCM	BDBiosciences
phospho-(Ser) PKC Substrate	All	-	Purified	Rabbit polyclonal	Western blots	Cell signalling Technology
Phospho-PKC (pan) (βIISer660)	Human, Mouse, rabbit, Monkey	-	Purified	Rabbit polyclonal	Western blots	Cell signalling Technology
Akt	Human, Mouse, Rat, Chicken, Drosophila	-	Purified	Rabbit polyclonal	Western blots	Cell signalling Technology
Phospho-Akt(Thr308)	Human, Mouse, Rat, Hamster	-	Purified	Rabbit polyclonal	Western blots	Cell signalling Technology
p42/44 MAP Kinase	Human, Mouse, Rat, Hamster, Zebra fish	-	Purified	Rabbit polyclonal	Western blots	Cell signalling Technology
Phospho-p42/44 MAP Kinase (Thr202/Tyr204)	Human, Mouse, Rat, Chicken, Hamster,	-	Purified	Rabbit polyclonal	Western blots	Cell signalling Technology
PKCα	Human, Mouse, Rat, Chicken, Dog, Frog	3	Purified	Mouse IgG2b	Western blots	BDBiosciences
Rabbit IgG (H+L)	mouse	-	HRP cojugated	goat polyclonal	Western blots	Cell signalling Technology
Mouse IgG (H+L)	mouse	-	HRP cojugated	horse polyclonal	Western blots	Cell signalling Technology

Table 2.2 PCR primers and conditions

Gene	expected size (bp)	[$MgCl_2$]	Denature	Anneal	Extension	Sequence
β2m	455	2.0 mM	94°C	59°C	72°C	U: 5' GGC GTC AAC AAT GCT GCT TCT 3'
			15 sec	30 sec	40 sec	L: 5' CTT TCT GTG TTT CCC GCT CCC 3'
Bcl-2	323	2.3mM	94°C	57°C	72°C	U: 5' GGG AGA ACA GGG TAT GA 3'
			15 sec	30 sec	30 sec	L: 5' ATC TCT GCG AAG TCA CG 3'
Bcl-xL	351	2.0 mM	94°C	57°C	72°C	U: 5' GAA GCA GAG AGG GAG ACC 3'
			15 sec	30 sec	25 sec	L: 5' CTC CTT GTC TAC GCT TTC 3'
IgM, D-J	120, 700,	3.0 mM	94°C	62°C	72°C	U: 5' AGG GAT CCT TGT GAA GGG ATC TAC TAC TGT G 3'
	1000, 1300		15 sec	30 sec	2.5 min	L: 5' AAA GAC CTG CAG AGG CCA TTC TTA CC 3'
IgM, V-J	400, 1000,	2.8 mM	94°C	62°C	72°C	U: 5' AGG T(G/C)(A/C) A(A/G)C TGC AG(C/G) AGT C(A/T)G G 3'
	1300, 1600		15 sec	30 sec	2.5 min	L: 5' AAA GAC CTG CAG AGG CCA TTC TTA CC 3'
$p21^{WAF1}$	235	2.9 mM	94°C	61.5°C	72°C	U: 5' CCC GTG GAC AGT GAG CAG T 3'
			20 sec	30 sec	20 sec	L: 5' GCA GCA GGG CAG AGG AAG T 3'
Mcl-1	163	2.0 mM	94°C	60°C	72°C	U: 5' TGG GGC AGG ATT GTG ACT CTT 3'
			30 sec	30 sec	30 sec	L: 5' ACC CAT CCC AGC CTC TTT GTT 3'
$p27^{Kip1}$	305	2.9 mM	94°C	61.5°C	72°C	U: 5' GAG CCT GGA GCG GAT GGA C 3'
			20 sec	30 sec	20 sec	L: 5' GGC TCC CGC TGA CAT CCT G 3'
IL7R	348	2.0 mM	94°C	58°C	72°C	U: 5' GAG GTG AAA GGC GTT GAA GC 3'
			15 sec	30 sec	40 sec	L: 5' CGA CTG GAA AGG CAA TGG TT 3'

Table 2.3 Suppliers addresses

Company	Address
BD Biosciences	21 Between Towns Road, Cowley, Oxford OX4 3LY, UK
Biodesign c/o AMS Biotechnology (Europe) Ltd.	63B Milton Park, Abingdon, Oxon, OX14 4RX, UK
Calbiochem, Merck Biosciences c/o VWR International Ltd.	Hunter Boulevard, Magna Park, Lutterworth, LE17 4XN, UK
Caltag-Medsystems Ltd	Botyl Road, Botolph Claydon, Buckingham, MK18 2LR, UK
Cambrex c/o Cambrex Bio Science Nottingham Ltd.	BioCity Nottingham, Pennyfoot Street, Nottingham, NG1 1GF, UK
Cedar Lane c/o VH Bio Ltd.	Unit 11b, Station Approach, Team Valley Trading Estate, Tyne & Wear NE11 0ZF, UK
Cell signalling Technology	73 Knowl Piece, Wilbury Way, Hitchin, Hertfordshire SG4 0TY
Eppendorf UK Ltd. c/o Helena Biosciences Europe Ltd.	Queensway South, Team Valley Trading Estate, Gateshead, Tyne&Wear, NE11 0SD, UK
Fermentas Life Sciences c/o Helena Biosciences Europe Ltd.	Queensway South, Team Valley Trading Estate, Gateshead, Tyne&Wear, NE11 0SD, UK
GE Healthcare UK Ltd. (Formaly Amersham Biosciences)	Pollards Wood, Nightingales Lane, Chalfont St.Giles, Bucks, UK
Harlan UK ltd	Shaw's Farm, Blackthorne, Bicester, Oxon OX25 1TP, UK
Invitrogen Life Technologies	3 Fountain Drive, Inchinnan Business Park, Paisley, UK
Kodak Ltd.	Kodak House, Station Road, Hemel Hempstead, Hertfordshire, HP1 1JU, UK
Millipore UK Ltd.	Units 3&5, The courtyards, Hatters lane, watford, WD18 8YH, UK
Miltenyi Biotec	Almac House, Church Lane, Bisley, Surrey GU24 9DR, UK
Molecular Biology Insight Inc	8685 US Highway 24, Cascade, CO 80809-1333, USA
MWG Biotech AG	Anzingerstr. 7a, 85560 Ebersberg, Germany
PeproTech EC Ltd	PeproTech House, 29 Margravine Road, London, W6 8LL, UK
Pierce c/o Perbio Science UK Ltd.	Unit 9, Atley Way, North Nelson Industrial Estate, Cramlington, Northumberland, NE231WA, UK
Qiagen Ltd.	QIAGEN House, Fleming Way, Crawley, West Sussex, RH10 9NQ, UK
Roche Diagnostics Ltd.	Bell Lane, Lewes, East Sussex, BN7 1LG, UK
Sigma-Aldrich company Ltd.	Fancy Road, Poole, Dorset BH12 4QH, UK
Takara Bio Europe/Clontech	2 Avenue du President Kennedy 78100 Saint-Germain-en-Laye, France
Tree Star	340 A Street Bd1 #203, Ashland, OR 97520, USA

Figure 2.1 pHACE and pHANE plasmids

pHACE is a mammalian expression vector that contains a cytomegalovirus promoter (CMV), Kozak translational initiation sequence, ATG start codon, EcoRI cloning site, C-terminal HA epitope tag, and stop codon. pHANE is a mammalian expression vector that contains a CMV promoter, Kozak translational initiation sequence, ATG start codon, N-terminal HA epitope tag, EcoRI cloning site, and stop codon. These plasmids are derived from the pcDNA3 vector.

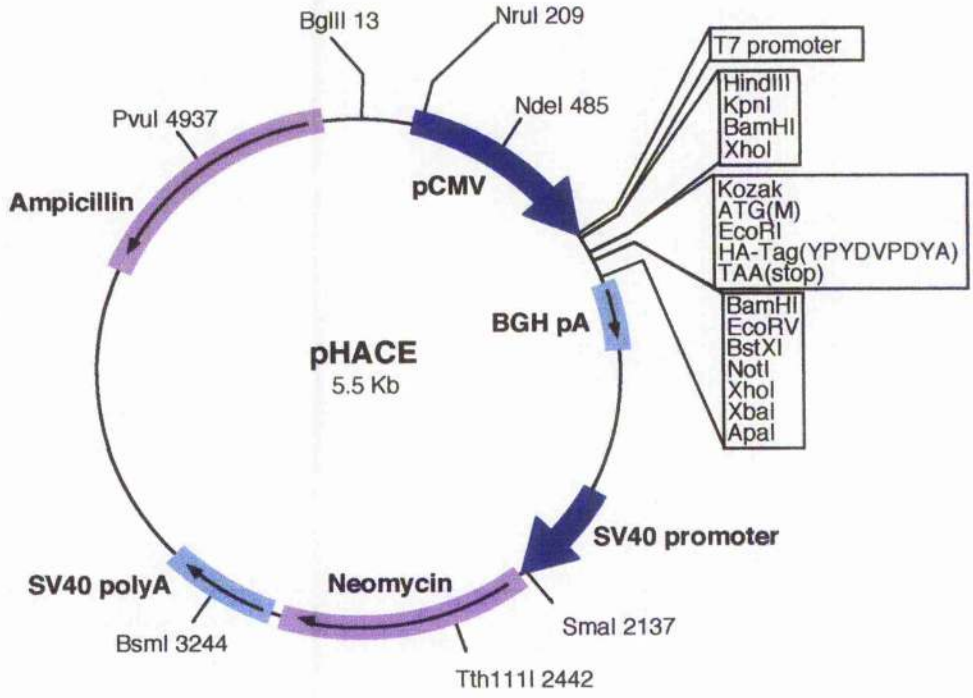
BglII 13
NruI 209
T7 promoter
HindIII
KpnI
BamHI
XhoI
NdeI 485
PvuI 4937
Ampicillin
pCMV
Kozak
ATG(M)
EcoRI
HA-Tag(YPYDVPDYA)
TAA(stop)
BamHI
EcoRV
BstXI
NotI
XhoI
XbaI
ApaI
BGH pA
pHACE
5.5 Kb
SV40 promoter
SV40 polyA
Neomycin
SmaI 2137
BsmI 3244
Tth111I 2442

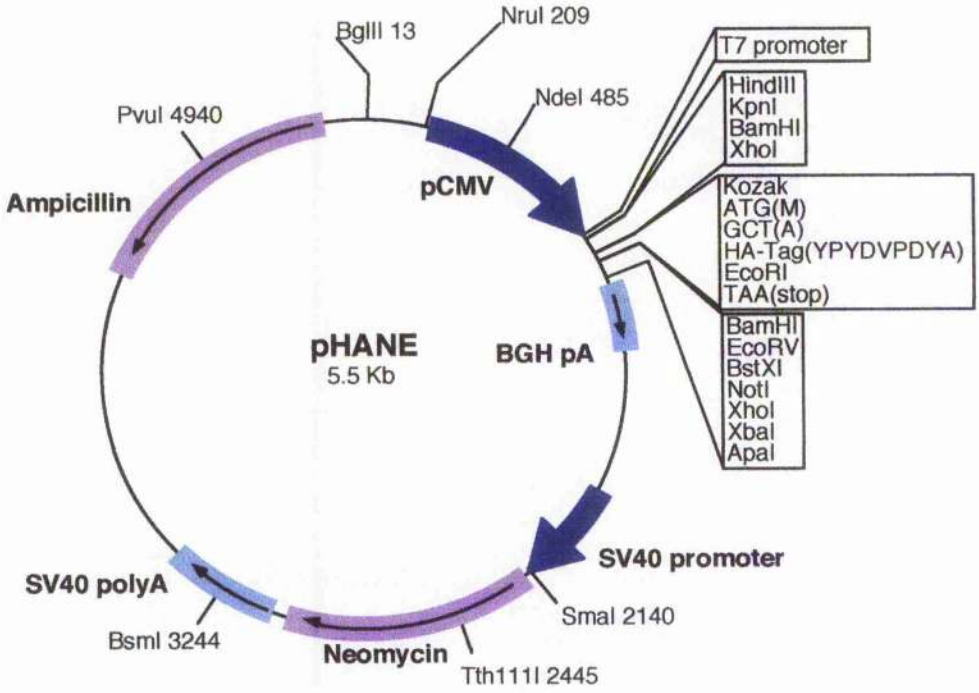
BglII 13
NruI 209
T7 promoter
HindIII
KpnI
BamHI
XhoI
NdeI 485
PvuI 4940
Ampicillin
pCMV
Kozak
ATG(M)
GCT(A)
HA-Tag(YPYDVPDYA)
EcoRI
TAA(stop)
BamHI
EcoRV
BstXI
NotI
XhoI
XbaI
ApaI
pHANE
5.5 Kb
BGH pA
SV40 promoter
SV40 polyA
SmaI 2140
BsmI 3244
Neomycin
Tth111I 2445

Figure 2.2 pGFP3 and MIEV plasmids

pGFP3 is a mammalian expression vector that contains a CMV promoter, Kozak translational initiation sequence, ATG start codon, EcoRI and BamHI cloning sites and EGFP. The plasmid is derived from the pEGFP-N1 vector. pMIEV is a retroviral vector that contains pgk promoter and 5' IRES which allows the bicistronic expression of the gene of interest and GFP.

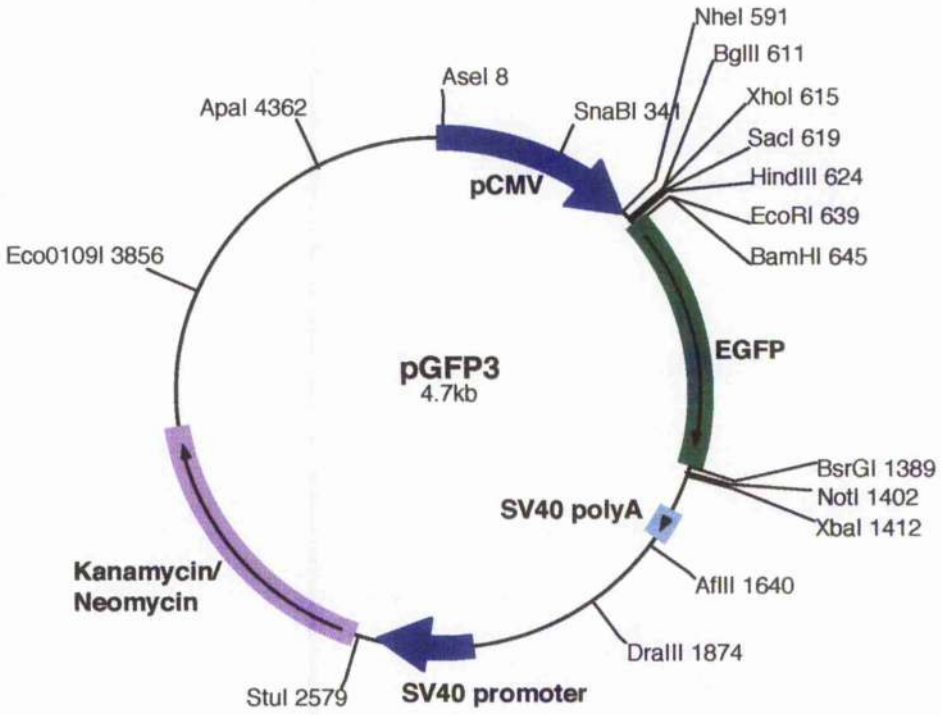
NheI 591
BglII 611
XhoI 615
SacI 619
HindIII 624
EcoRI 639
BamHI 645
AseI 8
SnaBI 341
ApaI 4362
pCMV
Eco0109I 3856
pGFP3
4.7kb
EGFP
BsrGI 1389
NotI 1402
XbaI 1412
SV40 polyA
AflII 1640
Kanamycin/
Neomycin
DraIII 1874
StuI 2579
SV40 promoter

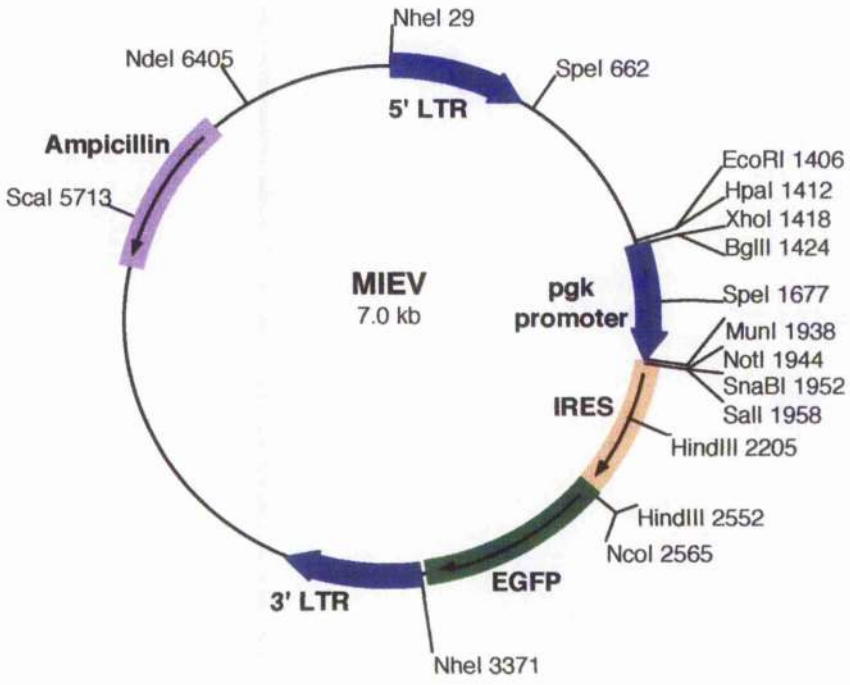
NheI 29
NdeI 6405
SpeI 662
5' LTR
Ampicillin
EcoRI 1406
HpaI 1412
XhoI 1418
BglII 1424
ScaI 5713
MIEV
7.0 kb
pgk
promoter
SpeI 1677
MunI 1938
NotI 1944
SnaBI 1952
IRES
SalI 1958
HindIII 2205
HindIII 2552
NcoI 2565
EGFP
3' LTR
NheI 3371

Figure 2.3 pMIEV-PKC-KR/PKCα and pMIEV-PKC-CAT plasmids

pMIEV-PKC-KR/PKCα expression plasmids were generated by subcloning full-length open reading frames of PKCα or full-length open reading frames of PKC isoforms with a point mutation at the ATP binding site into pMIEV. pMIEV-PKC-CAT expression plasmids were generated by subcloning cDNA fragments encoding the catalytic domains of PKC isoforms into pMIEV.

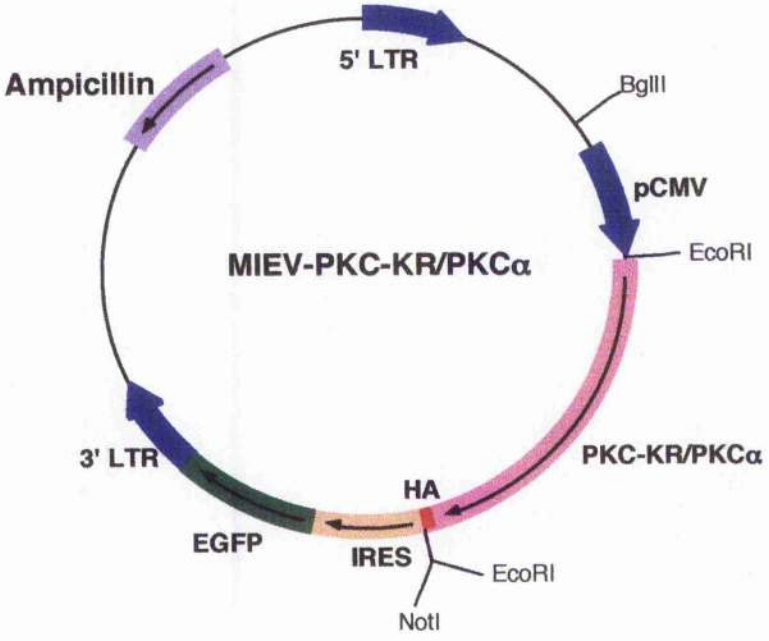
Ampicillin
5' LTR
BglII
pCMV
EcoRI
MIEV-PKC-KR/PKCα
PKC-KR/PKCα
HA
3' LTR
EGFP
IRES
EcoRI
NotI

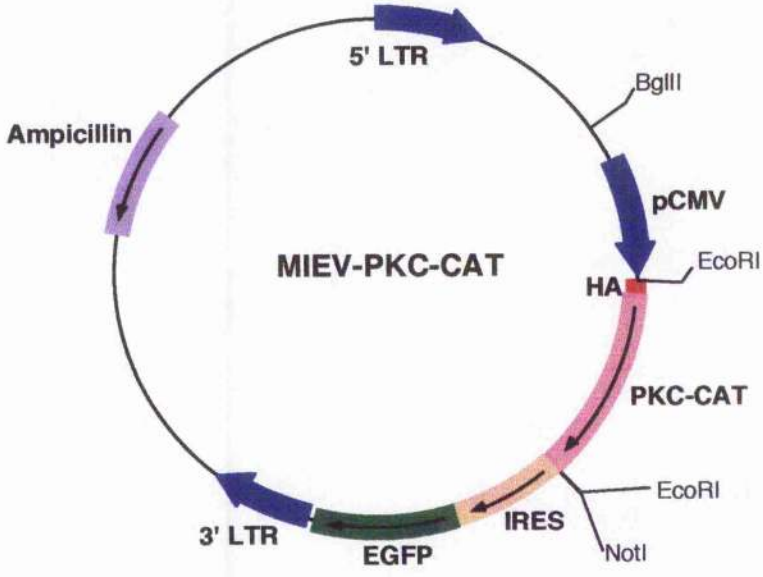
5' LTR
BglII
Ampicillin
pCMV
MIEV-PKC-CAT
EcoRI
HA
PKC-CAT
EcoRI
3' LTR
IRES
EGFP
NotI

Figure 2.4 pMIEV-PKCα-GFP and pMIEV-PKCαReg plamids

pMIEV-PKCα-GFP expression plasmid was generated by subcloning full-length open reading frames of PKCα fused with GFP into pMIEV digested with BglII and NotI. pMIEV-PKCαReg expression plasmid was generated by subcloning a part of open reading frames of regulatory domain (aa 2-383) into pMIEV digested with BglII and NotI.

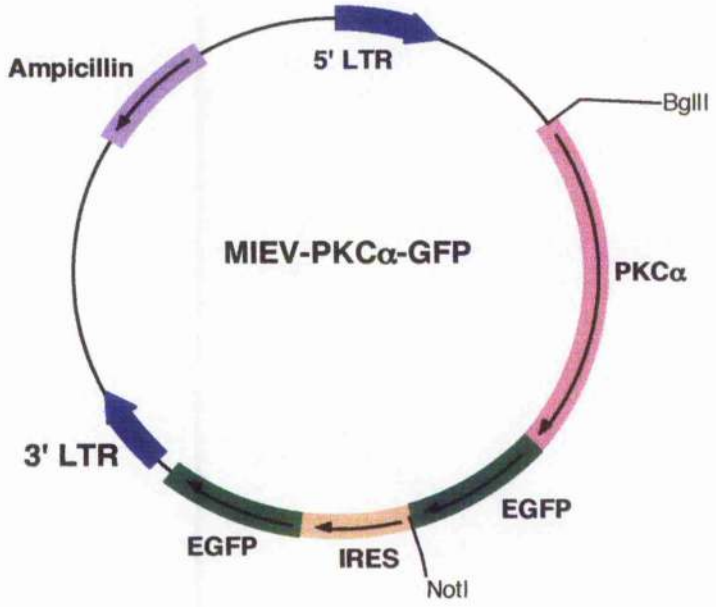
Ampicillin
5' LTR
BglII
MIEV-PKCα-GFP
PKCα
3' LTR
EGFP
EGFP
IRES
NotI

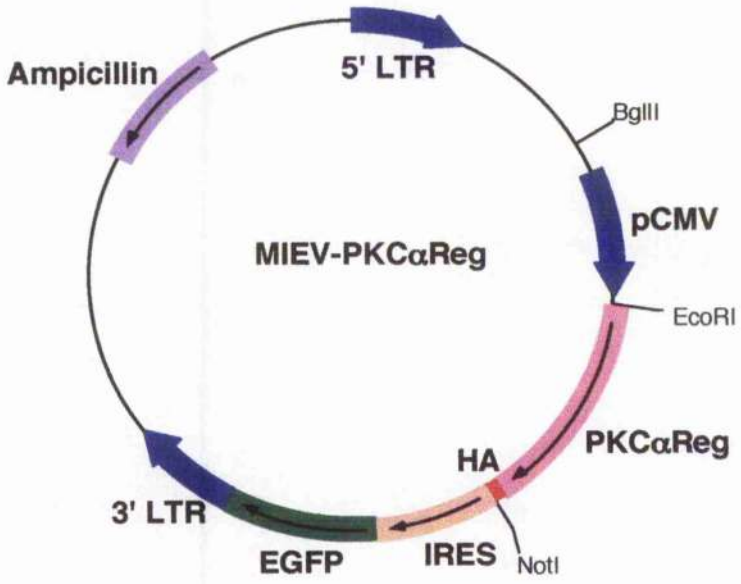
Ampicillin
5' LTR
BglII
pCMV
MIEV-PKCαReg
EcoRI
PKCαReg
HA
3' LTR
EGFP
IRES
NotI

Figure 2.5 Summary of the generation of a CD24 $^{lo/-}$ -HPC-enriched population

FL single cell suspensions were prepared by crushing FL and filtered in 70μm nylon mesh. The cells were incubated with anti-CD24 antibody and rabbit complement to permit complement-mediated CD24^{+} cell lysis. Viable CD24^{lo}-progenitor cells were recovered by Lympholyte-Mammal gradient centrifugation and CD24$^{lo/-}$ -HPC-enriched population was obtained. FCM plots CD24-APC vs. CD117-PE show typical enrichment of HPCs by analysing pre-antibody/complement mediated cell lysis and post-antibody/complement mediated cell lysis (24 % to 86 % CD117^{+} cells). The analysis was live and size gated.

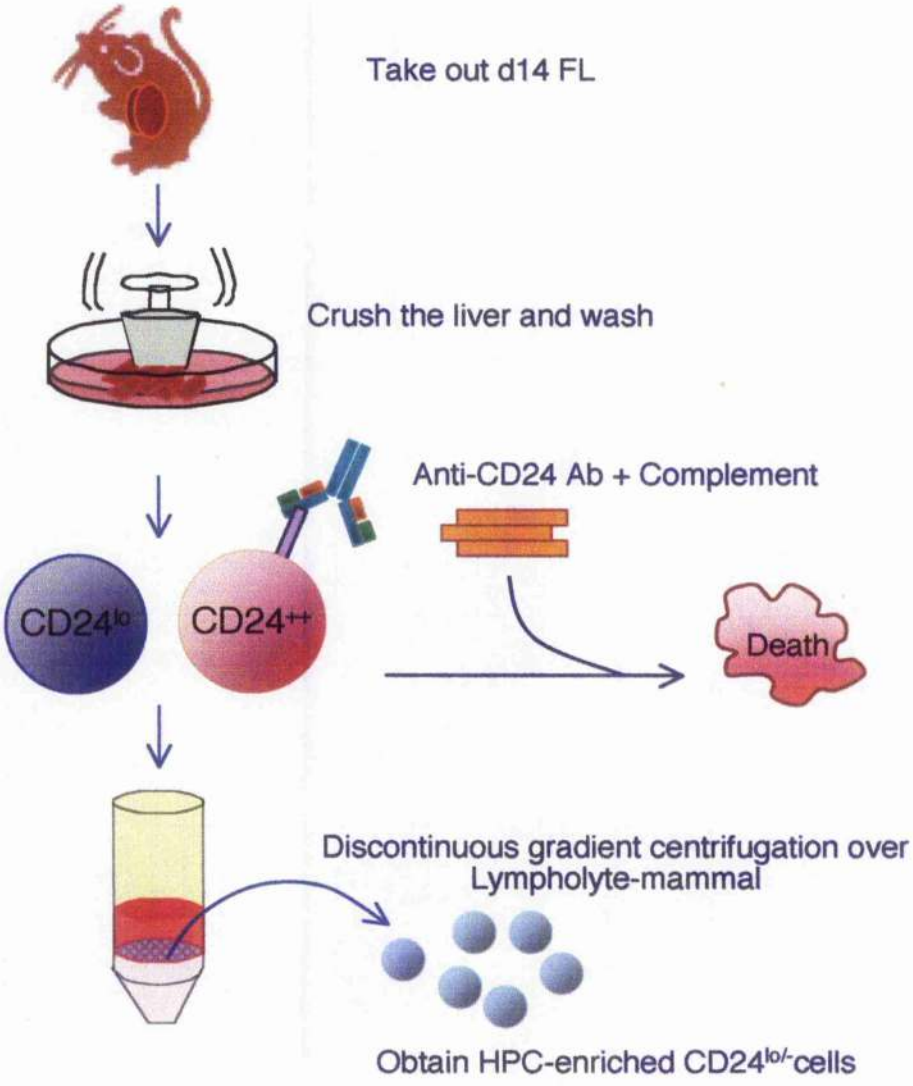
Take out d14 FL
Crush the liver and wash
Anti-CD24 Ab + Complement
CD24lo
CD24++
Death
Discontinuous gradient centrifugation over
Lympholyte-mammal
Obtain HPC-enriched CD24lo/- cells

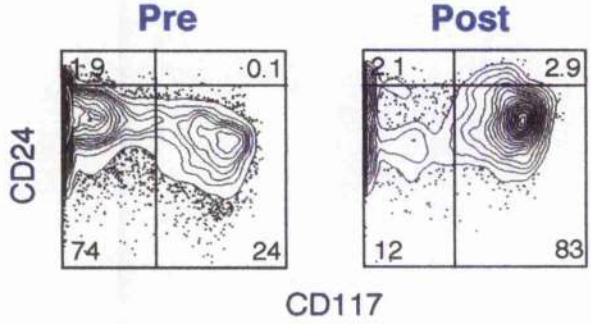
Pre
Post
1.9
0.1
74
24
2.1
2.9
12
83
CD24
CD117

Figure 2.6 Enrichment of cells utilising MACS-sorting

MACS sorting was applied for obtaining enriched population with expression of interested surface marker. The cells were incubated with biotinylated antibody (anti-CD19 in this figure). These cells were then labelled with MACS SA-micro beads and applied to a magnetic column to purify the population of interest. Typical flow cytometric plots before $CD19^+$ purification and after are presented. The analysis was live and size gated.

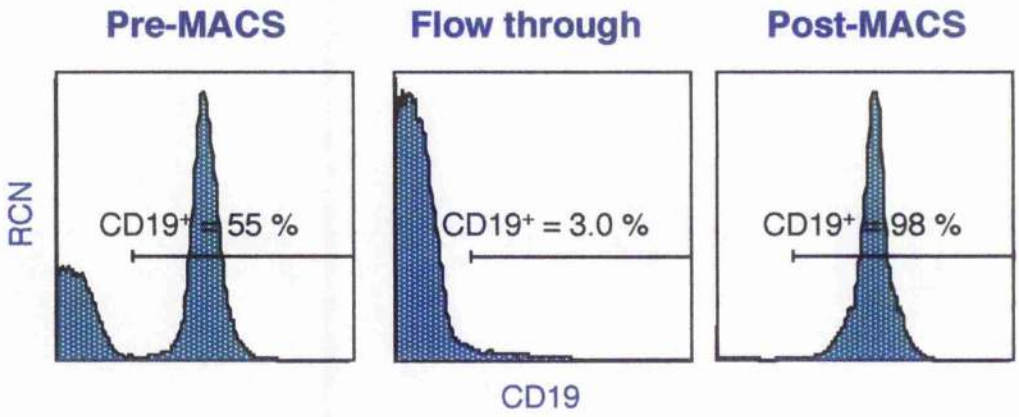
Pre-MACS
Flow through
Post-MACS
RCN
CD19+ = 55 %
CD19+ = 3.0 %
CD19+ = 98 %
CD19

Figure 2.7 *In vitro* B cell generation system

HPCs were prepared from d14 gestation FL and were cocultured on OP9 cells with growth factors. OP9 layers were replenished every 4-5 days and HPCs were cocultured until FCM analysis.

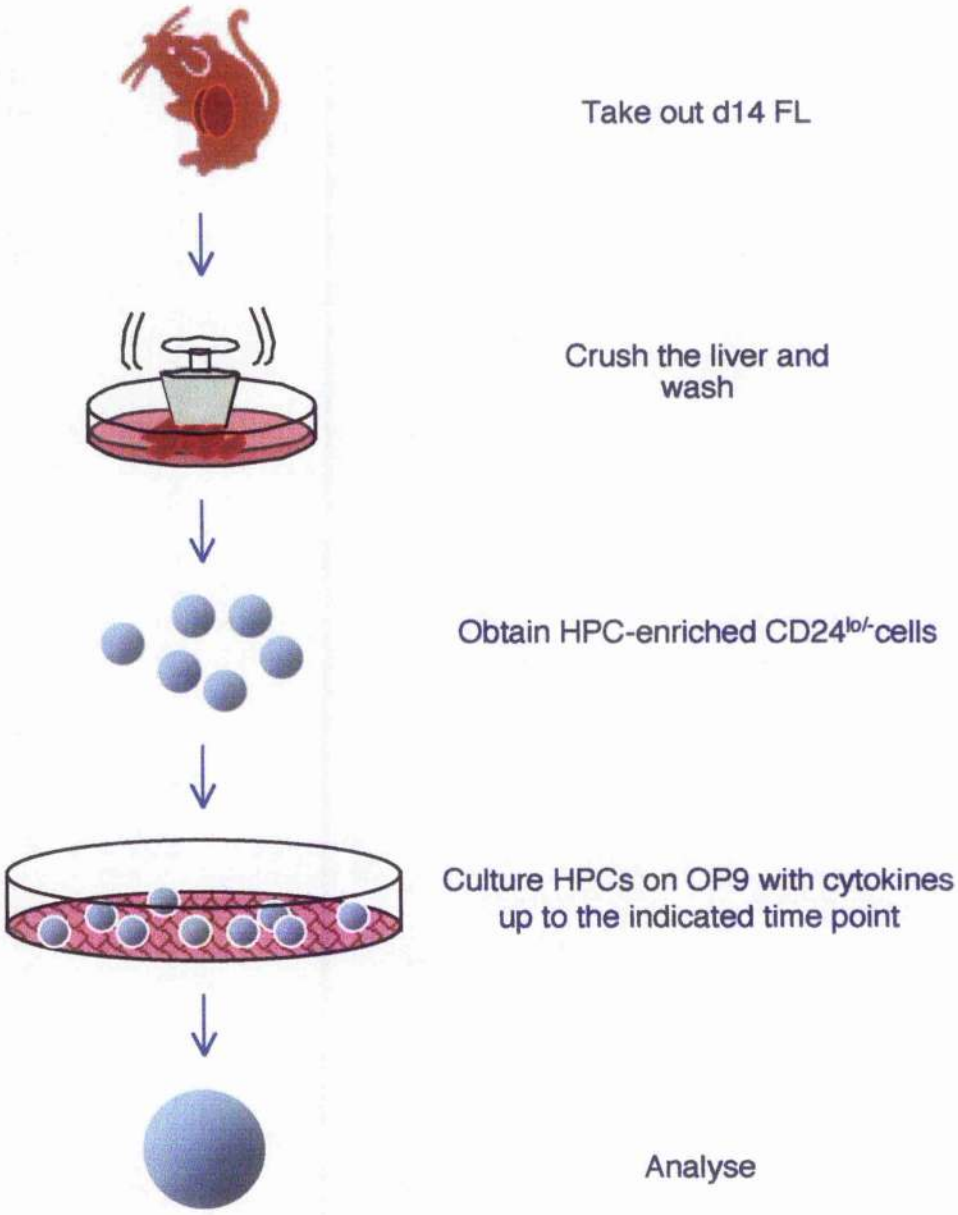
Take out d14 FL
Crush the liver and wash
Obtain HPC-enriched CD24lo/- cells
Culture HPCs on OP9 with cytokines up to the indicated time point
Analyse

Figure 2.8 *In vivo* B cell generation system

HPCs from ICR/RAG-1$^{-/-}$ mice were injected i.p. into neonatal RAG-1$^{-/-}$ mice. The mice were sacrificed by cervical dislocation at 2-6 weeks post-injection, and the BM, spleen, LN were harvested. A single cell suspension was obtained by crushing organs in PBS and by passing through a 70μm nylon mesh in PBS.

Take out d14 FL

Crush the liver and wash

Obtain HPC-enriched $CD24^{lo/-}$cells

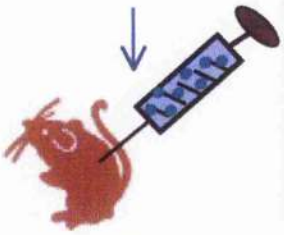

i.p. inject into RAG-$1^{-/-}$ neonates

Take out Spleen/LN/Thymus, analyse for lymphoid lineages

Obtain single suspension cellsby passing through the crushed organs

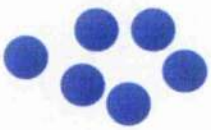

Obtain single suspension cells

Figure 2.9 FCM plot of cell cycle analysis

PI incorporation was analysed by FCM. The typical acquired data are shown. Sub-G_0/G_1, apoptosing (DNA amount<2); G_0, quiescent (DNA amount=2); G_1, growth and preparation of the chromosomes for replication (DNA amount=2); S, DNA synthesis (2<DNA amount<4); $G_2/$, mitosis preparation phase (DNA amount=4); M, mitosis (DNA amount=4).

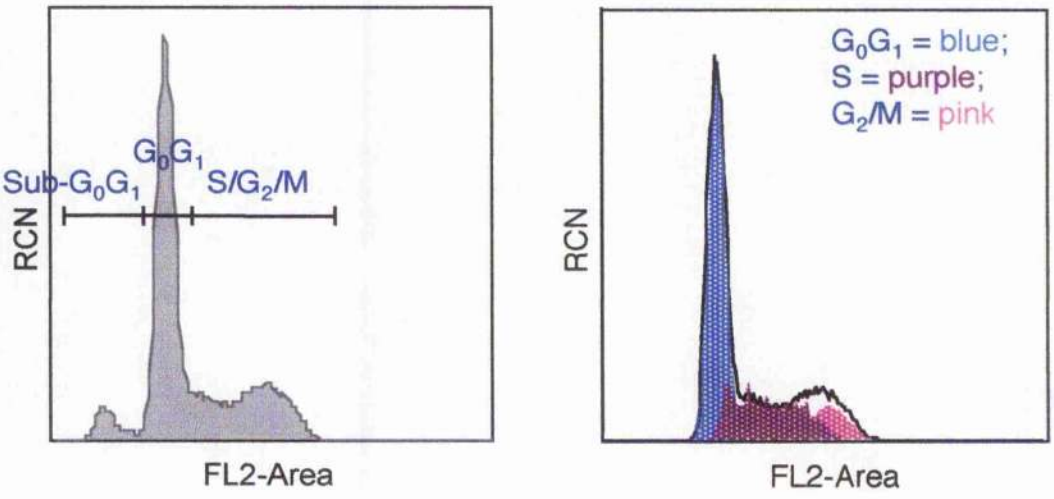
Sub-G0G1
G0G1
S/G2/M
RCN
FL2-Area
G0G1 = blue;
S = purple;
G2/M = pink
RCN
FL2-Area

Chapter 3:

Effects of mutated and wildtype PKC isotype expression during B cell development

3.1 Introduction

3.1.1 PKC mutants

PKC mutagenesis is a useful tool to examine the functions of specific PKC domains and to identify the roles of each PKC isotype, which can be difficult to define due to redundancy between PKC functions (Michie et al, 2001, Soh and Weinstein, 2003). Therefore, the following PKC mutants were used in this thesis, which were constructed as described in Section 2.1 and figure legends for Figure 2.3 and 2.4: PKC-KR (dominant negative PKC); PKC-CAT (kinase active PKC); PKCα-GFP, and PKCα-Reg. PKCα-KR and PKCδ-KR were generated by K to R point mutation, and PKCζ-KR were generated by K to M point mutation in ATP binding domain (Soh et al, 1999). PKCα-CAT, PKCδ-CAT and PKCζ-CAT were generated by deletion of the regulatory domain from the full length PKC open reading frames, which results in constitutive activation of PKC (Fig. 3.1) (Soh et al, 1999). PKCα-GFP was made by fusing GFP to the full length PKCα open reading frames at carboxyl-terminal. PKCα-Reg was constructed by deletion of a part of ATP binding domain and kinase domain from the full length PKCα open reading frames (Figure 3.1). In order to understand the mechanism of each PKC isotype during B cell development and transformation, the PKC constructs were stably expressed in HPCs using retroviral gene transfer technique as described in Section 2.4.5. The plasmids containing the above PKC mutants were subcloned into retroviral backbone to allow stable expression as described in Section 2.1.

3.2 Aims and Objectives

To assess the role of individual PKC isoforms during B cell development and transformation, the aims of this chapter were:

i. To validate the *in vitro* B cell generation system and phenotypically define B cell development *in vitro.*
ii. To validate the *in vivo* B cell generation system and phenotypically define B cell development *in vivo.*
iii. To develop the retroviral transfer technique, and validate the expression of PKC mutants at protein level.
iv. To test the effects of PKC mutant expression during B cell development.

3.3 Results

3.3.1 The *in vitro* B cell generation system supports mature B lymphocyte development

The calvarial stromal cell line, OP9 is able to support erythroid, myeloid, and B cell lineage differentiation (Nakano et al, 1994), and thus this *in vitro* system is a useful tool to examine lineage commitment and B cell development/maturation. FL cells were extracted from wildtype mice at day 14 of gestation and an HPC-enriched population was obtained by removing $CD24^{hi}$ cells with density gradient centrifugation as described in Section 2.4.2.1. The cells were cultured in the presence of OP9 cells and growth factors until analysis, as described in Section 2.4.7. To develop a model system to promote the development of B cells, phenotypic markers during B cell development were analysed by FCM. B cells express different surface molecules whose expression is developmentally regulated (Fig. 1.1): CD43, CD117, CD19, CD24, CD25, CD45R, kappa light chain (κ), IgM and IgD during the course of an OP9-HPC coculture. As shown in Figure 3.2, a significant percentage of HPCs differentiated towards the B cell lineage, as determined by expression of the B cell markers, CD19 and CD45R, as early as day 5. Upregulation of pre-B cell marker, CD24 and CD25, was detected, which is compatible with downregulation of stem cell marker, CD117. However, CD43 downregulation, which is observed *in vivo* (Nagata et al, 1997), at large pre-B cell stage was not observed in our system (Fig. 3.2). HPCs expressed IgM and IgD on surface by day 12, and developed into mature-B cell as observed normal B cell development *in vivo* (Mårtensson et al, 2002). These results support the use of this OP9-FL *in vitro* B cell development system to analyse the impact of PKC mutants throughout B cell development and transformation.

3.3.2 Establishment of an *in vivo* B cell generation system

HPCs derived from FL of wildtype mice were prepared, and 1×10^5, 3×10^5 or 1×10^6 cells were i.p. injected into RAG-$1^{-/-}$ neonatal mice. These mice lack V(D)J recombination activation gene-1, hence have no mature B or T cells. B

cell development is halted at pro-B stage, whereas T cell development is stopped at pre-T cell stage, since B and T cells are incapable of rearranging the genes encoding the IgH chains and T cell receptor β (TCRβ) chain respectively (Mombaerts et al, 1992). ICR mice have an outbred Swiss background, therefore, express H-2K^{q} type MHC-I molecule, and on the other hand, RAG-1$^{-/-}$ mice have a C57Bl/6 background, which express H-2K^{b} type MHC-I (Fig. 3.3). Therefore, as expected, no H-2K^{q+} cells were observed in either spleen or thymus from unreconstituted RAG-1$^{-/-}$ mice (Fig. 3.3). RAG-1$^{-/-}$ mice were sacrificed at 3-6 weeks from the injection, spleen cells were prepared, and the percentage of reconstitution was analysed by detecting surface MHC class I molecule, H-2K^{q}, which is expressed on ICR mouse-derived cells. The reconstitution average in the spleen was around 25 % in all mice injected with 1 $\times$ 10^5, 3 $\times$ 10^5 or 1 $\times$ 10^6 cell injection (Fig. 3.4). To examine the reconstitution potential of injected-HPCs, the B and T cell populations were examined using FCM. Surface marker expression, T cell markers: CD4 vs. CD8, TCRβ vs.CD90.2 (Thy1.2) and B cell markers: CD45R (B220) vs. IgM, were analysed by FCM in cells extracted from a spleen, thymus and LN of reconstituted mice. This analysis revealed that the reconstituted cell populations were different depending on the number of HPCs injected, despite the finding that the reconstitution efficiency appeared similar between 1 $\times$ 10^5, 3 $\times$ 10^5 and 1 $\times$ 10^6 cell injections. Only B cell reconstitution was observed in 1 $\times$ 10^5 MIEV-HPC injected mice (Fig. 3.5). In 3 $\times$ 10^5 MIEV-HPC injected mice, either B cell-oriented reconstitution (mouse 1) or T cell-oriented reconstitution (mouse 2) occurred (Fig. 3.6). Successfully, both T cells (TCRβ$^+$, CD90.2$^+$, CD4$^+$ or CD8$^+$) and B cells (CD45R$^+$ and IgM$^+$) were observed in 1 $\times$ 10^6 MIEV-HPC injected (Fig. 3.5), in spleen/thymus/LN and in spleen/LN, respectively. Taken together, 3 $\times$ 10^5 MIEV-HPC injection did not provide reliable reconstitution of both B and T populations, whereas 1 $\times$ 10^6 MIEV-HPC injection into RAG-1$^{-/-}$ mice allows the robust development of both B and T cells. Therefore, 1 $\times$ 10^6 cell injections were utilised to reconstitute B and T lymphocytes in mice for further examination of *in vivo* B cell development.

3.3.3 Confirmation of PKC expression in GP+E.86 by HA staining

The retroviral construct utilised during these studies generates a bicistronic message that encodes the mutant PKC isoform coupled to GFP, thus allowing retrovirally-infected HPCs to be monitored during the course of the experiment using cytometry by virtue of expression of GFP. In addition, all of the PKC mutants with the exception of PCKα-GFP are HA-tagged at either C or N terminus (Fig. 3.1). Therefore, direct expression of mutant PKC can be analysed using an anti-HA antibody. First, HA expression in the GP+E.86 retroviral packaging cell lines expressing PKCα-KR, PKCδ-KR or MIEV was confirmed by carrying out intracellular staining with anti-HA antibody. Both GP+E.86-PKCα-KR and -PKCδ-KR expressed HA, 62 % and 93 %, respectively compared to 0.32 % in MIEV (Fig. 3.7 top and middle). In contrast, GP+E.86-MIEV revealed the brightest in GFP fluorescence, however, as expected, this cell line did not express HA (Fig. 3.7 top and middle). In accordance with the above results, HA expression was recognised in the lysate from GP+E.86-PKCα-KR, but not in GP+E.86-MIEV by Western blots (Fig. 3.7 bottom).

3.3.4 The expression of PKC mutants in the retroviral GP+E.86 packaging line alters the activity of PKCα

The kinase activity in GP+E.86 retroviral packaging line stably expressing PKCα-KR, PKCα-CAT or MIEV was examined by ELISA-based non-radioactive kinase assay. GP+E.86-PKCα-KR, the kinase inactive form of PKCα expressing GP+E.86, attenuated its PKC kinase activity by 26 % and GP+E.86-PKCα-CAT, the constitutively kinase activated form of PKCα expressing GP+E.86, elevated its PKC kinase activity by 34 % compared to GP+E.86-MIEV (Fig. 3.8). Therefore, this suggests that the PKCα mutants being expressed in these cells are functional and thus is able to alter the level of PKCα activity in cells.

3.3.5 Retroviral transfer of PKC mutants revealed that GFP$^+$ PKCα-KR expressing cells exhibited growth advantage over GFP$^-$ cells

PKC regulates a wide variety of cellular processes that control cell growth, differentiation, cell cycle and apoptosis in response to diverse stimuli (Tan and Parker, 2003). In order to elucidate which PKC isotype mutants can affect B cell development and transformation, PKC constructs were retrovirally introduced into HPCs and cultured in the B cell generation system. To address this, HPCs from wildtype mice FL were retrovirally infected with PKC constructs; PKCα, PKCα-GFP, PKCα-Reg, PKCα-CAT, PKCα-KR, PKCδ-KR, PKCδ-CAT, PKCζ-KR and PKCζ-CAT, and empty MIEV vector control. Then, the cells were cultured in our *in vitro* B cell generation system. FCM analysis of HPC cultures immediately after retroviral infection revealed a GFP$^+$ population within each retroviral condition (Fig. 3.9A, day 2 MIEV 25 %, PKCα-KR 4.6 %, PKCδ-KR 11%, PKCζ-KR 3.5 %; Fig. 3.9B, day 2 PKCα-CAT 7.2 %, PKCδ-CAT 12 %, PKCζ-CAT 16 %, Fig. 3.9C; day 2 PKCα-GFP 16 %, PKCα 3.0 %, PKCα-Reg 16 %). Of note, a greater proportion of cells were retrovirally infected in the MIEV control culture (Fig. 3.9A). This is likely due to the absence of a gene of interest in the control vector 5' of GFP. As the OP9 coculture progressed, it became clear that PKCα-KR-expressing (GFP$^+$) cells displayed a growth advantage over the untransduced (GFP$^-$) cells as shown by a 20-fold increase in the percentage of GFP$^+$ cells from days 2 to 14 (4.2 % vs. 98 %; Fig. 3.9A). This was in contrast to cocultures containing PKCα-CAT-HPCs whose GFP$^+$ population was decreased from 7.2 % to 0.2 %, 36-fold loss within 12 days, which is not surprising considering PKCα-CAT has an enhanced kinase activity of PKCα, opposite to PKCα-KR (Fig. 3.9B). PKCζ-KR expressing cells started from 3.5 % GFP$^+$ and resulted in more than 3.2-fold decrease at day 14 (Fig. 3.9A). This tendency for GFP$^+$ population to reduce as the culture progresses was confirmed at least three separate experiments. GFP$^+$-PKCα-Reg-expressing cells also decreases 2.2-fold (Fig. 3.9C). None of the other constructs; PKCα-GFP, PKCα, PKCδ-KR, PKCδ-CAT, and PKCζ-CAT and MIEV had any effect on proliferation during B cell development, which maintained a relatively constant percentage of GFP expression (Fig. 3.9A, B

and C). The observed growth advantage of GFP$^+$ PKCα-KR expressing cells was accompanied by substantial elevation in cell numbers compared with MIEV-cocultures, and indeed, PKCα-KR-expressing cells proliferate 1.5-times faster than MIEV-expressing cells (data not shown). Taken together, these results demonstrate that the decrease of PKCα signals leads to an increase in the proliferative capacity of developing B cells.

3.3.6 PKCα-KR-FL cells revealed human CLL-like phenotype *in vitro*

HPCs were retrovirally infected with the PKC constructs described in the Figure 3.1 and were cocultured with OP9 cells and growth factors for 10 days. FCM analysis of the GFP$^+$ cells was carried out, utilising cell surface markers that can define the developmental stages of B cell maturation. More than 95 % of the GFP$^+$ cocultured cells expressed the pan-B cell markers CD45R and CD19, establishing that the retrovirally-infected cells had committed to the B cell lineage as seen in non-infected cells in the Figure 3.2 (Fig. 3.10A, B and C). Phenotypic analysis revealed that MIEV, PKCδ-KR, PKCδ-CAT, PKCζ-KR and PKCζ-CAT cocultures contained similar populations of normal developing B cells (CD19$^+$, CD23$^-$, IgM$^+$, CD5$^-$, CD45R$^+$; Fig. 3.10A, 3.10B). Interestingly, cocultures expressing PKCα mutants with kinase activity, such as, PKCα, PKCα-GFP and PKCα-CAT, resulted in less B cell population and the B cells express reduced amount of IgM on surface (0.9 %, PKCα; 0.3 %, PKCα-GFP; 0 %, PKCα-CAT; Fig. 3.10B and 3.10C). PKCα-CAT-expressing cells had the most obvious impacts, and only 55 % became CD19$^+$ B cells none of which expressed IgM on surface (Fig. 3.10B). PKCα-Reg expression in HPCs provided detrimental effects on B cell development, reducing the size of the B cell population and reducing the level of IgM on surface. Moreover, of surprise, PKCα-KR-expressing cells had upregulated CD19, CD23, CD21, a complement receptor (Rickert, 2005) and CD5 whilst expressing low levels of IgM and IgD by day 10 of coculture (Fig. 3.10A). Indeed, analysis of the mean fluorescence intensity (MFI) of key cell surface markers on B lineage cells in MIEV- compared with GFP$^+$ PKCα-KR populations revealed an upregulation of CD19 (271 vs. 476), CD23 (1.1 vs. 14), CD21 (9.8 vs. 15) and CD5 (5.1 vs. 50)

expression, while IgM and IgD expression were downregulated; IgM (19 vs. 2.8) and IgD (9.6 vs. 3.0) in GFP$^+$ PKCα-KR-expressing B cells. These findings indicate that stable expression of PKCα-KR leads to an outgrowth of cells that phenotypically resemble human CLL (CD19^{hi}, CD5$^+$, CD23$^+$, IgM^{lo}; Fig. 3.10A). In addition to the established phenotype of human CLL cells in PKCα-KR-expressing cultures, an elevation in CD2 levels was also noted compared with MIEV- or PKCδ-KR-expressing cultures; MFI of MIEV vs. PKCα-KR=19 vs. 204, thus broadening the CLL-like phenotype of the proliferating population in our *in vitro* mouse model system.

In contrast to GFP$^+$ PKCα-KR-expressing cells, GFP$^+$ PKCα-CAT expression appeared to inhibit the progenitor cells committing to the B lineage and developing towards the pre-B cell stage since the level of CD19$^+$ cells were significantly reduced in the culture compared to other PKC-CAT expressing cells (Fig. 3.10B). CD19$^+$ CD5$^+$ B-1 cells were not observed in these cultures. These findings indicate that PKCα-KR expression generates a population of cells that resembles CLL.

3.3.7 GFP$^+$ cells were reconstituted in MIEV-HPC-injected RAG-1$^{-/-}$ mice

The *in vivo* adoptive transfer system was established by transplanting retrovirally infected BM cells that express a gene of interest and GFP bicistronically, allowing injected cells to be monitored throughout the experiments (Pui et al, 1999). This system is a powerful tool to examine effects of a specific transduced gene on lymphopoiesis and transformation in a physiological environment. Prior to *in vivo* analysis on the role of PKCα-KR, a GFP$^-$ HPC reconstitution potential was tested by i.p. injecting MIEV-HPCs into RAG-1$^{-/-}$ mice. A correlation between percentage of GFP$^+$ cells in HPCs pre-injection and that of splenocytes derived from post-reconstitution of 1×10^6 MIEV-HPC-injected RAG-1$^{-/-}$ mice was determined by FCM analysis. Mice injected with 65 % GFP$^+$ MIEV-HPCs were able to achieve as much as the average of 11 % of GFP$^+$ cells in the spleen (Fig. 3.11, top). Two representative experiments from MIEV-reconstituted mice are shown in Figure

3.11 (bottom). Mouse 1 had 5.8 % and 42 % GFP$^+$ cells in spleen and LN, respectively, and mouse 2 had 10 % and 42 % GFP$^+$ cells in spleen and LN, respectively. Both mice had an adequate number of B and T cell reconstituted in both spleen and LN although the orientation toward B or T cell is slightly different: mouse 1 had T cell orientation; 43 % CD8$^+$ T cells, 46 % CD4$^+$ T cells and 3.3 % CD45R$^+$ IgM$^+$ B cells in GFP$^+$ gated LN cells, whereas mouse 2 had B cell orientation; 12 % CD8$^+$ T cells, 25 % CD4$^+$ T cells and 16 % CD45R$^+$ IgM$^+$ B cells in GFP$^+$ gated LN cells (Fig. 3.11 bottom). Taken together, it showed that the adoptive transfer provides successful T cell and B cell reconstitution *in vivo*, thus this system is sufficient for B cell generation system for further investigation for B cell development and transformation.

3.3.8 PKCα-KR-expressing cells displayed growth advantage *in vivo*

To test the impact of the stable expression of PKCα-KR *in vivo*, retrovirally-infected FL-HPCs were adoptively transferred into RAG-1$^{-/-}$ mice. Notably, FCM analysis of spleen and LN samples revealed an increase in the percentage of GFP$^+$ cells in PKCα-KR-HPC injected mice compared with MIEV-HPC injected mice, despite the fact that the percentage of GFP$^+$ cells in the PKCα-KR sample prior to injection was significantly less than that in the MIEV sample; prior to injection, MIEV vs. PKCα-KR=35 % (average 44.2 %) vs. 2.4 % (average 6.35 %), post reconstitution in spleen, MIEV vs. PKCα-KR=7.3 % (average 5.9 %) vs. 7.5 % (average 16 %) (Fig. 3.12, Table 3.1 and data not shown). This suggests that PKCα-KR expressing cells display an elevated proliferative potential *in vivo* and supports our *in vitro* data (Fig. 3.9A). This notion was supported by the finding that a reduction in the percentage of GFP$^+$ HPCs in the MIEV sample prior to injection resulted in a reduction in the percentage of GFP$^+$ cells recovered from the reconstituted spleen (Table 3.1).

3.3.9 PKCα-KR-FL cells also revealed human CLL-like phenotype *in vivo*

To assess whether the population of cells observed *in vitro* culture (Fig. 3.10A) could be also generated *in vivo*, MIEV- or PKCα-KR-retrovirally-infected FL-HPCs derived from wildtype mice were injected into RAG-1$^{-/-}$ mice and the

lymphocyte populations of the mice were analysed from 2 weeks to 6 weeks post injection. The representative data of spleen cells from either PKCα-KR or MIEV-HPCs injected RAG-1$^{-/-}$ mice is presented in Figure 3.13. Phenotypic analysis revealed that as expected, a population of mature B cells was present in the GFP$^-$ populations of both MIEV and PKCα-KR-injected mice (Fig. 3.13: CD19$^+$ IgM$^+$ IgD$^+$ CD23$^+$), indicating that the HPCs derived from wildtype mice reconstituted RAG-1$^{-/-}$ mice successfully as expected. FCM analysis of a spleen from an unreconstituted, age-matched RAG-1$^{-/-}$ mouse (no donor) highlights the presence of host-derived CD45R$^+$ CD19$^+$ IgM$^-$ IgD$^-$ CD23$^-$ cells which are also present in the GFP$^-$ population of MIEV- and PKCα-KR-HPC donor reconstituted mice (Fig. 3.13). Mice injected with-MIEV HPCs possess a significant elevation in the percentage of IgM$^+$ and IgD$^+$ B lymphocytes in the GFP$^+$ population, confirming that this is a successful method of generating mature B cells *in vivo* (Fig. 3.13). The phenotype of splenocytes from the PKCα-KR HPC-injected mice resembled that of cells generated by coculture of PKCα-KR-HPCs with OP9 cells *in vitro* (GFP$^+$, IgM^{lo}, CD23$^+$, CD5$^+$, CD19^{hi}, IgD^{lo}; Fig. 3.10A), representing hallmark of human CLL. Similar to that observed in the *in vitro* cocultures, analysis of the MFI of CLL cell surface markers on B lineage cells in MIEV- compared with PKCα-KR-GFP$^-$, GFP^{lo} and GFP^{hi} populations revealed an upregulation of CD19 and CD23 expression, while IgM and IgD expression was downregulated on GFP$^+$-PKCα-KR expressing B lineage cells as indicated: in the order of MIEV vs. PKCα-KR, GFP$^-$, GFP^{lo} and GFP^{hi}; IgM, 31, 351, 403 vs. 74, 77, 23; IgD, 5.2, 73. 25 vs. 9.1, 7.3, 4.5; CD23, 13, 55, 29 vs. 22, 142, 232; CD19, 91, 106, 102 vs. 101, 136, 149. The upregulation of CD19 and CD23 and downregulation of IgM and Ig D in PKCα-KR-expressing cells is concordant with the expression of GFP, thus, expression of PKCα-KR due to its bicistronic expression (Izon et al, 2001), but not in MIEV-expressing cells. Overall, subversion of PKCα causes transformation in developing B cells *in vivo* that are similar to human CLL cells *in vitro*.

3.4 Discussion

In this chapter, it is confirmed that our *in vitro* and *in vivo* B cell generation systems are sufficient for analysing the development of mature B cells. However, downregulation of CD43 in large pre-B cell stage and upregulation of CD23 in mature B cell stage could not be observed in our *in vitro* B cell generation system under natural circumstances (Fig. 3.2). The inability of OP9 cells to provide optimal niches for B cell development (Tokoyoda et al, 2004) can be a possible explanation for these.

Cellular analyses were carried out using the B cell generation system and retroviral technique to investigate a role of a specific PKC isotype. These systems indicate that stable expression of PKCα-KR in developing B cells results in the dysregulation of signalling pathways that control B cell differentiation and proliferation, thus driving the cells towards a CLL phenotype (Fig. 3.10A and 3.13). An intriguing feature of the cellular system is that B cell transformation is induced by the expression of a dominant negative PKCα molecule. This finding suggests that either PKCα kinase activity is not required for the generation of leukaemic cells or reduced PKC activity leads B cells to transform. There are reports that PKCα has a signalling role that is independent of its' kinase activity, and relies on the regulatory domain behaving as an adapter, thus allowing protein-protein interactions resulted in subsequent activation of signalling pathways (Melendez et al, 2001), morphology change (Mandil et al, 2001), proliferation (Mandil et al, 2001) and apoptosis (Soh et al, 2003). Yet, this seems not in the case because PKCα-Reg expression did not transform cells, but had rather harmful effects for B cell development. Of course the following possibility that it may simply be because the PKCα-Reg construct used contains a part of catalytic domain and may be incapable to translocate where the kinase should target can not be eliminated. In order to test whether the stable expression of the regulatory domain of PKCα, rather than catalytic domain, is responsible for the outgrowth of CLL cells, HPCs will be retrovirally infected with PKCα-regulatory domain only consists of PS, C1

and C2 domains and cultured in our B cell generation system *in vitro*. The resultant cell populations will be phenotypically characterised for the CLL cell surface markers, such as CD19, CD23, IgM, IgD and CD5. This set of studies will enable us to decipher whether the transformation can occur independently of kinase domain. Interestingly, increased PKCα activity resulted in giving detrimental effects on B cells, thus, among all the mutants with PKCα activity, PKCα-CAT that has most enhanced PKCα activity, appeared to promote B cell death (Fig. 3.10B). Several reports showed that PKCα activation negatively regulate cell cycle and growth in specific cells, such as pancreatic cells (Detjen et al, 2000), gastric cells (Okuda et al, 1999) and intestinal epithelial cells (Frey et al, 2000). Therefore, B cells may be one of cells that are negatively modulated by PKCα activity.

While knockout mouse models have highlighted the importance of PKCβ and PKCζ in controlling B cell activation, survival and proliferation (Leitges et al, 1996, Martin et al, 2002) and PKCδ in mediating B cell tolerance (Mecklenbräuker et al, 2002, Miyamoto et al, 2002), none of these models identify specific roles for individual PKC isoforms during early B cell maturation, suggesting a functional redundancy may exist between PKC family members. Interestingly, B cells from PKCδ$^{-/-}$ mice display splenomegaly and lymphadenopathy due to increases in the numbers of peripheral B cells (Mecklenbräuker et al, 2002, Miyamoto et al, 2002), therefore it is perhaps surprising that HPCs expressing PKCδ-KR do not display a growth advantage in our B cell generation systems. However, PKCδ$^{-/-}$ mouse-derived mature B cells proliferate because they are unable to undergo B cell anergy in response to self antigen (Mecklenbräuker et al, 2002, Miyamoto et al, 2002). Therefore, lack of proliferation observed in PKCδ-KR retrovirally-infected cells may be due to an absence of antigen in our *in vitro* HPC-OP9 coculture system. Previous findings showed that PKCζ knockout mice have abrogated BCR signalling results inhibition of proliferation and survival upon BCR stimulation. In PKCζ$^{-/-}$ mice, the matured B cell is the target and other co-stimulation signals delivered by anti-IgM or anti-CD28 antibody is required to see the inhibitory effects.

Even though decreased survival or proliferation was observed in our PKCζ-KR-expressing cell, this appeared to happen at early stage of the development (by day 5; Fig. 3.9A), therefore, these results appear to differ from the observation from PKCζ$^{-/-}$ mice.

The fact that PKCα-KR expression specifically transformed B cells in our system is perhaps unsurprising as our *in vitro* B cell generation system utilises the stromal cell line, OP9, derived from *op/op* mice, which are deficient in M-CSF (Nakano et al, 1994). OP9 cells support haemopoiesis and lymphopoiesis from HPCs, but the lack of M-CSF expression contributes to the preferential development of B cells over macrophages (Nakano et al, 1994). Our previous results suggest that expression of PKCα-KR does not trigger oncogenesis in developing T cells (Michie et al, 2001), however it remains to be established whether subversion of PKCα signalling can generate an oncogenic signal in other haematopoietic cell lineages such as NK cells, macrophages or granulocytes as has been established for a number of other cell types (Michie and Nakagawa, 2005).

Our results revealed that a CLL-like population of B cells develops on stable expression of PKCα-KR. Transgenic mouse with PKCα overexpression in the T cell lineage specifically, revealed that the T cells exhibited enhanced proliferation upon anti-CD3 stimulation and enhanced IL-2 production upon anti-CD3 and TPA stimulation (Iwamoto et al, 1992). Expression of PKCα-KR blocked development of T cells whereas PKCα-CAT promotes the development (Michie et al, 2001). Thus, PKCα expression in T cells induces proliferation and differentiation rather than hindrance. The studies using the PKCα$^{-/-}$ mouse model show that a lack of PKCα activity does not result in enhanced proliferation or development of spontaneous cancers, suggesting that PKCα does not normally behave as a tumour suppressor (Leitges et al, 2002). Indeed, overexpression of PKCα in MCF-7, human breast cancer cell line, causes enhanced proliferation, anchorage-independent growth and morphologic alterations and increased tumourigenicity (Ways et al, 1995). However, there

were reports showing that overexpression of PKCα in R6 cell, rat embryo fibroblast cell line, inhibits cellular growth (Burger et al, 1999, Burger et al, 2000). Thus, the impact of PKCα expression appears to depend on a kind of cell and functions of PKCα may be regulated by more complicated way. Taken together, our result that subversion of PKCα causes enhanced proliferation as well as tumourigenicity might be expected.

One of the hallmarks of CLL is the accumulation of B cells that are arrested in the G_0/G_1 phase of the cell cycle, due to a reluctance to undergo apoptosis (Bannerji and Byrd, 2000). This suggests that during the initial onset of CLL there is a proliferative stage, followed by cell cycle arrest. Indeed, there are reports that some circulating CLL cells are actually proliferating *in vivo* (Messmer et al, 2005, Quintanilla-Martinez et al, 1998). Interestingly, CLL cells generated from our *in vitro* and *in vivo* system are proliferating, as evidenced by the fact that they dominate the culture (Fig. 3.9A, 3.12 and Table 3.1). Recently, an orange dye called Orange CMRA from Invitrogen has been available as a replacement of green fluorescent, CFSE (5-(and-6)-carboxyfluoresceindiacetate-succinimidyl ester), which is a cytoplasmic fluorescent to track the number of cell division. The combination of this orange dye and GFP will make it possible to detect the number of cell divisions in our cells because the fluorescent range will not overlap with GFP, which is utilised to track the expression of PKC construct.

In summary, a novel system has been developed that leads to the generation of CLL both *in vitro* culture and *in vivo*, by expressing a plasmid-encoding a dominant negative PKCα in HPCs. In the next chapter, this powerful system will be utilized to address the molecular mechanisms that mediate PKCα-driven transformation events.

	% GFP pre-injection ± SEM	% GFP in spleen post-reconstitution ± SEM
MIEV	44.2 ± 6.75	5.94 ± 1.78
PKCα-KR	6.35 ± 1.16 ***	16.1 ± 5.09 **
MIEV-diluted I	6.35	0.22 ± 0.11
MIEV-diluted II	16.8	0.72 ± 0.55

Table 3.1 HPCs display a proliferative advantage upon subversion of PKCα signalling *in vivo*

The mean percentage of GFP expression is shown in MIEV- and PKCα-KR-HPCs prior to injection into RAG-1$^{-/-}$ mice (pre-injection; MIEV vs. PKCα-KR **=$p < 0.05$; n=7) and in the spleen of RAG-1$^{-/-}$ mice reconstituted with 1 x 10^6 MIEV- or PKCα-KR-retrovirally-infected HPCs (post-reconstitution; MIEV vs. PKCα-KR ***=$p < 0.001$; n=8). The results shown indicate that PKCα-KR-expressing cells possess an enhanced proliferative capacity *in vivo*, as an increase in the percentage of GFP$^-$ cells is observed in the spleens of PKCα-KR-HPC injected mice compared with MIEV-HPC injected mice, despite the fact that the percentage of GFP$^+$ cells in the PKCα-KR sample prior to injection was significantly less than that in the MIEV sample. Two individual experiments are shown where the percentage of GFP$^+$ MIEV cells is reduced/diluted prior to injection and the percentage of GFP$^+$ cells present in the spleen is further reduced at three weeks post injection (I: n=3; II: n=4).

Figure 3.1 Schematic representation of the structure of PKC mutants
PKCα construct contains full-length PKCα open reading frames (aa 2-672). PKCα-GFP construct has EGFP fused to full-length PKCα open reading frames at the C-terminus. PKC-KR constructs encode a full-length PKC open reading frames with a point mutation; lysine to arginine; PKCα (K368R) and PKCδ (K376R), lysine to methionine; PKCζ (K281M), in the C3 domain, ATP binding region. PKC-CAT constructs encode a truncated protein with a catalytic domain by deletion of the regulatory domain; PKCα (aa 326-672), PKCδ (aa 334-674) and PKCζ (aa 239-592). PKCα-Reg encodes the regulatory domain and truncated C3 domain (aa 2-383). PKCα, PKCα-GFP, PKCα-Reg and PKC-KRs have HA-tag on the N terminus and PKC-CATs have HA-tag on the C terminus.

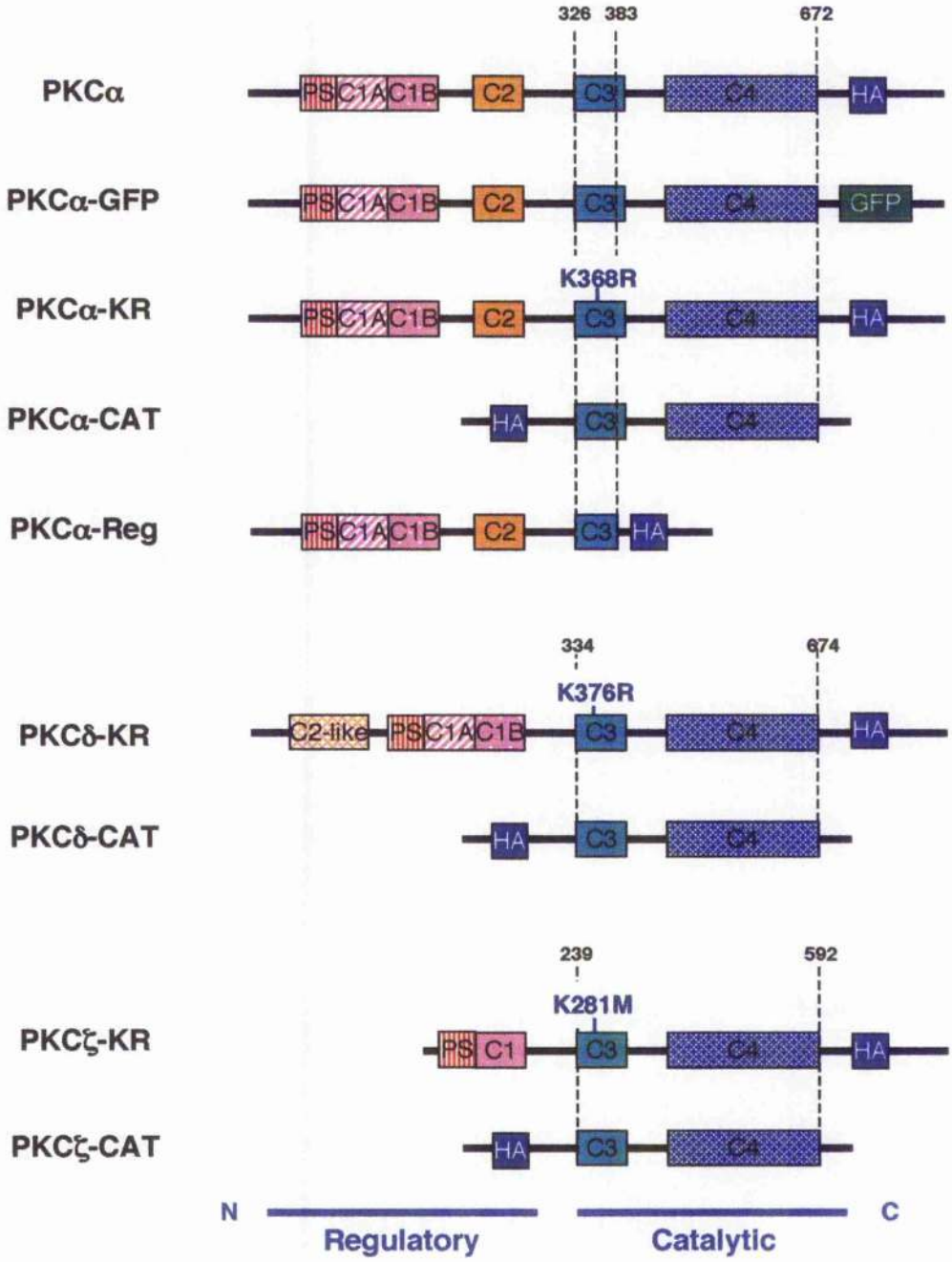
326
383
672
PKCα
PS
C1A
C1B
C2
C3
C4
HA
PKCα-GFP
GFP
K368R
PKCα-KR
PKCα-CAT
PKCα-Reg
334
674
K376R
PKCδ-KR
C2-like
PKCδ-CAT
239
592
K281M
PKCζ-KR
C1
PKCζ-CAT
N
C
Regulatory
Catalytic

Figure 3.2 The generation of mature B cells *in vitro*

Wildtype FL-derived HPCs were isolated from ICR mice at day 14 of gestation and HPCs were prepared as described in Section 2.4.2.1. The cells were cocultured on monolayer of OP9 cell line with growth factors, and FCM analysis was carried out at the indicated time point. Contour plots show the surface expression of CD43 vs. CD19, CD117 vs. CD19, CD24 vs. CD45R, CD25 vs. CD45R, κ vs. IgM and vs. IgD. Data was size gated on FSC vs. SSC and live gated based on exclusion of PI stained cells. Percentages as indicated in corner of quadrants. These data are from a single experiment, representative of three separate experiments.

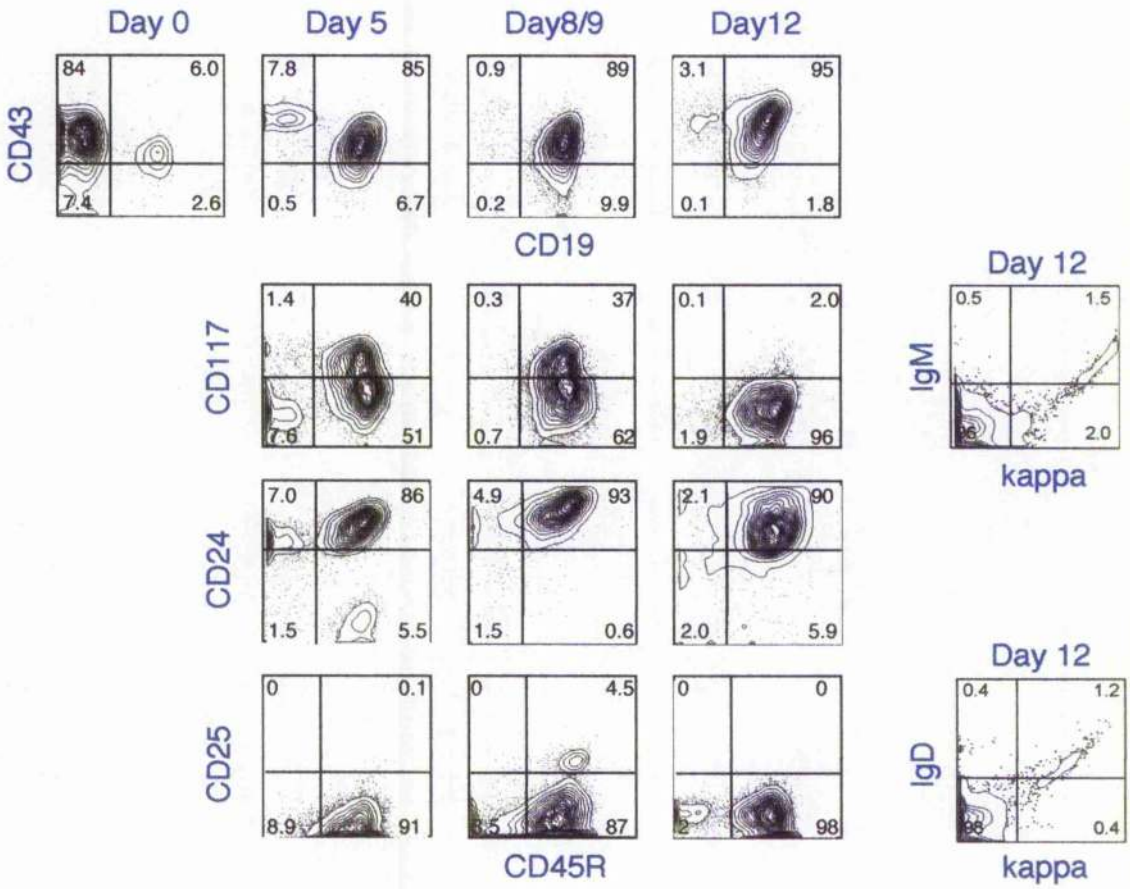
Day 0
Day 5
Day8/9
Day12
CD43
84
6.0
7.4
2.6
7.8
85
0.5
6.7
0.9
89
0.2
9.9
3.1
95
0.1
1.8
CD19
CD117
1.4
40
7.6
51
0.3
37
0.7
62
0.1
2.0
1.9
96
CD24
7.0
86
1.5
5.5
4.9
93
1.5
0.6
2.1
90
2.0
5.9
CD25
0
0.1
8.9
91
0
4.5
0
87
0
0
98
CD45R
Day 12
IgM
0.5
1.5
2.0
kappa
Day 12
IgD
0.4
1.2
0.4
kappa

Figure 3.3 Phenotypic analyses in cells derived from a RAG-1$^{-/-}$ mouse
The spleen and thymus was taken from a 3-week old RAG-1$^{-/-}$ mouse and analysed for the expression of mouse allo- and syngeneic-MHC class I, B cell markers and T cell markers; CD45R vs. IgM, CD90.2 vs. TCRβ and CD4 vs. CD8. H-2K^{b} and H-2K^{q} represent MHC class I for RAG-1$^{-/-}$ mice and for ICR mice, respectively. Data was size gated on FSC vs. SSC and live gated based on exclusion of PI stained cells. Percentages as indicated in corner of quadrants. These data are from a single experiment, representative of two separate experiments.

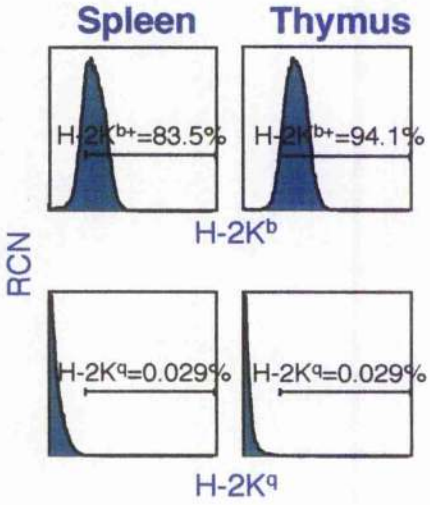
Spleen
Thymus
H-2K^{b+}=83.5%
H-2K^{b+}=94.1%
H-2K^{b}
RCN
H-2K^{q}=0.029%
H-2K^{q}=0.029%
H-2K^{q}

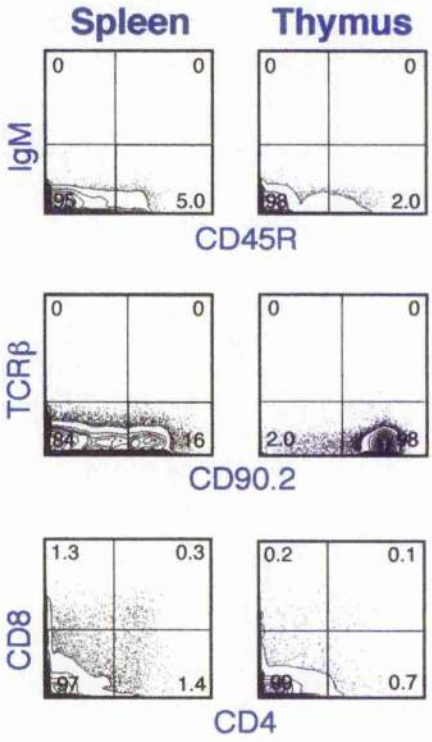
Spleen
Thymus
IgM
0
0
95
5.0
0
0
98
2.0
CD45R
TCRβ
0
0
84
16
0
0
2.0
98
CD90.2
CD8
1.3
0.3
97
1.4
0.2
0.1
99
0.7
CD4

Figure 3.4 Transplantation efficiency of HPCs in adoptive transfer into RAG-1$^{-/-}$ mice

Wildtype HPCs from ICR mice were i.p. injected into RAG-1$^{-/-}$ mice at the concentrations of 1×10^5, 3×10^5 and 1×10^6 as indicated and the amount of reconstituted cells was analysed by FCM with H-2K^q staining, which is a surface marker specific to donor, ICR derived cells. The values described were the average (n=3-9 mice/point) ± SEM.

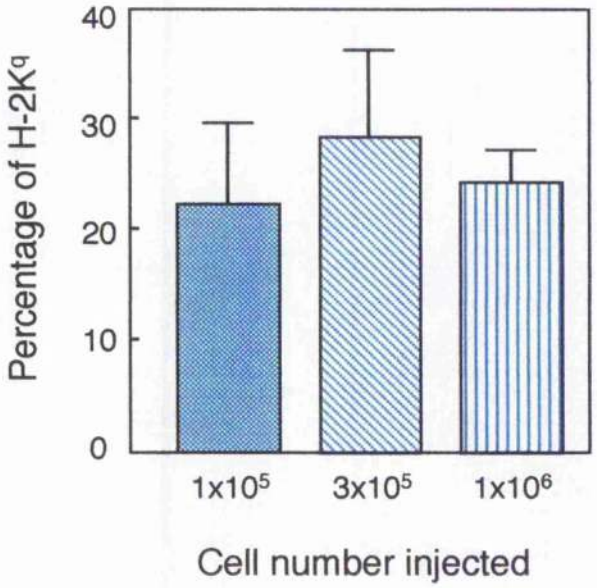
40
30
20
10
0
Percentage of H-2K^q
1x10^5
3x10^5
1x10^6
Cell number injected

Figure 3.5 Reconstitution of RAG-1$^{-/-}$ mice with FL-derived HPCs

RAG-1$^{-/-}$ mice i.p. injected with either 1×10^5 or 1×10^6 wildtype HPCs were sacrificed at 6 weeks post injection and spleen, LN and thymus were extracted and prepared for the FCM analysis; CD45R vs. IgM, CD90.2 vs. TCRβ and CD4 vs. CD8. Contour plots were size gated on FSC vs. SSC and live gated based on exclusion of PI stained cells. Percentages as indicated in corner of quadrants. These data are from a single experiment, representative of three separate experiments.

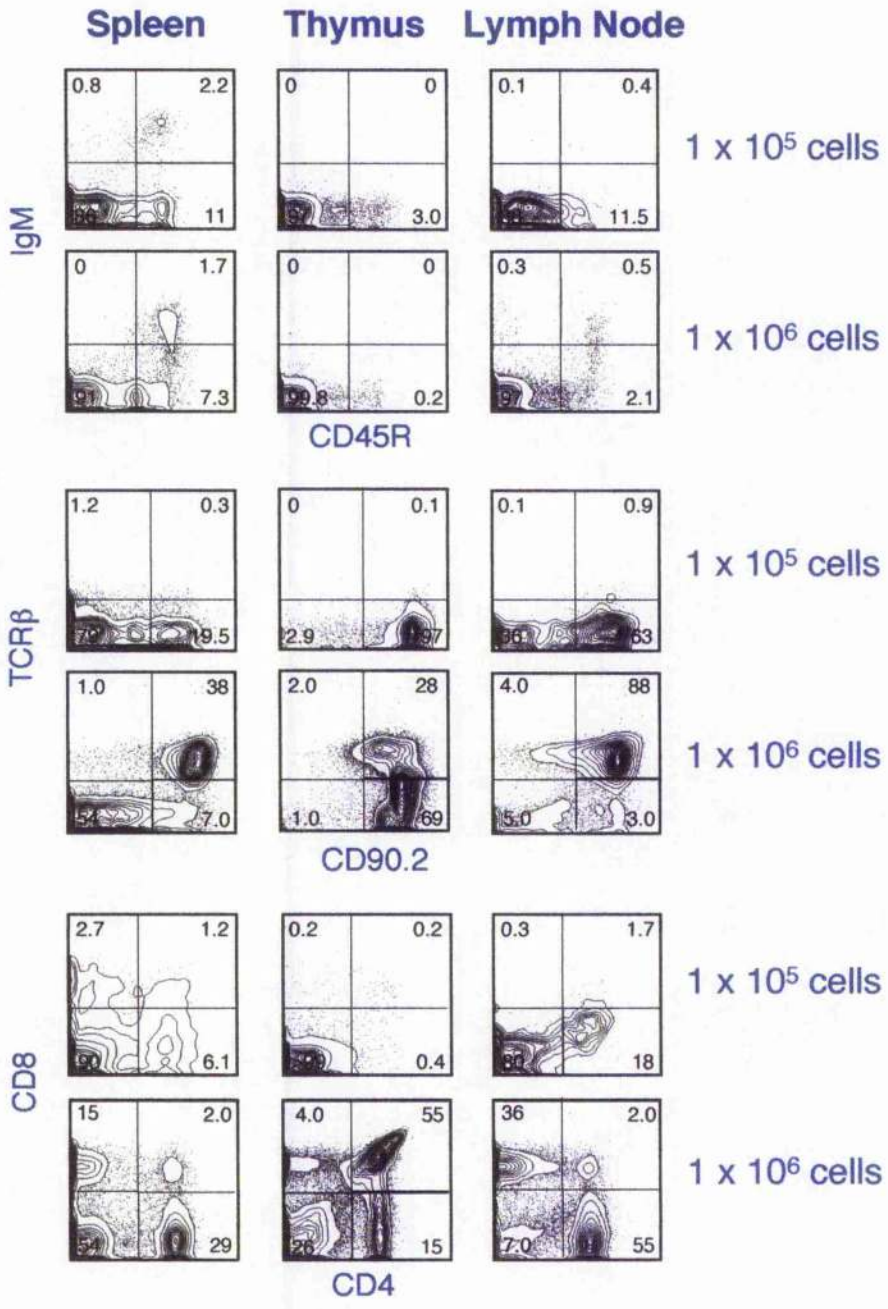
Spleen
Thymus
Lymph Node
IgM
TCRβ
CD8
CD45R
CD90.2
CD4
1 x 10⁵ cells
1 x 10⁶ cells
1 x 10⁵ cells
1 x 10⁶ cells
1 x 10⁵ cells
1 x 10⁶ cells
0.8
2.2
11
0
0
3.0
0.1
0.4
11.5
0
1.7
7.3
0
0
0.2
0.3
0.5
2.1
1.2
0.3
19.5
0
0.1
2.9
97
0.1
0.9
63
1.0
38
7.0
2.0
28
1.0
69
4.0
88
3.0
2.7
1.2
6.1
0.2
0.2
0.4
0.3
1.7
18
15
2.0
29
4.0
55
15
36
2.0
55

Figure 3.6 Reconstitution of RAG-1$^{-/-}$ mice with 3 × 10^5 FL-derived HPCs
RAG-1$^{-/-}$ mice i.p. injected with 3 × 10^5 MIEV-HPCs were sacrificed at 6 weeks post injection. Cells from spleen, LN and thymus were extracted and prepared for FCM analysis. The cells shown were analysed for the B and T cell markers; CD45R vs. IgM, CD90.2 vs. TCRβ and CD4 vs. CD8. Contour plots were size gated on FSC vs. SSC and live gated based on exclusion of PI stained cells. Percentages as indicated in corner of quadrants.

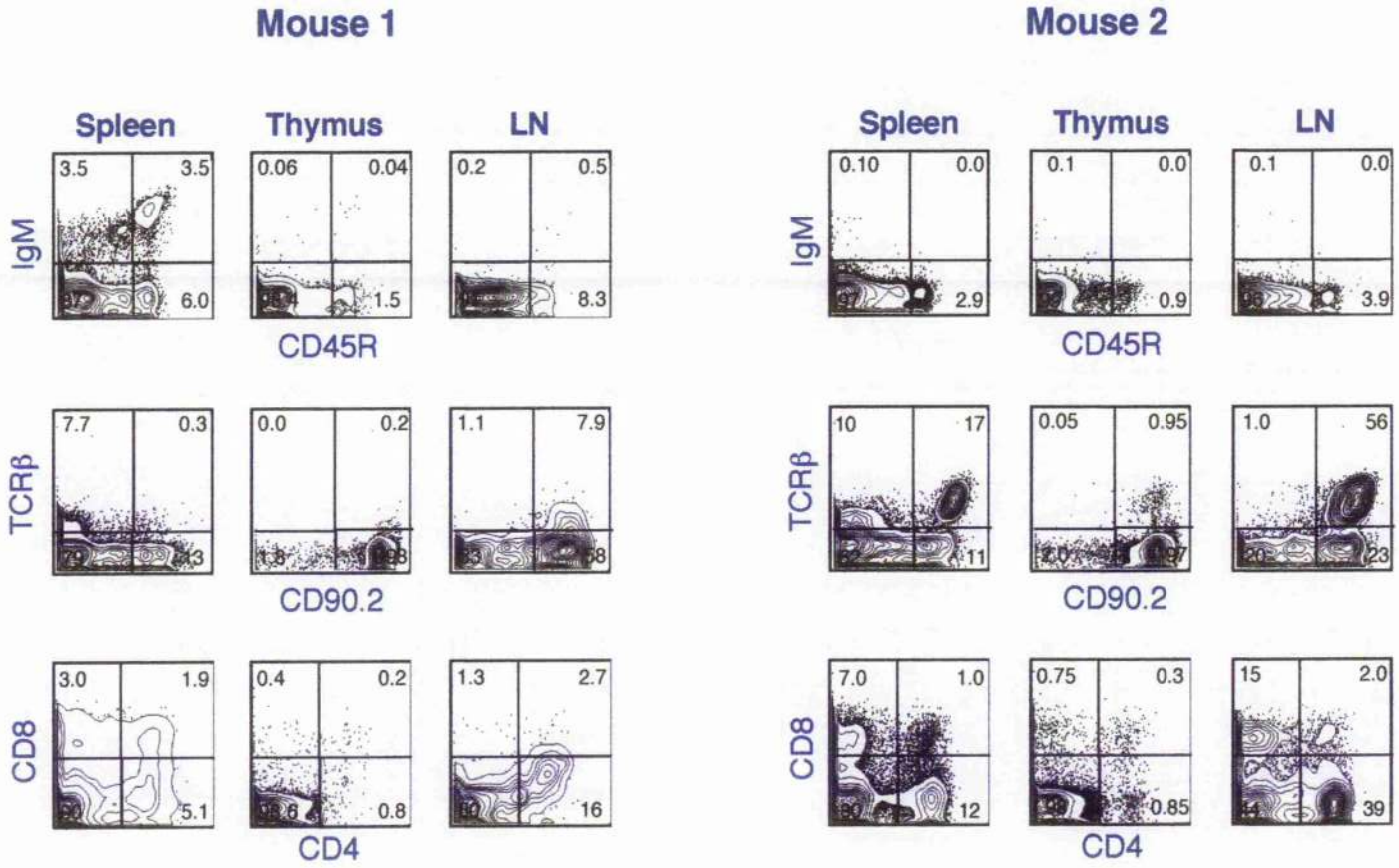
Mouse 1
Spleen
Thymus
LN
IgM
CD45R
TCRβ
CD90.2
CD8
CD4
3.5
3.5
6.0
0.06
0.04
1.5
0.2
0.5
8.3
7.7
0.3
0.0
0.2
1.1
7.9
3.0
1.9
5.1
0.4
0.2
0.8
1.3
2.7
16
Mouse 2
Spleen
Thymus
LN
IgM
CD45R
TCRβ
CD90.2
CD8
CD4
0.10
0.0
2.9
0.1
0.0
0.9
0.1
0.0
3.9
10
17
11
0.05
0.95
1.0
56
23
7.0
1.0
12
0.75
0.3
0.85
15
2.0
39

Figure 3.7 Expression of PKC constructs within GP+E.86 packaging lines
The constructs containing PKC-KR mutants bicistronically express GFP, and are also HA-tagged at the C-terminus, therefore PKC-KR expression was determined by both GFP fluorescence and intracellular staining with anti-HA antibody. The retroviral packaging cell line expressing vector alone (MIEV), PKCα-KR or PKCδ-KR were examined for GFP and HA expression (top and middle, respectively). These data are from a single experiment, representative of two separate experiments. The cell lysates from GP+E.86-MIEV and -PKCαKR were prepared and examined HA expression by Western blots with anti-HA antibody (bottom). The data are from a single experiment, representative of two separate experiments.

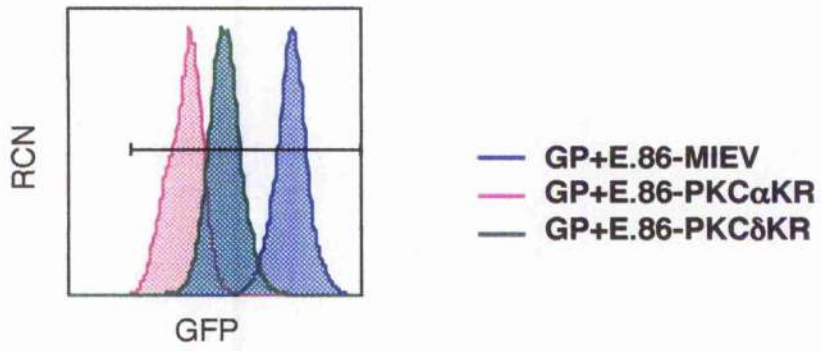

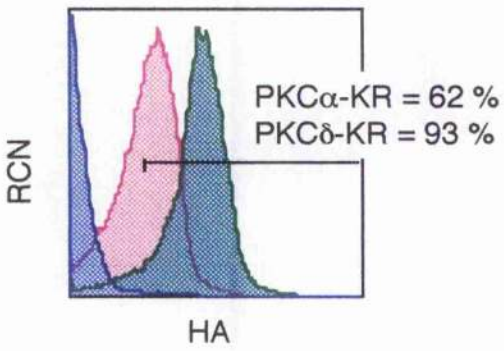

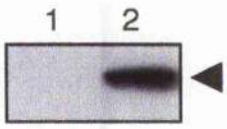

1. GP+E.86-MIEV
2. GP+E.86-PKCα-KR

Figure 3.8 GP+E.86-PKCα-KR decreased PKC activity and GP+E.86-PKCα-CAT increased PKC activity

Cell lysates were prepared from GP+E.86-MIEV and -PKCα-KR before the determination of PKC activity with non-radioactive PKA kinase kit. The graph shows the average % kinase activity (n=3/point) relative to MIEV-expressing control cells (100%); SEM shown. *=$p<0.05$ a value against MIEV. These data are from a single experiment, representative of two separate experiments.

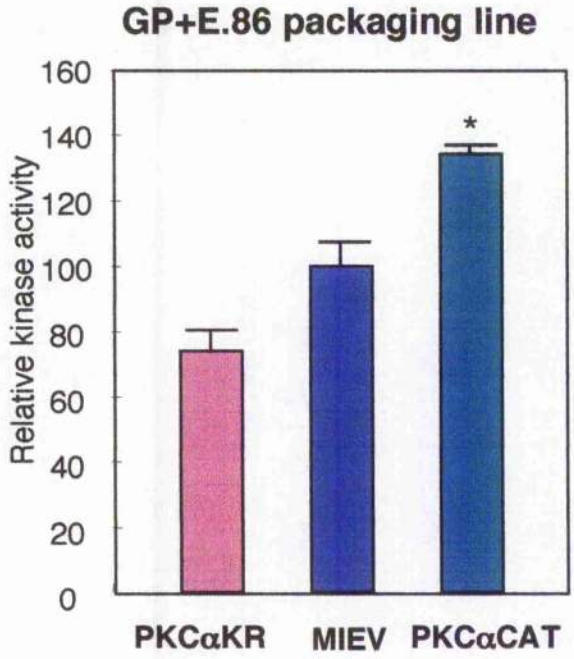
GP+E.86 packaging line
Relative kinase activity
160
140
120
100
80
60
40
20
0
*
PKCαKR
MIEV
PKCαCAT

Figure 3.9A Wildtype FL-derived HPCs retrovirally-infected with PKCα-KR display a growth advantage over GFP$^-$ and PKCα-CAT displayed a survival disadvantage over GFP$^-$ cells

Wildtype HPCs derived FL of ICR mice were retrovirally-infected with MIEV, PKCα-KR, PKCδ-KR or PKCζ-KR and then cultured in our *in vitro* B cell generation system. During this period, the cultures were sampled and analysed by FCM for relative amounts of GFP expression, percentages as indicated. Histogram plots were live and size gated. These data are from a single experiment, representative of six separate experiments.

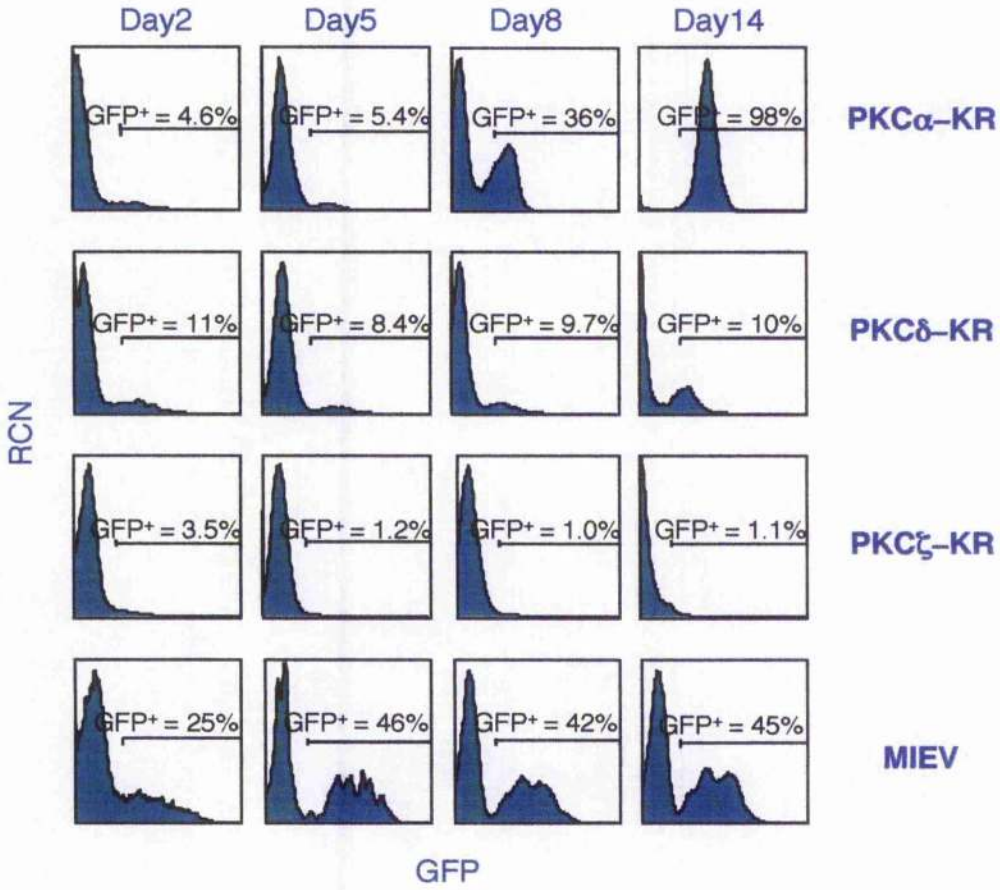
Day2
Day5
Day8
Day14
GFP+ = 4.6%
GFP+ = 5.4%
GFP+ = 36%
GFP+ = 98%
PKCα–KR
GFP+ = 11%
GFP+ = 8.4%
GFP+ = 9.7%
GFP+ = 10%
PKCδ–KR
GFP+ = 3.5%
GFP+ = 1.2%
GFP+ = 1.0%
GFP+ = 1.1%
PKCζ–KR
GFP+ = 25%
GFP+ = 46%
GFP+ = 42%
GFP+ = 45%
MIEV
RCN
GFP

Figure 3.9B Wildtype FL-derived HPCs retrovirally-infected with PKCα-KR display a growth advantage over GFP$^-$ and PKCα-CAT displayed a survival disadvantage over GFP$^-$ cells

Wildtype HPCs derived FL of ICR mice were retrovirally-infected with PKCα-CAT, PKCδ-CAT or PKCζ-CAT and then cultured in our *in vitro* B cell generation system. During this period, the cultures were sampled and analysed by FCM for relative amounts of GFP expression, percentages as indicated. Histogram plots were live and size gated. These data are from a single experiment, representative of five separate experiments.

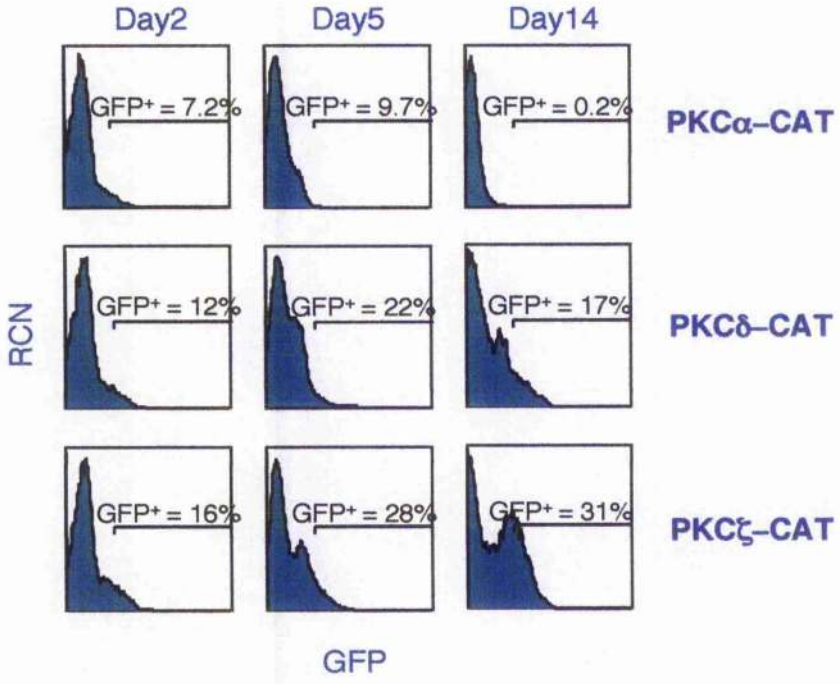
Day2
Day5
Day14
GFP+ = 7.2%
GFP+ = 9.7%
GFP+ = 0.2%
PKCα–CAT
GFP+ = 12%
GFP+ = 22%
GFP+ = 17%
PKCδ–CAT
GFP+ = 16%
GFP+ = 28%
GFP+ = 31%
PKCζ–CAT
RCN
GFP

Figure 3.9C Wildtype FL-derived HPCs retrovirally-infected with PKCα-KR display a growth advantage over GFP$^-$ and PKCα-CAT displayed a survival disadvantage over GFP$^-$ cells

Wildtype HPCs derived FL of ICR mice were retrovirally-infected with PKCα, PKCα-GFP or PKCα-Reg and then cultured in our *in vitro* B cell generation system. During this period, the cultures were sampled and analysed by FCM for relative amounts of GFP expression, percentages as indicated. Histogram plots were live and size gated. These data are from a single experiment, representative of three separate experiments.

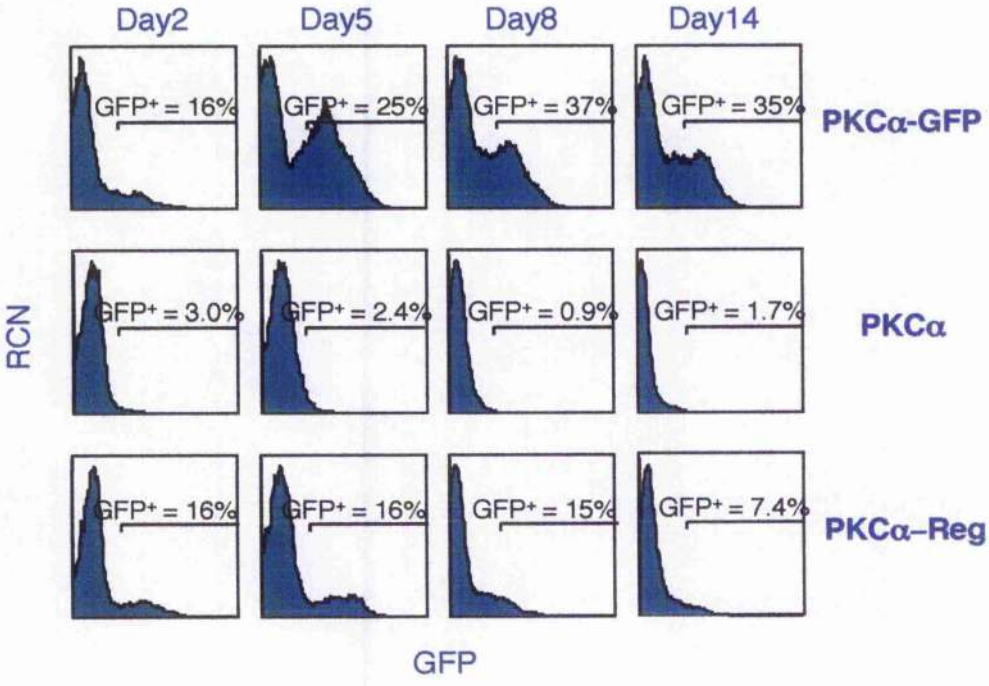
Day2
Day5
Day8
Day14
GFP+ = 16%
GFP+ = 25%
GFP+ = 37%
GFP+ = 35%
PKCα-GFP
GFP+ = 3.0%
GFP+ = 2.4%
GFP+ = 0.9%
GFP+ = 1.7%
PKCα
GFP+ = 16%
GFP+ = 16%
GFP+ = 15%
GFP+ = 7.4%
PKCα–Reg
RCN
GFP

Figure 3.10A Stable expression of PKCα-KR in wildtype HPCs results in the development of CLL-like cells

Wildtype HPCs derived from ICR mice infected with MIEV, PKCα-KR, PKCδ-KR and PKCζ-KR were phenotypically characterised by FCM. The cocultures were harvested at day 10. Analysis of IgM vs. κ, IgD vs. κ, CD5 vs. CD2, CD23 vs. CD19 and CD21 vs. CD19 expressions are shown for GFP^+ gated cells, percentages as indicated. Contour plots were live and size gated. N.D.=not determined. These data are from a single experiment, representative of six separate experiments.

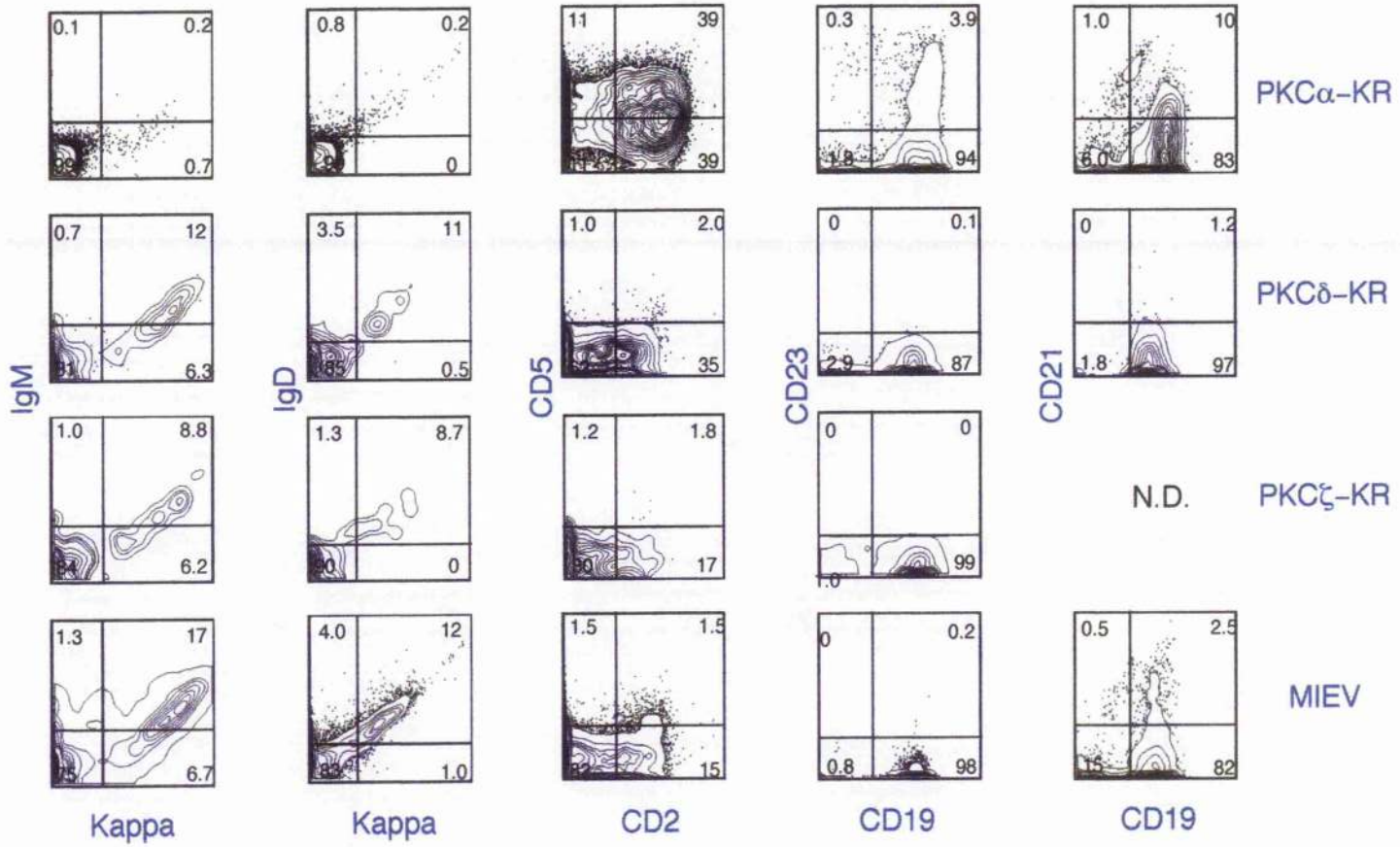
IgM
IgD
CD5
CD23
CD21
Kappa
Kappa
CD2
CD19
CD19
PKCα-KR
PKCδ-KR
N.D.
PKCζ-KR
MIEV

Figure 3.10B Stable expression of PKCα-KR in wildtype HPCs results in the development of CLL-like cells

Wildtype HPCs infected with PKCα-CAT, PKCδ-CAT and PKCζ-CAT were harvested at day 14 and phenotypically characterised by FCM. Analysis of IgM vs. κ, CD5 vs. CD2 and CD23 vs. CD19 expressions are shown for GFP^+ gated cells, percentages as indicated. Contour plots were live and size gated. These data are from a single experiment, representative of five separate experiments.

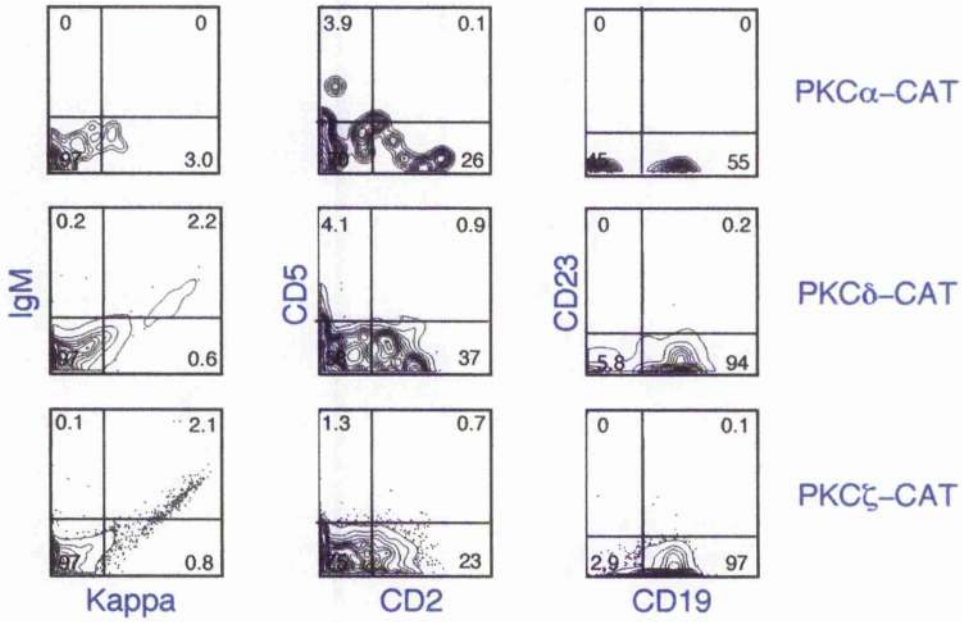
0
0
3.0
3.9
0.1
26
0
0
55
PKCα–CAT
IgM
0.2
2.2
0.6
CD5
4.1
0.9
37
CD23
0
0.2
5.8
94
PKCδ–CAT
0.1
2.1
0.8
1.3
0.7
23
0
0.1
2.9
97
PKCζ–CAT
Kappa
CD2
CD19

Figure 3.10C Stable expression of PKCα-KR in wildtype HPCs results in the development of CLL-like cells

Wildtype HPCs infected with PKCα, PKCα-GFP and PKCα-Reg were harvested at day 14 and phenotypically characterised by FCM. Analysis of IgM vs. κ, CD5 vs. CD2 and CD23 vs. CD19 expressions are shown for GFP^+ gated cells, percentages as indicated. Contour plots were live and size gated. These data are from a single experiment, representative of three separate experiments.

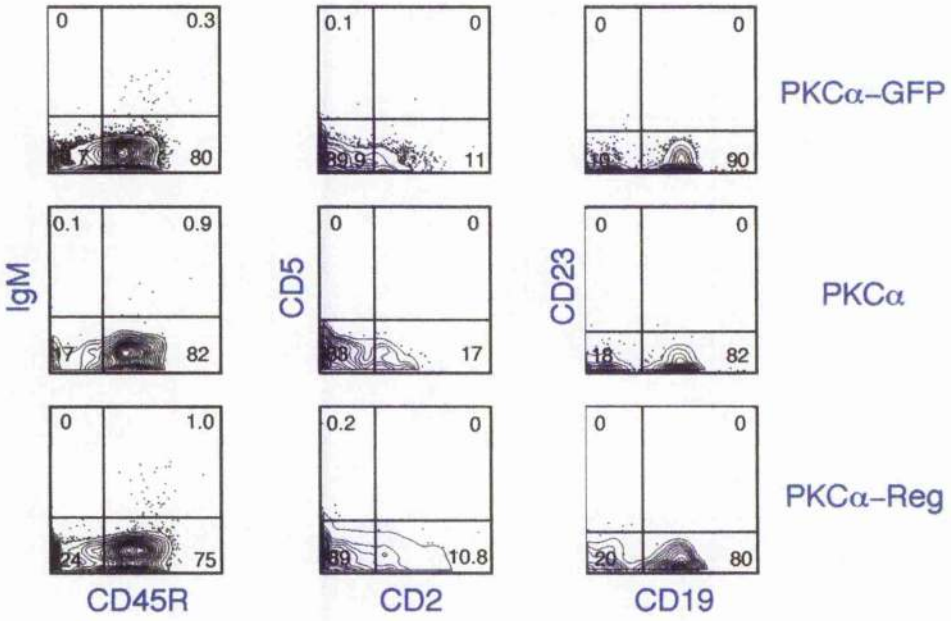
0
0.3
80
0.1
0
11
0
0
90
PKCα–GFP
IgM
CD5
CD23
0.1
0.9
17
82
0
0
17
0
0
18
82
PKCα
0
1.0
24
75
0.2
0
10.8
0
0
20
80
PKCα–Reg
CD45R
CD2
CD19

Figure 3.11 GFP$^+$ cells were detected in MIEV-HPC-reconstituted RAG-1$^{-/-}$ mice

The retroviral vector MIEV encode EGFP protein and MIEV infected cells can be monitored throughout the experiments by virtue of GFP. 1×10^6 HPCs from ICR mice were injected into RAG-1$^{-/-}$ mice and the amount of reconstituted cells was analysed at 4-6 weeks post injection by FCM with H-2K^q staining, which is a surface marker specific to donor, ICR mice. The correlation of the GFP$^+$ population in MIEV-HPCs before injection and the amount of reconstituted H-2K^{q+} cells is shown. The values described were the average (n=2-4 mice/point) ± SEM (top). RAG-1$^{-/-}$ mice injected with 1×10^6 MIEV-HPCs were sacrificed at 4-6 weeks post injection. Cells from spleen and thymus prepared for FCM and cells shown were gated on GFP and analysed for the B and T cell markers; CD45R vs. IgM and CD4 and CD8. Contour plots were size gated on FSC vs. SSC and live gated based on exclusion of PI stained cells. Percentages as indicated in corner of quadrants (bottom).

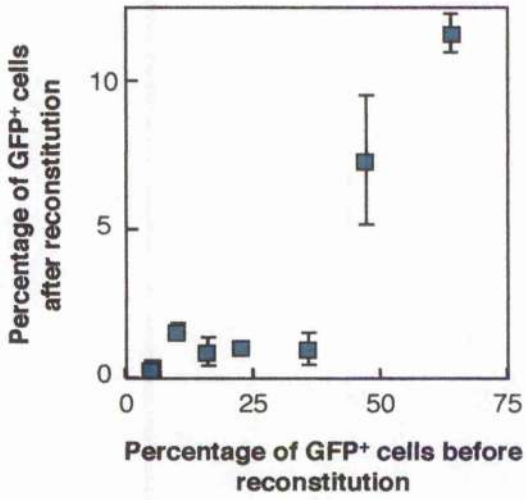
Percentage of GFP+ cells after reconstitution
10
5
0
0
25
50
75
Percentage of GFP+ cells before reconstitution

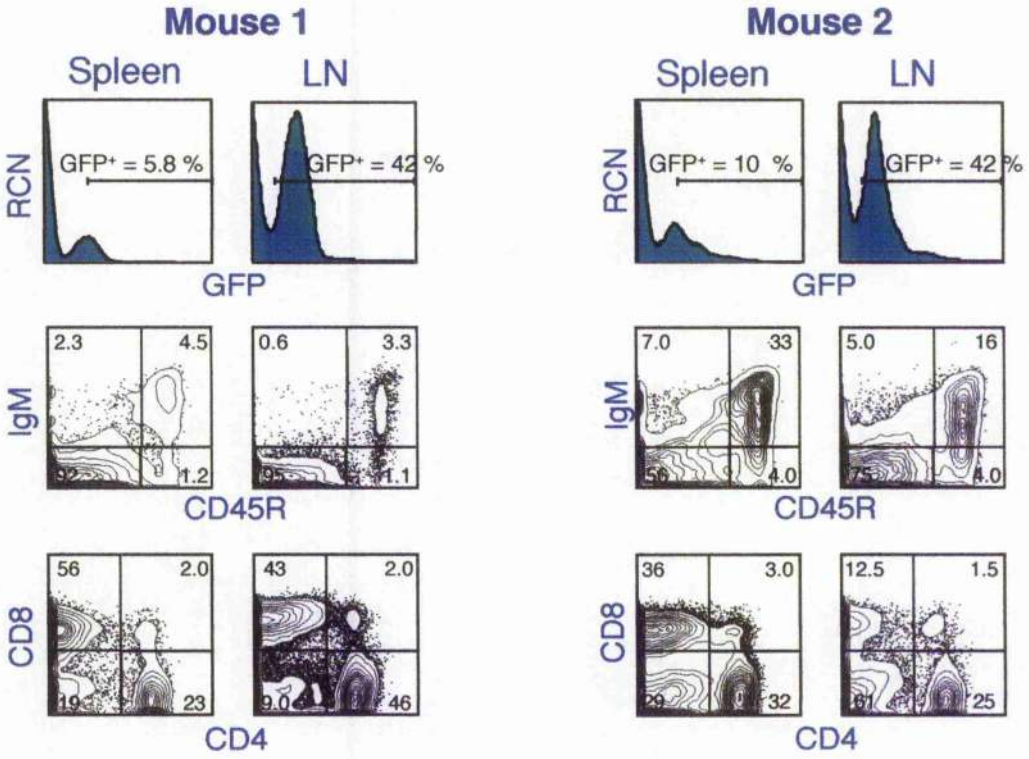
Mouse 1
Spleen
LN
RCN
GFP+ = 5.8 %
GFP+ = 42 %
GFP
IgM
2.3
4.5
92
1.2
0.6
3.3
95
1.1
CD45R
CD8
56
2.0
19
23
43
2.0
9.0
46
CD4
Mouse 2
Spleen
LN
RCN
GFP+ = 10 %
GFP+ = 42 %
GFP
IgM
7.0
33
56
4.0
5.0
16
75
4.0
CD45R
CD8
36
3.0
29
32
12.5
1.5
61
25
CD4

Figure 3.12 GFP$^+$ PKCα-KR-expressing cells showed enhanced proliferation *in vivo*

MIEV- and PKCα-KR-retrovirally-infected HPCs prior to injection into RAG-1$^{-/-}$ mice (pre-injection) and splenocytes derived from RAG-1$^{-/-}$ mice reconstituted with 1 x 10^6 MIEV- or PKCα-KR-retrovirally-infected HPCs (post-reconstitution) after 4-6 weeks injection were analysed their GFP intensity by FCM. The results were size gated on FSC vs. SSC and live gated based on exclusion of PI stained cells. Representative data of more than 10 separate experiments is shown.

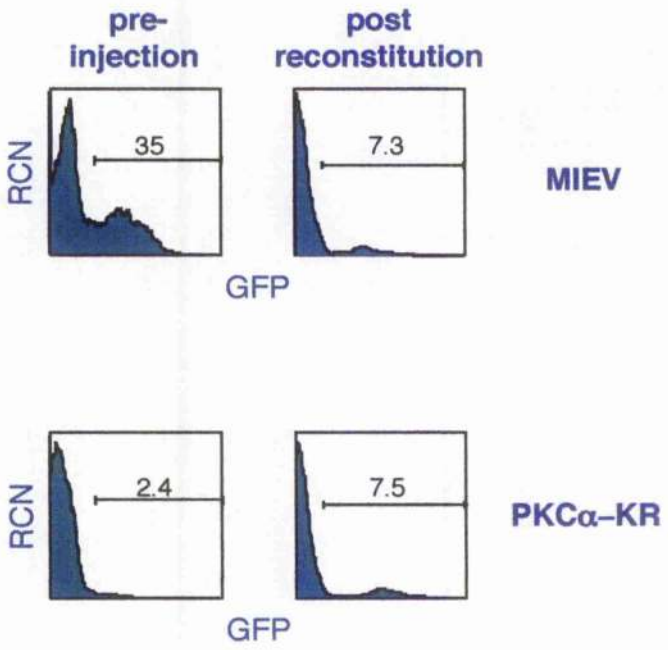
pre-
injection
post
reconstitution
RCN
35
7.3
MIEV
GFP
RCN
2.4
7.5
PKCα–KR
GFP

Figure 3.13 Splenocytes from PKCα-KR-infected-HPC injected RAG-1$^{-/-}$ mouse displayed a CLL-like phenotype

1×10^6 of either PKCα-KR- or MIEV-infected cells were i.p. injected into RAG-1$^{-/-}$ mouse. Spleen cells from reconstituted mice were analysed 3 week after the injection. FCM was carried out on GFP$^-$, GFP^{low} and GFP^{hi} populations, IgM vs. CD45R, IgD vs. CD45 and CD23 vs. CD19, percentages as indicated. Plots were live and size gated. This is a representative experiment from five separate adoptive transfers.

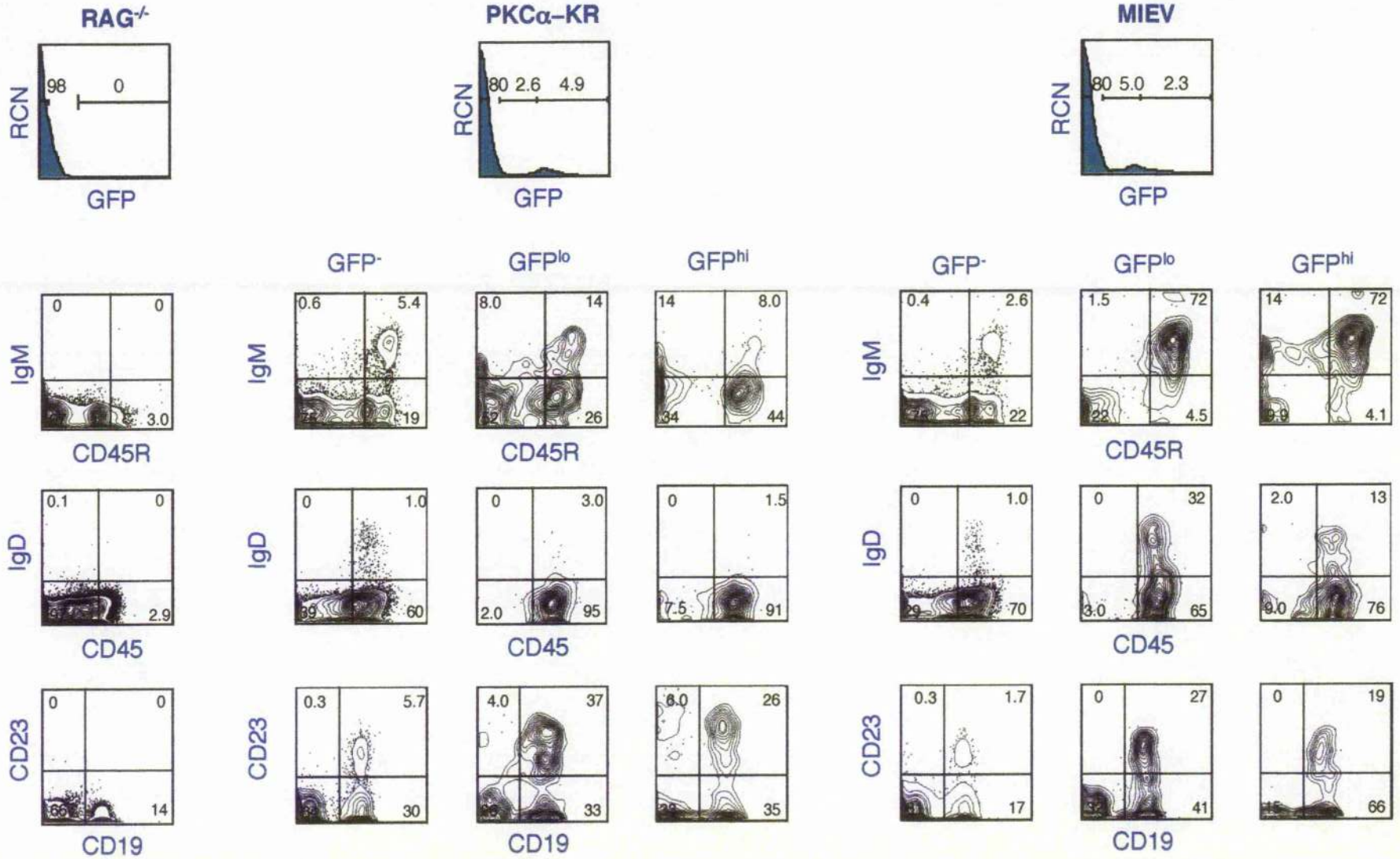
RAG-/-
PKCα–KR
MIEV
RCN
GFP
98
0
80
2.6
4.9
80
5.0
2.3
GFP-
GFPlo
GFPhi
IgM
CD45R
IgD
CD45
CD23
CD19
0
0
3.0
0.6
5.4
19
8.0
14
26
14
8.0
34
44
0.4
2.6
22
1.5
72
4.5
14
72
9.9
4.1
0.1
0
2.9
0
1.0
60
0
3.0
2.0
95
0
1.5
7.5
91
0
1.0
29
70
0
32
3.0
65
2.0
13
9.0
76
0
0
14
66
0.3
5.7
30
4.0
37
33
6.0
26
35
0.3
1.7
17
0
27
41
0
19
66

Chapter 4:

Subversion of PKCα signalling results in the outgrowth of a population of B lineage cells that have key hallmarks of CLL

4.1 Introduction

4.1.1 The potential link between PKC and CLL

Although PKC-mediated signalling pathways are suggested to be associated with the survival of CLL cells, the role of individual PKC isoforms has not been well elucidated. Previously, it was reported that activation of PKC with phorbol esters and bryostatin, which structurally mimic DAG and bind to the regulatory domain of cPKC and nPKC, thus triggering activation of these PKC isoforms, decreases spontaneous and chemotherapy-induced apoptosis in CLL cells (Barragan et al, 2003). Moreover, the PKC activation by byrostatin upregulates Mcl-1 and X-linked inhibitor of apoptosis proteins (IAP) expression, which correlates with cell survival (Kitada et al, 1999). In accordance with this, treatment of CLL cells with the nPKC inhibitor, rottlerin (Ringshausen et al, 2006, Ringshausen et al, 2002), or the pan PKC inhibitors, bisindolylmaleimide I (BisI) (Barragan et al, 2002) or UCN-01, a straurosporine derivative, (Kitada et al, 2000) induces apoptosis of CLL cells. Among all the isoforms, PKCδ is considered as a causative molecule in CLL because this PKC isoform is constitutively expressed in human samples and phosphorylated on tyrosine in a PI3K dependent manner (Alkan et al, 2005, Ringshausen et al, 2002). Therefore, PKCδ may act as a downstream effecter in the survival of these leukaemic cells. In addition to PKCδ, constitutive expression of PKCβ, γ, and ζ isoforms have been observed in human CLL, and at best, a low level of PKCα expression was detected in CLL samples (Alkan et al, 2005). Moreover, the overall PKC activity in CLL appeared lower compared to acute myeloid leukaemia (AML) and acute lymphoblastic leukaemia (ALL) samples (Komada et al, 1991). This relatively low PKC activity and lack of PKCα expression in human CLL may have an important bearing on our CLL model that results from the subversion of PKCα.

4.2 Aims and Objectives

It was interesting and surprising to find that the subversion of PKCα in HPCs resulted in the generation of CLL-like cells with enhanced proliferation. Therefore, the mechanisms that underlie this transform event both *in vitro* and *in vivo* were chosen to study, because to date, there are no good animal models available to study CLL. Therefore, to gain a deeper understanding of our CLL system, the aims of this chapter were:

i. To confirm the expression of PKCα-KR in retrovirally infected primary cells *in vitro*.
ii. To analyse cell cycle and proliferation level in PKCα-KR-expressing cells *in vitro*.
iii. To examine anti-apoptotic mechanisms in PKCα-KR-expressing cells *in vitro*.
iv. To test the effects of IL-7 in PKCα-KR-expressing cells *in vitro*.
v. To examine the expression of IgM molecules in PKCα-KR-expressing cells *in vitro*.
vi. To study the cell cycle in cells generated from PKCα-KR-HPCs and MIEV-HPCs *in vivo*.
vii. To assess the signalling pathways associated with CLL survival *in vitro*.
viii. To identify the molecular mechanisms that are modulated by PKCα-KR to drive oncogenesis.

4.3 Results

4.3.1 Confirmation of PKCα-KR expression in PKCα-KR-FL cells

Previously, PKCα-KR expression in GP+E.86-PKCα-KR packaging line was determined by HA staining due to a HA tag fused to C-terminus of the PKCα-KR construct as described in Section 3.3.3, now the intracellular HA expression in PKCα-KR-expressing FL cells was tested. FCM analysis revealed that 66 % of HA^+ cells among GFP^+ PKCα-KR-expressing cells, but not in GFP^+ MIEV-expressing cells at day 16 of coculture. Of note, MIEV-expressing cells expressed GFP higher than PKCα-KR-expressing cells, possibly due to the lack of gene of interest (Fig. 4.1).

4.3.2 Attenuation of kinase activity in PKCα-KR-expressing cells at early stage is important for leukaemic events

The level of PKC activity was examined in PKCα-KR- and MIEV-expressing cells at day 10 by non-radioactive ELISA-based kinase assay. As described in Section 3.3.4 that showed the reduction of kinase activity in GP+E.86-PKCα-KR, a 50 % reduction in kinase activity was detected in PKCα-KR-expressing cells compared to MIEV-expressing cells at d10 culture (Fig. 4.2). A radioactive PKC kinase assay detecting ^{32}P-labelled PKC-specific substrate peptide was also carried out and this revealed that 33 % attenuation in the activity in d10 PKCα-KR-expressing cells compared to d10 MIEV-expressing cells (Fig. 4.3 top), but surprisingly, PKC activity increased 16 % in d17 PKCα-KR-expressing cells relative to d17 MIEV-expressing cells (Fig. 4.3 bottom). In support of the decreased PKCα activity in PKCα-KR-expressing cells at day 10, Western blots analysis revealed a decreased level of serine phosphorylation of downstream substrates of PKC in lysates derived from PKCα-KR-expressing cells compared to MIEV-expressing cells. In addition, a reduction in the level of phosphorylation of PKC substrates was noted on TPA stimulation in PKCα-KR-expressing cells compared to MIEV (Fig. 4.4).

A similar expression level of PKCα was found in the lysate of PKCα-KR-expressing cells compared to that of MIEV-expressing cells at day 10 when they were probed with anti-PKCα antibody (Fig. 4.5). The same blot was stripped and reprobed with anti-pan-phospho-PKC antibody that can recognise PKC phosphorylated at a carboxyl-terminal residue homologous to serine 660 of PKC βII. Phosphoryl isoforms can be differentiated by virtue of size: PKCε, 85kDa; PKCα, 82kDa; PKCβI, βII, η and θ, 80 kDa; PKCδ, 78kDa. Utilising this antibody, it was demonstrated that PKCα is the only phosphorylated PKC isoform detected within these cells, as these bands were in the same location as those of anti-PKCα probed blot. The level of phosphorylation was similar among all the samples (Fig. 4.5).

4.3.3 Growth advantage in PKCα-KR-expressing cells occurs as a result of explosive proliferation

A growth advantage of GFP$^+$ PKCα-KR-expressing cells over GFP$^-$ population was observed as described in Section 3.3.5, therefore, PI staining was carried out to assess potential changes in the cell cycle. This set of analysis was performed on day 12 PKCα-KR- and MIEV-expressing cells as >90% of PKCα-KR-expressing cells were GFP$^+$ at this stage (Fig. 3.9A). The analysis showed that there was no significant difference in the cell cycle pattern between PKCα-KR-expressing cells and MIEV-expressing cells. However, these data confirmed that the relative elevation in cell number in PKCα-KR-expressing cells was not due to an increase in apoptosis in MIEV-expressing cells (Fig. 4.6). To address whether the elevation in cell number in GFP$^+$ PKCα-KR-expressing cells was due to an enhanced proliferation, the cells were analysed by BrdU incorporation to measure the level of DNA synthesis in the cell cultures. This set of analysis revealed that 55 % PKCα-KR-expressing cells were in the S phase compared with 42 % MIEV-expressing cells (Fig. 4.7). It was noted that PKCα-KR-expressing cells possessed an increased proliferative capacity as shown by their ability to incorporate 1.3 times more BrdU compared with MIEV-expressing cells. Taken together, these results show that in the presence of

OP9 cells and IL-7 the subversion of PKCα signals leads to an increase in the proliferative capacity of B lineage cells.

4.3.4 The level of expression of cyclin-dependent kinase inhibitors, $p21^{waf-1}$ and $p27^{kip-1}$, was relatively higher in PKCα-KR-expressing cells

In order to investigate the mechanism that underlies enhanced proliferative capacity in PKCα-KR-expressing cells, the transcript level of CDK inhibitors, $p21^{waf-1}$ and $p27^{kip-1}$, was examined. The mRNA was extracted from the PKCα-KR- and MIEV-cultures at the indicated day in the figure legend and semi-quantitative RT-PCR was carried out using either $p21^{waf-1}$ specific or $p27^{kip-1}$ specific primer pairs. Interestingly, the mRNA level of both $p21^{waf-1}$ and $p27^{kip-1}$ was maintained in PKCα-KR-expressing cells throughout the culture, whereas those of MIEV were diminished by day 14 compared with β2m (Fig. 4.8).

4.3.5 PKCα-KR-expressing cells are able to evade apoptosis

One of the hallmarks of CLL is the accumulation of B lineage cells that are arrested at the G_0/G_1 phase of the cell cycle and refractory to apoptosis (Bannerji and Byrd, 2000). To test whether PKCα-KR-expressing cells are able to survive in the absence of both OP9 cells and IL-7, GFP^+ cells were counted by FCM after withdrawal of both factors. PKCα-KR- and MIEV-expressing cells were cultured in the presence of OP9 cells and IL-7 up to day 12, and then 1×10^4 cells from each condition were cultured for 3 consecutive days in the absence of both OP9 cells and IL-7 and an aliquot from each culture was counted by FCM. The results showed that PKCα-KR-expressing cells were able to survive under these conditions for 3 days, while the majority of MIEV-expressing cells were dead after 2 days in culture, indicating that PKCα-KR-expressing cells are transformed and are able to evade cell death (Fig. 4.9). PI analysis on day 14 of culture, i.e. after 2 days in culture in the absence of OP9 cells and IL-7, revealed that 3.4-fold more cells were at the sub G_0/G_1 stage in MIEV-expressing cells, representing cells that were undergoing apoptosis. This finding indicated that the PKCα-KR-expressing cells were able to evade apoptosis (Fig. 4.10). Moreover, 75 % of PKCα-KR-expressing cells

were halted in the G_0/G_1 phase >2-fold higher than 35 % MIEV-expressing cells. When the capacity of cells to incorporate BrdU was analysed using day 14 cultures under the same condition, 20 % of the PKCα-KR-expressing cells were still cycling whereas only 6.5 % of MIEV-expressing cells were cycling (Fig. 4.11).

4.3.6 The level of Bcl-2 and Mcl-1 transcripts in PKCα-KR-expressing cells is relatively higher than in MIEV-expressing cells

To gain an understanding of the mechanism by which PKCα-KR-expressing cells modulate apoptotic rates, the level of mRNA expression on anti-apoptotic Bcl-2 family members was analysed. The results of RT-PCR showed that Bcl-2 and Mcl-1 transcript levels remained elevated in day 14 PKCα-KR-expressing cells although they were downregulated in MIEV cultures. When normalised to β2m expression, the expression levels of Bcl-2 and Mcl-1 were 3.7-fold and 1.5-fold higher than those of MIEV at day 14, respectively (Fig. 4.12). In contrast, the level of Bcl-xL transcripts remained unchanged in both MIEV and PKCα-expressing cells. Collectively, these studies provide a casual link between the subversion of PKCα signalling in developing B lineage cells and the generation of a transformed population that can escape apoptosis via a process that likely involves the upregulation of Bcl-2 and Mcl-1.

4.3.7 IL-7 accelerates proliferation in PKCα-KR-expressing cells

To test the effects of IL-7 on the survival and proliferation of CLL-like cells, 1×10^4 day 12 PKCα-KR- and MIEV-expressing cells were cultured for further 3 days in the absence of OP9 cells and in the presence of IL-7, and then an aliquot of each culture was counted by FCM as indicated in the figure legend. These experiments suggested that IL-7 supported survival of MIEV-expressing cells during the culture, as our previous results indicated that no live cells were left after 3 day culture in the absence of both OP9 cells and IL-7 (Fig. 4.9). Indeed, 45 % of MIEV-expressing cells survived after 3 days (Fig. 4.13). Interestingly, this cytokine in the absence of OP9 cells induced pronounced proliferation on PKCα-KR-expressing cells, and the cell number increased 4.7-

fold after 3 days in culture, suggesting these cells may be more sensitive to IL-7 and do not require OP9 to proliferate (Fig. 4.13). Therefore, the level of mRNA expression on IL-7 receptor (IL-7R) was analysed. The results of RT-PCR showed that IL-7R transcript levels were elevated in both the MIEV and PKCα-KR compared to day 0 cultures at day 8, PKCα-KR-expressing cells further upregulated IL-7R at day 14 compared with MIEV cultures, resulting in a 1.9-fold higher expression in PKCα-KR-expressing cells at day 14. Taken together, our results show that IL-7 is an essential cytokine for the proliferation in PKCα-KR expressing cells.

4.3.8 Long-term culture, M-1 cells were established from PKCα-KR-expressing cells

M-1 cells were generated by culturing PKCα-KR-HPCs in the absence of OP9 cells and IL-7, and GFP^+ $CD5^{lo}$ population was sorted out by cell sorter as described in Section 2.4.10. The sorted cells were characterised by post-sort FCM analysis (Fig. 4.15). The cells were >99 % GFP^+ and $CD45R^+$. Most cells are $CD19^-$ and $CD23^-$ and there is the mixture of $CD5^+$ and $CD5^-$ population (Fig. 4.15), suggesting M-1 cells consist of mixed oligoclonal population. These cells were established for molecular analysis of long-term cultured CLL cells.

4.3.9 Recombined IgM molecules are expressed in PKCα-KR- expressing cells

As described in Section 3.3.6, the surface expression of IgM in PKCα-KR-expressing cells was reduced. Therefore, to examine the level of intracellular IgM expression, intracellular staining using anti-IgM antibody was carried out in both PKCα-KR- and MIEV-expressing cells. Confirming previous data, the surface IgM expression on PKCα-KR-expressing cells was only 0.33 %, which was 3.9-fold less than that of MIEV-expressing cells (Fig. 4.16). On the other hand, the percentage of intracellular IgM expression in PKCα-KR-expressing cells was 1.5 %, 4.5-fold higher than that of surface expression, whereas the percentage of intracellular IgM expression in MIEV-expressing cells was 2.5 %,

only 1.9-fold higher than that of surface expression (Fig. 4.16), suggesting that IgM is synthesised in PKCα-KR expressing cells, but actively withheld within the cell. Molecular analysis of the IgH in the D to J locus in both MIEV and PKCα-KR cellular populations revealed that a similar pattern of multiple, random rearrangements occurred in both populations, which is similar as that of the control, normal B cells from spleen of a wildtype mouse (Fig. 4.17). M-1 cells mainly possessed 1300 bp and 120 bp bands, $D_{H1}J_{H1}$ and $D_{H1}J_{H4}$, respectively, indicating that this cell line possibly developed from 2 clones, thus, they contained oligoclonal populations. $D_{H1}J_{H1}$ band was brighter than the lower $D_{H1}J_{H4}$ band, suggesting that one clone has dominantly expanded in the culture in the absence of OP9 cells or IL-7. These results served to confirm that the proliferating PKCα-KR population arose from a number of distinct transformed progenitor cells.

4.3.10 RAG-1$^{-/-}$ mice injected PKCα-KR-HPCs bore subcutaneous tumour, lymphadenopathy and splenomegaly

In addition to the generation of human CLL-like populations within the spleen and LN of PKCα-KR-HPCs injected mice as described in Section 3.3.9, a subcutaneous (s.c.) tumour cell mass was also noted at the site of injection. These tumours were only present in PKCα-KR-HPC injected mice and resembled an enlarged LN (Fig. 4.18 top). PKCα-KR-HPCs injected mice survived no longer than 6 weeks (Fig. 4.18 bottom). This is possibly because of progression of tumours that seems to be early onset in this *in vivo* model. The spleen from 1×10^5 PKCα-KR-HPCs injected mice was larger than that of 1×10^6 MIEV-HPCs injected mice (Fig.4.19 top). The splenomegaly in 1×10^6 PKCα-KR-HPCs injected mice accompanied the increase of GFP$^+$ population and the cellularity is 18-fold higher compared to that of 1×10^6 MIEV-HPCs injected mice (Fig. 4.19 bottom). Similar to spleen, lymphadenopathy was observed in these mice.

4.3.11 Tumour cells also showed typical CLL phenotype

FCM analysis of the tumour mass revealed that the majority of the cells were GFP$^+$ (89 %; Fig. 4.20), and phenotypically the cells resembled the CLL population observed in the spleen and LN (IgM^{lo}, CD23$^+$, CD5$^+$, CD19^{hi}, IgD^{lo} as described in Section 3.3.9). It has been shown previously that the level of gene expression in bicistronic retroviral vectors can be directly related to the intensity of GFP expression (Izon et al, 2001), therefore it is interesting to note that the expression levels of CD23, CD19 and CD5 were elevated with increasing GFP expression in the s.c. tumours. This was demonstrated by comparing the MFI for specific cell surface markers on B lineage cells in PKCα-KR GFP^{lo} compared with GFP^{hi} populations: CD19 (98.0 vs. 99.2), CD23 (90.1 vs. 172) and CD5 (23.2 vs. 66.7) (Fig. 4.20). Additionally, in agreement with our previous *in vitro* and *in vivo* data, IgM expression was downregulated on the tumour cells with increasing GFP expression levels (16.2 vs. 11.6; Fig. 4.20). This finding suggests that the frequency of CLL cells increases with elevating levels of PKCα-KR expression *in vivo*.

4.3.12 Tumour cells are halted at G_0/G_1 phase of cell cycle *ex vivo*

As enhanced proliferation was observed in PKCα-KR-expressing cells *in vitro* as described in Section 4.3.3 and *in vivo* (Fig. 3.12 and Table 3.1), the cell cycle profile was analysed by PI staining in *in vivo* samples. To obtain a most homogenous population of mature B cells or GFP$^+$/CD23$^+$-PKCα-KR expressing cells from MIEV- or PKCα-KR-HPCs-injected mice, respectively, MACS-sorting was carried out: IgD$^+$ cells from a mixture of spleen and LN of MIEV-HPCs-injected mice; IgD$^-$/CD23$^+$ cells from a mixture of spleen and LN of PKCα-KR-HPCs-injected mice, and; CD23$^+$ cells from tumours of PKCα-KR-HPCs-injected mice. The results revealed that tumours had a higher percentage of cells arrested in the G_0/G_1 stage *ex vivo* (92 %) compared with LN and spleen cells (82 %) from the same PKCα-KR mouse, indicating tumour cells did not divide, which is another striking feature of CLL (Fig. 4.21, d0). The mature B cells from spleen and LN of MIEV-HPCs-injected mouse also arrested at G_0/G_1, (95 %) as expected due to their quiescence (Fig. 4.21, d0). This is probably

because cells from spleen and LN are proliferating whereas tumour cells have undergone cell cycle arrest.

To determine whether the tumour cells could be induced to proliferate, therefore overcoming the cell cycle arrest, all the *in vivo* derived cells were seeded onto OP9 cells in the presence of IL-7 and the cell cycle profile was determined after 5 days in culture. Of interest, PI analysis revealed that the tumour cells re-entered cell cycle (G_2M/S, 6.0 % to 31.3 %), and the spleen and LN cells from PKCα-KR-HPCs-injected mice also proliferated more vigorously compared to the day 0 profile (G_2M/S, 17 % to 40 %), suggesting that these cells maintain the ability to re-enter the cell cycle when introduced into the proliferative conditions of the *in vitro* cultures (Fig. 4.21). Of note, tumour cells and LN cells from PKCα-KR-HPCs-injected mice did not apoptose, indicating that these cells were protected from apoptosis in the presence of OP9 cells and IL-7. On the other hand, the spleen and LN cells from MIEV-HPCs-injected mice were prone to apoptosis (13 %) and majority of the cells were halted at G_0/G_1 (Fig. 4.21).

4.3.13 The impact of pharmacological inhibitors on PKCα-KR-expressing cells were different depending on their developing stage

PI3K-, ERK-MAPK- and PKC-mediated pathways have also been implicated in mediating the survival of human CLL cells (Barragan et al, 2002, Ringshausen et al, 2006, Ringshausen et al, 2002). Therefore, to address whether these signalling pathways play a role in the survival of PKCα-KR-expressing CLL cells, PKCα-KR- and MIEV-expressing cells and M-1 cells were treated with pharmacological inhibitors (Section 2.2) for 24 h; PKC inhibitors (chelerythrine and rottlerin), MAPK inhibitors (U0126, SB203580 and PD98059) and PI3K inhibitors (LY294002 and wortmannin) were used as indicated. HPCs derived from wildtype mice were retrovirally infected with MIEV or PKCα-KR and cocultured with OP9 for 16 days, therefore the majority of PKCα-KR cocultures consisted of the retrovirally infected GFP^+ population. Phosphatidylserine exposure on the outer PM, which is an early indication of apoptosis, was detected using Annexin V and analysed by FCM.

Our studies revealed that addition of PKC inhibitors did not induce spontaneous apoptosis on any of the cell populations tested (Fig. 4.22A). Both U0126 and PD98059 (MEK inhibitors) selectively induced a significant increase of apoptosis in long-term cultured PKCα-KR expressing cell, M-1 (Fig. 4.22 top and middle). Thus a 6.4-fold increase in apoptosis was observed compared to MIEV-expressing cells at 10 μM U0126. The p38-MAPK inhibitor, SB203580 did not affect either MIEV- or PKCα-KR-expressing cells, suggesting that p38-MAPK is not involved in CLL-survival. Indeed, M-1 cell survival was enhanced upon treatment with 5 μM SB203580 (Fig. 4.22B bottom). LY294002 appeared to induce apoptosis at 10 μM to all the cells, but PKCα-KR-expressing cells were most sensitive and thus the apoptosing ratio in PKCα-KR-expressing cells is 1.5-fold higher than MIEV-expressing cells (Fig. 4.22C top). Wortmannin caused apoptosis in both MIEV- and PKCα-KR-expressing cells, but not in M-1 cells (Fig. 4.22C bottom). Next, day 10 cocultures were treated with U0126 and LY294002 and the amount of apoptosis was analysed by FCM. Similar to that noted in d17 cocultures, apoptosis was observed in response to U0126 at day 10. However, day 10 MIEV-expressing cells were more sensitive than PKCα-KR-expressing cells to LY294002, which is opposite to that observed in day 17 cultures (Fig. 4.23). Taken together, ERK-MAPK and PI3K pathways seem to be key signalling pathways for survival in PKCα-KR-expressing cells and the mechanism of regulation by these pathways is different depending on the duration of culture.

4.3.14 PI3K and ERK signalling pathways were involved in PKCα-mediated transform

In order to further address the role played by the ERK-MAPK and PI3K pathways, the phosphorylation status of ERK1/2 and AKT, which is a downstream target of PI3K, was analysed in retrovirally infected HPCs and M-1 cells by Western blots. HPCs from wildtype mice FL were retrovirally infected with MIEV or PKCα-KR and cocultured with OP9 for up to 15 days. Whole cell lysates were prepared and resolved by SDS-PAGE. The resultant gel was

transferred to PVDF membrane and probed with anti-pERK1/2 antibody and anti-pAKT(T308). Of note, PKCα-KR-expressing cells exhibited an elevation in phosphorylation of ERK1/2, with a marked increase in ERK1 phosphorylation during the early stages of the coculture, whereas there was weak phosphorylation detected on ERK1/2 in MIEV-expressing cells (Fig. 4.24). The phosphorylation level of ERK1/2 was sustained in PKCα-KR-expressing cells, with stronger phosphorylation of ERK2. However, surprisingly, M-1 cells lost the high phosphorylation levels of ERK1/2 during long-term culture. These results suggest that ERK1 signal may preferentially mediate proliferation and survival in CLL-like cells at proliferative early stage. Phosphorylation on T308 of AKT, which is necessary for maximal AKT activation (Gold et al, 1999), was evident in the ICR-day 8 MIEV cocultures, whereas no signal was detected in ICR-day 8 and day 15 PKCα-KR cocultures or at later stages of the cultures. In samples derived from Rag-$1^{-/-}$ mice whose B cells are blocked pro-B cell stage, higher phosphorylation of AKT was noted compared with wildtype mice. This is possibly because AKT is important at the pro-B cell stage of development. Of note, AKT was less phosphorylated in PKCα-KR-expressing cells. These results support previous findings that AKT is essential for normal B lymphocyte development (Fruman et al, 1999), but may not be responsible for the aberrant survival of PKCα-KR cells.

4.4 Discussion

Collectively, these results indicate that the attenuation of PKCα signalling during early B cell development acts as an oncogenic trigger for developing B cells, resulting in the spontaneous generation of transformed cells that bear many of the hallmarks of CLL both *in vitro* and *in vivo*. The subversion of PKCα signalling in mouse HPCs generates a leukaemic population that has a striking resemblance to human CLL at the level of: (i) phenotype - $CD19^{hi}$ $CD5^{+}$ $CD23^{+}$ IgM^{lo}; (ii) cell cycle phase - halted in G_0/G_1 *ex vivo*, and; (iii) resistance to apoptosis - possibly due to an elevation in Bcl-2 and Mcl-1 expression. Moreover, PKCα-KR-expressing cells possess an enhanced proliferative capacity at the initiation of transformation both *in vitro* and *in vivo*. These data establish an important link between PKCα and CLL and provide an excellent model system to study the cellular and molecular mechanisms that drive the induction of CLL as well as role that PKCα specifically plays in the development of this disease.

This is to our knowledge the first time that PKCα has been specifically linked to the induction of CLL. PKC-mediated signalling pathways have been associated with the survival of CLL cells, but the role of individual PKC isoforms has not been elucidated (Barragan et al, 2002). As shown in the previous chapter, the ability to induce the development of CLL in HPCs only occurs upon PKCα, but not PKCδ or PKCζ subversion, suggesting that this is a unique property. This is supported by the fact that only PKCα is phosphorylated in early developing B cells (Fig. 4.5). When the PKCα-KR was expressed in developing B cells, certainly the reduction of PKCα activity was observed in the PKCα-KR early cultures (Fig. 4.2, 4.3 and 4.4), suggesting that the reduction in kinase activity at the early stage of B cell development is essential for B cell transformation. The different level of reduction in kinase activity was observed between non-radioactive ELISA kit (50 %) and radio active ^{32}P kit (33 %) (Fig. 4.2 and 4.3). The former is not PKC specific and thus is also able to assess

the PKA activity, suggesting that the activity of other kinase is reduced in PKCα-KR-expressing cells. However, an increased kinase activity was observed in the later PKCα-KR cultures, which may be caused by the transformation of B cells resulting in induction of enhanced PKCα activity. ^{32}P assay kit used is not specific for PKCα and may represent an increase in other PKC isoform activity, such as PKCδ, possible molecule for a cross-talk to PKCα (Koivunen et al, 2006). The growth advantage of PKCα-KR-expressing cells was accompanied by an enhanced proliferation and upregulation of $p21^{waf-1}$ and $p27^{kip-1}$ at mRNA level (Fig. 4.7 and 4.8). CDK inhibitors, $p21^{waf-1}$ and $p27^{kip-1}$, are known as a putative tumour suppressor, however, it has recently been suggested that they function as an oncogene when they are in cytoplasm not in nucleus (Blagosklonny, 2002). Therefore, the involvement of $p21^{waf-1}$ and $p27^{kip-1}$ in the progression of proliferation, is not counterintuitive.

IL-7 is an essential cytokine for mouse B cell development, survival and proliferation (Fry and Mackall, 2002). Murine developing B cells display a low threshold for IL-7-induced proliferation at pre-pro B cell stage and early pre-B cell stage. This sensitivity is lost at the late-pre B cell stage (Marshall et al, 1998). Proliferation of MIEV-expressing cells did not appear to be IL-7 dependent anymore (Fig. 4.13), indicating that MIEV cells had progressed beyond the late-pre B cell stage after day 12. However, the PKCα-KR-expressing cells exhibited pronounced level of IL-7 response, the transformation events may occur at either pre-pro B cell- or early pre-B cell-stage. IL-7Rα is upregulated as early as $CD45R^{+}$ $CD19^{-}$ B cell precursor stage and the expression is maintained until the early pre-B cell stage and is downregulated afterwards (Tudor et al, 2000). The RT-PCR results reveal that normal upregulation and downregulation of IL-7Rα occurred in MIEV-expressing cells, but PKCα-KR-expressing cells maintained the upregulated IL-7Rα (Fig. 4.14), which may be induced by their high response to IL-7. Moreover, IL-7 is known as a survival factor that induces anti-apoptotic Bcl-2 protein expression, such as Bcl-2 (Marsden and Strasser, 2003) and Mcl-1 (Opferman et al, 2003) in T cells. This high response to IL-7 and possible increased sensitivity to IL-7 by elevated

IL-7R expression in these cells may explain the relatively higher expression of Bcl-2 and Mcl-1.

It is becoming increasingly evident that CLL cells are resistant to apoptosis and arrested at the G_0/G_1 phase of the cell cycle (Bannerji and Byrd, 2000). In keeping with CLL cells, PKCα-KR-expressing cells have resistance to apoptosis induced by withdrawal of OP9 cells and IL-7, and moreover, majority of cells are arrested at G_0/G_1 cell cycle stage (Fig. 4.10). There was more BrdU incorporation in PKCα-KR-expressing cells compared to MIEV-expressing cells when they were cultured in the absence of OP9 cells and IL-7, therefore, indicating that PKCα-KR-expressing cells were still cycling in the absence of stroma and cytokines. The proliferative potential of PKCα-KR-expressing cells is reduced 2-fold in the absence of stroma and growth factors (Fig. 4.11) compared to normal culture conditions (Fig. 4.7) (58 % vs. 20 %), however, PKCα-KR-expressing cells did maintain their cellularity after 2 days in culture in the absence of OP9 cells and IL-7 (Fig. 4.9). *Bcl-2* family genes in CLL cells have long been reported to favour the suppression of apoptosis (Bannerji and Byrd, 2000), and a member of the Bcl-2 protein family, Mcl-1 was found to correlate with failure to undergo apoptosis in response to chemotherapy (Kitada et al, 1998). Therefore, the resistance of apoptosis in PKCα-KR-expressing cells may be explained by relatively higher level of Bcl-2 and Mcl-1 expression in these cells compared to control cells.

While tumours are not a characteristic of CLL, PKCα-KR-expressing cell injected mice generate s.c. tumour mass at the injection site *in vivo* (Fig. 4.18). Indeed, similar tumours develop when human CLL cells are s.c. injected into severe combined immuno deficiency (SCID) mice, suggesting that some PKCα-KR-HPCs became trapped s.c. at the time of injection and developed into tumours (Mohammad et al, 1996). Although spleen and LN cells from PKCα-KR-HPCs-injected mouse were in the G_2M/S phase when they were isolated, the tumour-derived cells arrested at G_0/G_1 stage, which is a hallmark of CLL. Presumably, there is no growth factor or stroma at the location where the

tumour formed, therefore, tumour cells may mirror the *in vitro* culture condition; no stroma or growth factor, which also arrested at G_0/G_1 stage. Interestingly, culture of these tumour-derived cells fresh *ex vivo* in the presence of OP9 cells and IL-7 renders them re-enter the cell cycle, which may explain two phases of this disease between proliferative and quiescent (Dighiero, 2005). Tumour-derived cells resulted in cell death when they were cultured in the absence of both OP9 cells and IL-7, a finding that is common in CLL cells isolated from patients (data not shown).

A previous report showed that human CLL samples expressed an increased percentage of IgM$^+$ cells intracellularly in spite of low surface IgM expression (Payelle-Brogard et al, 2002). This low level of surface expression is probably attributable to impairment of the glycosylation and folding of μ and Igα chains, leading to defective assembly and the retention of these chains in the ER compartment (Vuillier et al, 2005). It was demonstrated that PKCα-KR-expressing cells also displayed reduced level of the surface IgM expression, but there is a 4.5-fold more μ heavy chain in intracellular expression. Moreover, the D_H to J_H recombination pattern observed in PKCα-KR-expressing cells was similar to the control cells, therefore indicating that subversion of PKCα signalling in HPCs stimulates aberrant expansion of oligoclonal or possibly polyclonal population of developing B cells that resemble CLL. Further analysis is required to confirm this finding.

We have shown that treatment of both PKCα-KR- and MIEV-expressing cells with PI3K inhibitors induces an increase in apoptosis compared with the DMSO-treated control. These results support previous findings that AKT is essential for B lymphocyte development (Fruman et al, 1999). Previous studies in human CLL cells have demonstrated that while AKT phosphorylation was not detected using Western blotting techniques, these cells apoptose upon treatment with the PI3K inhibitor LY294002 (10 μM) (Ringshausen et al, 2002), this may also be the case in our PKCα-KR-expressing cells. However, as M-1 cells were not affected by LY294002 (Fig. 4.22C), PI3K may not be solely

responsible for the aberrant survival of PKCα-KR cells. Treatment of M-1 cells with MEK1 inhibitors induced a significant increase in apoptosis, while the level of apoptosis in MIEV- and PKCα-KR-expressing cells were unaffected upon treatment with these inhibitors. Studies assessing the phosphorylation status of ERK1/2 in MIEV-, PKCα-KR-expressing cells and M-1 cells reveal that while ERK1/2 are weakly phosphorylated in MIEV-expressing cells and M-1 cells, ERK1 is strongly phosphorylated in PKCα-KR-expressing cells (Fig. 4.24). In contrast, phosphorylation of AKT is evident only in MIEV-expressing cells at the early stage of development. The phosphorylation was most pronounced in RAG-1$^{-/-}$, supporting the notion that this is most important at the early stage. Despite of lack of detectable AKT phosphorylation in PKCα-expressing cells, these cells were more affected by PI3K inhibitors than MIEV-expressing cells. This implies that other downstream molecules of PI3K, such as Btk (Marshall et al, 2000), may be involved in the survival of PKCα-KR-expressing cells. Collectively, these studies suggest that PI3K- and ERK-MAPK-signalling pathways are differentially-regulated to induce survival during the progression of CLL cells. Further investigation of signalling pathways responsible for the induction of CLL will be performed using this model system.

In conclusion, this chapter reveals that PKCα-KR-expressing cells display a marked resemblance to human CLL at the level of: (i) phenotype - CD19^{hi} CD5^{+} CD23^{+} IgM^{lo}; (ii) resistance to apoptosis, possibly supported by elevation of Bcl-2 and Mcl-1; (iii) intracellular retention of IgM; and (iv) cell cycle phase (halted in G_0/G_1 *ex vivo*) coupled with potential for proliferation. Taken together, these showed important link between the subversion of PKCα signalling and the induction of CLL.

Figure 4.1 HA expression was confirmed in PKCα-KR-expressing cells
HPC-enriched FL cells were prepared from wildtype mice and retrovirally infected with MIEV or PKCα-KR and then seeded on OP9 cells in the presence of growth factors and cultured for 16 days. Unpermeabilised cells were analysed for GFP fluorescence by FCM, after PI discrimination of dead cells (upper plot). PKCα-KR expression was determined by examining HA expression. Cells were fixed and permeabilised before staining with an anti-HA antibody, to reveal the retrovirally introduced PKCα-KR construct (lower plot). These data are from a single experiment, representative of two separate experiments.

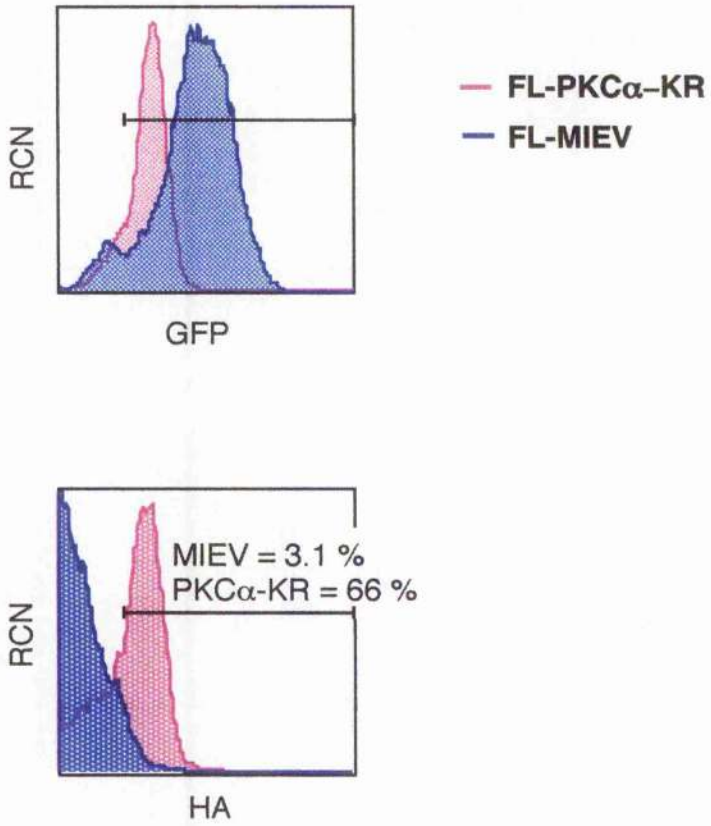
RCN
GFP
FL-PKCα–KR
FL-MIEV
RCN
MIEV = 3.1 %
PKCα-KR = 66 %
HA

Figure 4.2 PKCα-KR-expressing cells display a decrease in PKC activity at d10 of coculture

Cell lysates were prepared from MIEV and PKCα-KR retrovirally infected cells that were cultured for 10 days, before the determination of PKC activity with non-radioactive protein kinase assay kit. The graph shows the average % kinase activity (n=3/point) relative to MIEV-expressing control cells (100%); SEM shown. ***=p<0.0005 MIEV vs. PKCα-KR. The data are from a single experiment, representative of two separate experiments.

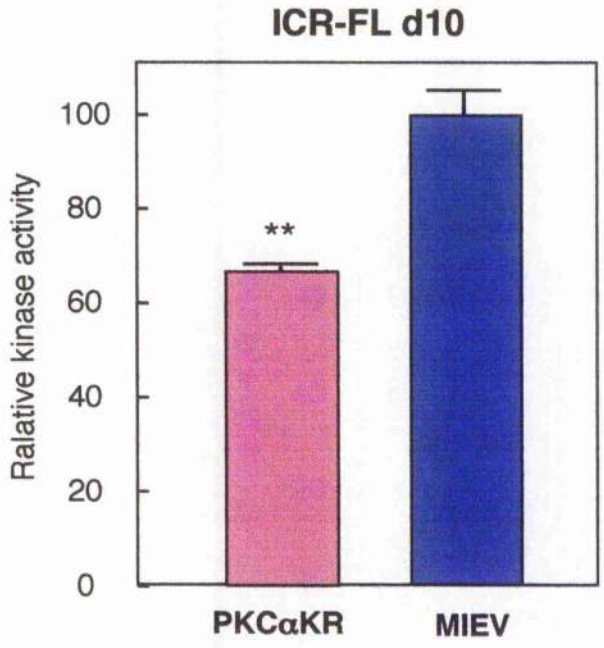

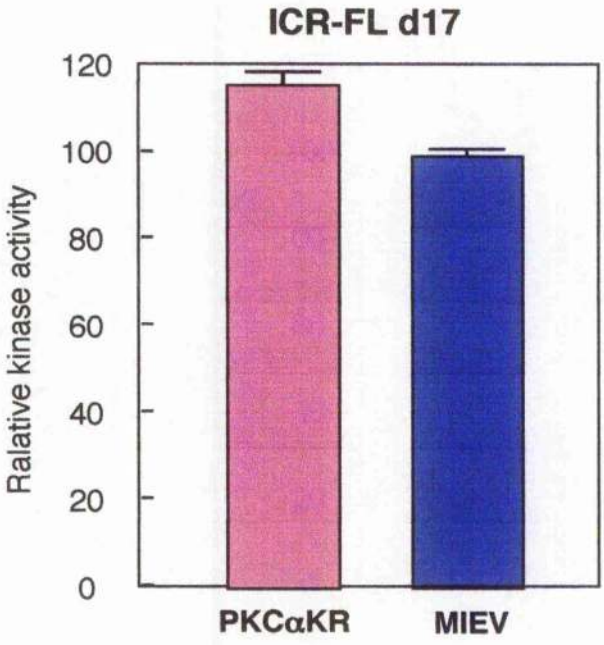

** $p < 0.005$ against MIEV

Figure 4.3 PKCα-KR-expressing cells display a decrease in PKC activity at early culture, but not in the late culture

Cell lysates were prepared from MIEV and PKCα-KR retrovirally infected cells that were cultured for either 10 or 17 days, before the determination of PKC activity with ^{32}P PKC kinase kit. The graph shows the average % kinase activity (n=2) relative to MIEV-expressing control cells (100%); SEM shown. **=p<0.005 MIEV vs. PKCα-KR. A representative of two separate experiments is shown.

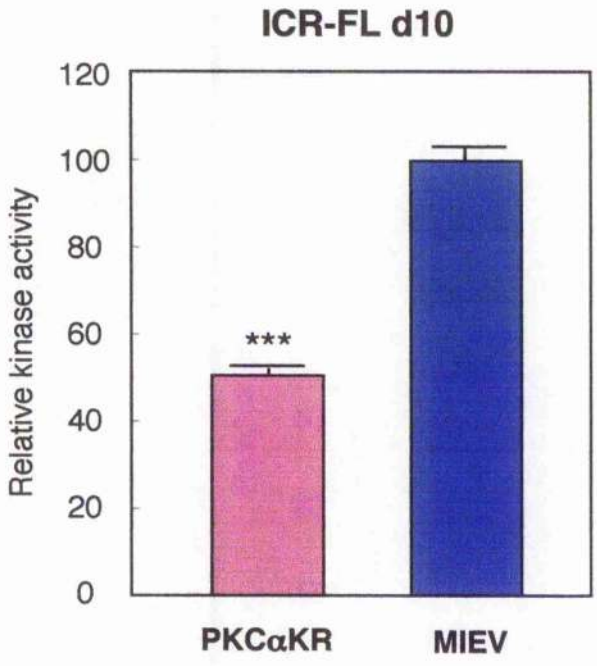

*** $p < 0.0005$ against MIEV

Figure 4.4 Phosphorylation level in PKC substrate was decreased in PKCα-KR-expressing cells

MIEV and PKCα-KR retrovirally infected cells cultured up to 10 day were incubated in the presence or absence of phorbol ester (0, 20, or 200 nmol/L TPA as indicated) for 30 min. Lysates were prepared and resolved by SDS-PAGE under reducing conditions and subsequently immunoblotted with a specific antibody against phosphoserine PKC substrates. The blot was stripped and reprobed with anti-ERK1/2 antibody. The data are from a single experiment, representative of two separate experiments.

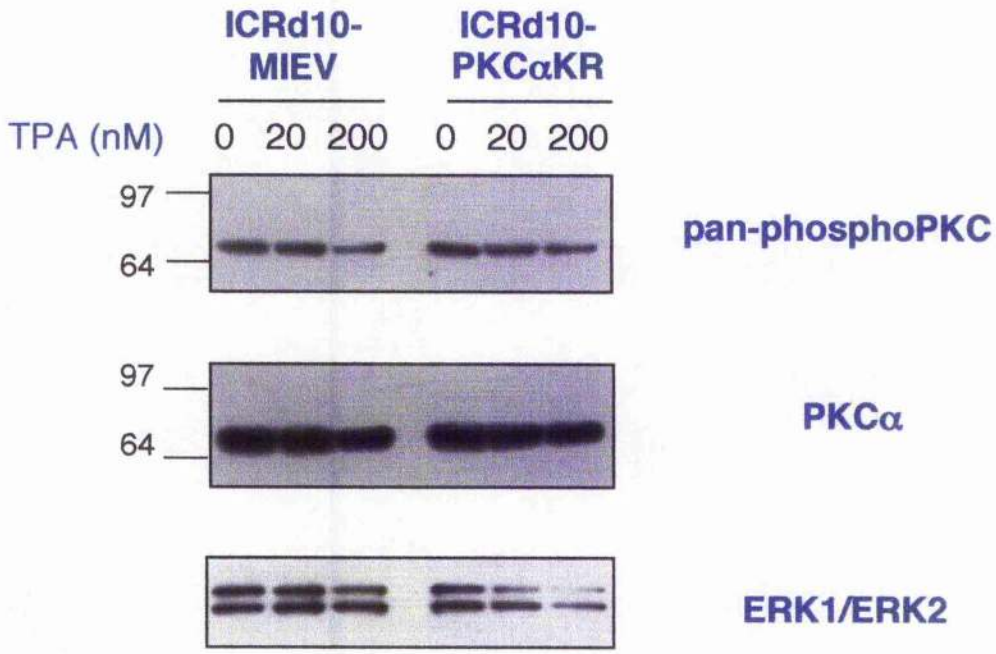
ICRd10-MIEV
ICRd10-PKCαKR
TPA (nM)
0 20 200 0 20 200
97
64
pan-phosphoPKC
97
64
PKCα
ERK1/ERK2

Figure 4.5 PKCα is not overexpressed in PKCα-KR expressing cells, but PKCα is the only phosphorylated isotype detected

MIEV and PKCα-KR retrovirally infected cells cultured up to 10 day were incubated in the presence or absence of phorbol ester (0, 20, or 200 nmol/L TPA as indicated) for 30 min. Lysates were prepared and resolved by SDS-PAGE under reducing conditions and subsequently immunoblotted with a specific antibody against PKCα. The blot was stripped and reprobed with anti-pan-phospho-PKC antibody. These data are from a single experiment, representative of two separate experiments.

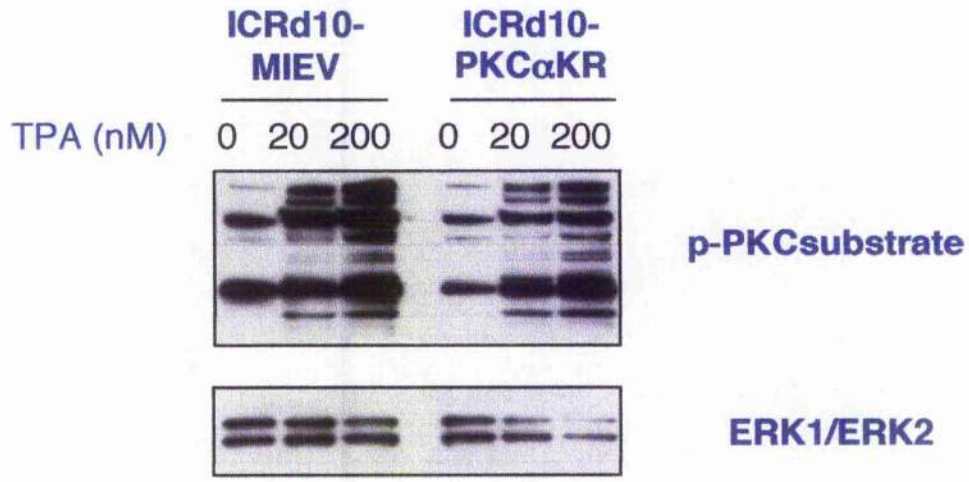
ICRd10-
MIEV
ICRd10-
PKCαKR
TPA (nM)
0 20 200 0 20 200
p-PKCsubstrate
ERK1/ERK2

Figure 4.6 There is no difference in the cell cycle between PKCα-KR-expressing and MIEV-expressing cells

MIEV and PKCα-KR retrovirally infected cells were seeded on OP9 cells in the presence of growth factors and cultured for 12 days. Then the cells were harvested by Lympholyte density gradient centrifugation and cultured in the same condition for further 2 days before PI analysis. Top, average ±SEM percentage of cells at the indicated cell cycle stage taken from four separate experiments. Bottom, histogram of DNA content vs. RCN is a representative of these experiments. The cellular data were size gated.

	$SubG_1$	G_0G_1	G_2M/S
MIEV	2.3 ± 0.47	58 ± 1.8	40 ± 1.8
PKCα-KR	2.3 ± 0.90	55 ± 1.4	43 ± 2.0

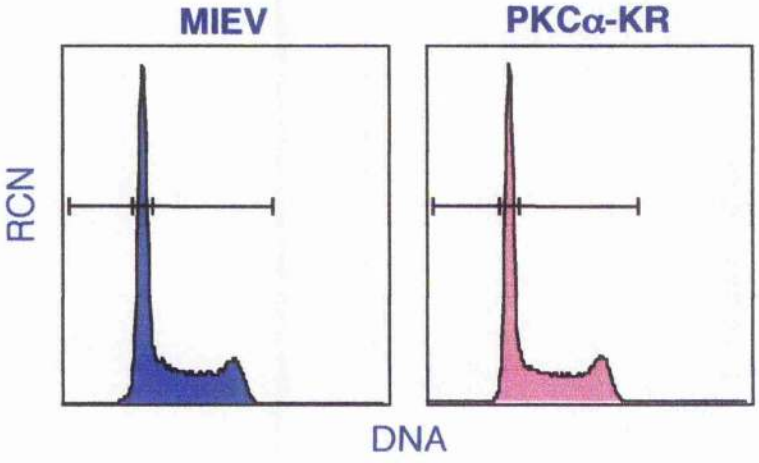

Figure 4.7 Enhanced proliferation gives PKCα-KR-expressing cells growth advantage

MIEV and PKCα-KR retrovirally infected cells were seeded on OP9 cells in the presence of growth factors and cultured for 12 days. Then, the cells were harvested by Lympholyte density gradient centrifugation and cultured on OP9 cells in the presence of growth factors for 2 days. BrdU solution was added 23 h prior to anti-BrdU antibody staining and subsequent FCM analysis. Cells were size gated before analysis of percentage of BrdU incorporation. The graph shows the average percentage of BrdU incorporated cells of three separate experiments; Average ±SEM shown. *=P<0.05, MIEV over PKCα-KR.

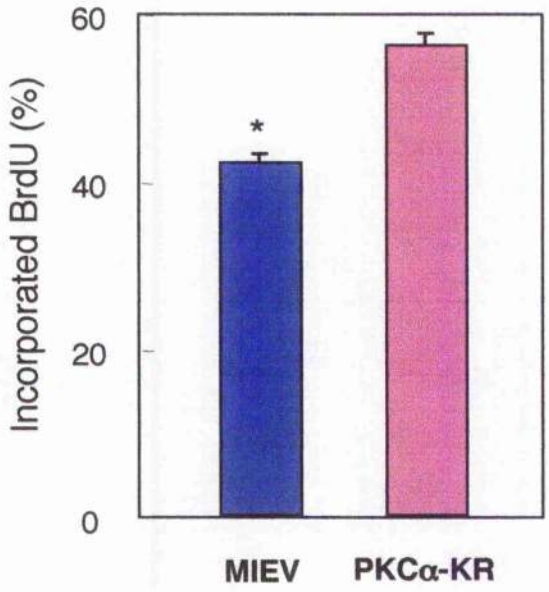
60
40
20
0
Incorporated BrdU (%)
*
MIEV
PKCα-KR

Figure 4.8 $p21^{waf-1}$ and $p27^{kip-1}$ mRNA was relatively higher in PKCα-KR-expressing cells to MIEV-expressing cells

MIEV and PKCα-KR retrovirally infected cells were seeded on OP9 cells in the presence of growth factors. Cells were removed at days 3, 8, and 14 of coculture and RNA/cDNA was prepared from the samples. Semi-quantitative RT-PCR was done with β2m, $p21^{waf-1}$, and $p27^{kip-1}$ primers (top). The bottom bar graph shows the relative expression of $p21^{waf-1}$ or $p27^{kip-1}$ normalized to β2m. The RNA level of indicated molecule in freshly prepared FL is calculated as 100 %. The representative is shown from two separate experiments.

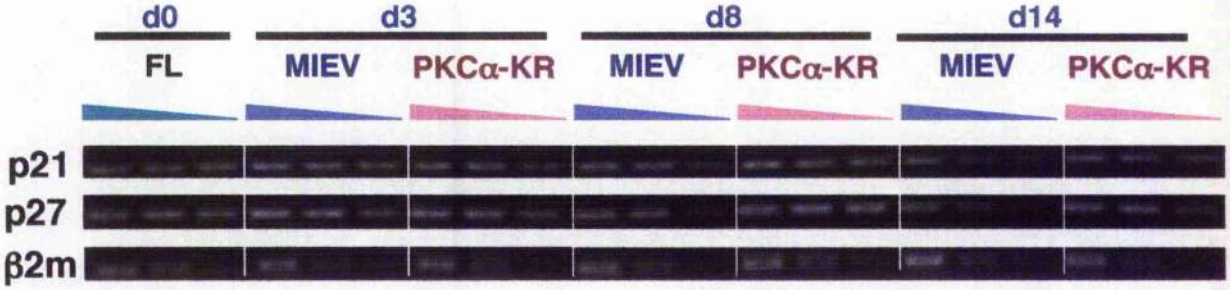
d0
d3
d8
d14
FL
MIEV
PKCα-KR
MIEV
PKCα-KR
MIEV
PKCα-KR
p21
p27
β2m

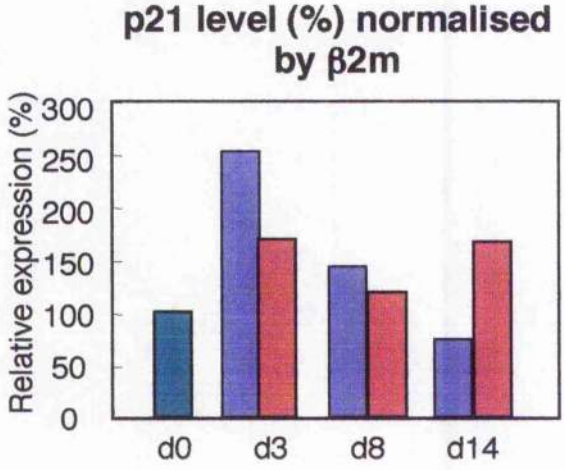
p21 level (%) normalised by β2m
Relative expression (%)
300
250
200
150
100
50
0
d0
d3
d8
d14

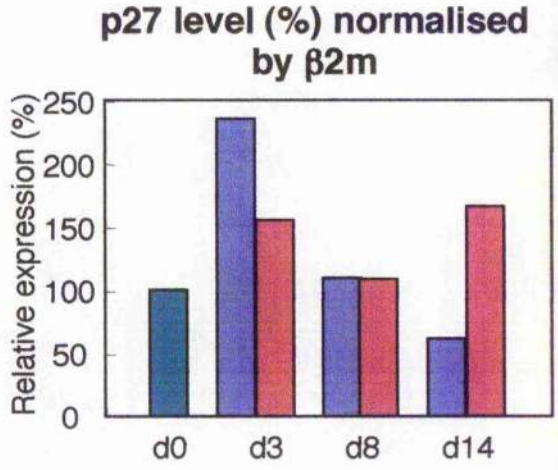
p27 level (%) normalised by β2m
Relative expression (%)
250
200
150
100
50
0
d0
d3
d8
d14

Figure 4.9 Subversion of PKCα signals enable cells to survive in the absence of stromal cells and growth factors

MIEV and PKCα-KR retrovirally infected cells were seeded on OP9 cells in the presence of growth factors and cultured for 12 days. Then the cells were harvested by Lympholyte density gradient centrifugation and cultured in the absence of both OP9 cells and growth factors (day 0; triplicate wells of a 24-well plate for each day of counting). Cells were then counted on the following 3 consecutive days by FCM. The graph shows the mean number of GFP^+ cells of three separate experiments; Average ± SEM shown. Cells were live and size gated.

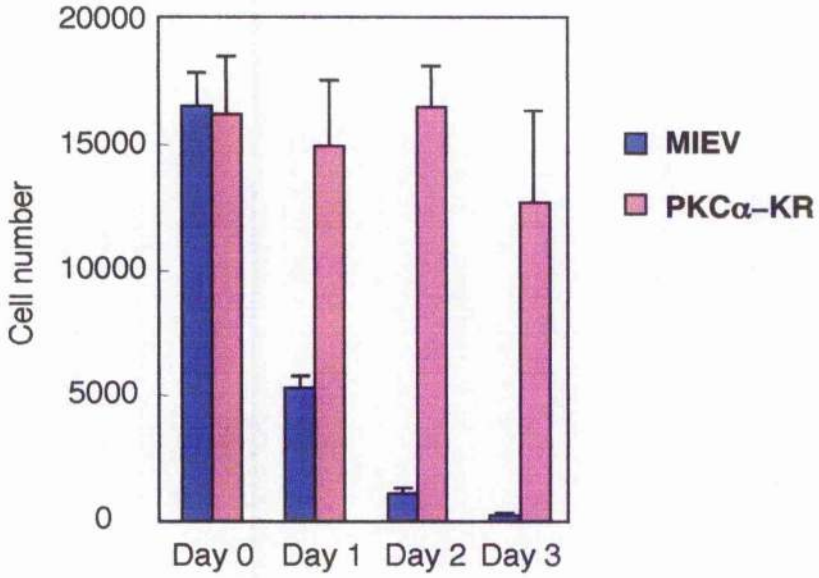
20000
15000
10000
5000
0
Cell number
Day 0
Day 1
Day 2
Day 3
MIEV
PKCα–KR

Figure 4.10 PKCα-KR-expressing cells were resistant to growth factor withdrawal-induced apoptosis

MIEV and PKCα-KR retrovirally infected cells were seeded on OP9 cells in the presence of growth factors and cultured for 12 days. Then the cells were harvested by Lympholyte density gradient centrifugation and cultured in the absence of OP9 cells and growth factors for further 2 days before PI analysis. Top, average ± SEM percentage of cells at the indicated cell cycle stage taken from four separate experiments. Bottom, histogram of DNA content vs. RCN is a representative of these experiments. The cellular data were size gated.

	SubG$_1$	G$_0$G$_1$	G$_2$M/S
MIEV	61 ± 4.9***	35 ± 4.6**	3.9 ± 0.46
PKCα-KR	18 ± 3.4	75 ± 3.9	7.7 ± 2.5

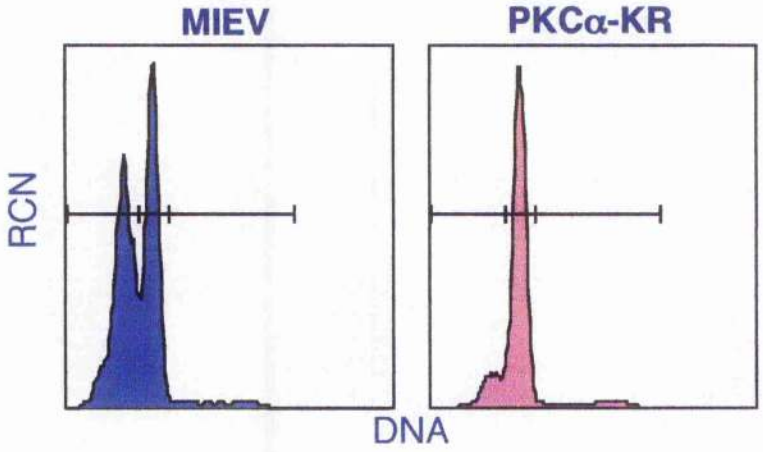

Figure 4.11 More PKCα-KR-expressing cells were cycling in the absence of OP9 cells and growth factors

MIEV and PKCα-KR retrovirally infected cells were seeded on OP9 cells in the presence of growth factors and cultured for 12 days. Then the cells were harvested by Lympholyte density gradient centrifugation and cultured on OP9 cells in the absence of growth factors for 2 days. BrdU solution was added 23 h prior to anti-BrdU antibody staining and subsequent FCM analysis. Cells were size gated before analysis of percentage of BrdU incorporation. The graph shows average percentage of BrdU incorporated cells of three separate experiments; Average ± SEM shown. *=$P<0.05$, MIEV over PKCα-KR.

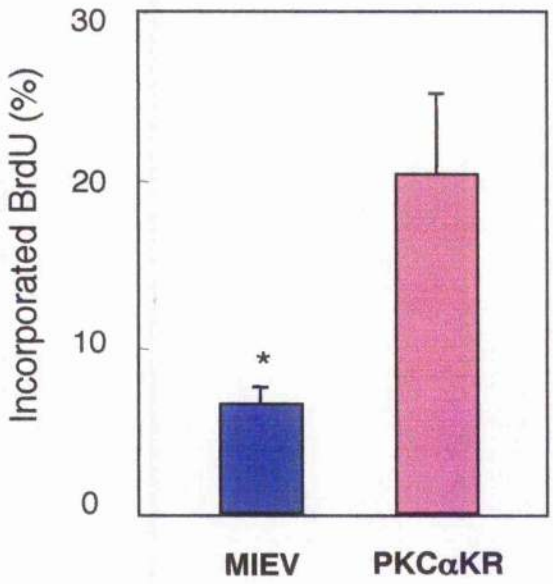
30
20
10
0
Incorporated BrdU (%)
*
MIEV
PKCαKR

Figure 4.12 Bcl-2 and Mcl-1 mRNA was relatively higher in PKCα-KR-expressing cells to MIEV-expressing cells

MIEV and PKCα-KR retrovirally infected cells were seeded on OP9 cells in the presence of growth factors. Cells were removed at days 3, 8, and 14 of coculture and RNA/cDNA was prepared from the samples. Semi-quantitative RT-PCR was done with β2m, Bcl-2, Mcl-1 and Bcl-xL primers (top). The bottom bar graph shows the relative expression of Bcl-2, Mcl-1 and Bcl-xL normalized to β2m. The RNA level of indicated molecule in freshly prepared FL is calculated as 100 %. The representative is shown from two separate experiments.

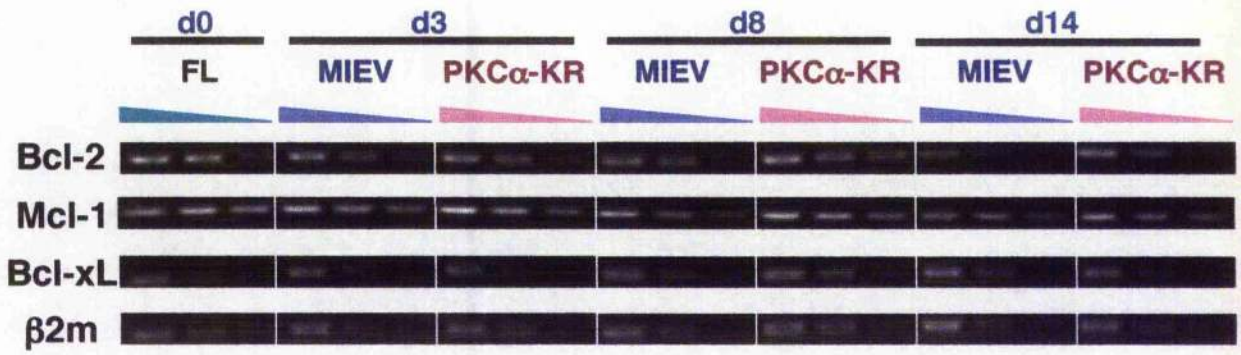
d0
d3
d8
d14
FL
MIEV
PKCα-KR
MIEV
PKCα-KR
MIEV
PKCα-KR
Bcl-2
Mcl-1
Bcl-xL
β2m

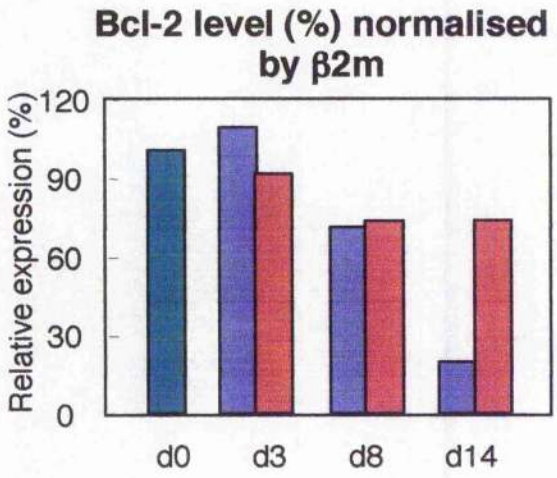
Bcl-2 level (%) normalised by β2m
Relative expression (%)
120
90
60
30
0
d0
d3
d8
d14

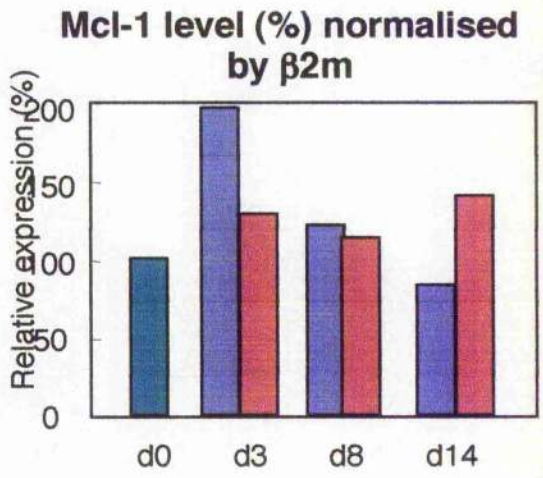
Mcl-1 level (%) normalised by β2m
Relative expression (%)
200
150
100
50
0
d0
d3
d8
d14

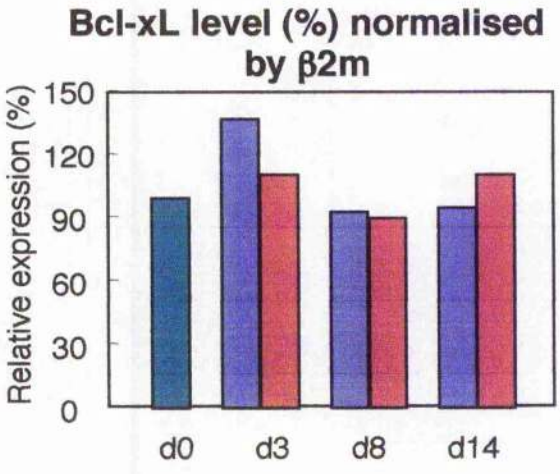
Bcl-xL level (%) normalised by β2m
Relative expression (%)
150
120
90
60
30
0
d0
d3
d8
d14

Figure 4.13 IL-7 induces PKCα-KR-expressing cells proliferate explosively
MIEV and PKCα-KR retrovirally infected cells were seeded on OP9 cells in the presence of growth factors and cultured for 12 days. Then the cells were harvested by Lympholyte density gradient centrifugation and cultured in the absence of OP9 cells and in the presence of IL-7 (day 0; triplicate wells of a 24-well plate for each day of counting). Cells were then counted on the following 3 consecutive days by FCM. The graph shows the mean number of GFP^+ cells of three separate experiments ±SEM. Cells were live and size gated. ***=P<0.0005, MIEV vs. PKCα-KR; **=P<0.005, MIEV vs. PKCα-KR.

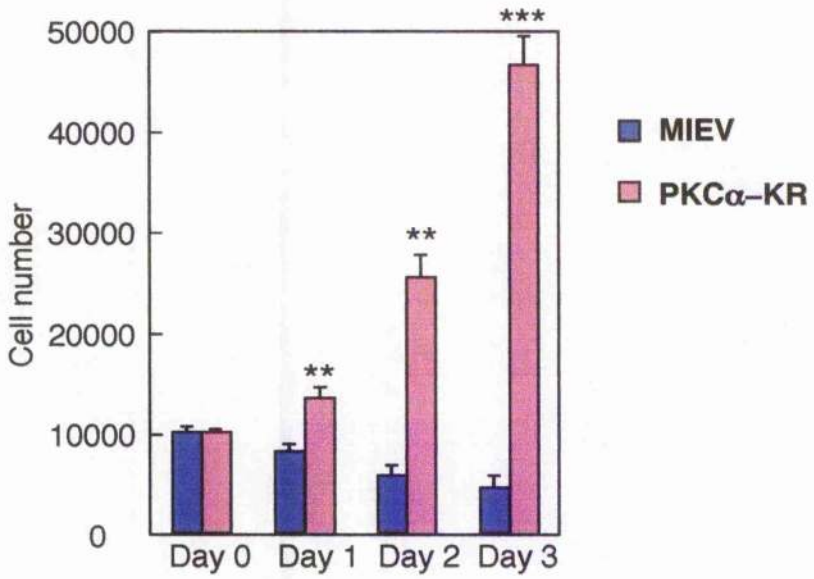
50000
40000
30000
20000
10000
0
Cell number
Day 0
Day 1
Day 2
Day 3
**
**
***
MIEV
PKCα–KR

Figure 4.14 IL-7Rα mRNA was upregulated in PKCα-KR-expressing cells
MIEV and PKCα-KR retrovirally infected cells were seeded on OP9 cells in the presence of growth factors. Cells were removed at days 3, 8, and 14 of coculture and RNA/cDNA was prepared from the samples. Semi-quantitative RT-PCR was done with β2m, IL-7Rα primers (top). The bottom bar graph shows the relative expression of IL-7Rα normalized to β2m. The RNA level of indicated molecule in freshly prepared FL is calculated as 100 %. The representative is shown from two separate experiments.


d0
d3
d8
d14
FL
MIEV
PKCα-KR
MIEV
PKCα-KR
MIEV
PKCα-KR
IL7-R
β2m

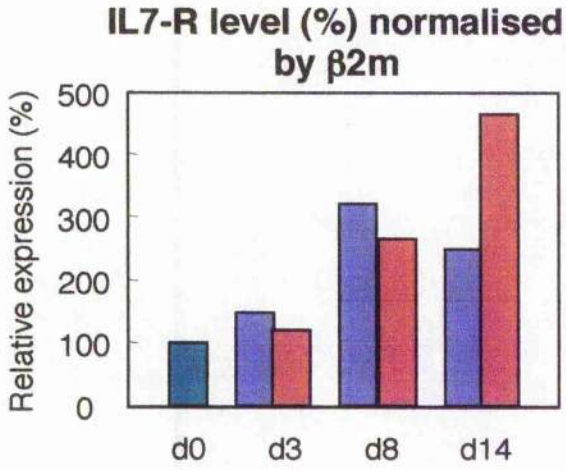
IL7-R level (%) normalised by β2m
Relative expression (%)
500
400
300
200
100
0
d0
d3
d8
d14

Figure 4.15 Phenotype analysis of M-1 cells

PKCα-KR retrovirally infected cells were cultured in the presence of OP9 cells and growth factors for 2 weeks, and cultured in the absence of OP9 cells and IL-7 as described in Section 2.4.10. M-1 cells were established by sorting out GFP^+ and $CD5^{lo}$ population. FCM analysis was carried out on established M-1 cells, CD5-APC vs. CD45R-PE and CD19-APC vs. CD23-PE; percentages are indicated. All FCM plots were live and size gated. These data are from a single experiment, representative of two separate experiments.

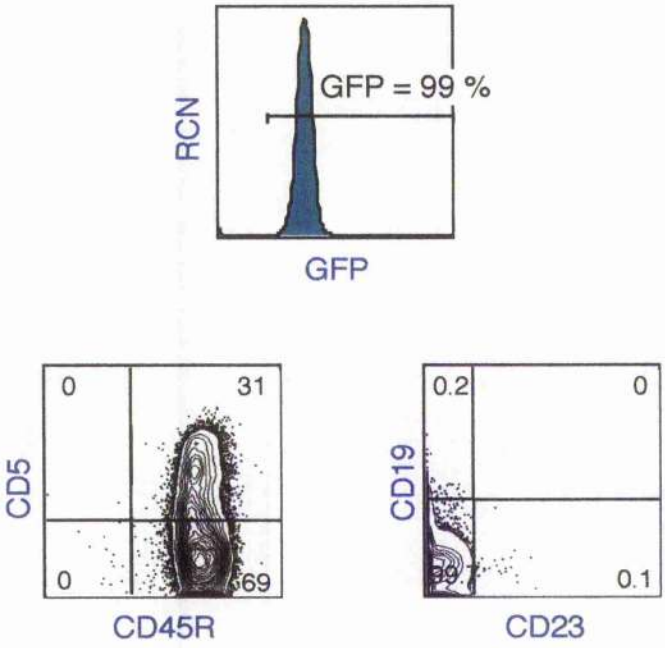
GFP = 99 %
RCN
GFP
0
31
0
69
CD5
CD45R
0.2
0
99.7
0.1
CD19
CD23

Figure 4.16 IgM is expressed intracellularly, but not on the surface in PKCα-KR-expressing cells

MIEV and PKCα-KR retrovirally infected cells were seeded on OP9 cells in the presence of growth factors and cultured for 19 days. Half of the cells were analysed for surface IgM expression (top). Half of the culture was fixed and permeabilised before staining with an anti-IgM antibody or isotype-matched antibody, to reveal the intracellular IgM level (bottom). An isotype-matched antibody was utilised for the control staining. Cells were size gated for both surface and intracellular staining, and dead cells were discriminated by gating out PI positive cells in surface staining. These data are from a single experiment, representative of three separate experiments.

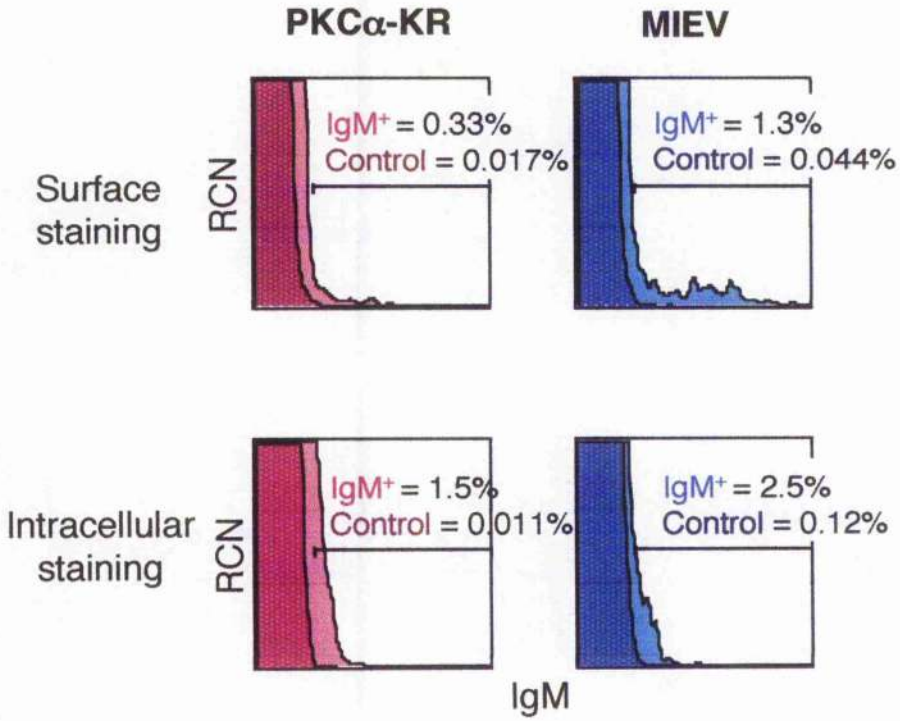
PKCα-KR
MIEV
Surface staining
Intracellular staining
RCN
IgM+ = 0.33%
Control = 0.017%
IgM+ = 1.3%
Control = 0.044%
IgM+ = 1.5%
Control = 0.011%
IgM+ = 2.5%
Control = 0.12%
IgM

Figure 4.17 IgM in PKCα-KR-expressing cells was D to J recombined

MIEV and PKCα-KR retrovirally infected cells were seeded on OP9 cells in the presence of growth factors and cultured for 15 days. Half of the cells were cultured under the same condition for further 4 days and the other half were cultured in the absence of OP9 cells and IL-7 for 4 days. Splenocytes from wildtype mouse and RAG-1$^{-/-}$ were obtained by crushing spleens followed by Lympholyte density graduation centrifugation. PCR was performed for the analysis of DNA rearrangements by amplifying DNA with specific primers flanking D_{H1} and J_{H4} of BCR locus. Amplifying the same DNA samples with primers specific for β2m. These data are from a single experiment, representative of two separate experiments.

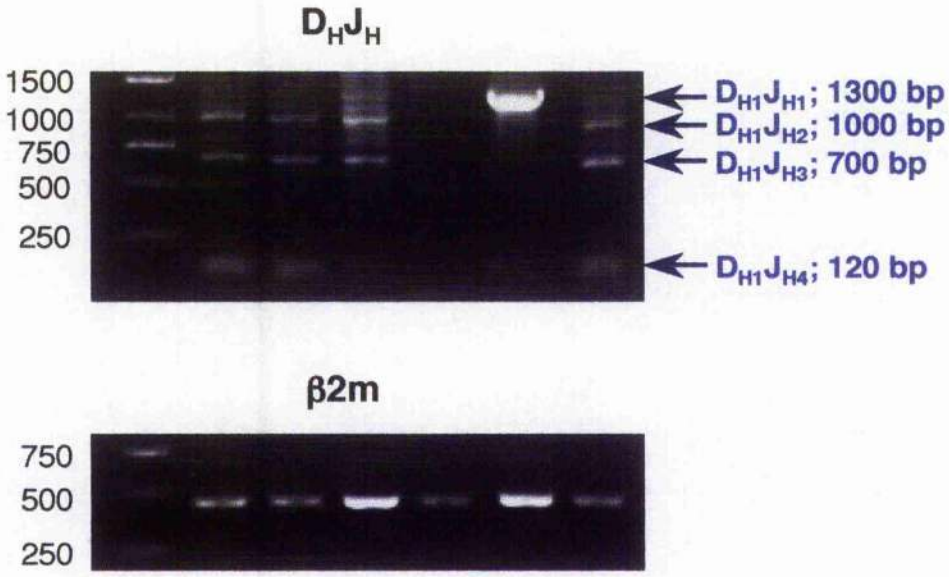

1. Marker
2. ICR-MIEV
3. ICR-PKCα-KR
4. ICR-adult splenocytes
5. RAG-adult splenocytes
6. M-1 cells
7. ICR-PKCα-KR w/o IL-7 for 4 days

Figure 4.18 A s.c. tumour mass was formed in PK-KR-HPCs-injected mice at the injection site and these mice could not survive more than 6 weeks

HPC-enriched FL cells were prepared from wildtype mice, retrovirally infected with PKCα-KR and were injected i.p. into neonatal RAG-1$^{-/-}$ mice (1×10^6 per mouse) (top). Analysis of the mice 3 weeks after injection revealed that GFP$^+$ tumour cell masses developed s.c. at the point of injection. Survival curve for PKCα-KR infected cell-adoptive transferred mice (bottom). * Include 2 mice sacrificed for the analysis. Both of them borne s.c. tumours. ** Include 3 mice sacrificed for the analysis. All of them borne s.c. tumours. *** Include 2 mice sacrificed for the analysis. One of them borne s.c. tumours. **** Include 1 mouse sacrificed for the analysis, which borne s.c. tumours. None of MIEV-HPCs-injected-mice died during the course of the experiments.

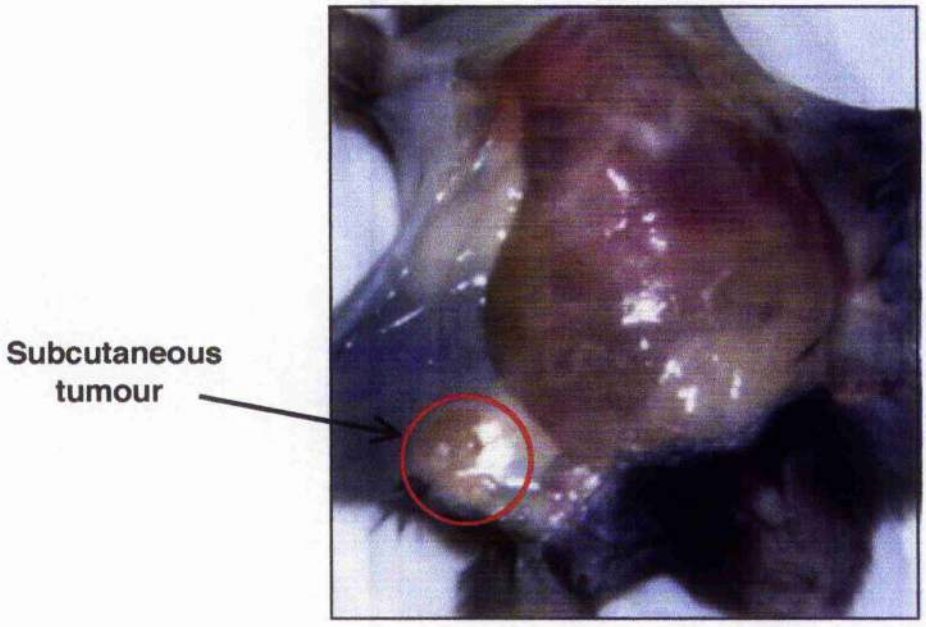
Subcutaneous
tumour

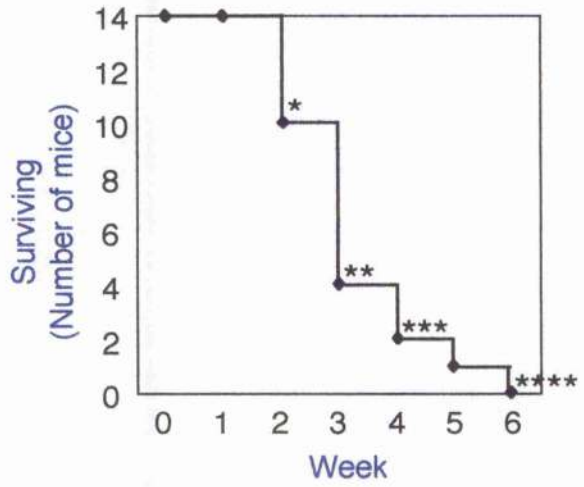
Surviving
(Number of mice)
14
12
10
8
6
4
2
0
*
**
***
****
0
1
2
3
4
5
6
Week

Figure 4.19 PKCα-KR-HPCs-injected mouse accompanied splenomegaly and the spleen enriched GFP$^+$ PKCα-KR-expressing cells

FL cells was prepared from wildtype mice, retrovirally infected with MIEV or PKCα-KR, and were injected i.p. into neonatal RAG-1$^{-/-}$ mice (1×10^6 or 1×10^5 and 1×10^6 per mouse, MIEV or PKCα-KR, respectively). The photo of the spleen was taken immediately after removal (top). Splenocytes were extracted from each mouse and analysed GFP intensity by FCM (bottom). The graph shows mean percentage of GFP$^+$ cells of three separate tubes. Average ±SEM shown. Cells were live and size gated. These data are from a single experiment, representative of three separate experiments.

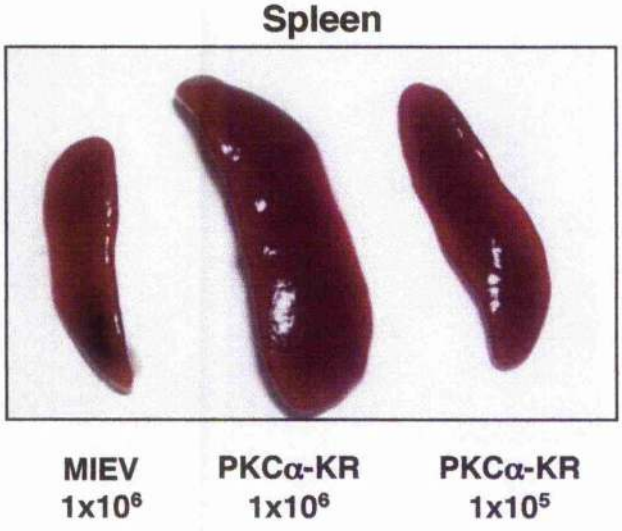
Spleen
MIEV
1x10⁶
PKCα-KR
1x10⁶
PKCα-KR
1x10⁵

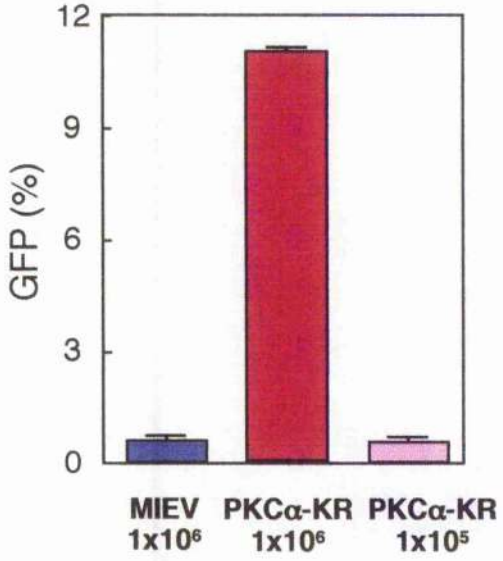
12
9
6
3
0
GFP (%)
MIEV
1x10⁶
PKCα-KR
1x10⁶
PKCα-KR
1x10⁵

Figure 4.20 A tumour cell mass phenotypically resembling CLL

Tumour mass was removed from PKCα-KR-HPCs-injected mouse and a single cell suspension was prepared. FCM analysis was carried out on GFP^{low} and GFP^{hi} populations, IgM-APC vs. CD45R-PE, IgD-APC vs. CD45-PE, CD19-APC vs. CD23-PE, and CD5-PE vs. CD45R; percentages are indicated. All FACS plots were live and size gated. These data are from a single experiment, representative of at least five separate experiments.

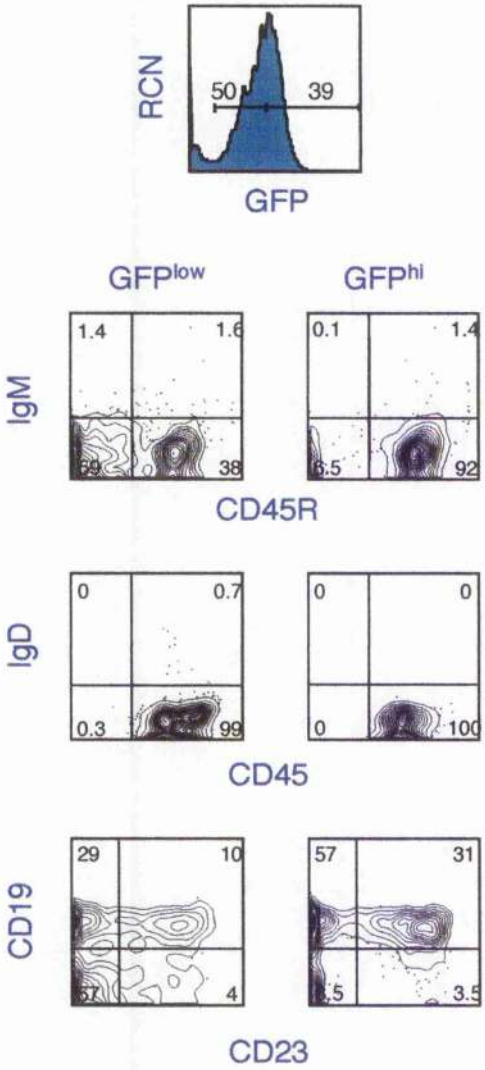
RCN
50
39
GFP
GFPlow
GFPhi
IgM
1.4
1.6
59
38
0.1
1.4
6.5
92
CD45R
IgD
0
0.7
0.3
99
0
0
0
100
CD45
CD19
29
10
57
4
57
31
3.5
3.5
CD23

Figure 4.21 Freshly prepared tumour cells arrested at G_0/G_1, but re-entered cell cycle upon culture in the presence of OP9 cells and IL-7

PI analysis was carried out on cell suspensions of isolated tumour, spleen and LN cells from PKCα-KR-HPCs-injected mouse and spleen and LN cells from MIEV-HPCs-injected mouse at day 0. The rest of the cells were seeded onto OP9 cells in the presence of IL-7 and samples as PI analysis (day 5). Top, value at the indicated cell cycle stage; bottom, histogram of DNA content vs. RCN. The cellular data were size gated. This is a representative result of two separate experiments.

Day0

	$SubG_0G_1$	G_0G_1	G_2M/S
MIEV	0.2	95	4.8
PKCα-KR	1.0	82	17
PKCα-KR Tumour	2.4	92	6.0

Day5

	$SubG_0G_1$	G_0G_1	G_2M/S
MIEV	13	77	10
PKCα-KR	0.0	60	40
PKCα-KR tumour	0.70	68	31.3

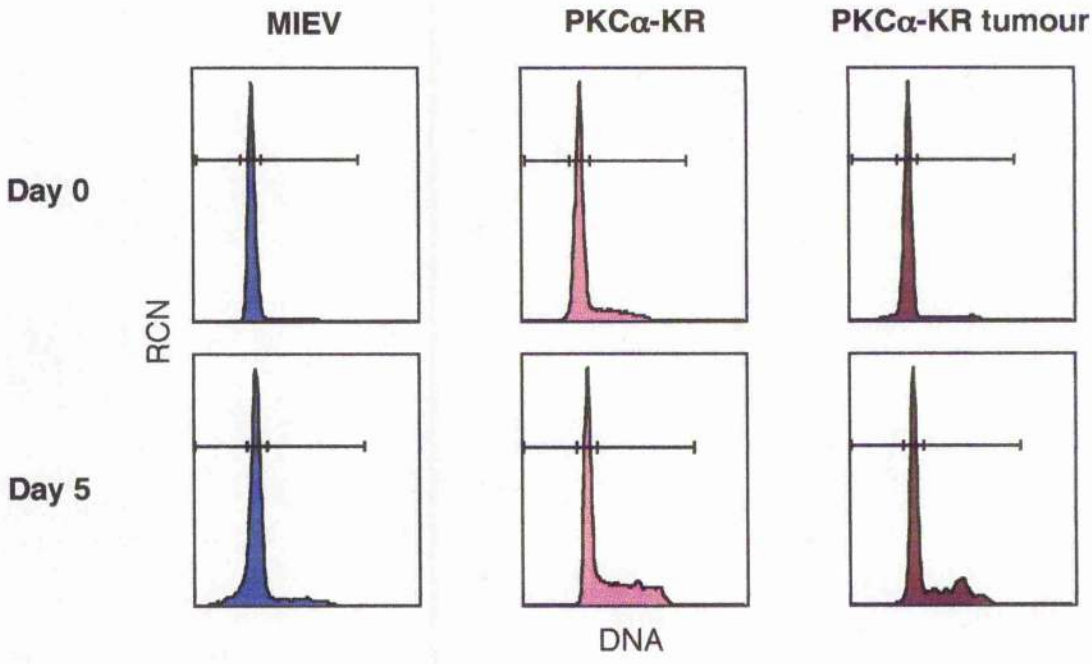

Figure 4.22A Effect of pharmacological inhibitors on apoptosis in mouse CLL-like cells

Retrovirally infected HPCs with MIEV or PKCα-KR were cocultured with OP9 for 16 days. Thereafter, 1 × 10^6 cells (MIEV- and PKCα-KR-expressing cells and M-1 cells) were plated and incubated in the absence or presence of pharmacological inhibitors for 24 h as indicated before Annexin V/7-AAD staining and subsequent FCM analysis was performed. The average ratio (n=5) against the control (DMSO-treated) ±SEM is shown. The concentration of pharmacological inhibitor is presented in a log scale. PKC inhibitors: 0.2, 2 μM chelerythrine (total PKC inhibitor); 2, 20 μM, rottlerin (nPKC inhibitor).

PKC inhibitors

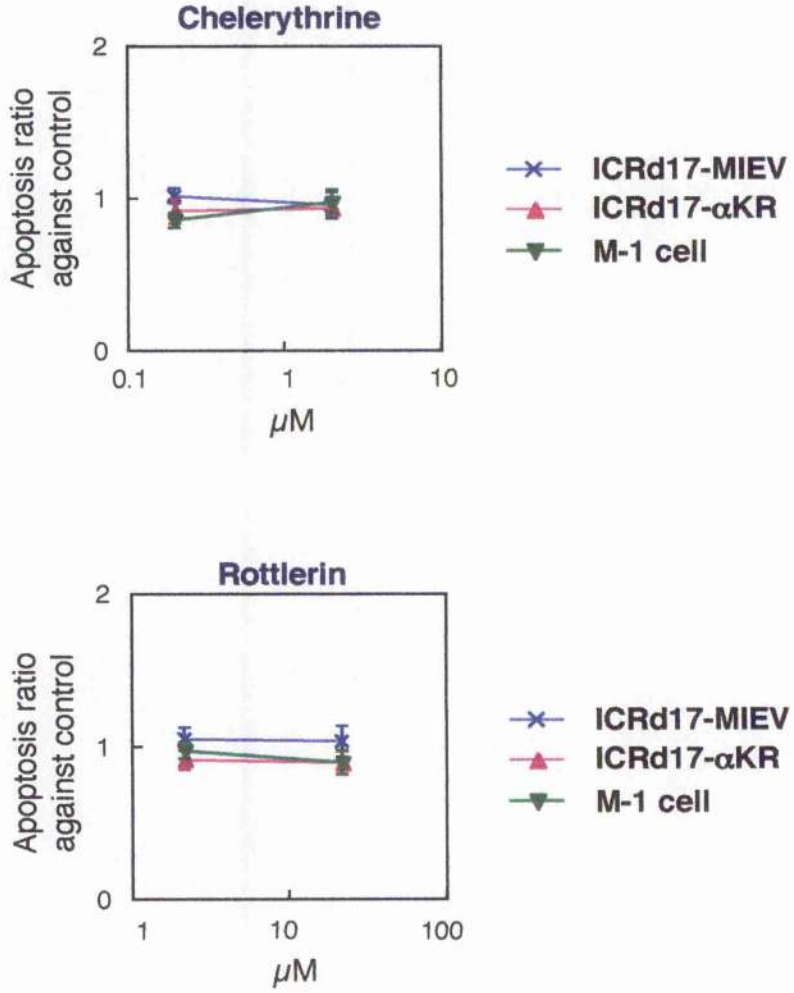

Figure 4.22B Effect of pharmacological inhibitors on apoptosis in mouse CLL-like cells

Retrovirally infected HPCs with MIEV or PKCα-KR were cocultured with OP9 for 16 days. Thereafter, 1×10^6 cells (MIEV- and PKCα-KR-expressing cells and M-1 cells) were plated and incubated in the absence or presence of pharmacological inhibitors for 24 h as indicated before Annexin V/7-AAD staining and subsequent FCM analysis was performed. The average ratio (n=5) against the control (DMSO-treated) ±SEM is shown. The concentration of pharmacological inhibitor is presented in a log scale. MAPK inhibitors: 1, 10 μM, U0126 (MEK1/2 inhibitor); 2, 20 μM, PD98059 (MEK1 inhibitor); 0.5, 5 μM, SB203580 (p38 inhibitor).

MAPK inhibitors

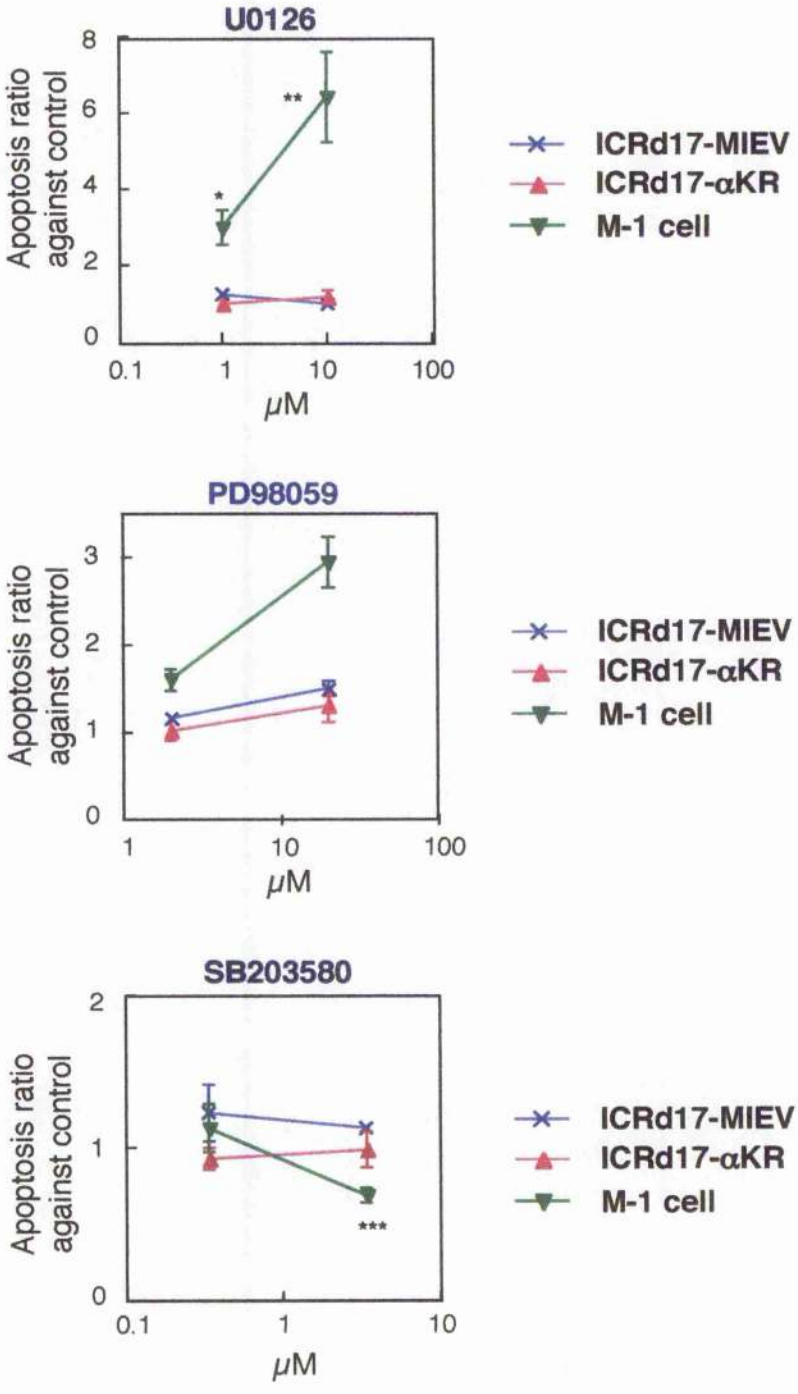

*** $p < 0.0005$, ** $p < 0.005$, *$p<0.01$ against MIEV

Figure 4.22C Effect of pharmacological inhibitors on apoptosis in mouse CLL-like cells

Retrovirally infected HPCs with MIEV or PKCα-KR were cocultured with OP9 for 16 days. Thereafter, 1×10^6 cells (MIEV- and PKCα-KR-expressing cells and M-1 cells) were plated and incubated in the absence or presence of pharmacological inhibitors for 24 h as indicated before Annexin V/7-AAD staining and subsequent FCM analysis was performed. The average ratio (n=5) against the control (DMSO-treated) ±SEM is shown. The concentration of pharmacological inhibitor is presented in a log scale. PI3K inhibitors: 1, 3, 10 μM, LY294002; 1, 10 μM, wortmannin.

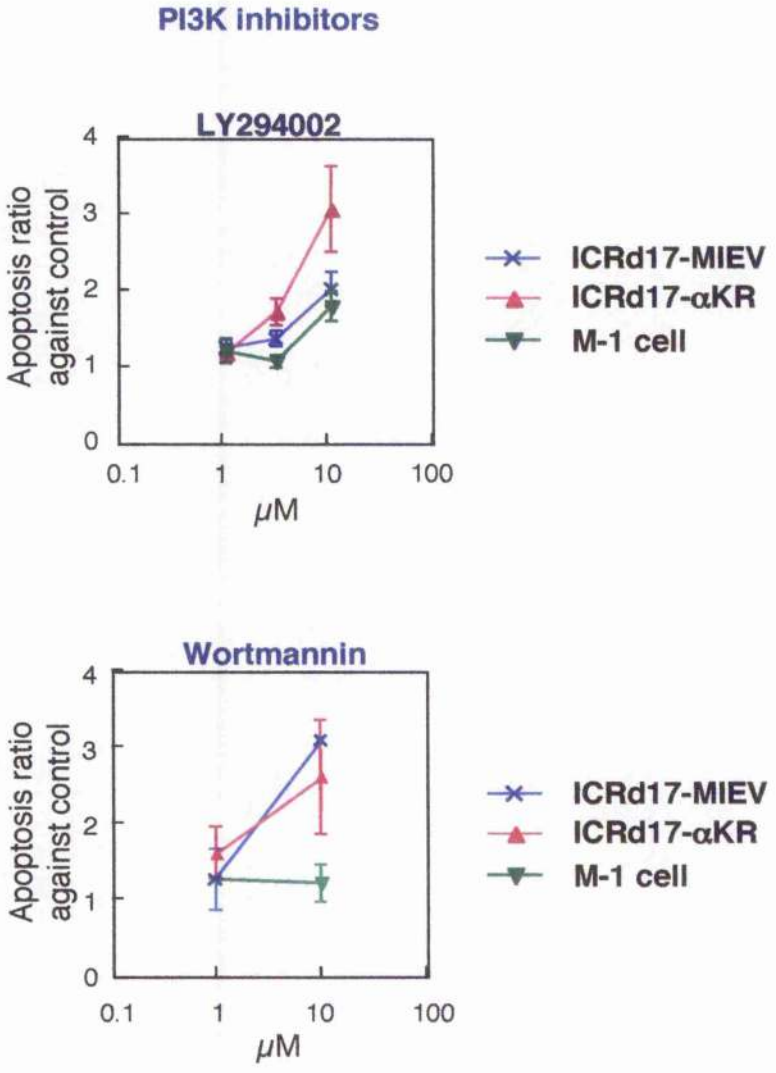
PI3K inhibitors
LY294002
Apoptosis ratio against control
0
1
2
3
4
0.1
1
10
100
μM
ICRd17-MIEV
ICRd17-αKR
M-1 cell
Wortmannin
Apoptosis ratio against control
0
1
2
3
4
0.1
1
10
100
μM
ICRd17-MIEV
ICRd17-αKR
M-1 cell

Figure 4.23 Effect of pharmacological inhibitors on apoptosis in early cocultures

Retrovirally infected HPCs with MIEV or PKCα-KR were cocultured with OP9 for 9 days. Thereafter, 1×10^6 cells were plated and incubated in the absence or presence of pharmacological inhibitors for 24 h as indicated before Annexin V/7-AAD staining and subsequent FCM analysis was performed. The ratio against the control (DMSO-treated) is shown. The concentration of pharmacological inhibitor is presented in a log scale. 1, 10 μM, U0126 (MEK1/2 inhibitor); 1, 3, 10 μM, LY294002 (PI3K inhibitor). This is a representative of two separate experiments.

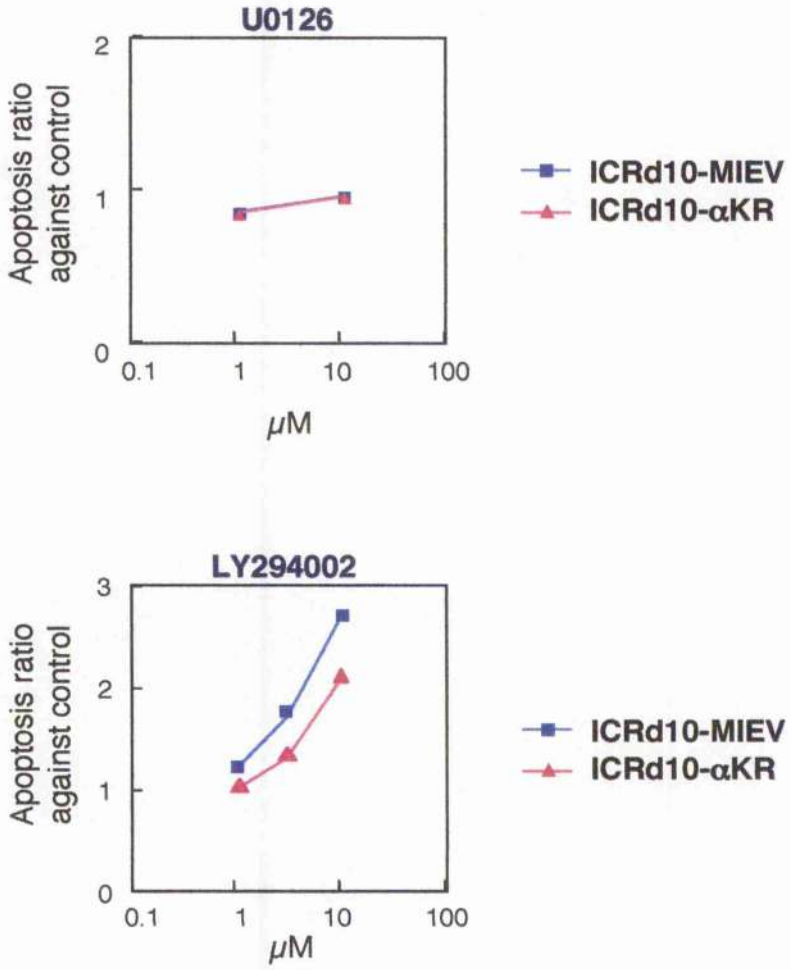
U0126
Apoptosis ratio against control
2
1
0
0.1
1
10
100
μM
ICRd10-MIEV
ICRd10-αKR
LY294002
Apoptosis ratio against control
3
2
1
0
0.1
1
10
100
μM
ICRd10-MIEV
ICRd10-αKR

Figure 4.24 Western blots showed the activation/phosphorylation status of AKT and ERK1/2 in B-CLL-like cells

HPCs derived from wildtype mice FL or RAG-1$^{-/-}$ mice FL were cocultured with OP9 and removed from the culture at day 8 and day 15 or day 6, respectively. The phosphorylation levels of AKT at the threonine residue 308 and ERK 1 and 2 were analysed by Western blotting. These are representative blots of three separate experiments.

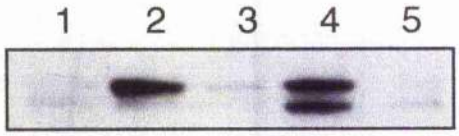

pERK1/2

1. ICRd8-MIEV
2. ICRd8-PKCα-KR
3. ICRd15-MIEV
4. ICRd15-PKCα-KR
5. M-1

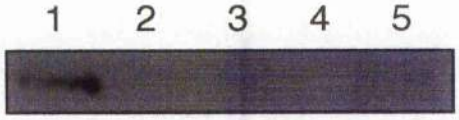

pAKT(T308)

1. ICRd8-MIEV
2. ICRd8-PKCα-KR
3. ICRd15-MIEV
4. ICRd15-PKCα-KR
5. M-1

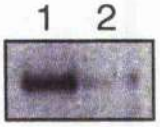

pAKT (T308)

1. RAGd6-MIEV
2. RAGd6-αKR

Chapter 5:
Which stage in the B-cell development does the tumourigenesis happen?

5.1 Introduction

5.1.1 T cell development

T cell progenitors are derived from BM or FL progenitors. Their development is dependent on the thymic organ. Developing thymocytes can be phenotypically characterised by expression of CD4 and CD8. When cells enter the thymus they lack the expression of CD4 and CD8, therefore being called $CD4^-$ $CD8^-$ double negative (DN) thymocytes. As development progresses, they become $CD4^+$ $CD8^+$ double positive (DP), and mature into single positive (SP) $CD4^+$ or $CD8^+$ T cells (Zúñiga-Pflücker, 2004) (Fig. 5.1). The DN stage is further subdivided based on CD25, CD44 and CD117 surface expression (Fig. 5.1). The earliest progenitors termed DN1 ($CD25^-$ $CD44^+$ $CD117^+$) maintain pluripotency, and thus can differentiate into T cells, B cells, NK cells, and DCs (Pear et al, 2004). The differentiation potential of DN2 ($CD25^+$ $CD44^+$ $CD117^+$) cells is limited to T cells and DCs (Pear et al, 2004). DN3 ($CD25^+$ $CD44^-$ $CD117^-$) cells are fully committed to the T cell lineage and start rearranging the TCRβ gene locus. DN4 ($CD25^-$ $CD44^-$ $CD117^-$) cells are the product of DN3 cells that have successfully rearranged TCRβ gene locus and express a functional TCRβ chain it in the context of the pre-TCR complex on cell surface (Schmitt et al, 2004).

5.1.2 Notch and T cell commitment

Notch, a gene that was originally identified in *Drosophila melanogaster*, is involved in binary cell fate decisions (Radtke et al, 2004). Mammals have four receptors (Notch 1-4) and five ligands (Jagged 1 and 2, and Delta-like 1, 3 and 4), which are widely expressed in the haematopoietic system (Radtke et al, 2004). Notch signalling is initiated through ligand-receptor interactions, leading to proteolytic cleavage of the receptor, which results in the release of cytoplasmic domain of Notch (NIC). NIC translocates to the nucleus and heterodimerises with the transcription factor CSL (CBF-1 [c-promoter binding factor 1] for humans, Su(H) [suppressor of hairless] for drosophila, Lag-2 [Lin-12 and Glp-1 phenotype 2] for *Caenorhabditis elegans*), also known as RBP-Jκ

[recombining binding protein-J kappa] in the mouse, leading to de-repression/activation of CSL-dependent downstream targets, such as *Hes* (Hairy enhancer of split) 1 and *Hes* 5 (Radtke et al, 2004).

The inhibition of Notch 1 signalling in thymus by Lunatic Fringe, a modulator of Notch 1, promoted the development of lymphoid progenitors towards the B cell lineage instead of T cell commitment (Koch et al, 2001). In contrast, the expression of activated Notch 1 in haemato-lymphoid progenitors resulted in the emergence of a population of thymic-independent T cells in BM, concomitant with a block of B cell maturation (Pui et al, 1999). Altogether, compelling evidence is provided that Notch 1 signalling is essential and sufficient to induce T cell lineage commitment in early lymphoid progenitors with a simultaneous block in B cell development, thus, the function of Notch 1 is vital in T cell versus B cell fate specification (Pear and Radtke, 2003). On the other hand, Notch signalling must be switched off during B cell development in BM despite the fact that Notch receptors and ligands are expressed on BM progenitors and stroma (Radtke et al, 2004). There are several reports that may explain this paradox. The expression of Pax5 represses transcription of Notch1 in B cell progenitors thus facilitating B lineage commitment (Souabni et al, 2002). Although a high density of Notch1 molecules promotes T cell fate and inhibit B cell fate, the lower density of DL-1 enhances $B220^-$ cells to an early T lymphoid generation and $B220^+$ cells to B lymphoid generation (Dalias et al, 2005). Alternatively, B cell progenitors can be protected in the specific niches of the BM (Tokoyoda et al, 2004). In order to understand the Notch signalling in T cell versus B cell fate, further investigations are required.

5.2 Aims and Objectives

The aims of this chapter were:

i. To examine if leukaemiagenesis can occur in other HPC sources.

ii. To define the developmental stage susceptible to PKCα-KR-mediated transformation by retrovirally infecting HPCs from RAG-1$^{-/-}$ mice.

iii. To examine the impact of Notch ligand DL1 on PKCα driven leukaemiagenesis.

5.3 Results

5.3.1 GFP$^+$ PKCα-KR-expressing FT and BM cells from wildtype mice exhibited the CLL-like phenotype

In order to elucidate whether cellular sources other than FL could lead to spontaneous tumourigenesis upon expression of PKCα-KR, FT and BM cells from wildtype mice were retrovirally infected with PKCα-KR or MIEV, and cultured in our *in vitro* B cell generation system. FCM analysis of cultures immediately after retroviral infection revealed a GFP$^+$ population in both sets of cocultures (FT: Fig. 5.2 top, day 1 MIEV 16 %, PKCα-KR 6.1 %; BM: Fig. 5.2 bottom, day 1 MIEV 17 %, PKCα-KR 11 %). As the BM cell coculture progressed, it became clear that PKCα-KR-expressing (GFP$^+$) cells displayed a growth advantage over the untransduced (GFP$^-$) cells as shown by a 8.4-fold increase in the percentage of GFP$^+$ PKCα-KR-expressing cells from days 1 to 16 (11 % vs. 93 %; Fig. 5.2 bottom). Although PKCα-KR-expressing GFP$^+$ FT exhibited growth advantage (PKCα-KR: day 1 to day 16, 16-fold increase; Fig. 5.2 top), it was clear that MIEV-expressing GFP$^+$ FT also exhibited an expansion growth (MIEV: day 1 to day 16, 5.0-fold increase; Fig. 5.2 top). The reason for this is not known and needs to be elucidated. When the growth speed was compared between PKCα-KR-expressing GFP$^+$ FL and BM, FL proliferated faster than BM (FL: 21-fold increase from day 2 to day 14, BM: 8.4-fold increase from day 1 to day 16). Next, the infected cells were analysed for CLL-markers; IgM, CD2, CD5, CD19 and CD23. The majority of the FT and BM cells retrovirally infected with MIEV committed towards the B cell lineage (FT: 99 % CD19$^+$ and BM: 97 % CD19$^+$, Fig. 5.3 top and bottom, respectively), and appeared to reach normal immature/mature B cell stage expressing κ and IgM molecules (Fig. 5.3 top and bottom). On the other hand, both FT and BM cells expressing PKCα-KR displayed CLL-like phenotype; IgM^{lo}, CD5$^+$ and CD23$^+$ (Fig. 5.3 top and bottom). These findings suggest that CLL cells may not only be generated from B cell committed cells as a result of PKCα subversion, but may also be generated from the pluripotent DN1 population, as these cells still retain the ability to commit to B cell lineage (Schmitt et al, 2004).

Of note, the subversion of PKCα also transformed BM cells, suggesting that this transformation process occurs in the adult system.

5.3.2 GFP$^+$ PKCα-KR-expressing cells derived from RAG-1$^{-/-}$-FL also exhibited growth advantage over GFP$^-$ cells and CLL-like phenotype

In order to identify how PKC mutants affect B cell development in RAG-1$^{-/-}$ mice, HPCs derived from RAG-1$^{-/-}$-FL were retrovirally infected. As B cells in RAG-1$^{-/-}$ mice are arrested in development at the pro-B cell stage (Mombaerts et al, 1992), transformation of RAG-1$^{-/-}$ derived lymphoid progenitors by subversion of PKCα, would suggest that this leukaemic event occurs before the pre-B cell stage. The infected PKC mutant expressing cells were cultured in our *in vitro* B cell generation system and analysed by FCM as indicated in the figure legend. As noted in wildtype mice (Fig. 3.9A), the percentage of GFP$^+$ population was relatively constant in PKCδ-KR- and MIEV-expressing cells from day 2 to day 18 (PKCδ-KR: day 2, 22 %, day 18, 26 %; MIEV: day 2, 83 %, day 18, 99 %; Fig. 5.4). PKCζ-KR expression in RAG-1$^{-/-}$ FL cells induced a decrease of GFP$^+$ population (2.7-foid reduction, day 2, 19 %; day 18, 6.9 %; Fig. 5.4) as observed in wildtype FL cells (Fig. 3.9A). Notably, the GFP$^+$ population in PKCα-KR-expressing cells reached 6.8-fold higher at day 18 compared to day 2 (day 2, 9.7 %, day 18, 67 %; Fig. 5.4), with major expansion noted after day 6 as noticed with wildtype cells (Fig. 3.9A). Therefore, GFP$^+$ PKCα-KR-expressing HPCs from RAG-1$^{-/-}$ also exhibited a growth advantage over GFP$^-$ population. Of note, the GFP$^+$ dominance over GFP$^-$ in RAG-1$^{-/-}$ PKCα-KR expressing FL cells progressed slower than that of wildtype FL (RAG-1$^{-/-}$: day 18, GFP$^+$=67 %; ICR, day 14, GFP$^+$=98 %, Fig. 5.4 and Fig. 3.9A). This may be due to the fact that developing B cells in RAG-1$^{-/-}$ mice can not express the pre-BCR complex, suggesting that the stimuli from pre-BCR might be required for more rapid transformation, although further studies are required to test this. Next, CLL marker expression (CD2, CD5, CD23 and CD19) on these PKC mutant expressing RAG-1$^{-/-}$ cells was analysed by FCM. In PKCδ-KR-, PKCζ-KR- and MIEV-expressing RAG-1$^{-/-}$ FL cells, >95 % cells became CD19$^+$ B cells and no CD23 expression was observed on surface (Fig. 5.5). PKCα-KR-expressing

RAG-1$^{-/-}$ cells upregulated CD2, CD23 and CD5 as observed in PKCα-KR-expressing wildtype derived FL (Fig. 3.10A). Analysis of the MFI of CD19 in MIEV-, PKCα-KR-, PKCδ-KR- and PKCζ-KR-expressing RAG-1$^{-/-}$ FL cells revealed an upregulation of CD19 on GFP^{+} PKCα-KR expressing B lineage cells as indicated: in the order of MIEV, PKCα-KR-, PKCδ-KR- and PKCζ-KR; 67, 164, 115 and 88 (Fig. 5.5). Therefore, these results suggest that this leukaemic event occurs at or before the early pre-B cell stage.

5.3.3 Subversion of PKCα initiated transformation in adult RAG-1$^{-/-}$ derived BM cells

In order to test whether this transformation can be initiated in cells derived from adult RAG-1$^{-/-}$ mice, BM cells were retrovirally infected. In agreement with wildtype mice (Fig. 5.2 bottom), GFP^{+} PKCα-KR-BM cells from adult RAG-1$^{-/-}$ mice also showed a growth advantage over the GFP^{-} cells (PKCα-KR: day 1, 4.9 %, day 8, 66 %; MIEV: day 1, 32 %, day 12, 46 %, Fig. 5.6). Of note, the growth advantage of GFP^{+} PKCα-KR-expressing cells from RAG-1$^{-/-}$ mouse lymphoid progenitors compared with those of wildtype mice in the earlier phase was similar in adult system (RAG-1$^{-/-}$, 6.3-fold increase in GFP^{+}(%) from day 1 to 8; ICR, 2.7-fold increase in GFP^{+}(%) from day 1 to 8), thus, an earlier expansion was observed. FCM analysis on CLL markers (CD2, CD5, CD23 and CD19) revealed that >92 % cells became CD19^{+} B cells in both PKCα-KR- and MIEV-expressing RAG-1$^{-/-}$ BM cells and PKCα-KR-expressing cells showed CLL-like phenotype, upreguiated CD2, CD23, CD5 and CD19 (Fig. 5.7). Therefore, these results suggest that transformation aiso occurs in RAG-1$^{-/-}$ adult system in a similar fashion to that in adult wildtype BM cells.

5.3.4 CLL-like phenotype developed *in vivo* by adoptive transfer of RAG-1$^{-/-}$-FL-derived PKCα-KR-expressing-HPCs into RAG-1$^{-/-}$ mice

To assess whether the population of cells observed *in vitro* culture (Fig. 5.5) could also be generated *in vivo*, MIEV- or PKCα-KR-retrovirally infected FL-HPCs derived from RAG-1$^{-/-}$ mice were injected into RAG-1$^{-/-}$ mice and the lymphocyte populations of the mice were analysed from 2 to 6 weeks post

injection. The GFP$^+$ population in LN cells from MIEV- and PKCα-KR-HPCs-injected mice was 0.76 % and 29 %, respectively, suggesting cells from GFP$^+$ PKCα-KR-HPCs-injected mice had growth advantage over GFP$^-$ and host derived cells compared with the GFP$^+$ population at day 2 (MIEV, 83 %; PKCα-KR, 9.7 %, Fig. 5.4). As observed in wildtype PKCα-KR-HPCs adoptive transfer mice (Fig. 4.18), some mice bore a s.c. tumour mass at the injection site. Representative data of reconstituted LN cells from either PKCα-KR or MIEV-HPCs injected RAG-1$^{-/-}$ mice and tumour are presented in Figure 5.8. Phenotypic analysis revealed that no GFP$^+$ CD19$^+$ B cells were present in either LN or spleen from MIEV-injected mice, and 20 % and 19 % was observed in LN cells and spleen, respectively, from PKCα-KR-injected mice (Fig. 5.8 and data not shown). Of interest, 37 % GFP$^+$ CD19$^+$ B cells were found in thymus (GFP$^+$=6.0 %) from PKCα-KR-HPCs injected RAG-1$^{-/-}$ mice, whereas none found in MIEV-HPCs injected RAG-1$^{-/-}$ mice (data not shown), indicating that these CLL-like cells are invasive. In contrast, >60 % HPCs became B cell in splenocytes from both MIEV- and PKCα-KR-wildtype HPCs-injected mice (Fig. 5.8), suggesting that the reconstituted B lineage population in RAG-1$^{-/-}$-HPCs-injected mice was either much lower or reconstituted cells die faster. The phenotype of LN cells from PKCα-KR HPC-injected mice resembled that of cells generated in *in vitro* cultures for RAG-1$^{-/-}$ FL cells in Figure 5.4 (GFP$^+$, CD23$^+$ and CD5$^+$; Fig. 5.8), representing a hallmark of human CLL. Overall, subversion of PKCα causes transformation in RAG-1$^{-/-}$ derived FL cells *in vivo* that are phenotypically similar to wildtype mouse PKCα-KR expressing FL, therefore, human CLL cells.

5.3.5 CLL-like phenotype was developed from retrovirally infected PKCα-KR-expressing splenocytes derived from adult wildtype mice

In order to test whether this transformation event could be initiated post pre-B cell stage, CD19$^+$ B cells-derived from splenocytes of a wildtype mouse were infected with MIEV- and PKCα-KR whilst being stimulated with 50 μg/ml LPS for 48 h to enhance retrovirus incorporation into genome of normally unproliferative mature CD19$^+$ B cells. Analysis of cells at day 3 revealed that there were

GFP$^+$ cells, indicating that retroviral infection was successful. GFP$^+$ PKCα-KR B cells showed growth advantage over the GFP$^-$ cells (PKCα-KR: day 3, 15 %, day 11, 94 %; MIEV: day 3, 51 %, day 11, 79 %, Fig. 5.9). FCM analysis on B cell marker expression (IgD vs. CD45, CD5 vs. CD45R, IgM vs. CD45R and CD23 vs. CD19) revealed a gradual upregulation of CD5 and CD23, and downregulation of IgM in PKCα-KR-expressing cells, thus displaying a CLL-like phenotype (Fig. 5.10). CD45R$^+$ CD5$^+$ cells reached 45 % in PKCα-KR-expressing cells, whereas only 6.0 % in MIEV-expressing cells (Fig. 5.10). Therefore, these results suggest that transformation can also occur in IgM expressing mature B cells.

5.3.6 Association with Notch ligand attenuates PKCα-KR-expressing cells to generate leukaemic cells

OP9-DL1 cells express Notch ligand, DL-1, and induce T cell differentiation of lymphoid progenitors in the absence of thymus (Schmitt and Zúñiga-Pflücker, 2002). OP9-DL1 cells can support normal B cell development if B cells are beyond the pre-B cell stage (Schmitt and Zúñiga-Pflücker, 2002). PKCα plays an important role in early T cell development from DN to DP stage (Michie et al, 2001). This paper shows that PKCα-KR blocks T cell development at the DN stage in the thymic environment, however, the potential that PKCα-KR-expressing DN subsets develop into B lineage cells was not assessed. Due to my findings showing PKCα-KR expression in HPCs generates CLL-like cells, the capacity of B cell commitment in PKCα-KR expressing DN and the possibility that this transformation event can occur in an *in vitro* T cell development system was tested. HPCs derived from wildtype FL were retrovirally infected with PKCα-CAT, PKCα-KR and MIEV and cocultured with OP9-DL1. FCM analysis of HPC cocultures revealed a shift in GFP$^+$ population within each retroviral condition (Fig. 5.11). There were 2.0 % GFP$^+$ cells at day 1 PKCα-CAT-expressing cells, but the number was decreased to 0.57 % at day 15. The same effect was observed when PKCα-CAT-expressing cells were cultured in OP9 (Fig. 3.9B), suggesting that the expression of PKCα-CAT is detrimental to HPCs. GFP$^+$ PKCα-KR-expressing

cells showed growth advantage, exhibiting 7.9-fold growth increase (day 1, 8.8 %; day 15, 69 %), whereas MIEV-expressing cells did not (day 1, 27 %; day 15, 56 %). Interestingly, while PKCα-KR showed a growth advantage compared to the MIEV- and PKCα-CAT cocultures, the increase of GFP^+ cells was milder in OP9-DL1 cocultures, 7.9-fold increase from day 4 to 15 (Fig. 5.11), compared with OP9 cocultures, 21-fold increase from day 2 to 14 (Fig. 3.9A).

Analysis of T cell maturation markers (CD25 vs. CD117 and CD4 vs. CD8) and B cell markers (CD23 vs. CD19) revealed that none of the MIEV-expressing cells became $CD19^+$ expressing B cells (Fig. 5.12A). More than 47 % of the cells committed to $CD25^+$ $CD117^+$ T cell lineage, and among them 7 % reaching DP stage in MIEV-expressing cells (Fig. 5.12A). Thus, confirming that T cell development occurred by co-culturing HPCs with OP9-DL1. In PKCα-CAT-expressing cells, T lineage cells developed as evidenced by the presence of DN and DP cells, but no B cells were observed. In the PKCα-KR GFP^+ cocultures, T cell development appeared to be severely blocked and as expected (Michie et al, 2001), and no DP cells were present (Fig. 5.12A). Moreover, 34 % of the cells were $CD117^-$ $CD25^-$, suggesting PKCα-KR-expressing cells were trapped at the pluripotent DN1 stage. Interestingly, only a small number of PKCα-KR-expressing cells became B cells (2.5 %), and they did not express CD23 (Fig. 5.12A), suggesting that they were not leukaemic. When cellularity was examined in the same coculture, the percentage in PKCα-KR-expressing cells was nearly half that of GFP^+ MIEV-expressing cells (Fig. 5.12B), despite the fact that more cells were GFP^+ in PKCα-KR-expressing cells (Fig. 5.11). This may suggest that PKCα-KR expression keeps HPCs from proliferating in the presence of DL1.

5.3.7 Notch signalling suppressed transformation of PKCα-KR-expressing cells

To define whether cells maintain their leukaemic potential when cultured on OP9-DL1, HPCs from wildtype FL were infected with MIEV and PKCα-KR and cocultured with either OP9 or OP9-DL1 up to day 6. Then the coculture was

divided into two, half was cultured with OP9 and the other half was cultured with OP9-DL1 until day13 (step 1: OP9-DL1 to OP9-DL1, step 2: OP9-DL1 to OP9, step 3: OP9 to OP9, step 4: OP9 to OP9-DL1). In MIEV-expressing cells, B cell development was not observed in the day 13 OP9-DL1 culture (step 1), but when cells were transferred to OP9 cells (step 2), the B cells expanded, resulting in 34 % B cells observed at the day 13 (Fig. 5.13A). This may be due to expansion of existing B lineage cells present in culture and/or commitment of HPCs to the B lineage possibly from the DN1 stage of thymocyte development. As expected, 97 % cells became $CD19^+$ B cells in the day 13 OP9 culture (step 3), which was reduced to 44 % B cells in the day 13 OP9 to OP9-DL1 culture (step 4). This is supported by a previous report showing that OP9-DL1 cells are able to support B cell development after pre-B cell stage (Schmitt and Zúñiga-Pflücker, 2002) (Fig. 5.13A). In PKCα-KR-expressing cells, not many B cells appeared in the day 13 OP9-DL1 culture although more B cells observed than in MIEV culture (MIEV; 4.8 %, PKCα-KR; 15 %) (step 1). Of interest, B cells explosively proliferated in the day 13 step 2 culture and indeed 0.4 % cells exhibited the CLL-like phenotype ($CD19^+$ $CD23^+$). As described in Section 3.3.6, most of PKCα-KR-expressing cells became B cells (98 %: Fig. 5.13B) and some of them expressed CLL phenotype when they were kept in culture on OP9, however, B cell growth was suppressed when they were cultured on OP9-DL1. Indeed only 3.3 % $CD19^+$ B cells were present in the cultures at day 13, these results suggest that Notch signalling functions as tumour suppressor for our CLL-like cells, compared with 85 % at the number of transfer at day 6 (Fig. 5.13B). PKCα-KR-expressing cells were not cancerous while they were cocultured with OP9-DL1, but tumourigenesis was reversible depending on the growing condition, suggesting that Notch signalling inhibits leukaemiagenesis in B lineage cells.

5.4 Discussion

In this chapter, other HPC sources were tested for their transformation potential and it was showed that stable PKCα-KR expression generated CLL-like cells in HPCs derived from wildtype BM and FT, and RAG-1$^{-/-}$ FL and BM. The mechanisms that underlie the leukaemiagenesis remain not unclear, however, ERK pathway is involved and the signals for transformation appears to be inhibited by Notch signalling.

CLL is commonly considered to arise from an outgrowth of a mature subset of B lymphocytes (Stevenson and Caligaris-Cappio, 2004). However, as B cell development is blocked at the pro-B cell stage in RAG$^{-/-}$ mice due to an inability to initiate recombination at the IgH chain gene locus, these results indicate that PKCα-mediated development of CLL occurs at an early stage of B cell development in this system.

MIEV-FT derived from wildtype mice successfully committed to CD19^{+} B cells (Fig. 5.3 top), thus it was confirmed B cells can be generated from thymocytes. The subversion of PKCα-KR in thymocytes generated CLL-like cells with the distinct phenotype, CD23^{+} CD5^{+} IgM^{lo}, indicating that B cell committed cells are not necessarily a target of transformation. Previously, it was shown that thymocytes at DN1 stage can give rise to B cells with relatively low frequency, but no later than DN1 stage (Schmitt et al, 2004). Therefore, it is most plausible that the both normal and leukaemic B cells were given rise from MIEV- and PKCα-KR-infected DN1 cells, respectively. In order to test until which stage of thymocytes can generate CLL-like cells by PKCα-KR expression, PKCα-KR infected cells will be separated into either DN1 or DN2 cells by virtue of CD25 and CD44 expression by cell sorting, and cultured in the B cell generation system, and analysed by FCM for CLL markers. Thymocytes seem to proliferate more than HPCs derived from FL, which increases chances for retroviral infection, and thus growth advantage was not observed in PKCα-KR-FT because both MIEV- and PKCα-KR-cocultures completely occupied with

GFP$^+$ cells (Fig. 5.2 top). We could generate CLL-like cells using BM cells derived from adult wiidtype mice, suggesting that this transforming event is not limited to foetal system. Although recent study showed that adult BM contains CD5$^+$ B-1 cell progenitor (Montecino-Rodriguez et al, 2006), the CD5$^-$ BM cells that generated in our *in vitro* culture are different from B-1 ceils due to lack of IgM expression (Fig. 5.10).

The origin of CLL is unknown, however, it is thought that mature B cells, such as naïve B ceils and memory B cells, are candidates due to their mature phenotype (Stevenson and Caligaris-Cappio, 2004). Curiously, PKCα-expressing RAG-1$^{-/-}$ cells also exhibited CLL-like phenotype (Fig. 5.5) that we observed in wildtype mice. This suggests that this transformation is induced before pre-B stage, where B cells in RAG-1$^{-/-}$ mice stop development. However, when adult CD19$^+$ splenocytes were infected with PKCα-KR upon LPS stimulation and were cocultured with OP9, they also displayed the CLL-phenotype. This is odd because adult CD19$^+$ splenocytes consist of populations of post immature B cells stage that express IgM on surface and thus, no late-pro-B cells (Mårtensson et al, 2002). To explain this controversy, there are two hypotheses. First, CLL is a heterogeneous leukaemia and thus PKCα-KR may target different developmental stages. For example, ALL is a heterogeneous disease with regard to clinical treatment response and prognosis, genetic changes resulted from chromosomal translocation and the involved causative proteins (Faderl et al, 1998). Recently, clinically and genetically different ALL subtypes have been shown to originate and transform at distinct stages of haematopoietic development. p210 BCR/ABL1 fusions originated in HPCs, whereas p190 BCR/ABL1 positive leukaemic cells were derived from committed B ceil progenitors (Castor et al, 2005). Therefore, it may be plausible that PKCα mediated transformation result in different consequences depending which stage of cells PKCα targets. As another possibility, there may be two transformation points for CLL induction, one before late-pro-B cell stage and the other after immature B cell stage. If so, it may explain why the growth speed of PKCα-KR-expressing RAG-1$^{-/-}$ FL cells was

slower than that of wildtype FL cells, the latter can fully bear both signals for transformation. This may also describe why there were less CLL-like B cells in the PKCα-KR-RAG-1$^{-/-}$-HPCs injected mice compared to PKCα-KR-wildtype HPCs injected mice even though GFP$^+$ population in the reconstituted mice was higher (PKCα-KR-RAG-1$^{-/-}$-HPCs injected mice, CD19$^+$ B cell=20 %, GFP$^+$=29 %; PKCα-KR-wildtype-HPCs injected mice, CD19$^+$ B cell=70 %, GFP$^+$=7.5 %; Fig. 5.8 and Fig. 3.13, respectively). The GFP$^-$ population in RAG-1$^{-/-}$ mice may not have developed as well as that in wildtype mice, which makes the GFP$^+$ population look elevated. Thus, the CLL-like cells without BCR, such as PKCα-KR-RAG-1$^{-/-}$-expressing cells may not survive as long as the CLL-like cells with BCR. As a future study to define the specific transformation stage and establish the cellular population targeted for transformation by PKCα, distinct populations of developing B cells will be isolated using FCM sorting, and thus the ability of cells to be transformed by PKCα-KR will be examined. First, HPCs derived from wildtype mice FL will be infected with PKCα-KR and discrete developmental stages of GFP$^+$ B cell will be isolated based on the expression of multiple cell surface markers, as follows: HSC (CD117$^-$, Sca-1$^+$); pre-pro-B cells (CD19$^-$, Sca-1$^-$CD117$^+$); pro-B cells (CD45R$^+$, CD19$^+$, CD24^{lo}), and; pre-B cells (CD45R$^+$, CD19$^+$, CD24^{hi}) (Hardy and Hayakawa, 2001, Kondo et al, 1997). The subsequent population will be stained with CLL markers, such as CD5, CD23 and IgM, and will be analysed by FCM. This experiment will elucidate which stage of haemopoiesis has a potential to be transformed by subversion of PKCα.

The OP9-DL1 cell line was generated by ectopically expressing the Notch ligand DL-1 in the OP9 cell line, thus enabling the OP9 cell line to support the induction of T cell differentiation (Schmitt and Zúñiga-Pflücker, 2002). The results gained from OP9-DL1 coculture showed that GFP$^+$ PKCα-CAT-cocultures express CD4 and CD8 on surface larger percentage than MIEV control, in contrast, PKCα-KR-cocultures did not express CD4 or CD8. This is consistent with a previous report showing that PKCα-CAT expression in FT facilitated T cell differentiation, while PKCα-KR expression blocked T cell

development (Michie et al, 2001). As we expected, OP9-DL1 did not support B cell development, which is consistent with the findings that Notch 1 signalling blocks B cell development before or during pre-pro-B cell stage (Pui et al, 1999). Yet, as it was observed that B cells that have matured beyond the pre-B cell stage are able to grow in the coculture with OP9 (Schmitt and Zúñiga-Pflücker, 2002), it is not surprising to see a population of B cells in MIEV-OP9-DL1 culture. B cell population in MIEV-OP9 culture started from 27 % at day 6, and it was slightly increased till 44 % at day 13. Whereas the leukaemic population of B cells generated by culturing PKCα-KR-expressing FL with OP9 started 85 % at day 6, and it was drastically decreased to 3.3 % at day 13 by co-culturing with OP9-DL1. Recently, it has been shown that Notch signalling induces growth arrest and apoptosis in malignant B cell via Hes1 (Zweidler-McKay et al, 2005). Our results support this data, and thus the level of Hes1 expression is of interest for a further study.

Considering the previous study showed that high density of DL-1 facilitates T cell development and inhibits B cell development (Dallas et al, 2005), and constitutively active Notch1 expression leads to T cell development fate and blocks B cell development at pre-pro-B cell stage (Pui et al, 1999), it is expected that OP9-DL1 cells which express DL1 with high density on surface interfere B lymphopoiesis and the B cell development is hindered at pre-pro-B cell stage. Thus, PKCα-KR-expressing HPCs that committed to B cells before transformation events would not proliferate in T cell environment unless they are transformed early enough to escape from Notch-mediated B cell block, which support the early transformation by PKCα-KR expression.

Altogether, it was shown that transformation events can occur before pre-B cells and possibly in an even earlier stage of B cell development. The progression of leukaemiagenesis could be hindered by Notch signalling. Further investigations are required to elucidate the origin of leukaemic cells as well as mechanisms of PKCα-KR mediated transformation.

Figure 5.1 T cell development

Thymocyte differentiation is characterised by the expression of well-defined cell-surface markers, including CD4, CD8, CD44, CD25 and CD117 as well as the expression of either pre-TCR or TCR.

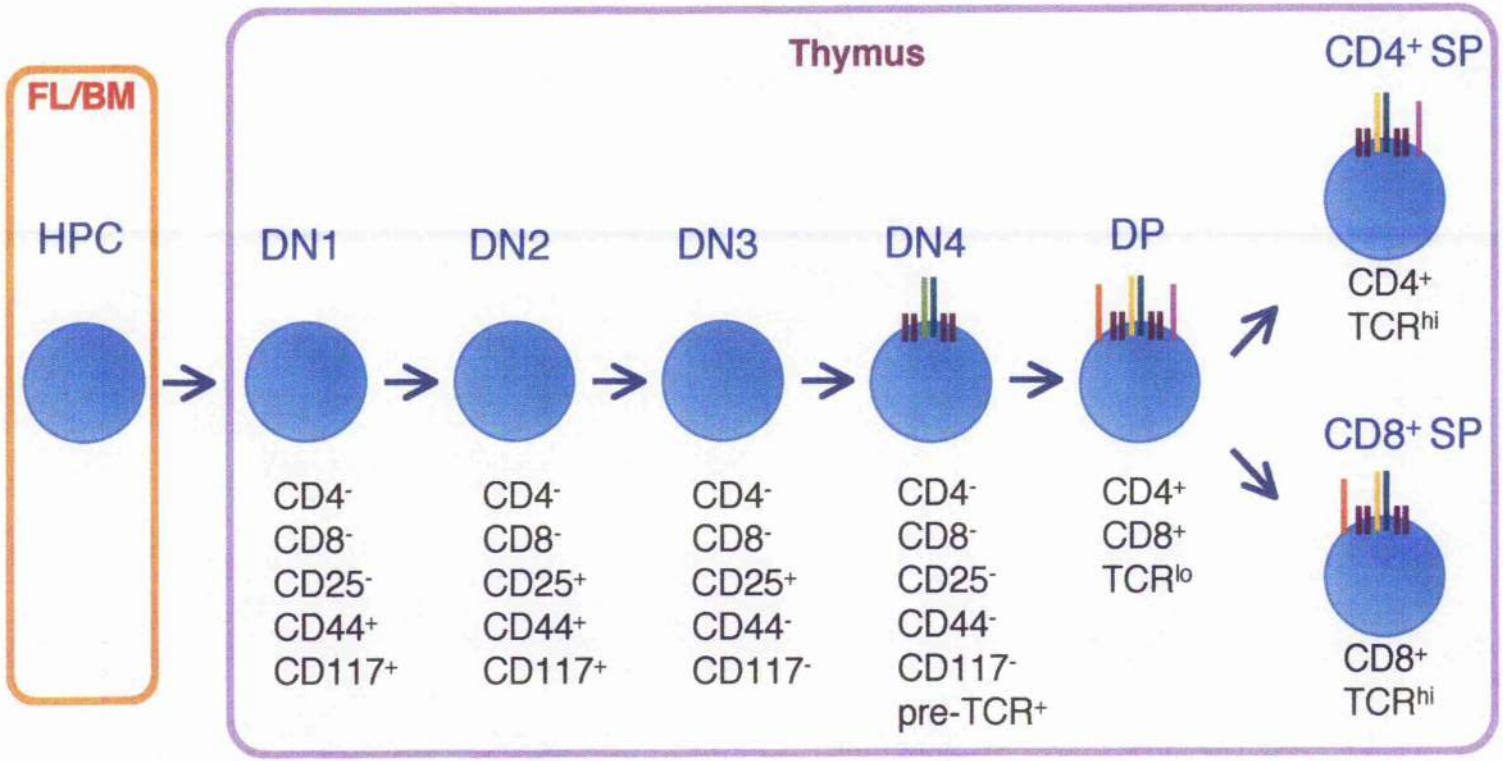
FL/BM
HPC
Thymus
DN1
DN2
DN3
DN4
DP
CD4+ SP
CD8+ SP
CD4- CD8- CD25- CD44+ CD117+
CD4- CD8- CD25+ CD44+ CD117+
CD4- CD8- CD25+ CD44- CD117-
CD4- CD8- CD25- CD44- CD117- pre-TCR+
CD4+ CD8+ TCRlo
CD4+ TCRhi
CD8+ TCRhi

Figure 5.2 Wildtype FT/BM-derived HPCs retrovirally infected with PKCα-KR display a growth advantage over GFP$^-$

Wildtype FT (top) and HPCs derived from adult BM (bottom) of ICR mice were retrovirally infected with MIEV and PKCα-KR and then cultured in our *in vitro* B cell generation system. During this period, the cultures were sampled and analysed by FCM for relative amounts of GFP expression, percentages as indicated. Histogram plots were live and size gated. These data are from a single experiment, representative of three separate experiments.

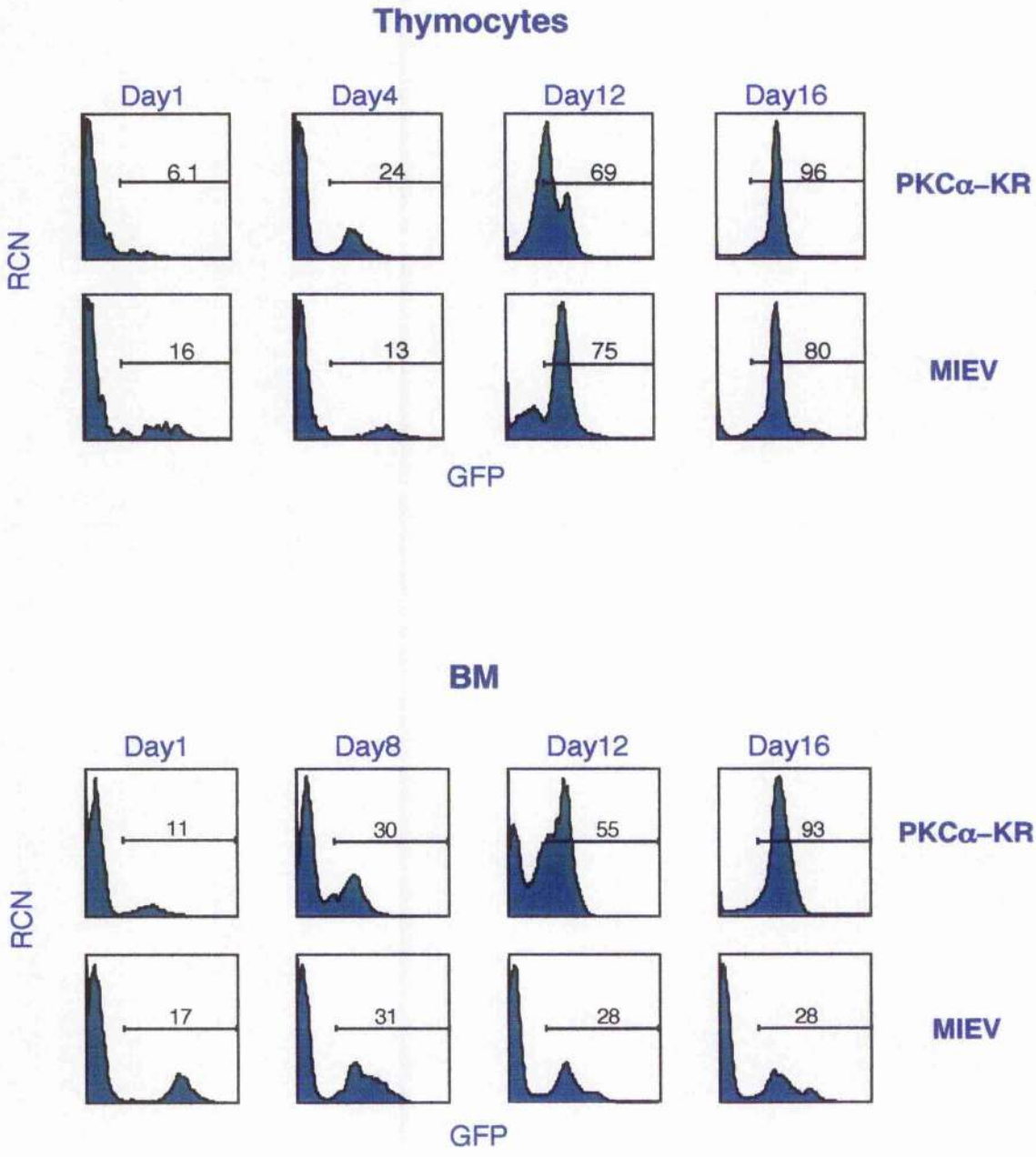
Thymocytes
Day1
Day4
Day12
Day16
6.1
24
69
96
PKCα–KR
RCN
16
13
75
80
MIEV
GFP
BM
Day1
Day8
Day12
Day16
11
30
55
93
PKCα–KR
RCN
17
31
28
28
MIEV
GFP

Figure 5.3 Stable expression of PKCα-KR in wildtype FT and BM results in the development of CLL-like cells

Wildtype FT (top) and HPCs derived from adult BM (bottom) of ICR mice were retrovirally infected with MIEV or PKCα-KR and cultured in our *in vitro* B cell generation system, and then phenotypically characterised by FCM. The cocultures were harvested at day 15 (top) or at day 16 (bottom). Analysis of IgM vs. κ, IgD vs. κ, CD5 vs. CD2 and CD23 vs. CD19 expression are shown for GFP^+ gated cells, percentages as indicated. Contour plots were live and size gated. These data are from a single experiment, representative of three separate experiments.

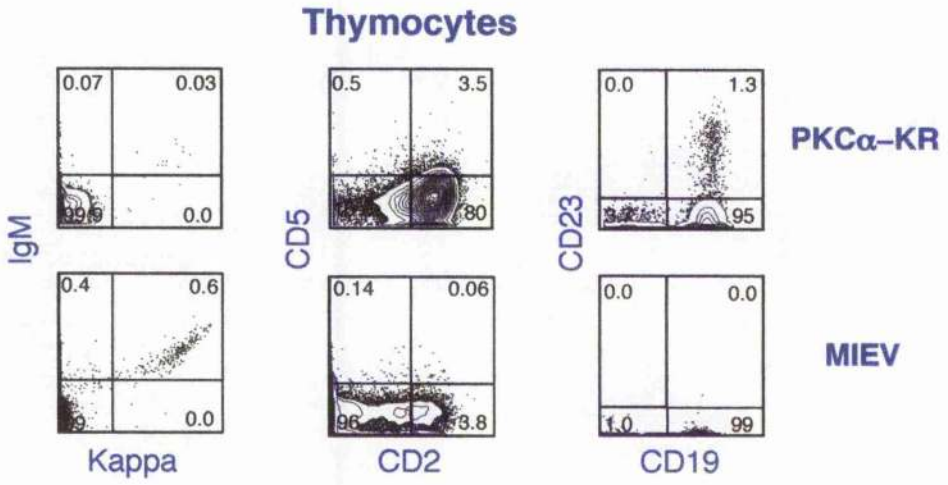
Thymocytes
0.07
0.03
99.9
0.0
0.5
3.5
80
0.0
1.3
95
PKCα–KR
IgM
CD5
CD23
0.4
0.6
0.0
0.14
0.06
96
3.8
0.0
0.0
1.0
99
MIEV
Kappa
CD2
CD19

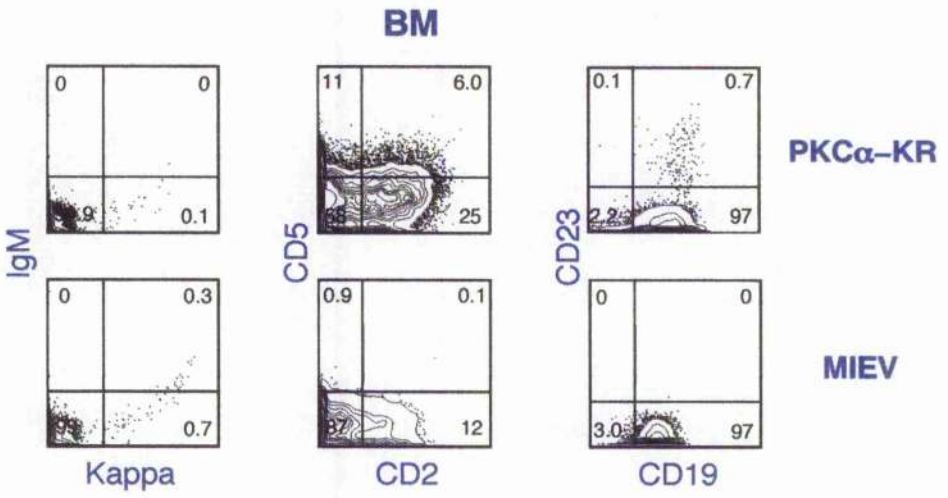
BM
0
0
0.1
11
6.0
25
0.1
0.7
97
PKCα–KR
IgM
CD5
CD23
0
0.3
0.7
0.9
0.1
12
0
0
3.0
97
MIEV
Kappa
CD2
CD19

Figure 5.4 RAG-1$^{-/-}$ FL-derived HPCs retrovirally infected with PKCα-KR display a growth advantage over GFP$^-$ cells

HPCs derived from RAG-1$^{-/-}$ mouse FL were retrovirally infected with MIEV, PKCα-KR, PKCδ-KR or PKCζ-KR and then cultured in our *in vitro* B cell generation system. During this period, the cultures were sampled and analysed by FCM for relative amounts of GFP expression, percentages as indicated. Histogram plots were live and size gated. These data are from a single experiment, representative of five separate experiments.

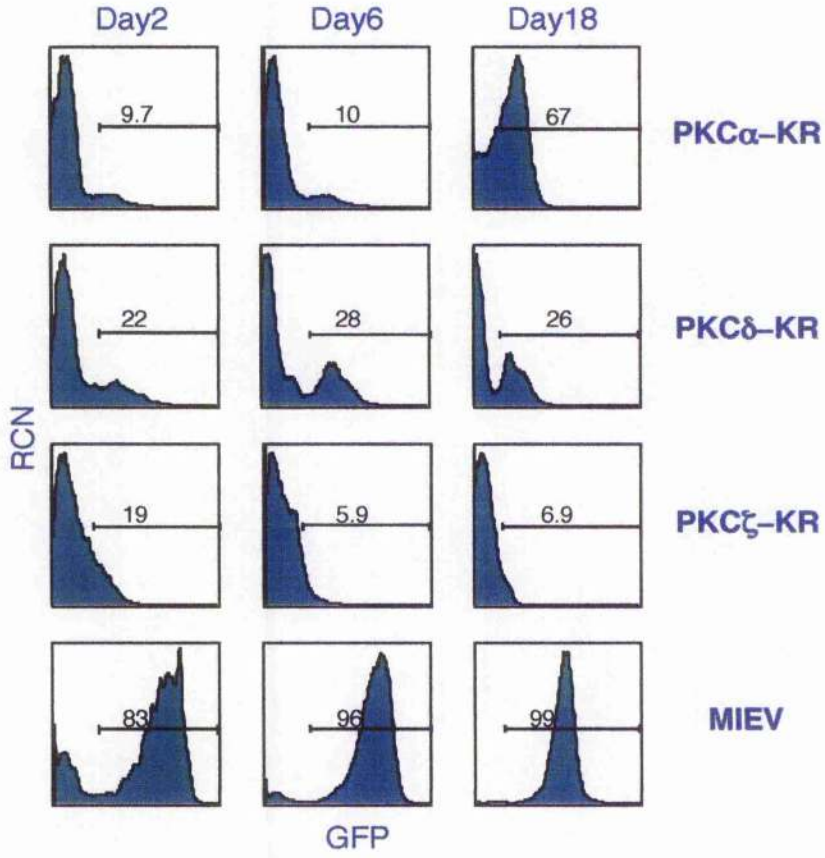
Day2
Day6
Day18
9.7
10
67
PKCα–KR
22
28
26
PKCδ–KR
19
5.9
6.9
PKCζ–KR
83
96
99
MIEV
RCN
GFP

Figure 5.5 Stable expression of PKCα-KR also renders CLL-like phenotype in HPCs derived from RAG-1$^{-/-}$

HPCs derived from FL of RAG-1$^{-/-}$ mice infected with MIEV, PKCα-KR, PKCδ-KR and PKCζ-KR were phenotypically characterised by FCM. The cocultures were harvested at day 18. Analysis of CD5 vs. CD2 and CD23 vs. CD19 expression are shown for GFP^{+} gated cells, percentages as indicated. Contour plots were live and size gated. These data are from a single experiment, representative of five separate experiments.

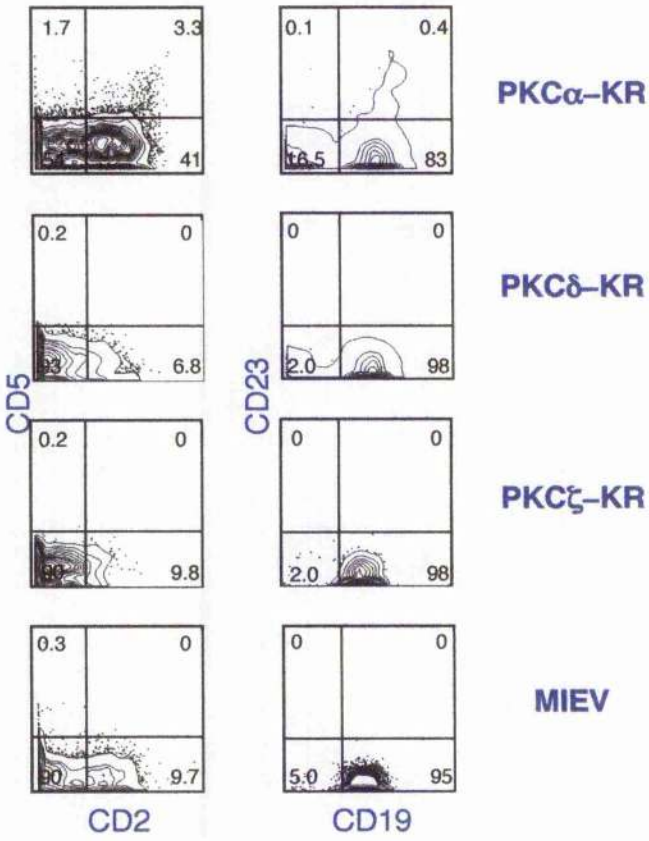
1.7
3.3
41
0.1
0.4
16.5
83
PKCα–KR
0.2
0
6.8
0
0
2.0
98
PKCδ–KR
CD5
CD23
0.2
0
9.8
0
0
2.0
98
PKCζ–KR
0.3
0
9.7
0
0
5.0
95
MIEV
CD2
CD19

Figure 5.6 RAG-1$^{-/-}$ BM cells retrovirally infected with PKCα-KR also display a growth advantage over GFP$^-$ cells

RAG-1$^{-/-}$ mice BM cells were retrovirally infected with MIEV or PKCα-KR and then cultured in our *in vitro* B cell generation system. During this period, the cultures were sampled and analysed by FCM for relative amounts of GFP expression, percentages as indicated. Histogram plots were live and size gated. These data are from a single experiment, representative of three separate experiments.

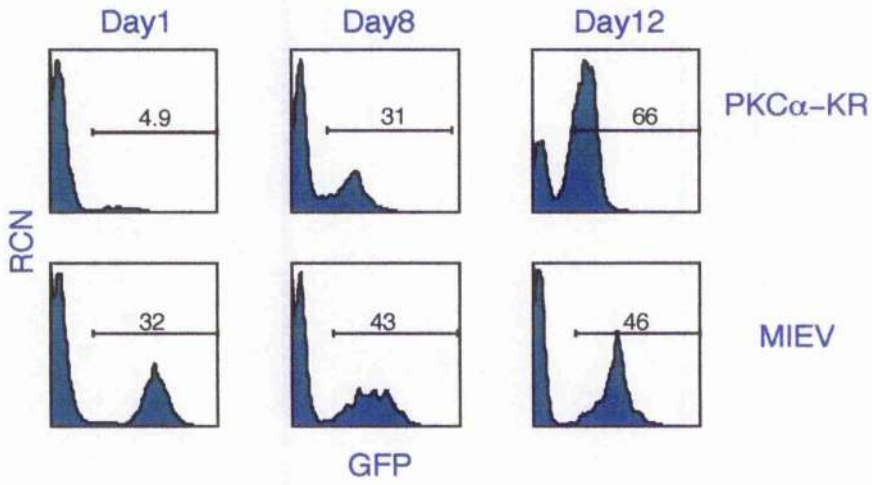
Day1
Day8
Day12
4.9
31
66
PKCα-KR
RCN
32
43
46
MIEV
GFP

Figure 5.7 Stable expression of PKCα-KR renders CLL-like phenotype in RAG-1$^{-/-}$ BM cells

RAG-1$^{-/-}$ derived BM cells infected with MIEV or PKCα-KR were phenotypically characterised by FCM. The cocultures were harvested at day 16. Analysis of CD5 vs. CD2 and CD23 vs. CD19 expression are shown for GFP^{+} gated cells, percentages as indicated. Contour plots were live and size gated. These data are from a single experiment, representative of three separate experiments.

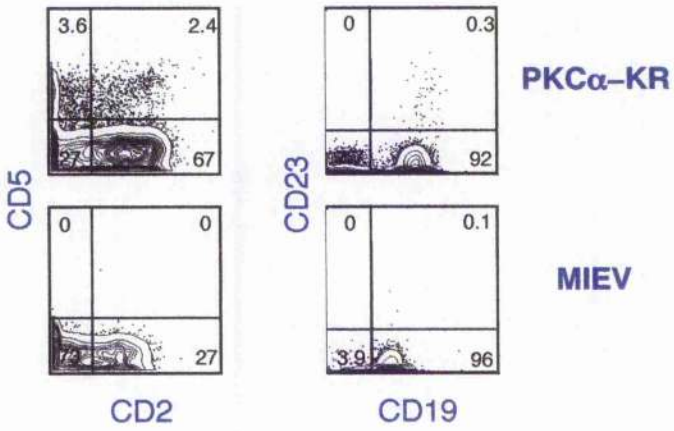
3.6
2.4
27
67
0
0
27
CD5
CD2
0
0.3
92
0
0.1
3.9
96
CD23
CD19
PKCα–KR
MIEV

Figure 5.8 LN cells from PKCα-KR-infected RAG-1$^{-/-}$-HPC-infected RAG-1$^{-/-}$ mouse displayed a CLL-like phenotype

1 × 10^6 of either PKCα-KR- or MIEV-infected RAG-1$^{-/-}$-HPCs were i.p. injected into RAG-1$^{-/-}$ mouse. LN cells and tumour mass from reconstituted mice were analysed 6 week after the injection. FCM was carried out on GFP$^+$ and GFP$^-$ populations, CD23 vs. CD19 and CD45R vs. CD5 percentages as indicated. Plots were live and size gated. This is a representative experiment from three separate adoptive transfers.

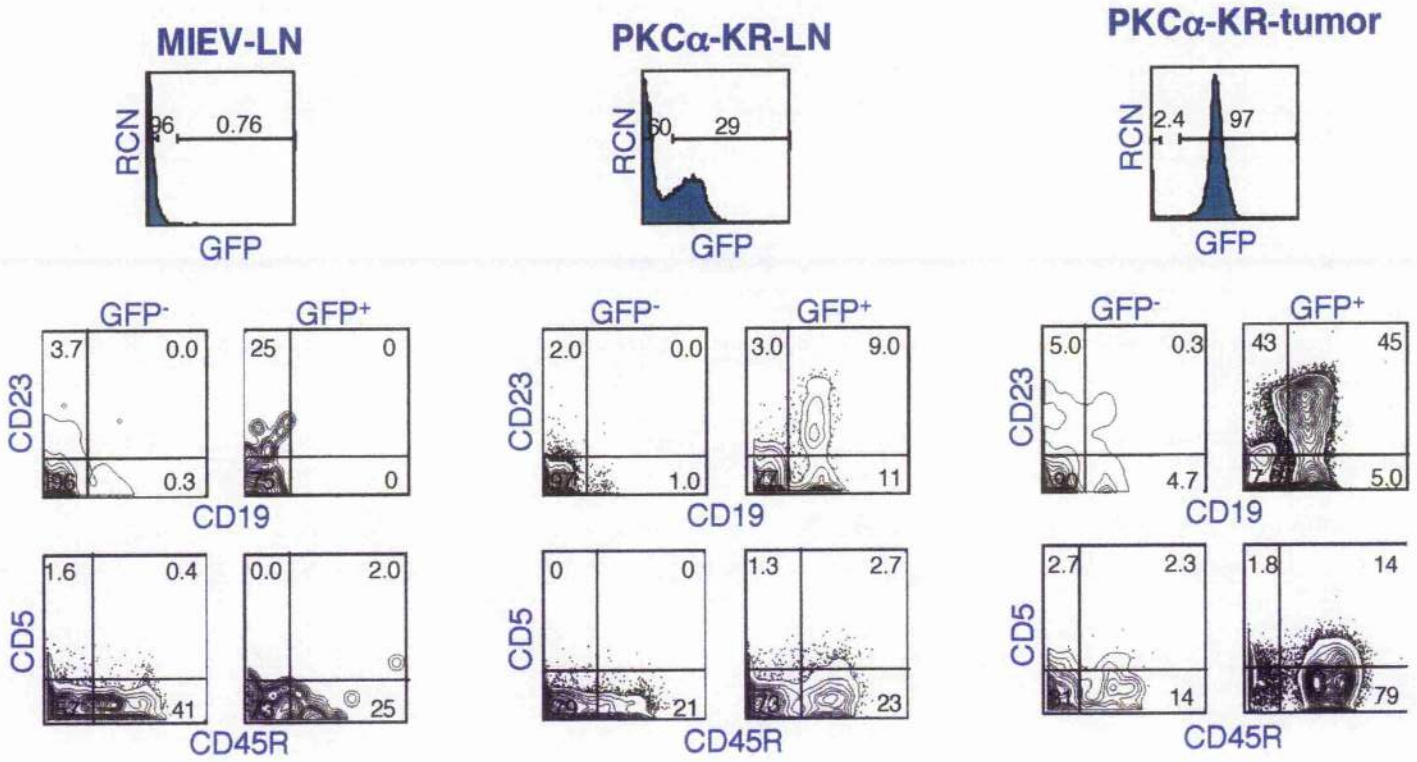
MIEV-LN
PKCα-KR-LN
PKCα-KR-tumor
RCN
96
0.76
60
29
2.4
97
GFP
GFP⁻
GFP⁺
CD23
CD19
3.7
0.0
0.3
25
0
2.0
1.0
3.0
9.0
11
5.0
4.7
43
45
5.0
CD5
CD45R
1.6
0.4
41
0.0
2.0
25
1.3
2.7
23
2.3
14
1.8
79

Figure 5.9 PKCα-KR-expressing-CD19$^+$ splenocytes from adult wildtype mice showed growth advantage

CD19$^+$ population in splenocytes derived from adult wildtype mice was enriched by MACS. CD19$^+$ splenocytes were retrovirally infected with MIEV or PKCα-KR under stimulation with 50 μg/ml LPS stimulation for 48 h and infected cells were cocultured with OP9. During this period, the cultures were sampled and analysed by FCM for relative amounts of GFP expression, percentages as indicated. Histogram plots were live and size gated. These data are from a single experiment, representative of two separate experiments.

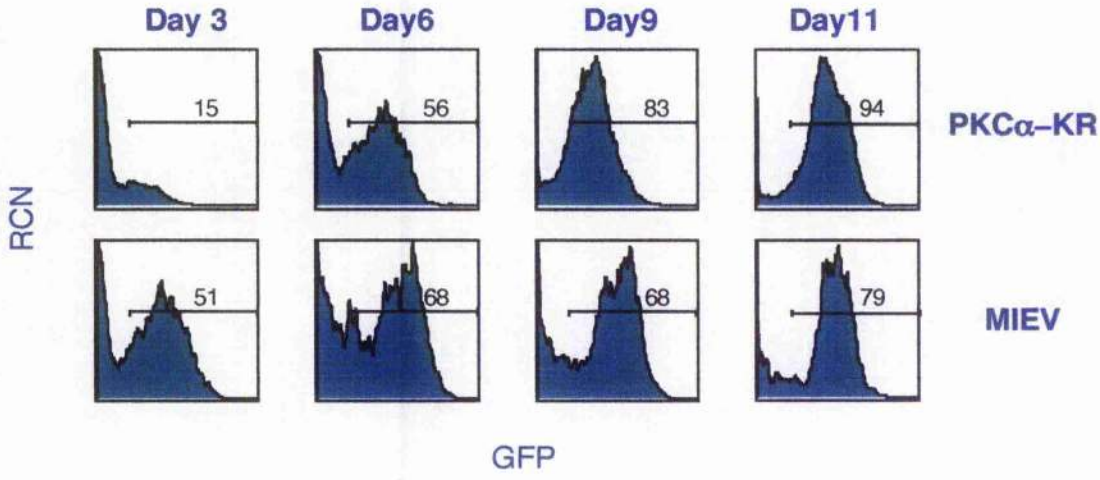
Day 3
Day6
Day9
Day11
15
56
83
94
PKCα–KR
51
68
68
79
MIEV
RCN
GFP

Figure 5.10 Stable expression of PKCα-KR in CD19$^+$ splenocytes from adult wildtype mice revealed CLL-like phenotype

CD19$^+$ splenocytes were infected with MIEV or PKCα-KR whilst being stimulated with 50 μg/ml LPS stimulation for 48 h and were phenotypically characterised by FCM. The cultures were sampled and analysed by FCM. Analysis of CD45 vs. IgD, CD45R vs. CD5, CD45R vs. IgM and CD23 vs. CD19 expressions are shown for GFP$^+$ gated cells, percentages as indicated. Contour plots were live and size gated. These data are from a single experiment, representative of two separate experiments.

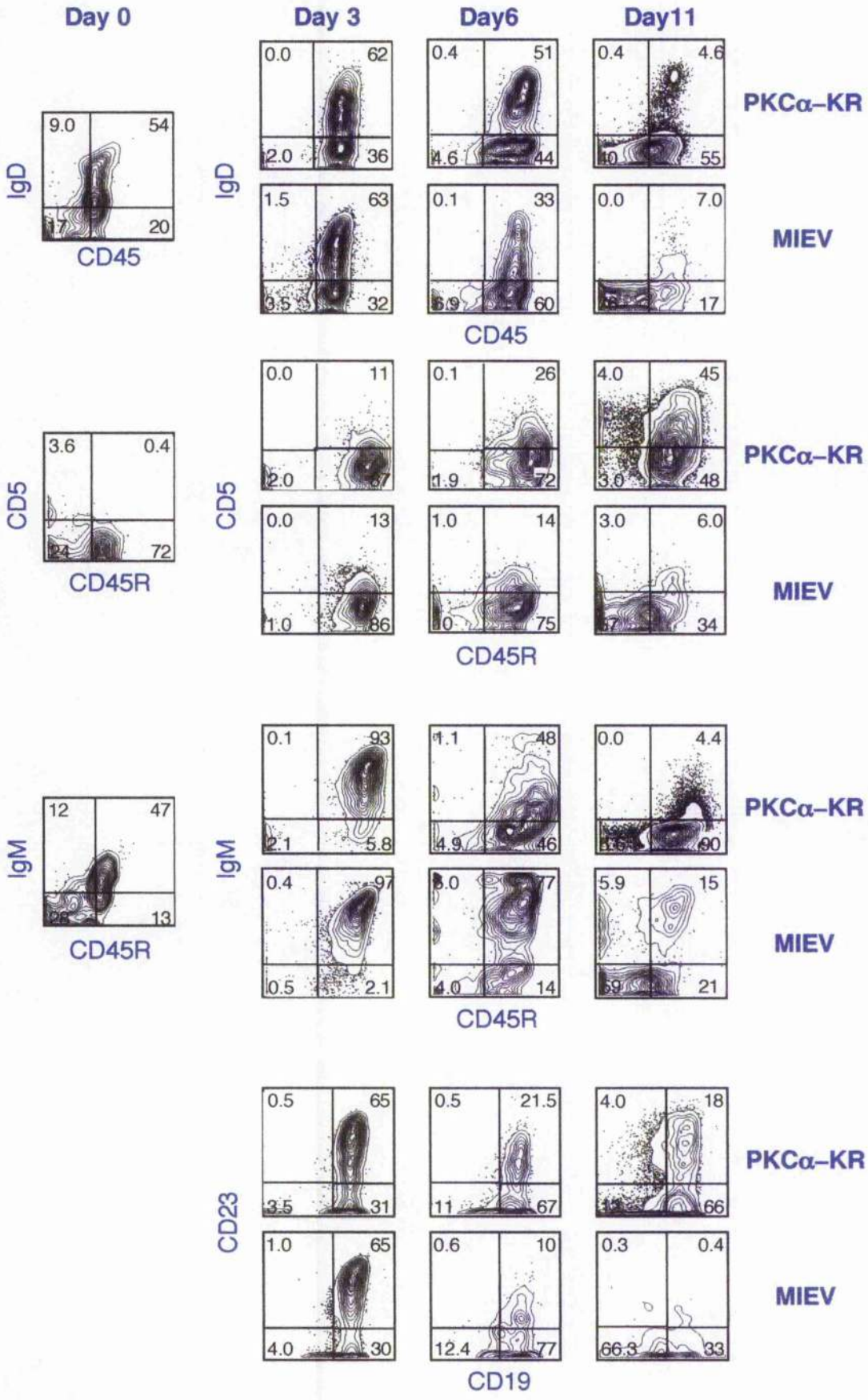
Day 0
Day 3
Day6
Day11
PKCα–KR
MIEV
IgD
CD45
CD5
CD45R
IgM
CD23
CD19
9.0
54
17
20
0.0
62
2.0
36
0.4
51
4.6
44
0.4
4.6
10
55
1.5
63
3.5
32
0.1
33
6.9
60
0.0
7.0
17
3.6
0.4
24
72
0.0
11
2.0
87
0.1
26
1.9
72
4.0
45
3.0
48
0.0
13
1.0
86
1.0
14
10
75
3.0
6.0
37
34
12
47
13
0.1
93
2.1
5.8
1.1
48
4.9
46
0.0
4.4
90
0.4
97
0.5
2.1
3.0
77
4.0
14
5.9
15
59
21
0.5
65
3.5
31
0.5
21.5
11
67
4.0
18
66
1.0
65
4.0
30
0.6
10
12.4
77
0.3
0.4
66.3
33

Figure 5.11 Coculture with OP9-DL1 inhibited growth of PKCα-CAT-expressing cells

Wildtype HPCs derived from FL of ICR mice were retrovirally infected with MIEV, PKCα-KR, and PKCα-CAT, and then cocultured with OP9-DL1 cells that support T cell development. During this period, the cultures were sampled and analysed by FCM for relative amounts of GFP expression, percentages as indicated. Histogram plots were live and size gated. These data are from a single experiment, representative of three separate experiments.

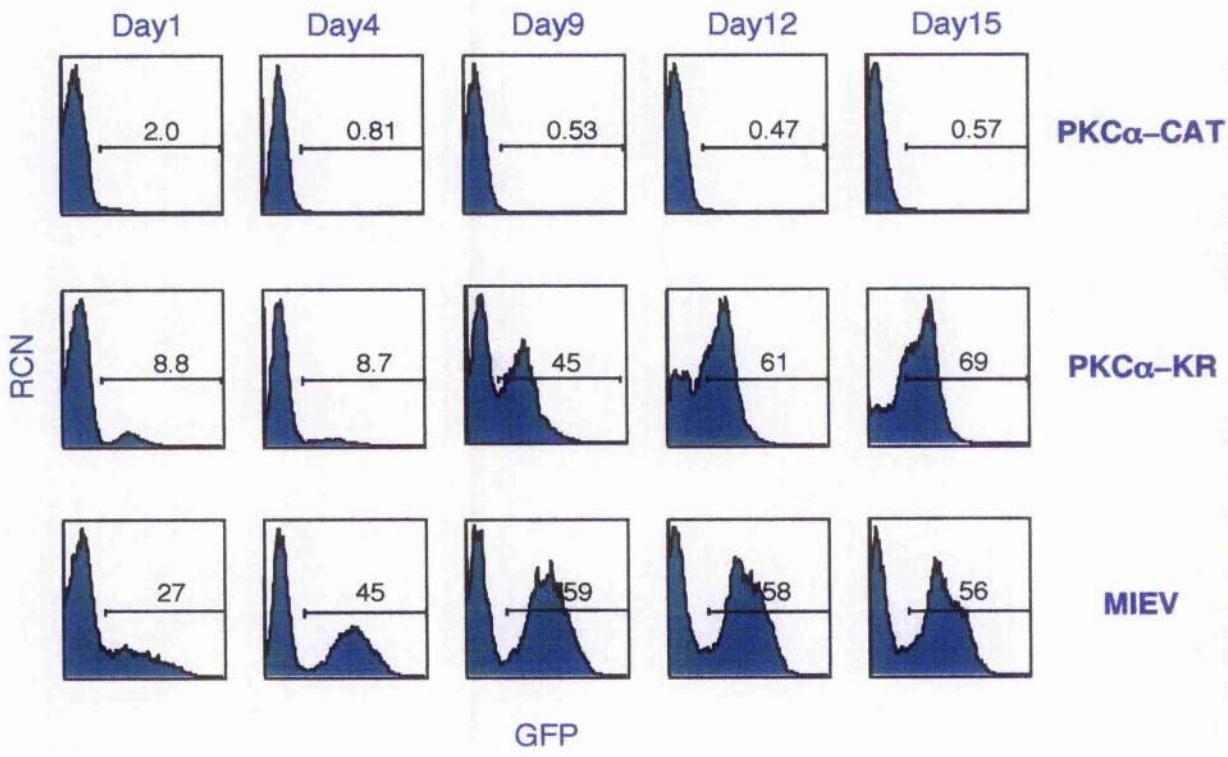
Day1
Day4
Day9
Day12
Day15
2.0
0.81
0.53
0.47
0.57
PKCα–CAT
8.8
8.7
45
61
69
PKCα–KR
RCN
27
45
59
58
56
MIEV
GFP

Figure 5.12A Notch ligation inhibited leukaemic cells' growth

Wildtype HPCs derived from ICR mice were retrovirally infected with MIEV, PKCα-KR, and PKCα-CAT, and then cocultured with OP9-DL1 cells. The cocultures were harvested at day 15 and phenotypically characterised by FCM. Analysis of CD23 vs. CD19, CD25 vs. CD117, and CD4 vs. CD8 expressions are shown for GFP^+ gated cells, percentages as indicated. Contour plots were live and size gated. These data are from a single experiment, representative of three separate experiments.

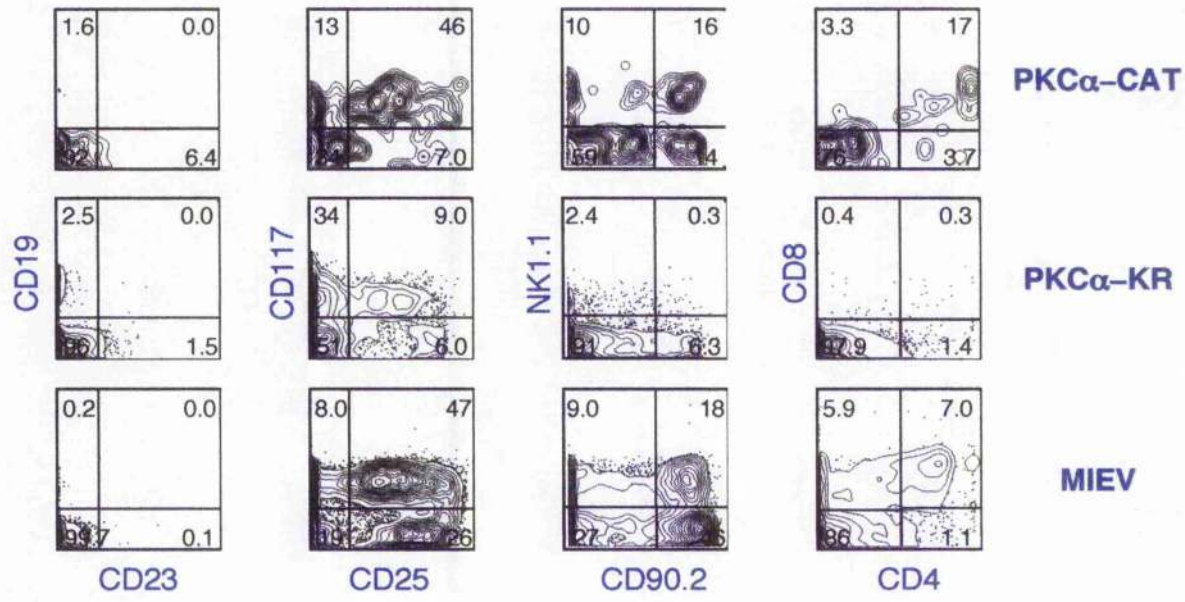
1.6
0.0
6.4
13
46
7.0
10
16
3.3
17
3.7
PKCα–CAT
2.5
0.0
1.5
34
9.0
6.0
2.4
0.3
6.3
0.4
0.3
1.4
PKCα–KR
0.2
0.0
0.1
8.0
47
9.0
18
5.9
7.0
1.1
MIEV
CD19
CD117
NK1.1
CD8
CD23
CD25
CD90.2
CD4

Figure 5.12B Notch ligation inhibited leukaemic cells' growth

Wildtype HPCs derived from ICR mice were retrovirally infected with MIEV, PKCα-KR, and PKCα-CAT, and then cocultured with OP9-DL1 cells. The GFP^+ cell number from the day 15 coculture was counted by FCM. The percentage was calculated against the number of MIEV coculture. The data are from a single experiment, representative of three separate experiments.

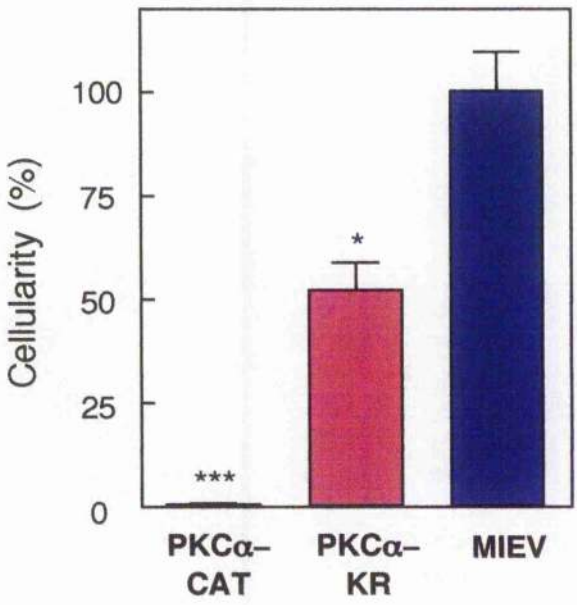

*** $p < 0.0001$ against MIEV
* $p < 0.01$ against MIEV

Figure 5.13A Leukaemic cells do not show CLL-like phenotype upon coculture with OP9-DL1, but they remain aberrant

Wildtype HPCs derived from ICR mice infected with MIEV were cocultured in either OP9 or OP9-DL1 for 6 day. At day 6, half of each coculture was exchanged into different feeder cells: step 1: OP9-DL1 to OP9-DL1; step 2: OP9-DL1 to OP9; step 3: OP9 to OP9; step 4: OP9 to OP9-DL-1. The cocultures were phenotypically characterised by FCM at day 10 and day 13. Analysis of CD23 vs. CD19 expressions are shown for GFP^+ gated cells, percentages as indicated. Contour plots were live and size gated. These data are from a single experiment, representative of three separate experiments.

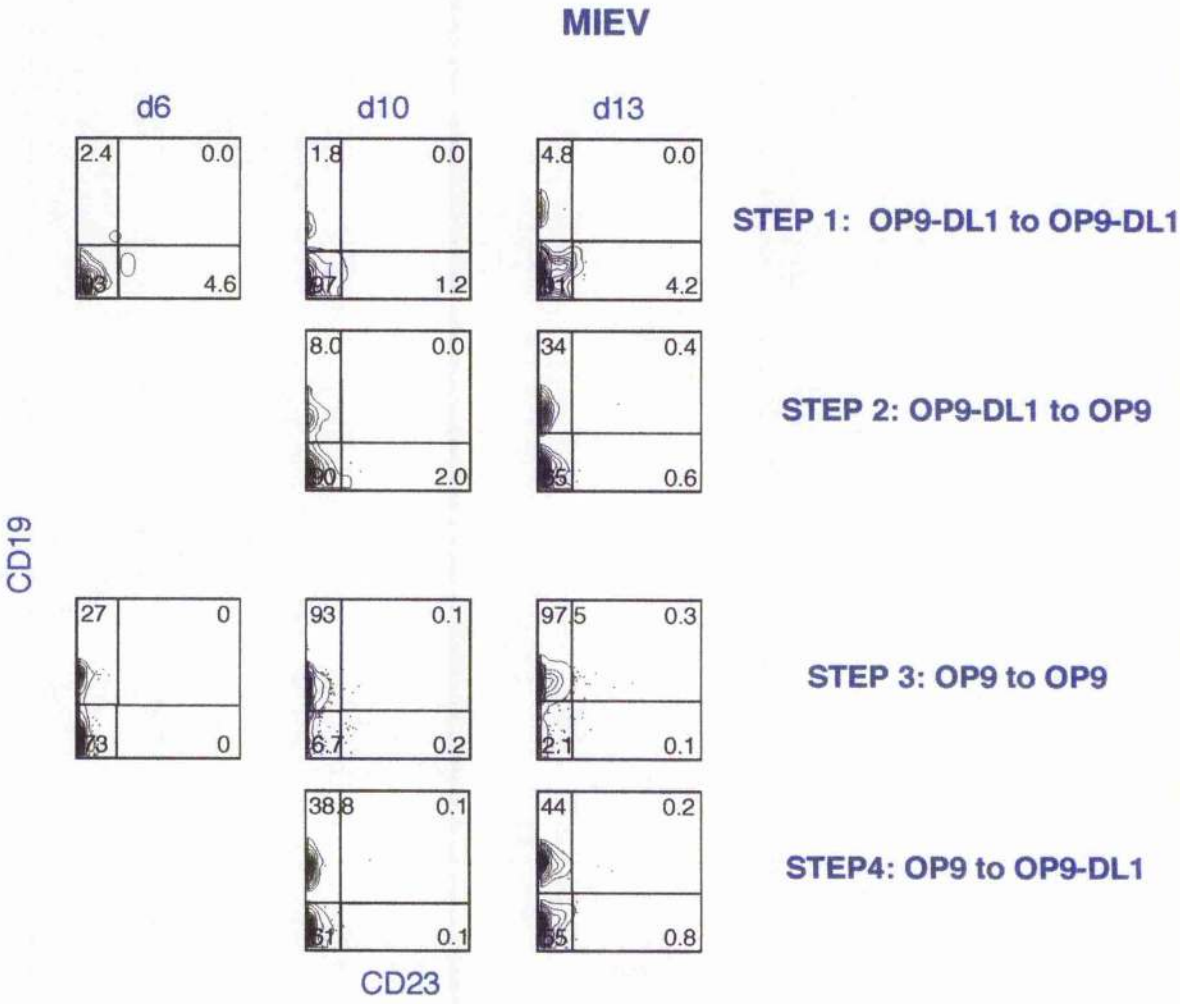
MIEV
d6
d10
d13
2.4
0.0
4.6
1.8
0.0
1.2
4.8
0.0
4.2
STEP 1: OP9-DL1 to OP9-DL1
8.0
0.0
2.0
34
0.4
0.6
STEP 2: OP9-DL1 to OP9
CD19
27
0
73
0
93
0.1
6.7
0.2
97.5
0.3
2.1
0.1
STEP 3: OP9 to OP9
38.8
0.1
0.1
44
0.2
0.8
STEP4: OP9 to OP9-DL1
CD23

Figure 5.13B Leukaemic cells do not show CLL-like phenotype upon coculture with OP9-DL1, but they remain aberrant

Wildtype HPCs derived from ICR mice infected with PKCα-KR were cocultured in either OP9 or OP9-DL1 for 6 day. At day 6, half of each coculture was exchanged into different feeder cells: step 1: OP9-DL1 to OP9-DL1; step 2: OP9-DL1 to OP9; step 3: OP9 to OP9; step 4: OP9 to OP9-DL-1. The cocultures were phenotypically characterised by FCM at day 10 and day 13. Analysis of CD23 vs. CD19 expressions are shown for GFP^+ gated cells, percentages as indicated. Contour plots were live and size gated. These data are from a single experiment, representative of three separate experiments.

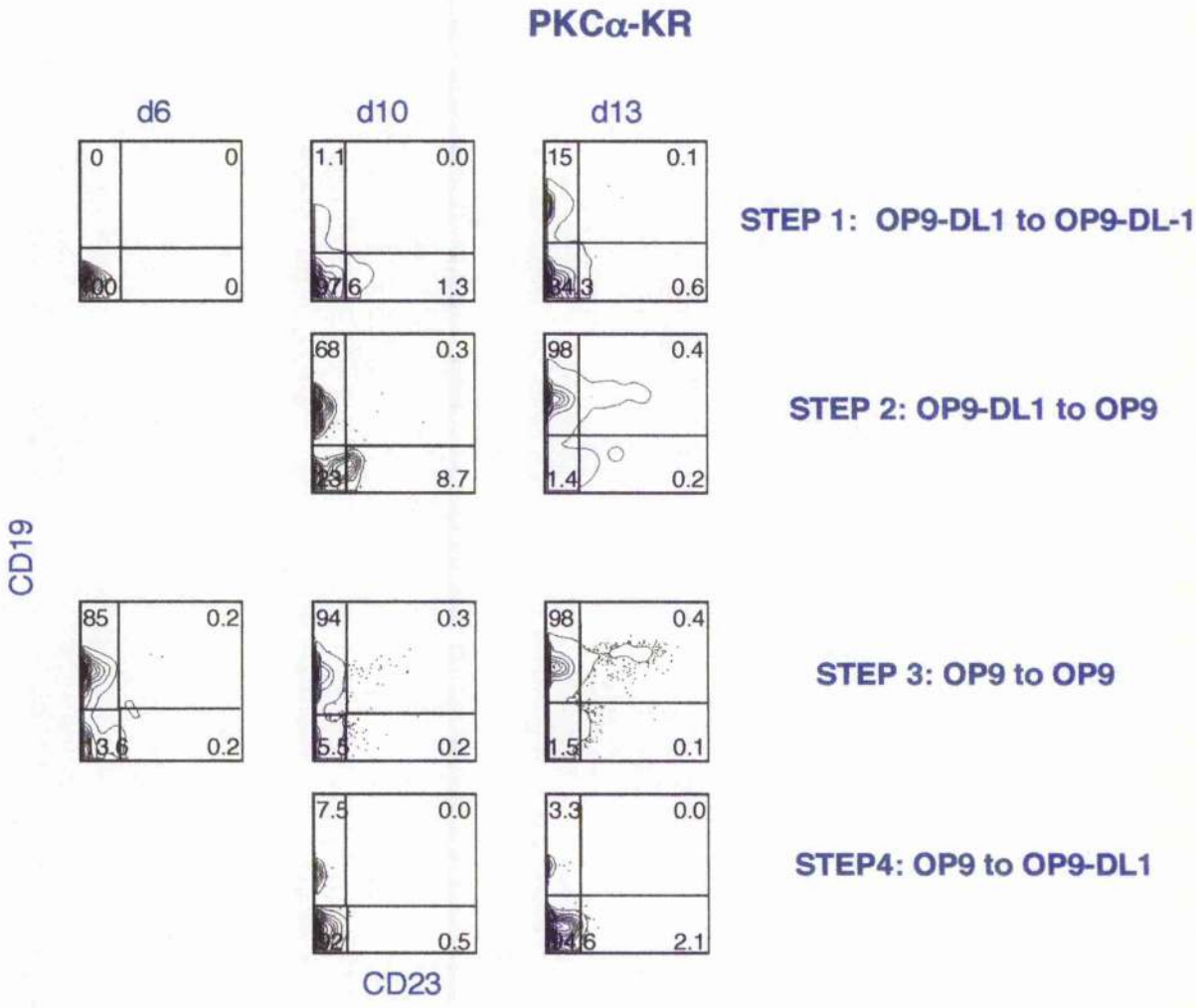
PKCα-KR
d6
d10
d13
0
0
0
0
1.1
0.0
97.6
1.3
15
0.1
34.3
0.6
STEP 1: OP9-DL1 to OP9-DL-1
68
0.3
8.7
98
0.4
1.4
0.2
STEP 2: OP9-DL1 to OP9
CD19
85
0.2
13.6
0.2
94
0.3
5.5
0.2
98
0.4
1.5
0.1
STEP 3: OP9 to OP9
7.5
0.0
0.5
3.3
0.0
2.1
STEP4: OP9 to OP9-DL1
CD23

Chapter 6:
General discussion

6.1 What mechanisms underly the subversion of PKCα generating CLL-like cells?

PKCα-KR-expression generated CLL-like cells with a reduction in PKC activity, which may occur as a consequence of discretely targeting PKCα activity. The ability to induce the development of CLL in HPCs appears to be a unique property of this isoform, PKCα, as subversion of PKCδ or PKCζ did not induce leukaemiagenesis. PKCα activation has generally been associated with the generation of anti-apoptotic cell responses (Jiffar et al, 2004, Ruvolo et al, 1998), however it is becoming apparent that the biological outcome of PKCα activation, whether it is survival or apoptosis is dependent on the cell type being studied (Michie and Nakagawa, 2005). As there is growing evidence that PKCα and PKCδ antagonise each other in order to regulate survival or apoptosis in a number of cell types (Hornia et al, 1999, Mandil et al, 2001) these studies, coupled with those of Ringshausen *et al.*, suggest that upsetting the balance of either of these isoforms may enable apoptosis of CLL cells (Nakagawa et al, 2006, Ringshausen et al, 2006).

BAFF and APRIL are TNF family ligands that are critical cytokines for maintenance of normal B cell development and homeostasis (Schiemann et al, 2001, Schneider et al, 2001, Thompson et al, 2000). Recent reports showed that BAFF and APRIL are expressed in CLL cells (He et al, 2004, Kern et al, 2004) and moreover, BAFF-R and receptors for both BAFF and APRIL, BCMA and TACI (Schneider, 2005) are expressed on CLL cells (He et al, 2004). The soluble forms of BAFF and APRIL prevented spontaneous/drug-induced apoptosis (Kern et al, 2004, Novak et al, 2002), suggesting autocrine secretion of these cytokines rescue CLL cells from apoptosis. To understand the mechanism of how PKCα-KR expressing cells evade apoptosis, it could be determined whether BAFF/APRIL and their receptors are expressed in our CLL-like cells by FCM. If expression of either BAFF or APRIL or both is determined, then anti-BAFF and -APRIL antibody could be added to the serum to block the autocrine survival action of BAFF/APRIL, and the apoptosis rate of CLL cells could be examined.

It is unknown how PKCα mediates transformation. A possible explanation is that PKCα phosphorylates and activates tumour suppressor downstream and therefore, the reduction of PKCα activity diminishes the tumour suppressing function. For example, the rasGTPase activating protein-associated docking proteins, Dok-1 and Dok-2 act as tumour suppressors of CML, as demonstrated by the development of CML in Dok-$1^{-/-}$ Dok-$2^{-/-}$ mice (Niki et al, 2004, Yasuda et al, 2004). In addition, reports establish that the signalling molecules SLP-65 (also known as BLNK/BASH) and Btk act as tumour suppressors in B lymphocytes, as evidenced by the observation that SLP-$65^{-/-}$ and SLP-$65^{-/-}$ $Btk^{-/-}$ mouse models display a high incidence of pre-B cell lymphomas (Flemming et al, 2003, Jumaa et al, 2003, Kersseboom et al, 2003). Detailed mechanisms remain unknown and need further examination.

6.2 Do CLL cells proliferate?

Two hallmarks of CLL is a defect in apoptosis and cell cycle arrest in the G_0/G_1 phase (Bannerji and Byrd, 2000). Yet, some studies showed that CLL cells are able to proliferate in the proliferating compartment (Ghia et al, 2002, Schmid and Isaacson, 1994) and the turnover between birth and death of the leukaemic cells is more vigorous than previously thought (Messmer et al, 2005). Proliferating CLL cells are Ki67 positive (Ghia et al, 2002, Granziero et al, 2001) and a member of the IAP family, survivin positive (Granziero et al, 2001). In addition, it seems that the stimulation provided by CD40L, which is mainly expressed on $CD4^+$ T cells, causes proliferation of CLL cells (Caligaris-Cappio, 2003, Fluckiger et al, 1992), and induces RNA expression of T cell attracting chemokines, CCL17 and CCL22 (Ghia et al, 2002). Thus, CLL does not appear to be a static disease that results of accumulation of long-lived lymphocytes, but rather consists of two phases, an accumulation and a proliferation phase (Caligaris-Cappio, 2003). The results in this thesis showed that our CLL-like cells exhibited prominent proliferation capacity *in vitro* and *in vivo*, but the cell cycle of tumour cells *in vivo* are arrested at the G_0/G_1 stage, thereby presenting two different phases. In order to understand what

mechanisms control proliferation, it would be interesting to determine the expression level of molecules that regulate proliferation, such as survivin, CCL22, CCL17, CD40, at the protein or transcript level by Western or RT-PCR, respectively. Although IL-4 is often examined for its role for CLL cell survival and proliferation, the results are still controversial (Fluckiger et al, 1992, Luo et al, 1991) in human CLL. The importance of IL-7 in CLL is not highlighted. This is probably because IL-7 in human B cell development is less essential than murine system (Fry and Mackall, 2002), therefore our murine CLL system may be substantially different from human CLL system regarding the dependence on cytokines. In our murine CLL system, IL-7 is a crucial cytokine for proliferation. IL-7 is secreted from multiple stromal tissues including spleen (Jiang et al, 2005), therefore, splenocytes and LN cells in PKCα-KR-injected mice access IL-7 and proliferate under the physiological concentration of IL-7. However, the cells from i.p. tumour mass probably could not obtain IL-7, thus, arresting the cell cycle at the G_0/G_1 stage.

6.3 Do CLL cells need stromal cells?

CLL cells die spontaneously *in vitro*, however, survival of CLL cells is promoted when stromal cells are added to cultures (Lagneaux et al, 1998). Tsukada *et al.*, have described that a subset of $CD14^+$ blood mononuclear cells can differentiate *in vitro* into large, round, adherent cells that contact with leukaemic cells and protect them from undergoing apoptosis *in vitro* and called these cells NLCs (Tsukada et al, 2002). The phenotypic characterization of NLCs suggests that they are related to stromal cells and NLCs prevent CLL cells from apoptosis by producing SDF-1, the chemokine that regulates B lymphopoiesis (Burger et al, 2000). Indeed, our CLL-like cells survived and even proliferated when they cultured with stromal cell line, OP9, in the presence of IL-7. Moreover, adherent, bigger $CD5^+$ cells were identified during the culture of M-1 cells (data not shown). These adherent cells may be NLCs in our system and help survival of long cultured M-1 cells. As a future direction, NLCs from M-1 cell culture will be isolated and phenotypically characterised, and assessed for their ability to secrete any chemokines or cytokines.

6.4 What is the role of BCR in CLL?

The BCR includes membrane Ig homodimer and the noncovalently bound disulphide-linked Igα and Igβ, which forms oligomeric complexes inside to process and amplify signals. Both Igα and Igβ play a key role in receptor expression and signal transduction through their ITAMs, and engagement of BCR induces phosphorylation on ITAMs, leading to recruitment of Src tyrosine kinase family including Syk and activation of intracellular signalling cascade (Gauld et al, 2002b). Signals delivered through the BCR may have different consequences depending on the stage of maturation of the cells, and thus BCR ligation results in apoptosis for immature cells or in proliferation for mature cells (Carey et al, 2000). Previously, Zupo *et al.*, reported that anti-IgM treatment of $CD38^+$ CLL cells causes apoptosis (Zupo et al, 1996), but Bernal *et al.*, reported that IgM ligation causes survival of CLL cells in the PI3K dependent way (Bernal et al, 2001). Nédellec *et al.*, examined 41 cases of CLL and categorised the cells on the basis of Ca^{2+} mobilisation upon surface IgM cross-linking: Group I; not respond, Group IIa; responded and proliferated, Group IIb; responded and apoptosed (Nédellec et al, 2005). Group IIa proliferated in a PI3K- and PKC-dependent manner, and ERK and PI3K were activated upon IgM ligation. In contrast, ERK and PI3K were inactive, but p38 is activated upon IgM engagement in Group IIb (Nédellec et al, 2005). CLL consist of heterogeneous cells, thereby it is not surprising that the response was varied.

ZAP-70, which is a receptor associated protein tyrosine kinase, is detected in most unmutated CLL cells (Rosenwald et al, 2001, Wiestner et al, 2003) and the ZAP-70 expression status is mostly correlated to clinically poor prognosis (Crespo et al, 2003, Orchard et al, 2004), thus ZAP-70 is an important clinical marker. Recent reports demonstrated that the level of Syk phosphorylation upon IgM cross-linking is greater in ZAP-70 positive CLL cells (Chen et al, 2002) and unmutated CLL cells (Lanham et al, 2003). Moreover, there are reports that CLL cells expressing CD38, a CLL clinical marker for poor prognosis, are more sensitive to IgM stimulation (Lanham et al, 2003, Zupo et al, 1996). This suggests that the expression of ZAP-70 and CD38 in CLL allows

more effective IgM signalling in CLL cells, which could contribute to the more aggressive course observed in ZAP-70 and CD38 positive CLL cells, mostly consisting of unmutated forms. The results presented in this thesis demonstrated that subversion of PKCα generates CLL-like cells, however, the expression levels of relevant clinical markers, such as ZAP-70 and CD38 remain undetermined. ZAP-70 is found abundantly in both human and murine T cells. Surprisingly, recent studies established that a subset of normal human B cells (Nolz et al, 2005) and normal murine B cells at the most stages of development (Schweighoffer et al, 2003) expressed ZAP-70 although there seems a difference in the expression level and cell type between human and murine system. Interestingly, murine ZAP-70 appears to be inducible by IL-7 (Meade et al, 2004), which is a proliferation inducing cytokine in our system. Analysis of ZAP-70 expression level by FCM in the presence/absence of IL-7 using our CLL system and comparison with that of MIEV may be useful for further understanding how our CLL-like cells transduce survival/proliferation signal to sustain malignancy. The amount of apoptosis/proliferation and the levels of Syk phosphorylation upon IgM engagement would also be interesting to be assessed. The outcome of IgM ligation will be linked to the expression level of either ZAP-70 or CD38 or both, thereby further characterising our CLL-like cells.

Although the survival of our CLL-like cells appears to depend on ERK and/or PI3K pathway, the response to IgM ligation or the signals involved have not examined. Therefore, further studies will investigate how PI3K-, ERK- and PKC-pathway are modulated when our CLL-like cells are treated with those pathway inhibitors upon IgM ligation by looking at expression level of particular signalling molecules, such as pAKT and pERK.

6.5 What stage do CLL cells mature at?

Somatic mutations in the Ig genes occur at GC during maturation of the B cells en route to production of high-affinity antibody. CLL can be divided into 2 subsets distinguished by the incidence of somatic mutations in the Ig V_H genes

(Stevenson and Caligaris-Cappio, 2004), and patients bearing unmutated V_H genes have a poorer clinical outcome compared to those with mutated V genes (Hamblin et al, 1999). If the development of IgV_H gene mutations requires BCR crosslinking/antigen stimulation, CLL cases with mutated V gene must have arisen from previously stimulated B cells, which is considered as memory B cells by similarity in phenotypical analysis (Klein et al, 2001, Rosenwald et al, 2001). Unmutated CLL is believed to be derived from a naïve B cell before entering a GC, or alternatively, from cells that did encounter antigen but it may have not been sufficient to induce antigen-stimulated maturation in a GC, thereby carrying germline IgV (Damle et al, 2002, Stevenson and Caligaris-Cappio, 2004). It has not been resolved whether this lack of mutations is either a consequence of the type of antigenic stimulation or a result of the timing of the transformation event. However, considering the results presented in this thesis regarding the transformation in RAG-1$^{-/-}$ mice and CD19$^+$ adult BM cells, it is suggested that transformation can be initiated at different stages of B cell development, prior to the pro-B stage or post immature B cells stage. Thus PKCα-KR may target different population of cells and result in CLL with similar phenotype. A malignant cancer stem cell population has been identified in other leukaemias, such as AML (Bonnet and Dick, 1997), ALL (Cobaleda et al, 2000) and chronic myeloid leukaemia (CML) (Holyoake et al, 1999). The cellular origin of cancer stem cells has not been clarified, but they have a self-renewal ability to generate additional cancer stem cells and can differentiate to generate phenotypically diverse cancer cells. Therefore, a possibility cannot be excluded that CLL originates from cancer stem cells at least in our system, and thus, PKCα-KR may target the HPC population. In order to define the origin of CLL, HPCs will be retrovirally infected with PKCα-KR, and distinct populations of developing B cells will be isolated using FCM sorting with the virtue of GFP$^+$ and the expression of surface markers: HPC (CD117$^+$, Sca-1$^+$); pre-pro-B cells (CD19$^-$, Sca-1$^-$CD117$^+$); pro-B cells (CD45R$^+$, CD19$^+$, CD24^{lo}), and; pre-B cells (CD45R$^+$, CD19$^+$, CD24^{hi}) (Hardy and Hayakawa, 2001, Kondo et al, 1997). The developed population will be stained with CLL marker, such as CD5, CD23 and IgM, and will be analysed by FCM. This experiment will

elucidate which stage(s) of B haematopoiesis has a potential to be transformed by subversion of PKCα. Furthermore, a limiting dilution analysis will be performed to determine the frequency of transformation into CLL cells from each developmental stage.

6.6 Concluding remarks

These studies provide vital information regarding a unique oncogenic trigger for the development of a CLL-like disease resulting from the subversion of PKCα signalling. Further investigation will uncover novel avenues not only for the study of the induction and maintenance of CLL, but also for the development of potential diagnostic tools and therapeutic drugs to identify and combat CLL.

Bibliography

Adams, B., Dörfler, P., Aguzzi, A., et al. Pax-5 encodes the transcription factor BSAP and is expressed in B lymphocytes, the developing CNS, and adult testis. Genes Dev (1992); 6: 1589-1607.

Ajiro, K. Histone H2B phosphorylation in mammalian apoptotic cells. An association with DNA fragmentation. J Biol Chem (2000); 275: 439-443.

Alkan, S., Huang, Q., Ergin, M., et al. Survival role of protein kinase C (PKC) in chronic lymphocytic leukemia and determination of isoform expression pattern and genes altered by PKC inhibition. Am J Hematol (2005); 79: 97-106.

Alvaro, V., Prevostel, C., Joubert, D., Slosberg, E. and Weinstein, B.I. Ectopic expression of a mutant form of PKCalpha originally found in human tumors: aberrant subcellular translocation and effects on growth control. Oncogene (1997); 14: 677-685.

Anderson, J.S., Teutsch, M., Dong, Z. and Wortis, H.H. An essential role for tyrosine kinase in the regulation of Bruton's B-cell apoptosis. Proc Natl Acad Sci U S A (1996); 93: 10966-10971.

Anilkumar, N., Parsons, M., Monk, R., Ng, T. and Adams, J.C. Interaction of fascin and protein kinase Calpha: a novel intersection in cell adhesion and motility. Embo J (2003); 22: 5390-5402.

Bain, G., Maandag, E.C., Izon, D.J., et al. E2A proteins are required for proper B cell development and initiation of immunoglobulin gene rearrangements. Cell (1994); 79: 885-892.

Bain, G., Robanus Maandag, E.C., te Riele, H.P., et al. Both E12 and E47 allow commitment to the B cell lineage. Immunity (1997); 6: 145-154.

Bajpai, U.D., Zhang, K., Teutsch, M., Sen, R. and Wortis, H.H. Bruton's tyrosine kinase links the B cell receptor to nuclear factor kappaB activation. J Exp Med (2000); 191: 1735-1744.

Bannerji, R. and Byrd, J.C. Update on the biology of chronic lymphocytic leukemia. Curr Opin Oncol (2000); 12: 22-29.

Barragán, M., Bellosillo, B., Campàs, C., Colomer, D., Pons, G. and Gil, J. Involvement of protein kinase C and phosphatidylinositol 3-kinase pathways in the survival of B-cell chronic lymphocytic leukemia cells. Blood (2002); 99: 2969-2976.

Barragán, M., Campàs, C., Bellosillo, B. and Gil, J. Protein kinases in the regulation of apoptosis in B-cell chronic lymphocytic leukemia. Leuk Lymphoma (2003); 44: 1865-1870.

Batata, A. and Shen, B. Immunophenotyping of subtypes of B-chronic (mature) lymphoid leukemia. A study of 242 cases. Cancer (1992); 70: 2436-2443.

Benschop, R.J. and Cambier, J.C. B cell development: signal transduction by antigen receptors and their surrogates. Curr Opin Immunol (1999); 11: 143-151.

Berland, R. and Wortis, H.H. Origins and functions of B-1 cells with notes on the role of CD5. Annu Rev Immunol (2002); 20: 253-300.

Bernal, A., Pastore, R.D., Asgary, Z., et al. Survival of leukemic B cells promoted by engagement of the antigen receptor. Blood (2001); 98: 3050-3057.

Besson, A. and Yong, V.W. Involvement of p21(Waf1/Cip1) in protein kinase C alpha-induced cell cycle progression. Mol Cell Biol (2000); 20: 4580-4590.

Binet, J.L., Auquier, A., Dighiero, G., et al. A new prognostic classification of chronic lymphocytic leukemia derived from a multivariate survival analysis. Cancer (1981); 48: 198-206.

Blackburn, R.V., Galoforo, S.S., Berns, C.M., Motwani, N.M., Corry, P.M. and Lee, Y.J. Differential induction of cell death in human glioma cell lines by sodium nitroprusside. Cancer (1998); 82: 1137-1145.

Blagosklonny, M.V. Are p27 and p21 cytoplasmic oncoproteins? Cell Cycle (2002); 1: 391-393.

Boes, M., Prodeus, A.P., Schmidt, T., Carroll, M.C. and Chen, J. A critical role of natural immunoglobulin M in immediate defense against systemic bacterial infection. J Exp Med (1998); 188: 2381-2386.

Bonnet, D. and Dick, J.E. Human acute myeloid leukemia is organized as a hierarchy that originates from a primitive hematopoietic cell. Nat Med (1997); 3: 730-737.

Bornancin, F. and Parker, P.J. Phosphorylation of threonine 638 critically controls the dephosphorylation and inactivation of protein kinase Calpha. Curr Biol (1996); 6: 1114-1123.

Bornancin, F. and Parker, P.J. Phosphorylation of protein kinase C-alpha on serine 657 controls the accumulation of active enzyme and contributes to its phosphatase-resistant state. J Biol Chem (1997); 272: 3544-3549.

Boudreau, R.T., Garduno, R. and Lin, T.J. Protein phosphatase 2A and protein kinase Calpha are physically associated and are involved in Pseudomonas aeruginosa-induced interleukin 6 production by mast cells. J Biol Chem (2002); 277: 5322-5329.

Bradford, M.M. A rapid and sensitive method for the quantitation of microgram quantities of protein utilizing the principle of protein-dye binding. Anal Biochem (1976); 72: 248-254.

Buitrago, C.G., Pardo, V.G., de Boland, A.R. and Boland, R. Activation of RAF-1 through Ras and protein kinase Calpha mediates 1alpha,25(OH)2-vitamin D3 regulation of the mitogen-activated protein kinase pathway in muscle cells. J Biol Chem (2003); 278: 2199-2205.

Bullrich, F., Rasio, D., Kitada, S., et al. ATM mutations in B-cell chronic lymphocytic leukemia. Cancer Res (1999); 59: 24-27.

Burger, J.A., Burger, M. and Kipps, T.J. Chronic lymphocytic leukemia B cells express functional CXCR4 chemokine receptors that mediate spontaneous migration beneath bone marrow stromal cells. Blood (1999); 94: 3658-3667.

Burger, J.A., Tsukada, N., Burger, M., Zvaifler, N.J., Dell'Aquila, M. and Kipps, T.J. Blood-derived nurse-like cells protect chronic lymphocytic leukemia B cells from spontaneous apoptosis through stromal cell-derived factor-1. Blood (2000); 96: 2655-2663.

Busslinger, M. Transcriptional control of early B cell development. Annu Rev Immunol (2004); 22: 55-79.

Caligaris-Cappio, F. Role of the microenvironment in chronic lymphocytic leukaemia. Br J Haematol (2003); 123: 380-388.

Campbell, S.L., Khosravi-Far, R., Rossman, K.L., Clark, G.J. and Der, C.J. Increasing complexity of Ras signaling. Oncogene (1998); 17: 1395-1413.

Cardone, M.H., Roy, N., Stennicke, H.R., et al. Regulation of cell death protease caspase-9 by phosphorylation. Science (1998); 282: 1318-1321.

Carey, G.B., Donjerkovic, D., Mueller, C.M., et al. B-cell receptor and Fas-mediated signals for life and death. Immunol Rev (2000); 176: 105-115.

Carlyle, J.R. and Zuniga-Pflucker, J.C. Requirement for the thymus in alphabeta T lymphocyte lineage commitment. Immunity (1998); 9: 187-197.

Carpenter, G. and Ji, Q. Phospholipase C-gamma as a signal-transducing element. Exp Cell Res (1999); 253: 15-24.

Castor, A., Nilsson, L., Astrand-Grundstrom, I., et al. Distinct patterns of hematopoietic stem cell involvement in acute lymphoblastic leukemia. Nat Med (2005); 11: 630-637.

Cazaubon, S., Bornancin, F. and Parker, P.J. Threonine-497 is a critical site for permissive activation of protein kinase C alpha. Biochem J (1994); 301: 443-448.

Chen, L., Widhopf, G., Huynh, L., et al. Expression of ZAP-70 is associated with increased B-cell receptor signaling in chronic lymphocytic leukemia. Blood (2002); 100: 4609-4614.

Chen, Z., Gibson, T.B., Robinson, F., et al. MAP kinases. Chem Rev (2001); 101: 2449-2476.

Cepko, C. and Pear, W.S. Current Protocols in Molecular Biology: Transduction of genes using retrovirus vectors. New York: John Wiley & Sons (2003): 9.9.1-9.9.16

Cheng, A.M., Rowley, B., Pao, W., Hayday, A., Bolen, J.B. and Pawson, T. Syk tyrosine kinase required for mouse viability and B-cell development. Nature (1995); 378: 303-306.

Cheung, W.L., Ajiro, K., Samejima, K., et al. Apoptotic phosphorylation of histone H2B is mediated by mammalian sterile twenty kinase. Cell (2003); 113: 507-517.

Chiorazzi, N. and Ferrarini, M. B cell chronic lymphocytic leukemia: lessons learned from studies of the B cell antigen receptor. Annu Rev Immunol (2003); 21: 841-894.

Chiorazzi, N., Hatzi, K. and Albesiano, E. B-Cell chronic lymphocytic leukemia, a clonal disease of B lymphocytes with receptors that vary in specificity for (auto)antigens. Ann N Y Acad Sci (2005); 1062: 1-12.

Chiu, C.W., Dalton, M., Ishiai, M., Kurosaki, T. and Chan, A.C. BLNK: molecular scaffolding through 'cis'-mediated organization of signaling proteins. Embo J (2002); 21: 6461-6472.

Clayton, E., Bardi, G., Bell, S.E., et al. A crucial role for the p110delta subunit of phosphatidylinositol 3-kinase in B cell development and activation. J Exp Med (2002); 196: 753-763.

Cobaleda, C., Gutierrez-Cianca, N., Perez-Losada, J., et al. A primitive hematopoietic cell is the target for the leukemic transformation in human philadelphia-positive acute lymphoblastic leukemia. Blood (2000); 95: 1007-1013.

Conley, M.E., Rohrer, J., Rapalus, L., Boylin, E.C. and Minegishi, Y. Defects in early B-cell development: comparing the consequences of abnormalities in pre-BCR signaling in the human and the mouse. Immunol Rev (2000); 178: 75-90.

Cordone, I., Masi, S., Mauro, F.R., et al. p53 expression in B-cell chronic lymphocytic leukemia: a marker of disease progression and poor prognosis. Blood (1998); 91: 4342-4349.

Crespo, M., Bosch, F., Villamor, N., et al. ZAP-70 expression as a surrogate for immunoglobulin-variable-region mutations in chronic lymphocytic leukemia. N Engl J Med (2003); 348: 1764-1775.

Crespo, M., Villamor, N., Gine, E., et al. ZAP-70 expression in normal pro/pre B cells, mature B cells, and in B-cell acute lymphoblastic leukemia. Clin Cancer Res (2006); 12: 726-734.

Dal Porto, J.M., Gauld, S.B., Merrell, K.T., Mills, D., Pugh-Bernard, A.E. and Cambier, J. B cell antigen receptor signaling 101. Mol Immunol (2004); 41: 599-613.

Dallas, M.H., Varnum-Finney, B., Delaney, C., Kato, K. and Bernstein, I.D. Density of the Notch ligand Delta1 determines generation of B and T cell precursors from hematopoietic stem cells. J Exp Med (2005); 201: 1361-1366.

Damle, R.N., Ghiotto, F., Valetto, A., et al. B-cell chronic lymphocytic leukemia cells express a surface membrane phenotype of activated, antigen-experienced B lymphocytes. Blood (2002); 99: 4087-4093.

Damle, R.N., Wasil, T., Fais, F., et al. Ig V gene mutation status and CD38 expression as novel prognostic indicators in chronic lymphocytic leukemia. Blood (1999); 94: 1840-1847.

Dancescu, M., Rubio-Trujillo, M., Biron, G., Bron, D., Delespesse, G. and Sarfati, M. Interleukin 4 protects chronic lymphocytic leukemic B cells from death by apoptosis and upregulates Bcl-2 expression. J Exp Med (1992); 176: 1319-1326.

de Waard, R., Dammers, P.M., Tung, J.W., et al. Presence of germline and full-length IgA RNA transcripts among peritoneal B-1 cells. Dev Immunol (1998); 6: 81-87.

Deaglio, S., Vaisitti, T., Bergui, L., et al. CD38 and CD100 lead a network of surface receptors relaying positive signals for B-CLL growth and survival. Blood (2005); 105: 3042-3050.

DeKoter, R.P., Lee, H.J. and Singh, H. PU.1 regulates expression of the interleukin-7 receptor in lymphoid progenitors. Immunity (2002); 16: 297-309.

DeKoter, R.P. and Singh, H. Regulation of B lymphocyte and macrophage development by graded expression of PU.1. Science (2000); 288: 1439-1441.

del Peso, L., Gonzalez-Garcia, M., Page, C., Herrera, R. and Nunez, G. Interleukin-3-induced phosphorylation of BAD through the protein kinase Akt. Science (1997); 278: 687-689.

Detjen, K.M., Brembeck, F.H., Welzel, M., et al. Activation of protein kinase Calpha inhibits growth of pancreatic cancer cells via p21(cip)-mediated G(1) arrest. J Cell Sci (2000); 113: 3025-3035.

Diaz, M. and Casali, P. Somatic immunoglobulin hypermutation. Curr Opin Immunol (2002); 14: 235-240.

Dighiero, G. CLL Biology and Prognosis. Hematology (Am Soc Hematol Educ Program) (2005); 278-284.

Döhner, H., Fischer, K., Bentz, M., et al. p53 gene deletion predicts for poor survival and non-response to therapy with purine analogs in chronic B-cell leukemias. Blood (1995); 85: 1580-1589.

Döhner, H., Stilgenbauer, S., Benner, A., et al. Genomic aberrations and survival in chronic lymphocytic leukemia. N Engl J Med (2000); 343: 1910-1916.

Dutil, E.M. and Newton, A.C. Dual role of pseudosubstrate in the coordinated regulation of protein kinase C by phosphorylation and diacylglycerol. J Biol Chem (2000); 275: 10697-10701.

Dutil, E.M., Toker, A. and Newton, A.C. Regulation of conventional protein kinase C isozymes by phosphoinositide-dependent kinase 1 (PDK-1). Curr Biol (1998); 8: 1366-1375.

Faderl, S., Kantarjian, H.M., Talpaz, M. and Estrov, Z. Clinical significance of cytogenetic abnormalities in adult acute lymphoblastic leukemia. Blood (1998); 91: 3995-4019.

Fais, F., Ghiotto, F., Hashimoto, S., et al. Chronic lymphocytic leukemia B cells express restricted sets of mutated and unmutated antigen receptors. J Clin Invest (1998); 102: 1515-1525.

Flemming, A., Brummer, T., Reth, M. and Jumaa, H. The adaptor protein SLP-65 acts as a tumor suppressor that limits pre-B cell expansion. Nat Immunol (2003); 4: 38-43.

Fluckiger, A.C., Rossi, J.F., Bussel, A., Bryon, P., Banchereau, J. and Defrance, T. Responsiveness of chronic lymphocytic leukemia B cells activated via surface Igs or CD40 to B-cell tropic factors. Blood (1992); 80: 3173-3181.

Fournier, S., Delespesse, G., Rubio, M., Biron, G. and Sarfati, M. CD23 antigen regulation and signaling in chronic lymphocytic leukemia. J Clin Invest (1992); 89: 1312-1321.

Frey, M.R., Clark, J.A., Leontieva, O., Uronis, J.M., Black, A.R. and Black, J.D. Protein kinase C signaling mediates a program of cell cycle withdrawal in the intestinal epithelium. J Cell Biol (2000); 151: 763-778.

Fruman, D.A. Phosphoinositide 3-kinase and its targets in B-cell and T-cell signaling. Curr Opin Immunol (2004); 16: 314-320.

Fruman, D.A., Snapper, S.B., Yballe, C.M., et al. Impaired B cell development and proliferation in absence of phosphoinositide 3-kinase p85alpha. Science (1999); 283: 393-397.

Fry, T.J. and Mackall, C.L. Interleukin-7: from bench to clinic. Blood (2002); 99: 3892-3904.

Fu, C., Turck, C.W., Kurosaki, T. and Chan, A.C. BLNK: a central linker protein in B cell activation. Immunity (1998); 9: 93-103.

Gauld, S.B., Blair, D., Moss, C.A., Reid, S.D. and Harnett, M.M. Differential roles for extracellularly regulated kinase-mitogen-activated protein kinase in B cell antigen receptor-induced apoptosis and CD40-mediated rescue of WEHI-231 immature B cells. J Immunol (2002a); 168: 3855-3864.

Gauld, S.B., Dal Porto, J.M. and Cambier, J.C. B cell antigen receptor signaling: roles in cell development and disease. Science (2002b); 296: 1641-1642.

Ghia, P., Strola, G., Granziero, L., et al. Chronic lymphocytic leukemia B cells are endowed with the capacity to attract $CD4^+$, $CD40L^+$ T cells by producing CCL22. Eur J Immunol (2002); 32: 1403-1413.

Ghosh, S., May, M.J. and Kopp, E.B. NF-kappa B and Rel proteins: evolutionarily conserved mediators of immune responses. Annu Rev Immunol (1998); 16: 225-260.

Gisler, R. and Sigvardsson, M. The human V-preB promoter is a target for coordinated activation by early B cell factor and E47. J Immunol (2002); 168: 5130-5138.

Goebel, P., Janney, N., Valenzuela, J.R., Romanow, W.J., Murre, C. and Feeney, A.J. Localized gene-specific induction of accessibility to V(D)J recombination induced by E2A and early B cell factor in nonlymphoid cells. J Exp Med (2001); 194: 645-656.

Gold, M.R., Scheid, M.P., Santos, L., et al. The B cell antigen receptor activates the Akt (protein kinase B)/glycogen synthase kinase-3 signaling pathway via phosphatidylinositol 3-kinase. J Immunol (1999); 163: 1894-1905.

Grady, G.C., Mason, S.M., Stephen, J., Zúñiga-Pflücker, J. C. and Michie, A.M. Cyclic adenosine 5'-monophosphate response element binding protein plays a central role in mediating proliferation and differentiation downstream of the pre-TCR complex in developing thymocytes. J Immunol (2004); 173: 1802-1810.

Granziero, L., Ghia, P., Circosta, P., et al. Survivin is expressed on CD40 stimulation and interfaces proliferation and apoptosis in B-cell chronic lymphocytic leukemia. Blood (2001); 97: 2777-2783.

Guo, B., Su, T.T. and Rawlings, D.J. Protein kinase C family functions in B-cell activation. Curr Opin Immunol (2004); 16: 367-373.

Gutierrez-Ramos, J.C. and Palacios, R. *In vitro* differentiation of embryonic stem cells into lymphocyte precursors able to generate T and B lymphocytes *in vivo*. Proc Natl Acad Sci U S A (1992); 89: 9171-9175.

Hagman, J. and Lukin, K. Early B-cell factor 'pioneers' the way for B-cell development. Trends Immunol (2005); 26: 455-461.

Hahne, M., Kataoka, T., Schroter, M., et al. APRIL, a new ligand of the tumor necrosis factor family, stimulates tumor cell growth. J Exp Med (1998); 188: 1185-1190.

Hallek, M. Chronic Lymphocytic Leukemia (CLL): First-Line Treatment. Hematology (Am Soc Hematol Educ Program) (2005); 285-291.

Hamblin, T.J., Davis, Z., Gardiner, A., Oscier, D.G. and Stevenson, F.K. Unmutated Ig V(H) genes are associated with a more aggressive form of chronic lymphocytic leukemia. Blood (1999); 94: 1848-1854.

Hamblin, T.J., Orchard, J.A., Ibbotson, R.E., et al. CD38 expression and immunoglobulin variable region mutations are independent prognostic variables in chronic lymphocytic leukemia, but CD38 expression may vary during the course of the disease. Blood (2002); 99: 1023-1029.

Hamblin, T.J. and Oscier, D.G. Chronic lymphocytic leukaemia: the nature of the leukaemic cell. Blood Rev (1997); 11: 119-128.

Hanada, M., Delia, D., Aiello, A., Stadtmauer, E. and Reed, J.C. bcl-2 gene hypomethylation and high-level expression in B-cell chronic lymphocytic leukemia. Blood (1993); 82: 1820-1828.

Hansra, G., Bornancin, F., Whelan, R., Hemmings, B.A. and Parker, P.J. 12-O-Tetradecanoylphorbol-13-acetate-induced dephosphorylation of protein kinase Calpha correlates with the presence of a membrane-associated protein phosphatase 2A heterotrimer. J Biol Chem (1996); 271: 32785-32788.

Harding, A., Tian, T., Westbury, E., Frische, E. and Hancock, J.F. Subcellular localization determines MAP kinase signal output. Curr Biol (2005); 15: 869-873.

Hardy, R.R., Carmack, C.E., Shinton, S.A., Kemp, J.D. and Hayakawa, K. Resolution and characterization of pro-B and pre-pro-B cell stages in normal mouse bone marrow. J Exp Med (1991); 173: 1213-1225.

Hardy, R.R. and Hayakawa, K. B cell development pathways. Annu Rev Immunol (2001); 19: 595-621.

Harnett, M.M., Katz, E. and Ford, C.A. Differential signalling during B-cell maturation. Immunol Lett (2005); 98: 33-44.

Hashimoto, S., Iwamatsu, A., Ishiai, M., et al. Identification of the SH2 domain binding protein of Bruton's tyrosine kinase as BLNK-functional significance of Btk-SH2 domain in B-cell antigen receptor-coupled calcium signaling. Blood (1999); 94: 2357-2364.

Havran, W.L., DiGiusto, D.L. and Cambier, J.C. mIgM:mIgD ratios on B cells: mean mIgD expression exceeds mIgM by 10-fold on most splenic B cells. J Immunol (1984); 132: 1712-1716.

Hayakawa, K., Asano, M., Shinton, S.A., et al. Positive selection of natural autoreactive B cells. Science (1999); 285: 113-116.

Hayakawa, K. and Hardy, R.R. Development and function of B-1 cells. Curr Opin Immunol (2000); 12: 346-353.

Hayakawa, K., Hardy, R.R., Honda, M., Herzenberg, L.A. and Steinberg, A.D. Ly-1 B cells: functionally distinct lymphocytes that secrete IgM autoantibodies. Proc Natl Acad Sci U S A (1984); 81: 2494-2498.

Hayashi, K., Nittono, R., Okamoto, N., et al. The B cell-restricted adaptor BASH is required for normal development and antigen receptor-mediated activation of B cells. Proc Natl Acad Sci U S A (2000); 97: 2755-2760.

He, B., Chadburn, A., Jou, E., Schattner, E.J., Knowles, D.M. and Cerutti, A. Lymphoma B cells evade apoptosis through the TNF family members BAFF/BLyS and APRIL. J Immunol (2004); 172: 3268-3279.

Herzenberg, L.A. B-1 cells: the lineage question revisited. Immunol Rev (2000); 175: 9-22.

Herzenberg, L.A. and Tung, J.W. B cell lineages: documented at last! Nat Immunol (2006); 7: 225-226.

Holinstat, M., Mehta, D., Kozasa, T., Minshall, R.D. and Malik, A.B. Protein kinase Calpha-induced p115RhoGEF phosphorylation signals endothelial cytoskeletal rearrangement. J Biol Chem (2003); 278: 28793-28798.

Holyoake, T., Jiang, X., Eaves, C. and Eaves, A. Isolation of a highly quiescent subpopulation of primitive leukemic cells in chronic myeloid leukemia. Blood (1999); 94: 2056-2064.

Hornia, A., Lu, Z., Sukezane, T., et al. Antagonistic effects of protein kinase C alpha and delta on both transformation and phospholipase D activity mediated by the epidermal growth factor receptor. Mol Cell Biol (1999); 19: 7672-7680.

Hsu, L.Y., Lauring, J., Liang, H.E., et al. A conserved transcriptional enhancer regulates RAG gene expression in developing B cells. Immunity (2003); 19: 105-117.

Hubmann, R., Schwarzmeier, J.D., Shehata, M., et al. Notch2 is involved in the overexpression of CD23 in B-cell chronic lymphocytic leukemia. Blood (2002); 99: 3742-3747.

Iritani, B.M., Forbush, K.A., Farrar, M.A. and Perlmutter, R.M. Control of B cell development by Ras-mediated activation of Raf. Embo J (1997); 16: 7019-7031.

Ishiai, M., Kurosaki, M., Pappu, R., et al. BLNK required for coupling Syk to PLC gamma 2 and Rac1-JNK in B cells. Immunity (1999); 10: 117-125.

Iwamoto, T., Hagiwara, M., Hidaka, H., Isomura, T., Kioussis, D. and Nakashima, I. Accelerated proliferation and interleukin-2 production of thymocytes by stimulation of soluble anti-CD3 monoclonal antibody in transgenic mice carrying a rabbit protein kinase C alpha. J Biol Chem (1992); 267: 18644-18648.

Izon, D.J., Punt, J.A., Xu, L., et al. Notch1 regulates maturation of $CD4^+$ and $CD8^+$ thymocytes by modulating TCR signal strength. Immunity (2001); 14: 253-264.

Janeway, C.A.Jr., Travers, P., Walport, M. and Shlomchik, M.J. Immunobiology 5th ed.: The humoral immune response. Edinburgh: Churchill Livingstone (2001): 341-380.

Jiang, Q., Li, W.Q., Aiello, F.B., et al. Cell biology of IL-7, a key lymphotrophin. Cytokine Growth Factor Rev (2005); 16: 513-533.

Jiffar, T., Kurinna, S., Suck, G., et al. PKC alpha mediates chemoresistance in acute lymphoblastic leukemia through effects on Bcl2 phosphorylation. Leukemia (2004); 18: 505-512.

Jou, S.T., Carpino, N., Takahashi, Y., et al. Essential, nonredundant role for the phosphoinositide 3-kinase p110delta in signaling by the B-cell receptor complex. Mol Cell Biol (2002); 22: 8580-8591.

Jumaa, H., Bossaller, L., Portugal, K., et al. Deficiency of the adaptor SLP-65 in pre-B-cell acute lymphoblastic leukaemia. Nature (2003); 423: 452-456.

Jumaa, H., Wollscheid, B., Mitterer, M., Wienands, J., Reth, M. and Nielsen, P.J. Abnormal development and function of B lymphocytes in mice deficient for the signaling adaptor protein SLP-65. Immunity (1999); 11: 547-554.

Kandel, E.S. and Hay, N. The regulation and activities of the multifunctional serine/threonine kinase Akt/PKB. Exp Cell Res (1999); 253: 210-229.

Kantor, A.B. and Herzenberg, L.A. Origin of murine B cell lineages. Annu Rev Immunol (1993); 11: 501-538.

Kantor, A.B., Stall, A.M., Adams, S. and Herzenberg, L.A. Differential development of progenitor activity for three B-cell lineages. Proc Natl Acad Sci U S A (1992); 89: 3320-3324.

Karin, M. and Ben-Neriah, Y. Phosphorylation meets ubiquitination: the control of NF-[kappa]B activity. Annu Rev Immunol (2000); 18: 621-663.

Karin, M. and Lin, A. NF-kappaB at the crossroads of life and death. Nat Immunol (2002); 3: 221-227.

Kern, C., Cornuel, J.F., Billard, C., et al. Involvement of BAFF and APRIL in the resistance to apoptosis of B-CLL through an autocrine pathway. Blood (2004); 103: 679-688.

Kerner, J.D., Appleby, M.W., Mohr, R.N., et al. Impaired expansion of mouse B cell progenitors lacking Btk. Immunity (1995); 3: 301-312.

Kersseboom, R., Middendorp, S., Dingjan, G.M., et al. Bruton's tyrosine kinase cooperates with the B cell linker protein SLP-65 as a tumor suppressor in Pre-B cells. J Exp Med (2003); 198: 91-98.

Khan, W.N., Alt, F.W., Gerstein, R.M., et al. Defective B cell development and function in Btk-deficient mice. Immunity (1995); 3: 283-299.

Kitada, S., Andersen, J., Akar, S., et al. Expression of apoptosis-regulating proteins in chronic lymphocytic leukemia: correlations with *In vitro* and *In vivo* chemoresponses. Blood (1998); 91: 3379-3389.

Kitada, S., Zapata, J.M., Andreeff, M. and Reed, J.C. Bryostatin and CD40-ligand enhance apoptosis resistance and induce expression of cell survival genes in B-cell chronic lymphocytic leukaemia. Br J Haematol (1999); 106: 995-1004.

Kitada, S., Zapata, J.M., Andreeff, M. and Reed, J.C. Protein kinase inhibitors flavopiridol and 7-hydroxy-staurosporine down-regulate antiapoptosis proteins in B-cell chronic lymphocytic leukemia. Blood (2000); 96: 393-397.

Klauck, T.M., Faux, M.C., Labudda, K., Langeberg, L.K., Jaken, S. and Scott, J.D. Coordination of three signaling enzymes by AKAP79, a mammalian scaffold protein. Science (1996); 271: 1589-1592.

Klein, U., Tu, Y., Stolovitzky, G.A., et al. Gene expression profiling of B cell chronic lymphocytic leukemia reveals a homogeneous phenotype related to memory B cells. J Exp Med (2001); 194: 1625-1638.

Koch, U., Lacombe, T.A., Holland, D., et al. Subversion of the T/B lineage decision in the thymus by lunatic fringe-mediated inhibition of Notch-1. Immunity (2001); 15: 225-236.

Kodama, H., Sudo, H., Koyama, H., Kasai, S. and Yamamoto, S. In vitro hemopoiesis within a microenvironment created by MC3T3-G2/PA6 preadipocytes. J Cell Physiol (1984); 118: 233-240.

Koivunen, J., Aaltonen, V. and Peltonen, J. Protein kinase C (PKC) family in cancer progression. Cancer Lett (2006); 235: 1-10.

Kolch, W. Coordinating ERK/MAPK signalling through scaffolds and inhibitors. Nat Rev Mol Cell Biol (2005); 6: 827-837.

Kolch, W., Heidecker, G., Kochs, G., et al. Protein kinase C alpha activates RAF-1 by direct phosphorylation. Nature (1993); 364: 249-252.

Komada, F., Nishikawa, M., Uemura, Y., Morita, K., Hidaka, H. and Shirakawa, S. Expression of three major protein kinase C isozymes in various types of human leukemic cells. Cancer Res (1991); 51: 4271-4278.

Kondo, M., Weissman, I.L. and Akashi, K. Identification of clonogenic common lymphoid progenitors in mouse bone marrow. Cell (1997); 91: 661-672.

Koyasu, S. The role of PI3K in immune cells. Nat Immunol (2003); 4: 313-319.

Kozmik, Z., Wang, S., Dörfler, P., Adams, B. and Busslinger, M. The promoter of the CD19 gene is a target for the B-cell-specific transcription factor BSAP. Mol Cell Biol (1992); 12: 2662-2672.

Kröber, A., Bloehdorn, J., Hafner, S., et al. Additional genetic high-risk features such as 11q deletion, 17p deletion, and V3-21 usage characterize discordance of ZAP-70 and VH mutation status in chronic lymphocytic leukemia. J Clin Oncol (2006); 24: 969-975.

Kröber, A., Seiler, T., Benner, A., et al. V(H) mutation status, CD38 expression level, genomic aberrations, and survival in chronic lymphocytic leukemia. Blood (2002); 100: 1410-1416.

Kroese, F.G., Ammerlaan, W.A. and Kantor, A.B. Evidence that intestinal IgA plasma cells in mu, kappa transgenic mice are derived from B-1 (Ly-1 B) cells. Int Immunol (1993); 5: 1317-1327.

Kurosaki, T. Molecular mechanisms in B cell antigen receptor signaling. Curr Opin Immunol (1997); 9: 309-318.

Kurosaki, T., Maeda, A., Ishiai, M., Hashimoto, A., Inabe, K. and Takata, M. Regulation of the phospholipase C-gamma2 pathway in B cells. Immunol Rev (2000); 176: 19-29.

Lagneaux, L., Delforge, A., Bron, D., De Bruyn, C. and Stryckmans, P. Chronic lymphocytic leukemic B cells but not normal B cells are rescued from apoptosis by contact with normal bone marrow stromal cells. Blood (1998); 91: 2387-2396.

Lanham, S., Hamblin, T., Oscier, D., Ibbotson, R., Stevenson, F. and Packham, G. Differential signaling via surface IgM is associated with V_H gene mutational status and CD38 expression in chronic lymphocytic leukemia. Blood (2003); 101: 1087-1093.

Lee, J.R. and Koretzky, G.A. Extracellular signal-regulated kinase-2, but not c-Jun NH2-terminal kinase, activation correlates with surface IgM-mediated apoptosis in the WEHI 231 B cell line. J Immunol (1998); 161: 1637-1644.

Leirdal, M. and Sioud, M. Ribozyme inhibition of the protein kinase C alpha triggers apoptosis in glioma cells. Br J Cancer (1999); 80: 1558-1564.

Leitges, M., Plomann, M., Standaert, M.L., et al. Knockout of PKC alpha enhances insulin signaling through PI3K. Mol Endocrinol (2002); 16: 847-858.

Leitges, M., Sanz, L., Martin, P., et al. Targeted disruption of the zetaPKC gene results in the impairment of the NF-kappaB pathway. Mol Cell (2001); 8: 771-780.

Leitges, M., Schmedt, C., Guinamard, R., et al. Immunodeficiency in protein kinase cbeta-deficient mice. Science (1996); 273: 788-791.

Levine, A.J., Momand, J. and Finlay, C.A. The p53 tumour suppressor gene. Nature (1991); 351: 453-456.

Li, Y.S., Wasserman, R., Hayakawa, K. and Hardy, R.R. Identification of the earliest B lineage stage in mouse bone marrow. Immunity (1996); 5: 527-535.

Lim, S.T., Longley, R.L., Couchman, J.R. and Woods, A. Direct binding of syndecan-4 cytoplasmic domain to the catalytic domain of protein kinase C alpha (PKC alpha) increases focal adhesion localization of PKC alpha. J Biol Chem (2003); 278: 13795-13802.

Lin, H. and Grosschedl, R. Failure of B-cell differentiation in mice lacking the transcription factor EBF. Nature (1995); 376: 263-267.

Lin, K., Sherrington, P.D., Dennis, M., Matrai, Z., Cawley, J.C. and Pettitt, A.R. Relationship between p53 dysfunction, CD38 expression, and IgV(H) mutation in chronic lymphocytic leukemia. Blood (2002); 100: 1404-1409.

Liu, Y.J. and Banchereau, J. Regulation of B-cell commitment to plasma cells or to memory B cells. Semin Immunol (1997); 9: 235-240.

Luo, H.Y., Rubio, M., Biron, G., Delespesse, G. and Sarfati, M. Antiproliferative effect of interleukin-4 in B chronic lymphocytic leukemia. J Immunother (1991); 10: 418-425.

MacLennan, I.C. Germinal centers. Annu Rev Immunol (1994); 12: 117-139.

Mandil, R., Ashkenazi, E., Blass, M., et al. Protein kinase Calpha and protein kinase Cdelta play opposite roles in the proliferation and apoptosis of glioma cells. Cancer Res (2001); 61: 4612-4619.

Markowitz, D., Goff, S. and Bank, A. A safe packaging line for gene transfer: separating viral genes on two different plasmids. J Virol (1988); 62: 1120-1124.

Marsden, V.S. and Strasser, A. Control of apoptosis in the immune system: Bcl-2, BH3-only proteins and more. Annu Rev Immunol (2003); 21: 71-105.

Marshall, A.J., Fleming, H.E., Wu, G.E. and Paige, C.J. Modulation of the IL-7 dose-response threshold during pro-B cell differentiation is dependent on pre-B cell receptor expression. J Immunol (1998); 161: 6038-6045.

Marshall, A.J., Niiro, H., Yun, T.J. and Clark, E.A. Regulation of B-cell activation and differentiation by the phosphatidylinositol 3-kinase and phospholipase Cgamma pathway. Immunol Rev (2000); 176: 30-46.

Marshall, C.J. Specificity of receptor tyrosine kinase signaling: transient versus sustained extracellular signal-regulated kinase activation. Cell (1995); 80: 179-185.

Mårtensson, I.L., Rolink, A., Melchers, F., Mundt, C., Licence, S. and Shimizu, T. The pre-B cell receptor and its role in proliferation and Ig heavy chain allelic exclusion. Semin Immunol (2002); 14: 335-342.

Martin, P., Duran, A., Minguet, S., et al. Role of zeta PKC in B-cell signaling and function. Embo J (2002); 21: 4049-4057.

Matutes, E., Owusu-Ankomah, K., Morilla, R., et al. The immunological profile of B-cell disorders and proposal of a scoring system for the diagnosis of CLL. Leukemia (1994); 8: 1640-1645.

McConkey, D.J., Chandra, J., Wright, S., et al. Apoptosis sensitivity in chronic lymphocytic leukemia is determined by endogenous endonuclease content and relative expression of BCL-2 and BAX. J Immunol (1996); 156: 2624-2630.

McMahon, S.B., Norvell, A., Levine, K.J. and Monroe, J.G. Transient transfection of murine B lymphocyte blasts as a method for examining gene regulation in primary B cells. J Immunol Methods (1995); 179: 251-259.

Meade, J., Tybulewicz, V.L. and Turner, M. The tyrosine kinase Syk is required for light chain isotype exclusion but dispensable for the negative selection of B cells. Eur J Immunol (2004); 34: 1102-1110.

Mecklenbräuker, I., Kalled, S.L., Leitges, M., Mackay, F. and Tarakhovsky, A. Regulation of B-cell survival by BAFF-dependent PKCdelta-mediated nuclear signalling. Nature (2004); 431: 456-461.

Mecklenbräuker, I., Saijo, K., Zheng, N.Y., Leitges, M. and Tarakhovsky, A. Protein kinase Cdelta controls self-antigen-induced B-cell tolerance. Nature (2002); 416: 860-865.

Melchers, F., ten Boekel, E., Yamagami, T., Andersson, J. and Rolink, A. The roles of preB and B cell receptors in the stepwise allelic exclusion of mouse IgH and L chain gene loci. Semin Immunol (1999); 11: 307-317.

Melendez, A.J., Harnett, M.M. and Allen, J.M. Crosstalk between ARF6 and protein kinase Calpha in Fc(gamma)RI-mediated activation of phospholipase D1. Curr Biol (2001); 11: 869-874.

Messmer, B.T., Messmer, D., Allen, S.L., et al. *In vivo* measurements document the dynamic cellular kinetics of chronic lymphocytic leukemia B cells. J Clin Invest (2005); 115: 755-764.

Michie, A.M. and Nakagawa, R. The link between PKCalpha regulation and cellular transformation. Immunol Lett (2005); 96: 155-162.

Michie, A.M., Soh, J.W., Hawley, R.G., Weinstein, I.B. and Zúñiga-Pflücker, J. C. Allelic exclusion and differentiation by protein kinase C-mediated signals in immature thymocytes. Proc Natl Acad Sci U S A (2001); 98: 609-614.

Miller, A.D. and Chen, F. Retrovirus packaging cells based on 10A1 murine leukemia virus for production of vectors that use multiple receptors for cell entry. J Virol (1996); 70: 5564-5571.

Miller, D.G., Adam, M.A. and Miller, A.D. Gene transfer by retrovirus vectors occurs only in cells that are actively replicating at the time of infection. Mol Cell Biol (1990); 10: 4239-4242.

Minegishi, Y., Rohrer, J., Coustan-Smith, E., et al. An essential role for BLNK in human B cell development. Science (1999); 286: 1954-1957.

Miyamoto, A., Nakayama, K., Imaki, H., et al. Increased proliferation of B cells and auto-immunity in mice lacking protein kinase Cdelta. Nature (2002); 416: 865-869.

Mohammad, R.M., Mohamed, A.N., Hamdan, M.Y., et al. Establishment of a human B-CLL xenograft model: utility as a preclinical therapeutic model. Leukemia (1996); 10: 130-137.

Mombaerts, P., Iacomini, J., Johnson, R.S., Herrup, K., Tonegawa, S. and Papaioannou, V.E. RAG-1-deficient mice have no mature B and T lymphocytes. Cell (1992); 68: 869-877.

Montecino-Rodriguez, E., Leathers, H. and Dorshkind, K. Identification of a B-1 B cell-specified progenitor. Nat Immunol (2006); 7: 293-301.

Moore, P.A., Belvedere, O., Orr, A., et al. BLyS: member of the tumor necrosis factor family and B lymphocyte stimulator. Science (1999); 285: 260-263.

Moreau, E.J., Matutes, E., A'Hern, R.P., et al. Improvement of the chronic lymphocytic leukemia scoring system with the monoclonal antibody SN8 (CD79b). Am J Clin Pathol (1997); 108: 378-382.

Mostafavi-Pour, Z., Askari, J.A., Parkinson, S.J., Parker, P.J., Ng, T.T. and Humphries, M.J. Integrin-specific signaling pathways controlling focal adhesion formation and cell migration. J Cell Biol (2003); 161: 155-167.

Murphy, L.O., Smith, S., Chen, R.H., Fingar, D.C. and Blenis, J. Molecular interpretation of ERK signal duration by immediate early gene products. Nat Cell Biol (2002); 4: 556-564.

Nagasawa, T., Kikutani, H. and Kishimoto, T. Molecular cloning and structure of a pre-B-cell growth-stimulating factor. Proc Natl Acad Sci U S A (1994); 91: 2305-2309.

Nagata, K., Nakamura, T., Kitamura, F., et al. The Ig alpha/Igbeta heterodimer on mu-negative proB cells is competent for transducing signals to induce early B cell differentiation. Immunity (1997); 7: 559-570.

Nakagawa, R., Soh, J.W. and Michie, A.M. Subversion of protein kinase C alpha signaling in hematopoietic progenitor cells results in the generation of a B-cell chronic lymphocytic leukemia-like population *in vivo*. Cancer Res (2006); 66: 527-534.

Nakano, T. Lymphohematopoietic development from embryonic stem cells in vitro. Semin Immunol (1995); 7: 197-203.

Nakano, T., Kodama, H. and Honjo, T. Generation of lymphohematopoietic cells from embryonic stem cells in culture. Science (1994); 265: 1098-1101.

Nakashima, S. Protein kinase C alpha (PKC alpha): regulation and biological function. J Biochem (Tokyo) (2002); 132: 669-675.

Nédellec, S., Renaudineau, Y., Bordron, A., et al. B cell response to surface IgM cross-linking identifies different prognostic groups of B-chronic lymphocytic leukemia patients. J Immunol (2005); 174: 3749-3756.

Newton, A.C. Protein kinase C: structure, function, and regulation. J Biol Chem (1995); 270: 28495-28498.

Ng, T., Shima, D., Squire, A., et al. PKCalpha regulates beta1 integrin-dependent cell motility through association and control of integrin traffic. Embo J (1999); 18: 3909-3923.

Niki, M., Di Cristofano, A., Zhao, M., et al. Role of Dok-1 and Dok-2 in leukemia suppression. J Exp Med (2004); 200: 1689-1695.

Nishio, M., Endo, T., Tsukada, N., et al. Nurselike cells express BAFF and APRIL, which can promote survival of chronic lymphocytic leukemia cells via a paracrine pathway distinct from that of SDF-1alpha. Blood (2005); 106: 1012-1020.

Nisitani, S., Tsubata, T. and Honjo, T. Lineage marker-negative lymphocyte precursors derived from embryonic stem cells in vitro differentiate into mature lymphocytes *in vivo*. Int Immunol (1994); 6: 909-916.

Nolz, J.C., Tschumper, R.C., Pittner, B.T., Darce, J.R., Kay, N.E. and Jelinek, D.F. ZAP-70 is expressed by a subset of normal human B-lymphocytes displaying an activated phenotype. Leukemia (2005); 19: 1018-1024.

Notarangelo, L.D., Villa, A. and Schwarz, K. RAG and RAG defects. Curr Opin Immunol (1999); 11: 435-442

Novak, A.J., Bram, R.J., Kay, N.E. and Jelinek, D.F. Aberrant expression of B-lymphocyte stimulator by B chronic lymphocytic leukemia cells: a mechanism for survival. Blood (2002); 100: 2973-2979.

Nutt, S.L., Heavey, B., Rolink, A.G. and Busslinger, M. Commitment to the B-lymphoid lineage depends on the transcription factor Pax5. Nature (1999); 401: 556-562.

Nutt, S.L., Morrison, A.M., Dörfler, P., Rolink, A. and Busslinger, M. Identification of BSAP (Pax-5) target genes in early B-cell development by loss- and gain-of-function experiments. Embo J (1998); 17: 2319-2333.

Nutt, S.L., Urbánek, P., Rolink, A. and Busslinger, M. Essential functions of Pax5 (BSAP) in pro-B cell development: difference between fetal and adult B lymphopoiesis and reduced V-to-DJ recombination at the IgH locus. Genes Dev (1997); 11: 476-491.

Ohkusu, K., Du, J., Isobe, K.I., et al. Protein kinase C alpha-mediated chronic signal transduction for immunosenescence. J Immunol (1997); 159: 2082-2084.

Okkenhaug, K., Bilancio, A., Farjot, G., et al. Impaired B and T cell antigen receptor signaling in p110delta PI 3-kinase mutant mice. Science (2002); 297: 1031-1034.

Okuda, H., Adachi, M., Miyazawa, M., Hinoda, Y. and Imai, K. Protein kinase Calpha promotes apoptotic cell death in gastric cancer cells depending upon loss of anchorage. Oncogene (1999); 18: 5604-5609.

Opferman, J.T., Letai, A., Beard, C., Sorcinelli, M.D., Ong, C.C. and Korsmeyer, S.J. Development and maintenance of B and T lymphocytes requires antiapoptotic MCL-1. Nature (2003); 426: 671-676.

Orchard, J., Ibbotson, R., Best, G., Parker, A. and Oscier, D. ZAP-70 in B cell malignancies. Leuk Lymphoma (2005); 46: 1689-1698.

Orchard, J.A., Ibbotson, R.E., Davis, Z., et al. ZAP-70 expression and prognosis in chronic lymphocytic leukaemia. Lancet (2004); 363: 105-111.

Oscier, D.G., Gardiner, A.C., Mould, S.J., et al. Multivariate analysis of prognostic factors in CLL: clinical stage, IGVH gene mutational status, and loss or mutation of the p53 gene are independent prognostic factors. Blood (2002); 100: 1177-1184.

Oscier, D.G., Thompsett, A., Zhu, D. and Stevenson, F.K. Differential rates of somatic hypermutation in V(H) genes among subsets of chronic lymphocytic leukemia defined by chromosomal abnormalities. Blood (1997); 89: 4153-4160.

Osmond, D.G., Rolink, A. and Melchers, F. Murine B lymphopoiesis: towards a unified model. Immunol Today (1998); 19: 65-68.

Ozes, O.N., Mayo, L.D., Gustin, J.A., Pfeffer, S.R., Pfeffer, L.M. and Donner, D.B. NF-kappaB activation by tumour necrosis factor requires the Akt serine-threonine kinase. Nature (1999); 401: 82-85.

Panayiotidis, P., Ganeshaguru, K., Jabbar, S.A. and Hoffbrand, A.V. Interleukin-4 inhibits apoptotic cell death and loss of the bcl-2 protein in B-chronic lymphocytic leukaemia cells in vitro. Br J Haematol (1993); 85: 439-445.

Papavasiliou, F., Jankovic, M., Suh, H. and Nussenzweig, M.C. The cytoplasmic domains of immunoglobulin (Ig) alpha and Ig beta can independently induce the precursor B cell transition and allelic exclusion. J Exp Med (1995); 182: 1389-1394.

Pappu, R., Cheng, A.M., Li, B., et al. Requirement for B cell linker protein (BLNK) in B cell development. Science (1999); 286: 1949-1954.

Parekh, D.B., Ziegler, W. and Parker, P.J. Multiple pathways control protein kinase C phosphorylation. Embo J (2000); 19: 496-503.

Payelle-Brogard, B., Magnac, C., Alcover, A., Roux, P. and Dighiero, G. Defective assembly of the B-cell receptor chains accounts for its low expression in B-chronic lymphocytic leukaemia. Br J Haematol (2002); 118: 976-985.

Pear, W.S. and Radtke, F. Notch signaling in lymphopoiesis. Semin Immunol (2003); 15: 69-79.

Pear, W.S., Tu, L. and Stein, P.L. Lineage choices in the developing thymus: choosing the T and NKT pathways. Curr Opin Immunol (2004); 16: 167-173.

Pedersen, I.M., Kitada, S., Leoni, L.M., et al. Protection of CLL B cells by a follicular dendritic cell line is dependent on induction of Mcl-1. Blood (2002); 100: 1795-1801.

Perez-Chacon, G., Vargas, J.A., Jorda, J., et al. CD5 provides viability signals to B cells from a subset of B-CLL patients by a mechanism that involves PKC. Leuk Res (2006).

Pettitt, A.R., Sherrington, P.D., Stewart, G., Cawley, J.C., Taylor, A.M. and Stankovic, T. p53 dysfunction in B-cell chronic lymphocytic leukemia: inactivation of ATM as an alternative to TP53 mutation. Blood (2001); 98: 814-822.

Petro, J.B., Rahman, S.M., Ballard, D.W. and Khan, W.N. Bruton's tyrosine kinase is required for activation of IkappaB kinase and nuclear factor kappaB in response to B cell receptor engagement. J Exp Med (2000); 191: 1745-1754.

Pierce, A., Heyworth, C.M., Nicholls, S.E., et al. An activated protein kinase C alpha gives a differentiation signal for hematopoietic progenitor cells and mimicks macrophage colony-stimulating factor-stimulated signaling events. J Cell Biol (1998); 140: 1511-1518.

Pui, J.C., Allman, D., Xu, L., et al. Notch1 expression in early lymphopoiesis influences B versus T lineage determination. Immunity (1999); 11: 299-308.

Quintanilla-Martinez, L., Thieblemont, C., Fend, F., et al. Mantle cell lymphomas lack expression of p27Kip1, a cyclin-dependent kinase inhibitor. Am J Pathol (1998); 153: 175-182.

Radtke, F., Wilson, A., Mancini, S.J. and MacDonald, H.R. Notch regulation of lymphocyte development and function. Nat Immunol (2004); 5: 247-253.

Rai, K.R., Sawitsky, A., Cronkite, E.P., Chanana, A.D., Levy, R.N. and Pasternack, B.S. Clinical staging of chronic lymphocytic leukemia. Blood (1975); 46: 219-234.

Rassenti, L.Z., Huynh, L., Toy, T.L., et al. ZAP-70 compared with immunoglobulin heavy-chain gene mutation status as a predictor of disease progression in chronic lymphocytic leukemia. N Engl J Med (2004); 351: 893-901.

Rawlings, D.J., Saffran, D.C., Tsukada, S., et al. Mutation of unique region of Bruton's tyrosine kinase in immunodeficient XID mice. Science (1993); 261: 358-361.

Reinisch, W., Willheim, M., Hilgarth, M., et al. Soluble CD23 reliably reflects disease activity in B-cell chronic lymphocytic leukemia. J Clin Oncol (1994); 12: 2146-2152.

Rickert, R.C. Regulation of B lymphocyte activation by complement C3 and the B cell coreceptor complex. Curr Opin Immunol (2005); 17: 237-243.

Ringshausen, I., Oelsner, M., Weick, K., Bogner, C., Peschel, C. and Decker, T. Mechanisms of apoptosis-induction by rottlerin: therapeutic implications for B-CLL. Leukemia (2006); 20: 514-520.

Ringshausen, I., Schneller, F., Bogner, C., et al. Constitutively activated phosphatidylinositol-3 kinase (PI-3K) is involved in the defect of apoptosis in B-CLL: association with protein kinase Cdelta. Blood (2002); 100: 3741-3748.

Rojnuckarin, P. and Kaushansky, K. Actin reorganization and proplatelet formation in murine megakaryocytes: the role of protein kinase calpha. Blood (2001); 97: 154-161.

Rolink, A.G., Nutt, S.L., Melchers, F. and Busslinger, M. Long-term *in vivo* reconstitution of T-cell development by Pax5-deficient B-cell progenitors. Nature (1999); 401: 603-606.

Rolink, A.G., Winkler, T., Melchers, F. and Andersson, J. Precursor B cell receptor-dependent B cell proliferation and differentiation does not require the bone marrow or fetal liver environment. J Exp Med (2000); 191: 23-32.

Romanow, W.J., Langerak, A.W., Goebel, P., et al. E2A and EBF act in synergy with the V(D)J recombinase to generate a diverse immunoglobulin repertoire in nonlymphoid cells. Mol Cell (2000); 5: 343-353.

Romashkova, J.A. and Makarov, S.S. NF-kappaB is a target of AKT in anti-apoptotic PDGF signalling. Nature (1999); 401: 86-90.

Rosenwald, A., Alizadeh, A.A., Widhopf, G., et al. Relation of gene expression phenotype to immunoglobulin mutation genotype in B cell chronic lymphocytic leukemia. J Exp Med (2001); 194: 1639-1647.

Roux, P.P. and Blenis, J. ERK and p38 MAPK-activated protein kinases: a family of protein kinases with diverse biological functions. Microbiol Mol Biol Rev (2004); 68: 320-344.

Rowley, R.B., Burkhardt, A.L., Chao, H.G., Matsueda, G.R. and Bolen, J.B. Syk protein-tyrosine kinase is regulated by tyrosine-phosphorylated Ig alpha/Ig beta immunoreceptor tyrosine activation motif binding and autophosphorylation. J Biol Chem (1995); 270: 11590-11594.

Rozman, C. and Montserrat, E. Chronic lymphocytic leukemia. N Engl J Med (1995); 333: 1052-1057.

Ruvolo, P.P., Deng, X., Carr, B.K. and May, W.S. A functional role for mitochondrial protein kinase Calpha in Bcl2 phosphorylation and suppression of apoptosis. J Biol Chem (1998); 273: 25436-25442.

Sagaert, X. and De Wolf-Peeters, C. Classification of B-cells according to their differentiation status, their micro-anatomical localisation and their developmental lineage. Immunol Lett (2003); 90: 179-186.

Saijo, K., Mecklenbrauker, I., Santana, A., Leitger, M., Schmedt, C. and Tarakhovsky, A. Protein kinase C beta controls nuclear factor kappaB activation in B cells through selective regulation of the IkappaB kinase alpha. J Exp Med (2002); 195: 1647-1652.

Saoncella, S., Echtermeyer, F., Denhez, F., et al. Syndecan-4 signals cooperatively with integrins in a Rho-dependent manner in the assembly of focal adhesions and actin stress fibers. Proc Natl Acad Sci U S A (1999); 96: 2805-2810.

Sarfati, M., Chevret, S., Chastang, C., et al. Prognostic importance of serum soluble CD23 level in chronic lymphocytic leukemia. Blood (1996); 88: 4259-4264.

Schaffner, C., Stilgenbauer, S., Rappold, G.A., Dohner, H. and Lichter, P. Somatic ATM mutations indicate a pathogenic role of ATM in B-cell chronic lymphocytic leukemia. Blood (1999); 94: 748-753.

Schebesta, M., Pfeffer, P.L. and Busslinger, M. Control of pre-BCR signaling by Pax5-dependent activation of the BLNK gene. Immunity (2002); 17: 473-485.

Schechtman, D. and Mochly-Rosen, D. Adaptor proteins in protein kinase C-mediated signal transduction. Oncogene (2001); 20: 6339-6347.

Schena, M., Larsson, L.G., Gottardi, D., et al. Growth- and differentiation-associated expression of bcl-2 in B-chronic lymphocytic leukemia cells. Blood (1992); 79: 2981-2989.

Schiemann, B., Gommerman, J.L., Vora, K., et al. An essential role for BAFF in the normal development of B cells through a BCMA-independent pathway. Science (2001); 293: 2111-2114.

Schmid, C. and Isaacson, P.G. Proliferation centres in B-cell malignant lymphoma, lymphocytic (B-CLL): an immunophenotypic study. Histopathology (1994); 24: 445-451.

Schmitt, T.M., Ciofani, M., Petrie, H.T. and Zúñiga-Pflücker, J.C. Maintenance of T cell specification and differentiation requires recurrent notch receptor-ligand interactions. J Exp Med (2004); 200: 469-479.

Schmitt, T.M. and Zúñiga-Pflücker, J.C. Induction of T cell development from hematopoietic progenitor cells by delta-like-1 in vitro. Immunity (2002); 17: 749-756.

Schneider, P. The role of APRIL and BAFF in lymphocyte activation. Curr Opin Immunol (2005); 17: 282-289.

Schneider, P., Takatsuka, H., Wilson, A., et al. Maturation of marginal zone and follicular B cells requires B cell activating factor of the tumor necrosis factor family and is independent of B cell maturation antigen. J Exp Med (2001); 194: 1691-1697.

Schönwasser, D.C., Marais, R.M., Marshall, C.J. and Parker, P.J. Activation of the mitogen-activated protein kinase/extracellular signal-regulated kinase pathway by conventional, novel, and atypical protein kinase C isotypes. Mol Cell Biol (1998); 18: 790-798.

Schwarzmeier, J.D., Hubmann, R., Düchler, M., Jäger, U. and Shehata, M. Regulation of CD23 expression by Notch2 in B-cell chronic lymphocytic leukemia. Leuk Lymphoma (2005); 46: 157-165.

Schweighoffer, E., Vanes, L., Mathiot, A., Nakamura, T. and Tybulewicz, V.L. Unexpected requirement for ZAP-70 in pre-B cell development and allelic exclusion. Immunity (2003); 18: 523-533.

Scott, E.W., Fisher, R.C., Olson, M.C., Kehrli, E.W., Simon, M.C. and Singh, H. PU.1 functions in a cell-autonomous manner to control the differentiation of multipotential lymphoid-myeloid progenitors. Immunity (1997); 6: 437-447.

Scott, E.W., Simon, M.C., Anastasi, J. and Singh, H. Requirement of transcription factor PU.1 in the development of multiple hematopoietic lineages. Science (1994); 265: 1573-1577.

Shaw, A.C., Swat, W., Davidson, L. and Alt, F.W. Induction of Ig light chain gene rearrangement in heavy chain-deficient B cells by activated Ras. Proc Natl Acad Sci U S A (1999a); 96: 2239-2243.

Shaw, A.C., Swat, W., Ferrini, R., Davidson, L. and Alt, F.W. Activated Ras signals developmental progression of recombinase-activating gene (RAG)-deficient pro-B lymphocytes. J Exp Med (1999b); 189: 123-129.

Shinkai, Y., Rathbun, G., Lam, K.P., et al. RAG-2-deficient mice lack mature lymphocytes owing to inability to initiate V(D)J rearrangement. Cell (1992); 68: 855-867.

Sigvardsson, M. Overlapping expression of early B-cell factor and basic helix-loop-helix proteins as a mechanism to dictate B-lineage-specific activity of the lambda5 promoter. Mol Cell Biol (2000); 20: 3640-3654.

Sigvardsson, M., Clark, D.R., Fitzsimmons, D., et al. Early B-cell factor, E2A, and Pax-5 cooperate to activate the early B cell-specific mb-1 promoter. Mol Cell Biol (2002); 22: 8539-8551.

Sigvardsson, M., O'Riordan, M. and Grosschedl, R. EBF and E47 collaborate to induce expression of the endogenous immunoglobulin surrogate light chain genes. Immunity (1997); 7: 25-36.

Soh, J.W., Lee, E.H., Prywes, R. and Weinstein, I.B. Novel roles of specific isoforms of protein kinase C in activation of the c-fos serum response element. Mol Cell Biol (1999); 19: 1313-1324.

Soh, J.W., Lee, Y.S. and Weinstein, I.B. Effects of regulatory domains of specific isoforms of protein kinase C on growth control and apoptosis in MCF-7 breast cancer cells. J Exp Ther Oncol (2003); 3: 115-126.

Soh, J.W. and Weinstein, I.B. Roles of specific isoforms of protein kinase C in the transcriptional control of cyclin D1 and related genes. J Biol Chem (2003); 278: 34709-34716.

Souabni, A., Cobaleda, C., Schebesta, M. and Busslinger, M. Pax5 promotes B lymphopoiesis and blocks T cell development by repressing Notch1. Immunity (2002); 17: 781-793.

Stankovic, T., Stewart, G.S., Fegan, C., et al. Ataxia telangiectasia mutated-deficient B-cell chronic lymphocytic leukemia occurs in pregerminal center cells and results in defective damage response and unrepaired chromosome damage. Blood (2002); 99: 300-309.

Staudinger, J., Zhou, J., Burgess, R., Elledge, S.J. and Olson, E.N. PICK1: a perinuclear binding protein and substrate for protein kinase C isolated by the yeast two-hybrid system. J Cell Biol (1995); 128: 263-271.

Stevenson, F.K. and Caligaris-Cappio, F. Chronic lymphocytic leukemia: revelations from the B-cell receptor. Blood (2004); 103: 4389-4395.

Stilgenbauer, S., Bullinger, L., Lichter, P. and Dohner, H. Genetics of chronic lymphocytic leukemia: genomic aberrations and V(H) gene mutation status in pathogenesis and clinical course. Leukemia (2002); 16: 993-1007.

Su, T.T., Guo, B., Kawakami, Y., et al. PKC-beta controls I kappa B kinase lipid raft recruitment and activation in response to BCR signaling. Nat Immunol (2002); 3: 780-786.

Suzuki, H., Terauchi, Y., Fujiwara, M., et al. Xid-like immunodeficiency in mice with disruption of the p85alpha subunit of phosphoinositide 3-kinase. Science (1999); 283: 390-392.

Takata, M., Homma, Y. and Kurosaki, T. Requirement of phospholipase C-gamma 2 activation in surface immunoglobulin M-induced B cell apoptosis. J Exp Med (1995); 182: 907-914.

Takata, M. and Kurosaki, T. A role for Bruton's tyrosine kinase in B cell antigen receptor-mediated activation of phospholipase C-gamma 2. J Exp Med (1996); 184: 31-40.

Tan, S.L. and Parker, P.J. Emerging and diverse roles of protein kinase C in immune cell signalling. Biochem J (2003); 376: 545-552.

Teh, Y.M. and Neuberger, M.S. The immunoglobulin (Ig)alpha and Igbeta cytoplasmic domains are independently sufficient to signal B cell maturation and activation in transgenic mice. J Exp Med (1997); 185: 1753-1758.

ten Boekel, E., Melchers, F. and Rolink, A.G. Precursor B cells showing H chain allelic inclusion display allelic exclusion at the level of pre-B cell receptor surface expression. Immunity (1998); 8: 199-207.

Thomas, J.D., Sideras, P., Smith, C.I., Vorechovsky, I., Chapman, V. and Paul, W.E. Colocalization of X-linked agammaglobulinemia and X-linked immunodeficiency genes. Science (1993); 261: 355-358.

Thompson, J.S., Schneider, P., Kalled, S.L., et al. BAFF binds to the tumor necrosis factor receptor-like molecule B cell maturation antigen and is important for maintaining the peripheral B cell population. J Exp Med (2000); 192: 129-135.

Thunberg, U., Johnson, A., Roos, G., et al. CD38 expression is a poor predictor for V_H gene mutational status and prognosis in chronic lymphocytic leukemia. Blood (2001); 97: 1892-1894.

Ting, H.C., Christian, S.L., Burgess, A.E. and Gold, M.R. Activation and phosphatidylinositol 3-kinase-dependent phosphorylation of protein kinase C-epsilon by the B cell antigen receptor. Immunol Lett (2002); 82: 205-215.

Tobin, G., Thunberg, U., Johnson, A., et al. Chronic lymphocytic leukemias utilizing the V_H3-21 gene display highly restricted Vlambda2-14 gene use and homologous CDR3s: implicating recognition of a common antigen epitope. Blood (2003); 101: 4952-4957.

Tobin, G., Thunberg, U., Johnson, A., et al. Somatically mutated Ig V(H)3-21 genes characterize a new subset of chronic lymphocytic leukemia. Blood (2002); 99: 2262-2264.

Tojima, Y., Fujimoto, A., Delhase, M., et al. NAK is an IkappaB kinase-activating kinase. Nature (2000); 404: 778-782.

Tokoyoda, K., Egawa, T., Sugiyama, T., Choi, B.I. and Nagasawa, T. Cellular niches controlling B lymphocyte behavior within bone marrow during development. Immunity (2004); 20: 707-718.

Trushin, S.A., Pennington, K.N., Carmona, E.M., et al. Protein kinase Calpha (PKCalpha) acts upstream of PKCtheta to activate IkappaB kinase and NF-kappaB in T lymphocytes. Mol Cell Biol (2003); 23: 7068-7081.

Tsukada, N., Burger, J.A., Zvaifler, N.J. and Kipps, T.J. Distinctive features of "nurselike" cells that differentiate in the context of chronic lymphocytic leukemia. Blood (2002); 99: 1030-1037.

Tsukada, S., Saffran, D.C., Rawlings, D.J., et al. Deficient expression of a B cell cytoplasmic tyrosine kinase in human X-linked agammaglobulinemia. Cell (1993); 72: 279-290.

Tsuruta, F., Masuyama, N. and Gotoh, Y. The phosphatidylinositol 3-kinase (PI3K)-Akt pathway suppresses Bax translocation to mitochondria. J Biol Chem (2002); 277: 14040-14047.

Tudor, K.S., Payne, K.J., Yamashita, Y. and Kincade, P.W. Functional assessment of precursors from murine bone marrow suggests a sequence of early B lineage differentiation events. Immunity (2000); 12: 335-345.

Tung, J.W., Mrazek, M.D., Yang, Y. and Herzenberg, L.A. Phenotypically distinct B cell development pathways map to the three B cell lineages in the mouse. Proc Natl Acad Sci U S A (2006); 103: 6293-6298.

Turner, M., Mee, P.J., Costello, P.S., et al. Perinatal lethality and blocked B-cell development in mice lacking the tyrosine kinase Syk. Nature (1995); 378: 298-302.

Úrbanek, P., Wang, Z.Q., Fetka, I., Wagner, E.F. and Busslinger, M. Complete block of early B cell differentiation and altered patterning of the posterior midbrain in mice lacking Pax5/BSAP. Cell (1994); 79: 901-912.

Vallentin, A., Lo, T.C. and Joubert, D. A single point mutation in the V3 region affects protein kinase Calpha targeting and accumulation at cell-cell contacts. Mol Cell Biol (2001); 21: 3351-3363.

Vetrie, D., Vorechovsky, I., Sideras, P., et al. The gene involved in X-linked agammaglobulinaemia is a member of the src family of protein-tyrosine kinases. Nature (1993); 361: 226-233.

Vindelov, L.L., Christensen, I.J. and Nissen, N.I. A detergent-trypsin method for the preparation of nuclei for flow cytometric DNA analysis. Cytometry (1983); 3: 323-327.

Vuillier, F., Dumas, G., Magnac, C., et al. Lower levels of surface B-cell-receptor expression in chronic lymphocytic leukemia are associated with glycosylation and folding defects of the mu and CD79a chains. Blood (2005); 105: 2933-2940.

Wang, D., Feng, J., Wen, R., et al. Phospholipase Cgamma2 is essential in the functions of B cell and several Fc receptors. Immunity (2000); 13: 25-35.

Wang, W.L., Yeh, S.F., Chang, Y.I., et al. PICK1, an anchoring protein that specifically targets protein kinase Calpha to mitochondria selectively upon serum stimulation in NIH 3T3 cells. J Biol Chem (2003); 278: 37705-37712.

Wang, X.Y., Repasky, E. and Liu, H.T. Antisense inhibition of protein kinase Calpha reverses the transformed phenotype in human lung carcinoma cells. Exp Cell Res (1999); 250: 253-263.

Ways, D.K., Kukoly, C.A., deVente, J., et al. MCF-7 breast cancer cells transfected with protein kinase C-alpha exhibit altered expression of other protein kinase C isoforms and display a more aggressive neoplastic phenotype. J Clin Invest (1995); 95: 1906-1915.

Whelan, R.D. and Parker, P.J. Loss of protein kinase C function induces an apoptotic response. Oncogene (1998); 16: 1939-1944.

Wiestner, A., Rosenwald, A., Barry, T.S., et al. ZAP-70 expression identifies a chronic lymphocytic leukemia subtype with unmutated immunoglobulin genes, inferior clinical outcome, and distinct gene expression profile. Blood (2003); 101: 4944-4951.

Witt, C.M., Hurez, V., Swindle, C.S., Hamada, Y. and Klug, C.A. Activated Notch2 potentiates CD8 lineage maturation and promotes the selective development of B1 B cells. Mol Cell Biol (2003); 23: 8637-8650.

Xu, S., Wong, S.C. and Lam, K.P. Cutting edge: B cell linker protein is dispensable for the allelic exclusion of immunoglobulin heavy chain locus but required for the persistence of $CD5^+$ B cells. J Immunol (2000); 165: 4153-4157.

Yasuda, T., Shirakata, M., Iwama, A., et al. Role of Dok-1 and Dok-2 in myeloid homeostasis and suppression of leukemia. J Exp Med (2004); 200: 1681-1687.

Yoshida, H., Hayashi, S., Kunisada, T., et al. The murine mutation osteopetrosis is in the coding region of the macrophage colony stimulating factor gene. Nature (1990); 345: 442-444.

Zeng, X., Xu, H. and Glazer, R.I. Transformation of mammary epithelial cells by 3-phosphoinositide-dependent protein kinase-1 (PDK1) is associated with the induction of protein kinase Calpha. Cancer Res (2002); 62: 3538-3543.

Zhu, Y., Dong, Q., Tan, B.J., Lim, W.G., Zhou, S. and Duan, W. The PKCalpha-D294G mutant found in pituitary and thyroid tumors fails to transduce extracellular signals. Cancer Res (2005); 65: 4520-4524.

Zhuang, Y., Barndt, R.J., Pan, L., Kelley, R. and Dai, M. Functional replacement of the mouse E2A gene with a human HEB cDNA. Mol Cell Biol (1998); 18: 3340-3349.

Zúñiga-Pflücker, J.C. T-cell development made simple. Nat Rev Immunol (2004); 4: 67-72.

Zupo, S., Isnardi, L., Megna, M., et al. CD38 expression distinguishes two groups of B-cell chronic lymphocytic leukemias with different responses to anti-IgM antibodies and propensity to apoptosis. Blood (1996); 88: 1365-1374.

Zupo, S., Massara, R., Dono, M., et al. Apoptosis or plasma cell differentiation of CD38-positive B-chronic lymphocytic leukemia cells induced by cross-linking of surface IgM or IgD. Blood (2000); 95: 1199-1206.

Zweidler-McKay, P.A., He, Y., Xu, L., et al. Notch signaling is a potent inducer of growth arrest and apoptosis in a wide range of B-cell malignancies. Blood (2005); 106: 3898-3906.

Publications

A.M. Michie and **R. Nakagawa**

The link between PKCα regulation and cellular transformation. Immunological Letters (2005); 96: 155-162

R. Nakagawa, J.W. Soh and A.M. Michie

Subversion of PKCα signaling in hematopoietic progenitor cells results in the generation of a B-CLL-like population *in vivo*. Cancer Research (2006); 66: 527-534.

A.M. Michie and **R. Nakagawa**

Elucidating the role of protein kinase C in chronic lymphocytic leukaemia. Hematological Oncology (2006); 24: 134-138.

R. Nakagawa, S.M. Mason and A.M. Michie

A protocol to determine the role of specific signalling molecules during lymphocyte development *in vivo*: instant transgenesis. Nature Protocols (2006); 1: 1185-1193